Assessment of Utricular Nerve, Hair Cell and Mechanical Function, *in vivo.*

A thesis submitted in fulfilment of the requirements for the degree of Doctor of Philosophy

By

Christopher John Pastras

School of Medical Sciences
The University of Sydney

20th December 2018

Acknowledgements

First, I would like to thank my Supervisor Daniel Brown, who has been very supportive throughout my studies and enabled me to undertake this research journey. I am very thankful for Daniel's hands-on supervision, and for the knowledge and wisdom he has imparted on me. Notably, he has given me an understanding of how to undertake new and novel research, once you realize how to question, learn, think and develop for yourself.

Second, I would like to thank my Associate Supervisor Ian Curthoys, who has also been very encouraging and has helped steer me through my candidature. Despite a large h-index, a highly respected reputation, and many major contributions to the research field, Ian has always been very kind, helpful, and has provided the additional supervisory support necessary.

A very special mention goes to my wife Cassandra, who has been an ongoing source of encouragement and calming reassurance throughout this thesis. Through many long days and nights spent analyzing data or writing, Cass has been there, to provide unconditional love and support. Importantly, she has helped provide distraction and humor during some stressful times.

I owe many thanks to my parents, Christina and Steven, who provided me with a supportive and memorable upbringing. Mum has always been there to provide encouragement for anything I chose to do, and Dad catalyzed an interest in science, with many trips to various museums and zoos, as well as many interesting scientific discussions. Thank you both. Additional thanks go to my brother, Paul and sister, Katherine who have been a healthy source of sibling rivalry and competition, growing up. Both continue to support everything I do, including this PhD. Much gratitude goes to my family-in-law, Leisa, Dave, Alanna, Jonati, Jon, and Olivia, for their ongoing hospitality, kindness and support. A special mention goes to my best mates, Michael and Ryan, who have provided a much-needed outlet during the tough times, including humorous chats and visits to the pub.

Table of Contents

List of tables and figures

As many chapters in the thesis are presented in journal format the figures are presented as follows:

Authorship attribution statement

Three peer-reviewed journal articles published in *Hearing Research* have been included as chapters in this thesis. The first-person plural ("we") was used throughout this thesis for overall consistency, as three chapters featured co-authored publications. In chapter 5 where I performed functional and mechanical measurements during experimental manipulations, assistance and advice were provided by both my supervisors.

Chapter 2 contains the publication: **Pastras, C. J.**, Curthoys, I. S., Sokolic, L., & Brown, D. J. (2018). Suppression of the vestibular short-latency evoked potential by electrical stimulation of the central vestibular system. *Hearing research*, *361*, 23-35. For this paper, I performed the experiments, collected and analyzed the data, and drafted and edited the manuscript. IS Curthoys provided advice on the project and edited the manuscript. L Sokolic aided with the histology. DJ Brown developed the experimental equipment, provided experimental assistance and edited the manuscript.

Chapter 3 contains the publication: **Pastras, C. J.**, Curthoys, I. S., & Brown, D. J. (2017). In vivo recording of the vestibular microphonic in mammals. *Hearing research*, *354*, 38-47. I performed the experiments, collected and analyzed the data, and drafted and edited the manuscript. IS Curthoys provided advice on the project and edited the manuscript. DJ Brown developed the experimental equipment, provided experimental assistance and edited the manuscript.

Chapter 4 contains the publication: **Pastras, C. J.**, Curthoys, I. S., & Brown, D. J. (2018). Dynamic response to sound and vibration of the guinea pig utricular macula, measured in vivo using Laser Doppler Vibrometry. *Hearing research*. I performed the experiments, collected and analyzed the data, drafted and edited the manuscript. IS Curthoys provided advice and equipment for the project and edited the manuscript. DJ Brown developed the experimental equipment, provided experimental assistance and edited the manuscript.

In addition to the statements above, in cases where I am not the corresponding author of a published item, permission to include the published material has been granted by the corresponding author.

Christopher John Pastras …… **Date:** 22nd October 2018

As supervisor for the candidature upon which this thesis is based, I can confirm that the authorship attribution statements above are correct.

Daniel J Brown ……. **Date:** 22nd October 2018

Statement of originality

I, Christopher John Pastras certify that to the best of my knowledge the content of this thesis is my own work. This thesis has not been submitted for any degree or other purposes. I certify that the intellectual content of this thesis is the product of my own work and that all the assistance received in preparing this thesis and sources have been acknowledged.

Christopher John Pastras …… **Date:** 22nd October 2018

Publications presented for examination

The following publications form the main body of the thesis:

Pastras, C. J., Curthoys, I. S., Sokolic, L., & Brown, D. J. (2018). Suppression of the vestibular short-latency evoked potential by electrical stimulation of the central vestibular system. *Hearing research*, *361*, 23-35.

This paper is presented in *Chapter 2* of this thesis

Pastras, C. J., Curthoys, I. S., & Brown, D. J. (2017). In vivo recording of the vestibular microphonic in mammals. *Hearing research*, *354*, 38-47.

This paper is presented in *Chapter 3* of this thesis

Pastras, C. J., Curthoys, I. S., & Brown, D. J. (2018). Dynamic response to sound and vibration of the guinea pig utricular macula, measured in vivo using laser doppler vibrometry. *Hearing research*.

This paper is presented in *Chapter 4* of this thesis

Additional relevant publications

A substantial contribution was also made to the following papers which are presented in the appendix:

Brown, D. J., **Pastras, C. J.**, & Curthoys, I. S. (2017). Electrophysiological Measurements of Peripheral Vestibular Function—A Review of Electrovestibulography. *Frontiers in systems neuroscience*, *11*, 34.

This paper is presented in *Appendix 3* of this thesis

Curthoys, I. S., Grant, J. W., Burgess, A. M., **Pastras, C. J.**, Brown, D. J., & Manzari, L. (2018). Otolithic Receptor Mechanisms for Vestibular-Evoked Myogenic Potentials: A Review. *Frontiers in neurology*, *9*.

This paper is presented in *Appendix 4* of this thesis

Conference abstracts during candidature

Pastras, C.J., Curthoys, I.S., Brown, D.J. Assessment of Utricular Nerve, Hair cell and Mechanical function, *in vivo*. The 16th Australasian Auditory Neuroscience Workshop. The Women's College, UQ campus, St. Lucia, 1st December 2018 (Podium).

Pastras, C.J., Curthoys, I.S., Brown, D.J. Dynamic Response of the Utricular Macula using Laser Doppler Vibrometry *in vivo*. Poster Blitz Presentation ARO – 41st Midwinter Meeting of the Association for Research in Otolaryngology, San Diego, California, 10 - 15 February 2018 (Podium).

Pastras, C.J., Curthoys, I.S., Brown, D.J. Suppression of the Vestibular Short Latency Evoked Potential with Electrical Stimulation of the Central Vestibular System. Poster PS 547 at the 41st Midwinter Meeting of the Association for Research in Otolaryngology, San Diego, California, 10 - 15 February 2018 (Poster).

Pastras, C.J., Curthoys, I.S., Brown, D.J. Dynamic Response and sensitivity of the Utricular Macula using Laser Doppler Vibrometry *in vivo*. Poster PS 544 at the 41st Midwinter Meeting of the Association for Research in Otolaryngology, San Diego, California, 10 - 15 February 2018 (Poster).

Pastras, C.J., Curthoys, I.S., Brown, D.J. The Vestibular Short Latency Evoked Potential with Electrical Stimulation of the Efferent Vestibular System. The 15th Australasian Auditory Neuroscience Workshop. School of Medical Sciences, University of New South Wales, 2nd December 2017 (Podium).

Pastras, C.J., Curthoys, I.S., Brown, D.J. Dynamic response and sensitivity of the utricular macula, measured *in vivo* using Laser Doppler Vibrometry in guinea pigs. The 15th Australasian Auditory Neuroscience Workshop. School of Medical Sciences, University of New South Wales, 2nd December 2017 (Poster).

Pastras, C.J., Curthoys, I.S., Brown, D. J. *In vivo* Vestibular Microphonic recordings in guinea pigs. Poster PS 905 presented at the 40th Midwinter Meeting of the Association for Research in Otolaryngology, Baltimore, Maryland, 7-12 February 2017 (Poster).

Pastras, C.J., Curthoys, I.S., Brown, D.J. In vivo Vestibular Microphonic recordings in guinea pigs. The 14th Australasian Auditory Neuroscience Workshop. Medical Science Precinct, Hobart, 4-5th December 2016 (Podium).

Pastras, C.J., Curthoys, I.S., Brown, D.J. Characterisation of the mammalian Vestibular Microphonic. The 26th annual meeting of the Neuro-otology Society of Australia (NOTSA). University of Newcastle, 23rd-25th September 2016 (Podium).

Pastras, C.J., Curthoys, I.S., Brown, D.J. Vestibular Microphonics: a new in vivo tool for measuring otolith hair cell function. RPA vestibular Seminar, Royal Prince Alfred Hospital, Camperdown. Department of Neurology. 7th September 2016 (Podium).

Pastras, C.J., Brown, D.J., Curthoys, I.S., Mukherjee, P. and Gibson, W.P. Experimental support for Cochlear implantation in Post-Labyrinthectomy Patients. The 25th annual meeting of the Neuro- otology Society of Australia (NOTSA). Alfred Hospital, Melbourne, 18-20 September 2015 (Podium).

Pastras, C.J., Brown, D.J., Curthoys, I.S., Mukherjee, P. and Gibson, W.P. Cochlear implantation in post-labyrinthectomy guinea pigs. Australasian Auditory Neuroscience Workshop (AANW), Mt Eliza, Melbourne, 30 Nov – 1 Dec 2015 (Podium).

List of common abbreviations

ACAP: Antidromic Compound Action Potential

AChR: Acetylcholine Receptor

ACS: Air Conducted Sound

BCV: Bone Conducted Vibration

CAP: Compound Action Potential

CM: Cochlear Microphonic

COCB: Crossed Olivocochlear Bundle

ES: Electrical Stimulation

EVS: Efferent Vestibular System

I/O: Input/Output

LDV: Laser Doppler Vibrometer/Vibrometry

MET: Mechanoelectrical Transduction

MOC: Medial Olivocochlear

MVN: Medial Vestibular Nucleus

pps: pulses per second

SCC: Semicircular Canal

THD: Total Harmonic Distortion

UM: Utricular Microphonic

VEMP: Vestibular Evoked Myogenic Potential

VM: Vestibular Microphonic

VsEP: Vestibular short-latency Evoked Potential

Abstract

Vestibular research currently relies on single response measures such as *ex vivo* hair cell and *in vivo* single unit recordings. Although these methods allow detailed insight into the response properties of individual vestibular hair cells and neurons, they do not provide a holistic understanding of peripheral vestibular functioning and its relationship to vestibular pathology in a living system. For this to take place, *in vivo* recordings of peripheral vestibular nerve, hair cell and mechanical function are needed. The previous inability to record vestibular hair cell responses stemmed from a difficulty in accessing the vestibular end-organs and stimulating them in isolation of the cochlea. To circumvent this, we developed a ventral surgical approach, removing the cochlea, to provide full access to the basal surface of the utricular macula. This allowed functional and mechanical utricular hair cell recordings, alongside gross utricular nerve responses. Recordings were performed in anaesthetized guinea pigs using Bone Conducted Vibration (BCV) and Air Conducted Sound (ACS) stimuli, providing a clinical link to vestibular reflex testing. We have thus far performed experiments involving: 1) Selective manipulation of vestibular nerve function, using electrical stimulation of the central vestibular system. 2) Glass micropipette recordings from the basal surface of the macular epithelium, which provided a robust and localized measure of extracellular utricular hair cell function. 3) With the macular exposed, we have measured the dynamic motion of the macula using Laser Doppler Vibrometry, which was recorded alongside the hair cell and nerve response recordings. 4) We have used physiological and pharmacological experimental manipulations to selectively modulate utricular nerve, hair cell or mechanical function, demonstrating the ability to differentially diagnose the basis of peripheral vestibular disorders in the mammalian utricle. These tools allow for a more complete understanding of peripheral vestibular function and a first order perspective into clinical disorders effecting the otoliths.

Chapter 1: Thesis introduction

Since Von Békésy's cadaveric recording of the cochlear traveling wave (Békésy 1928), a number of objective *in vivo* measures of auditory function have been developed, which independently assess cochlear nerve, hair cell and mechanical function (see Table 1, below). These measures include the CM (Wever and Bray 1930), CAP (Fromm, Nylen et al. 1935, Tasaki and Fernandez 1951), Summating Potential (Davis, Deatherage et al. 1958), basilar membrane vibration (Johnstone and Boyle 1967), Auditory Nerve Neurophonic (Weinberger, Kitzes et al. 1970), and Otoacoustic Emission (Kemp 1978). The ability to evaluate different aspects of cochlear physiology allows us to differentially diagnose the cause of peripheral dysfunction and determine the roots of auditory pathologies such as acoustic trauma (Patuzzi, Yates et al. 1989), endolymphatic hydrops (Brown, Chihara et al. 2013), tinnitus (Evans and Borerwe 1982) and ototoxicity (Stypulkowski 1990, Fitzgerald, Robertson et al. 1993, Sheppard, Hayes et al. 2014). Moreover, these tools have helped characterize the fundamental mechanisms underpinning hearing sensitivity such as the cochlear amplifier and top-down auditory feedback driven by the olivocochlear efferents.

COCHLEAR			
Electrophysiological measurements			
Name	**Stimulus**	**Source**	**Example**
Single unit potential	Spont. or ACS	Neuron(s)	(Webster and Aitkin 1971)
Auditory Nerve Neurophonic	Spont. or ACS	Nerve	(Weinberger, Kitzes et al. 1970)
Compound Action Potential (CAP)	ACS	Nerve	(Deatherage, Eldredge et al. 1959)
Cochlear Microphonic (CM)	ACS	Hair cells	(Tasaki and Fernandez 1951)
Summating potential	ACS	Hair cells	(Davis, Deatherage et al. 1958)
Endocochlear potential	Spont.	Stria vascularis	(Salt, Melichar et al. 1987)
Auditory Brainstem Response (ABR)	ACS	Nerve/Brainstem	(Ozdamar 1979)
Otoacoustic Emission	ACS	Hair cells	(Kemp 1978)
Electrically-evoked CAP	Current	Nerve	(Killian, Klis et al. 1994)
Mechanical measurements			

Recording location	**Recording technique**	**Example**
Organ of Corti	Mössbauer technique	(Johnstone and Boyle 1967)
	Laser speckle	(Kohllöffel 1972)
	Capacitive probe	(Wilson and Johnstone 1975)
	Light lever	(LePage 1989)
	Laser Doppler Velocimetry	(Ruggero and Rich 1991)
	Optical Coherence Tomography	(Lee, Raphael et al. 2015)

VESTIBULAR			
Electrophysiological measurements			
Name	**Stimulus**	**Source**	**Example**
Single unit potential	Spont., BCV or ACS	Neuron(s)	(Curthoys, Vulovic et al. 2016)
Vestibular Evoked Myogenic Potential (VEMP)	BCV, ACS or current	Myocytes	(Hsu, Wang et al. 2008)
Vestibular Ocular Reflex	Rotation or current	Myocytes	(Hubner, Khan et al. 2017)
Vestibular short-latency evoked potential (VsEP)	BCV or ACS	Neural	(Jones, Jones et al. 2011)
Mechanical measurements			
Recording location	**Recording technique**		**Example**
N/A	**-**		**-**

Table 1: List of mammalian *in vivo* electrophysiological and mechanical recordings from the cochlea and vestibular system. Abbreviations: ACS: Air-conducted sound; BCV: Bone-conducted vibration; Spont.: Spontaneous Activity.

In contrast to the host of cochlear response measures, to probe vestibular function researchers have mostly relied on either single neuron ('unit') recordings, *ex vivo* hair cell measurements, or reflex response recordings. Unfortunately, there are several limitations to these response measures. Although single-unit recordings have helped form the basis of our understanding regarding peripheral vestibular sensitivity (Curthoys and Vulovic 2011, Curthoys, Vulovic et al. 2016). Such measurements are difficult to perform, particularly for long experiments where researchers may wish to longitudinally investigate the effects of an experimental manipulation. Moreover, these effects cannot be compared between control and experimental animals, thus limiting their utility.

More recently, the Vestibular short-latency Evoked Potential (VsEP) has been used to assess peripheral vestibular function in experimental animals (Jones, Subramanian et al. 2002). The VsEP is a compound action potential of the irregular otolithic afferent neurons in response to changes in linear acceleration (Jones, Jones et al. 2011), and can easily be recorded longitudinally, or compared between animal groups. The VsEP has been used to explore changes in peripheral vestibular sensitivity due to endolymphatic hydrops (Kingma and Wit 2009, Brown, Chihara et al. 2013), noise exposure (Sohmer, Elidan et al. 1999, Biron, Freeman et al. 2002, Stewart, Kanicki et al. 2018), ototoxic agents (Oei, Segenhout et al. 2004, Bremer, De Groot et al. 2012), and genetic mutations (Jones, Erway et al. 2004). Unfortunately, in isolation the VsEP cannot identify the root cause of the loss of sensitivity, where abnormal neural, hair cell or mechanical responses may underlie changes in peripheral function.

From a clinical standpoint, there are numerous balance disorders that lack a clear pathophysiological understanding, which may originate from either hair cell, mechanical or neural dysfunction. In peripheral hearing assessment, the development of objective functional measures such as the Auditory Brainstem Response (ABR) and otoacoustic emissions has allowed rapid screening of peripheral auditory function, even in infants. Unfortunately, the same level of testing is not available in the vestibular system, where reflex responses are used to identify the occurrence, but not the cause of vestibular loss.

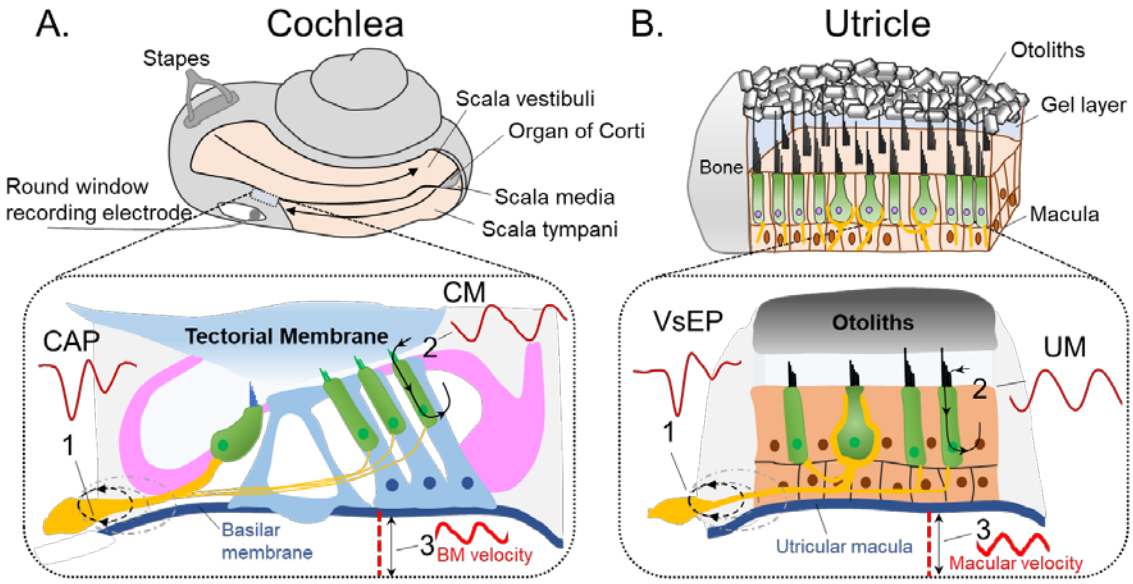

Figure 1: (A) For decades auditory researchers have used objective measures of cochlear nerve, hair cell and mechanical function in the CAP, CM and basilar membrane vibration to understand the cellular basis of hearing loss. (B) This thesis aimed to develop and characterize analogous functional

and mechanical recordings from the utricle, in the VsEP, UM and macular vibration to differentially diagnose peripheral vestibular dysfunction.

The aim of this thesis was to develop and characterize functional and mechanical hair cell recordings of the vestibular system, alongside neural responses, *in vivo*. Additionally, experimental manipulations were performed to selectively modulate peripheral nerve, hair cell or mechanical function, as a simple demonstration of scenarios where these response measures behave independently. For simplicity, we have focused on the function of the utricle and have used BCV and ACS stimuli.

In chapter 2, we attempt to manipulate the VsEP without altering hair cell responses. This involved electrically stimulating the Efferent Vestibular System (EVS) cell bodies at the brainstem. Chapter 3 explores the measurement of the Vestibular Microphonic. Since this response was typically recorded from the surface of utricular macula we will refer to it throughout the thesis as the Utricular Microphonic (UM). Experimental evidence demonstrates the UM is a utricular hair cell potential local to the recording electrode at the surface of the macula. In Chapter 4, we recorded mechanical responses of the utricular macular to BCV and ACS, alongside functional responses in the UM and VsEP. Chapter 5 demonstrates the simultaneous use of the VsEP, UM and macular vibration measures during various experimental manipulations of the utricle. Finally, chapter 6 provides an overall discussion of these novel response measures, and how they may be used to further explore vestibular function, in the laboratory or clinic.

Chapter 2: Modulation of utricular nerve function

2.1. Introduction

A complete *in vivo* assessment of peripheral utricular function requires an objective measure of utricular nerve function. Current available techniques include the single unit potential (Curthoys, Kim et al. 2006, Curthoys, Vulovic et al. 2016) and VsEP (Jones, Jones et al. 2011). The VsEP has been previously recorded in our laboratory (Brown, Chihara et al. 2013), and shown to originate from the utricle (Chihara, Wang et al. 2013), making it an appropriate tool to differentially diagnose peripheral utricular nerve function, *in vivo*. The VsEP is easily recorded via a facial nerve wire electrode, and allows longitudinal, intra-animal (Kingma and Wit 2009) and inter-animal monitoring (Lee, Holt et al. 2017) during experimental manipulations. For a more detailed overview of the VsEP see appendix 3 (Brown, Pastras et al. 2017). However, being a nerve response to ACS or BCV, the amplitude of the VsEP is dependent upon the sensitivity of both macular vibration and utricular hair cells, and thus experimental manipulations of the VsEP amplitude *may* be due to changes in mechanical or hair cell function, rather than manipulations of the nerve function *per se*.

Researchers have used the VsEP to study the effect of experimental manipulations on peripheral otolith function, such as the effect of ototoxic drugs (Bremer, De Groot et al. 2012), endolymphatic hydrops (Brown, Chihara et al. 2013), potassium toxicity (Kingma and Wit 2010) and noise exposure (Sohmer, Elidan et al. 1999). In such studies the origin of vestibular dysfunction could not be determined, despite most studies assuming that changes in the VsEP amplitude arose due to hair cell dysfunction. In auditory research, we are now starting to appreciate that substantial changes in hearing or objective measures of cochlear sensitivity (i.e. the CAP or ABR) following noise trauma, ototoxicity or aging can arise due to a loss of cochlear neurons – a phenomenon termed 'hidden hearing loss' (Liberman and Kujawa 2017, Parthasarathy and Kujawa 2018), where mechanical and hair cell function can remain unaltered. Similarly, it is plausible that a loss of vestibular nerve sensitivity, without changes in hair cell or mechanical sensitivity, may underlie some forms of peripheral vestibular dysfunction. Thus, we sought to establish a simple demonstration that the VsEP amplitude can change independently of changes in hair cell or mechanical sensitivity.

In order to *directly* manipulate peripheral utricular nerve function, we aimed to electrically stimulate the EVS at the floor of the fourth ventricle, as the EVS densely innervates peripheral vestibular afferents (Lysakowski and Goldberg 1997, Lysakowski and Goldberg 2004, Holt, Kewin et al. 2015). Previous studies demonstrated that electrical stimulation of the mammalian EVS resulted in large increases in the

spontaneous firing rate of irregular, vestibular neurons (Goldberg and Fernandez 1980, Marlinski, Plotnik et al. 2004), and it was assumed that this was due to a direct effect of the EVS on the primary afferents.

Ultimately, the following study shows that we were successful in modulating the amplitude of the VsEP, although the effects were NOT mediated via EVS activation. Rather, our electrical stimulation resulted in antidromic blockage of the VsEP response. Fortuitously, this result provides an *even more* elegant demonstration that the VsEP amplitude can be manipulated independent of changes in the utricular macular vibration or hair cell sensitivity.

2.2. Suppression of the VsEP by electrical stimulation of the central vestibular system

Pastras, C. J., Curthoys, I. S., Sokolic, L., & Brown, D. J. (2018). Suppression of the vestibular short-latency evoked potential by electrical stimulation of the central vestibular system. *Hearing research*, *361*, 23-35.

Hearing Research 361 (2018) 23–35

Contents lists available at ScienceDirect

Hearing Research

journal homepage: www.elsevier.com/locate/heares

Research Paper

Suppression of the vestibular short-latency evoked potential by electrical stimulation of the central vestibular system

Christopher J. Pastras [a], Ian S. Curthoys [b], Ljiljana Sokolic [a], Daniel J. Brown [a, *]

[a] The Meniere's Laboratory, Sydney Medical School, The University of Sydney, Sydney, NSW, 2050, Australia
[b] Vestibular Research Laboratory, The University of Sydney, School of Psychology, Sydney, NSW, 2050, Australia

ARTICLE INFO

Article history:
Received 9 October 2017
Received in revised form
15 January 2018
Accepted 22 January 2018
Available online 2 February 2018

Keywords:
Vestibular short-latency evoked potential
Central vestibular system
Vestibular nuclei
Efferent vestibular system
Antidromic CAP
Guinea pig
Bone conducted vibration

ABSTRACT

In an attempt to view the effects of the efferent vestibular system (EVS) on peripheral dynamic vestibular function, we have monitored the Vestibular short-latency Evoked Potential (VsEP) evoked by pulses of bone conducted vibration during electrical stimulation of the EVS neurons near the floor of the fourth ventricle in the brainstem of anesthetized guinea pigs. Given the reported effects of EVS on primary afferent activity, we hypothesized that EVS stimulation would cause a slight reduction in the VsEP amplitude. Our results show a substantial (>50%) suppression of the VsEP, occurring immediately after a single EVS current pulse. The effect could not be blocked by cholinergic drugs which have been shown to block efferent-mediated vestibular effects. Shocks produced a short-latency P1-N1 response immediately after the electrical artifact which correlated closely to the VsEP suppression. Ultimately, we have identified that this suppression results from antidromic blockade of the afferent response (the VsEP). It would appear that this effect is unavoidable for EVS stimulation, as we found no other effects.

1. Introduction

The mammalian EVS has a bilateral and symmetric origin in the dorsal brainstem, at the floor of the fourth ventricle, lateral of the facial nerve genu (Goldberg and Fernandez, 1980; Strutz, 1982; Motts et al., 2008). It has an extensive and non-selective top-down projection to the periphery, where efferent fibers bifurcate and densely innervate type I calyx afferents, type II hair cells and also likely bouton afferents of all vestibular end-organs (Lysakowski and Goldberg., 1997, 2004; Holt et al., 2015).

EVS effects are mediated by cholinergic neurotransmission with both fast nicotinic (ionotropic) and slow muscarinic (metabotropic) kinetics (Luebke et al., 2005; Holt et al., 2017). Less understood pathways have also been implicated such as the Calcitonin Gene-Related Peptide (Wackym et al., 1991; Chi et al., 1999), Adenoside 5′-Triphosphate (Rennie and Ashmore, 1993; Rossi et al., 1994; Syeda and Lysakowski, 2001), Nitric Oxide (Lysakowski and Singer, 2000), Opioid peptides (Popper and Wackym, 2001), and GABA (Didier et al., 1990; Lopez et al., 1990). It is therefore likely the EVS has a range of functional time scales, with both rapid and gradual peripheral modulatory effects. Pharmacological modulation of the EVS in turtles using specific acetylcholine receptor (AChR) agonists and antagonists have demonstrated that fast calyx-dimorphic excitation is mediated by α4, α6 and β2 nicotinic AChR subunits, whereas fast bouton inhibition is attributed to the activation of α9/10 nicotinic AChRs on type II hair cells (Holt et al., 2006, 2015). Slow calyx-dimorphic excitation has also been implicated by M-current activation through muscarinic acetylcholine receptors (Holt et al., 2017). Knock-out mice for specific nAChR homomeric and heteromeric subtypes produced variations in VsEP threshold, latency and amplitude, suggesting a complex relationship between peripheral efferent cholinergic activation and primary dynamic afferent activity (Morley et al., 2017). However, despite ongoing work, the functional role of the EVS is currently unknown.

Plotnik et al. (2005) found large fluctuations in the background firing of irregular afferents which was shown to originate from the EVS. This was confirmed to be an artifact of the chinchillas

Abbreviations: AChR, Acetylcholine Receptor; BCV, Bone Conducted Vibration; CAP, Compound Action Potential; CM, Cochlear Microphonic; DMPP, 1,1-Dimethyl-4-phenylpiperazinium iodide; eCAP, electrically-evoked Compound Action Potential; ECG, Electrocardiography; ES, Electrical Stimulation; EVS, Efferent Vestibular System; I/O, Input/Output; VsEP, Vestibular short-latency Evoked Potential

* Corresponding author. Brain and Mind Centre, The University of Sydney, 100 Mallett St. Camperdown, Sydney, NSW, 2050, Australia.
E-mail address: daniel.brown@sydney.edu.au (D.J. Brown).

https://doi.org/10.1016/j.heares.2018.01.013
0378-5955/

decerebrate state and lack of inhibitory feedback pathways, hence the explanation that the EVS may modulate peripheral afferent activity by a non-linear positive feedback mechanism (Plotnik et al., 2005). Experiments in the toadfish have demonstrated the EVS is activated during arousal, a behavior which precedes predatory movement in that species (Highstein and Baker, 1985), hence, the idea that the EVS may modify peripheral vestibular gain before or during specific activities. If the function of the EVS is somewhat specific to the behavioral requirements of an animal, it may explain the different vestibular efferent neuroanatomy and neurophysiology across species (Meredith, 1988).

It was originally hypothesized that the vestibular efferents send corollary discharges to the peripheral vestibular system to suppress afferent activity during active motions. However, whilst recent studies have shown that there is a strong corollary suppression of actively driven afferent throughput at the level of the vestibular nucleus (Cullen et al., 2011), this does not seem to occur in mammalian peripheral vestibular afferents (Cullen, 2012), unlike that of the amphibian species, Xenopus (Chagnaud et al., 2015). This suggests that the function of the mammalian vestibular efferents at the periphery is likely not involved with inhibitory silencing or distinguishing passive and active movements, but rather may be involved with slow adaptation and homeostasis. Recent research has demonstrated that mice lacking the α9-nAChR have impaired VOR adaptation (Hübner et al., 2015) and compensation (Hübner et al., 2017), further supporting this hypothesis.

Electrical stimulation of the efferent vestibular system has been used to study efferent-mediated effects on the peripheral vestibular afferents (Goldberg and Fernandez, 1980; Brichta and Goldberg, 2000), and experiments in mammals (Marlinski et al., 2004), toadfish (Boyle and Highstein, 1990; Boyle et al., 1991), frogs (Rossi et al., 1980; Bernard et al., 1985) and turtles (Brichta and Peterson, 1994; Holt et al., 2006) demonstrate the EVS plays an active role in modulating peripheral vestibular afferent activity. Specifically, in mammals, high-frequency shocks to the floor of the fourth ventricle result in both fast (10–100 ms) and slow (5–20 s) increases in spontaneous irregular afferent firing, and slow yet smaller regular primary afferent excitation (Goldberg and Fernandez, 1980; Goldberg, 2000). Results are not homogenous across species, and show mixed excitatory and inhibitory spontaneous afferent activity in frogs (Sugai et al., 1992) and turtles (Brichta and Goldberg, 1996) depending on neuroepithelial location (Holt et al., 2006). Moreover, electrical stimulation in the EVS region may potentially evoke antidromic stimulation of the vestibular afferents (Goldberg and Fernandez, 1980), which terminate in close proximity to, or indeed within the EVS nucleus (Ohgaki et al., 1988). Such antidromic effects may potentially confound any efferent-mediated effects. Presently, it is thought such antidromic affects occur secondary to efferent-mediated effects.

That high frequency electrical stimulation of the EVS is needed to modify afferent activity suggests the vestibular efferents may act as a high-pass filter, attenuating tonic low-frequency stimuli whilst amplifying phasic high-frequency information, which may function to rapidly modify peripheral vestibular gain during large dynamic stimuli (Holt et al., 2011).

Despite continued research, the functional role of the peripheral EVS remains elusive. We have attempted to further study the function of the EVS by electrically stimulating the efferent vestibular cell bodies at the floor of the fourth ventricle, whilst monitoring the VsEP, evoked by Bone-Conducted Vibration (BCV) in guinea pigs. This is analogous to the research undertaken in auditory physiology, with medial-olivocochlear (MOC) stimulation, whilst monitoring the acoustic Compound Action Potential (CAP) (Galambos, 1956; Gifford and Guinan, 1987). Since the VsEP is a measure of irregular jerk-sensitive afferent activity (Jones et al., 2011; Chihara et al., 2013), which primarily innervate the calyx/dimorphic units at the striola (Curthoys et al., 2006, 2016), we are solely interested in the efferent driven mechanisms of these irregular units. Based on the few studies available, and the known characteristics of efferent-mediated calyx/dimorphic excitation, we hypothesized EVS stimulation will result in VsEP suppression. This is supported by Goldberg and Fernandez (1980), who found that pairing fast efferent-mediated excitation with rotation, resulted in a modest reduction in the rotational gain of irregular vestibular afferents. Recordings in the turtle showed that canal duct indentation paired with an efferent-mediatedfast response resulted in a gain decrease (Holt, 2008), and Boyle and Highstein (1990) noticed an inhibition of the dynamically driven vestibular response during EVS stimulation. These results can be explained by a parallel-conductance model, whereby fast efferent responses cause large conductance increases at the efferent-afferent synapse, resulting in a decreased conductance of the main afferent terminal through electrical shunting (Holt et al., 2011). In this study, suppression of the VsEP by electrical stimulation of the central vestibular system at the floor of the fourth ventricle does not appear to rely on the activation of EVS neurons.

2. Materials and methods

2.1. Animal preparation & surgery

Experiments were performed on 15 adult tri-colored guinea pigs (*Cavia porcellus*), of either sex weighing between 200 and 600 g. All experimental procedures were approved by The University of Sydney Animal Ethics Committee (protocol #829). Animals received pre-anaesthetic intraperitoneal injections of Atropine Sulphate (0.6 mg/ml; Apex Laboratories, NSW, Australia), and were thereafter anaesthetized using either Ketamine (Ketamil, Ilium – 100 mg/kg) and Xylazine (Xylazil-20, Ilium – 4 mg/kg) (n = 6) or Isoflurane (IsoFlo - 2–4%) (n = 9). Animals anesthetized using Isoflurane received 0.05 ml intraperitoneal pre-anaesthetic injections of the analgesic Temgesic (Buprenorphreine Hydrochloride, 324 μg/ml; Reckitt Benckiser, Auckland, NZ). In experiments using Ketamine and Xylazine anesthesia, for the first 4 h animals received hourly injections of Ketamine and Xylazine at half the initial dose, delivered intramuscularly. Thereafter, animals received top up injections of only Ketamine (50 mg/kg) every 45 min. In both anaesthetic regimes, once sedated and lacking a foot-withdrawal reflex, animals were transferred to the surgical table to be tracheotomized and artificially ventilated with oxygen. Heart rate and blood oxygen saturation were continuously monitored throughout the experiment, and body temperature was maintained using a blanket and infrared heating pad (Kent Scientific, CT, USA).

The animal's head was mounted between custom-made ear bars, housing a canalphone speaker (ATH-IM70, Audio-Technica, Tokyo, Japan). A BCV vibration/modal shaker device was attached to the ipsilateral earbar in a lateral-medial orientation via a 5 cm metal rod, with an attached 3-axis accelerometer (bandpass: 0.02–6 kHz; TE Connectivity, Ch-8200, Switzerland) (Fig. 1). In the dorsal position, a small incision was made behind the pinna, removing musculature and exposing the dorsolateral bulla, so that a small window of bone could be removed (~2 mm^2), providing a clear view of the round window and facial nerve canal.

A Teflon-coated Ag/AgCl wire with the tip exposed was used as a non-inverting electrode, and was either inserted onto the round window niche, or 3 mm into the facial nerve canal. A bare Ag/AgCl wire inserted into the neck musculature served as the inverting electrode. The animal was grounded via a low-resistance Ag/AgCl electrode placed in the nape of the neck.

For most experiments where the focus was on VsEP recordings,

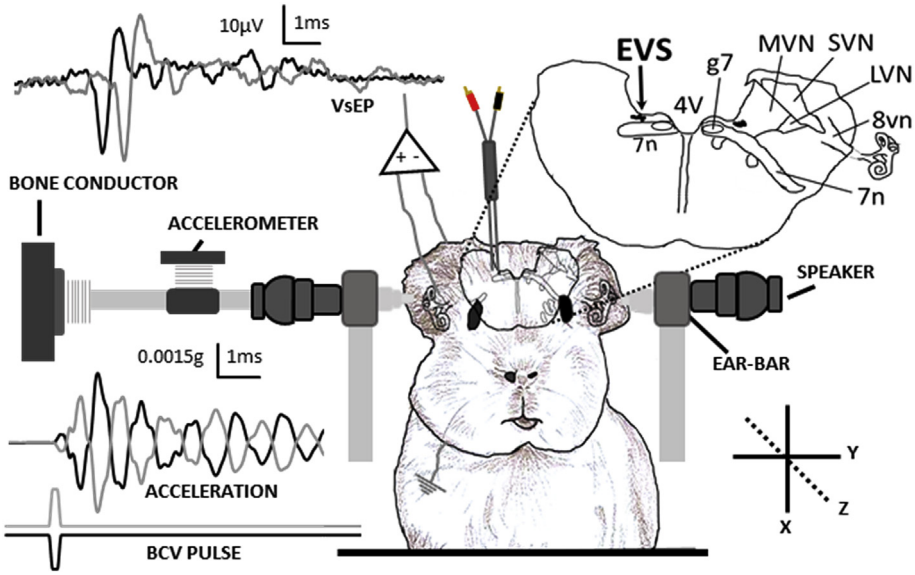

Fig. 1. Schematic diagram of the experimental preparation. Animal is secured between custom-made ear bars housing an ipsilateral and contralateral speaker, and a bolt connecting both a 3-axis accelerometer and a bone-conductor on the ipsilateral recording side. BCV pulse command voltages are shown with associated acceleration (bottom left), and VsEP waveforms (top middle), averaged 100 times. A schematic diagram of the guinea pig brainstem with key regions labelled (top right; adapted from Motts et al., 2008), with our stimulation location and the EVS highlighted in bold. Abbreviations: EVS: Efferent Vestibular System, 4V: 4th ventricle; g7: Facial nerve genu; 7n: 7th cranial nerve; 8vn: Vestibular branch of 8th cranial nerve; LVN: Lateral Vestibular Nucleus; MVN: Medial Vestibular Nucleus; SVN: Superior Vestibular Nucleus. Animal #523.

subsequent to recordings of the CAP from the round window, the cochlea was surgically destroyed with the use of a surgical pick. However, in select experiments the VsEP was recorded with the cochlea intact, but with constant acoustic masking noise presented to both ears to suppress cochlear responses.

2.2. Stimuli & recordings

Stimuli and responses were generated and recorded using custom-developed LabVIEW (National Instruments, TX, USA) programs. BCV, auditory and shock stimuli were generated using an external soundcard (SoundblasterX7, Creative Inc., Singapore). Analogue responses were amplified by 60 dB (×1000), with a 1 Hz to 10 kHz band-pass filter (IsoDAM 8, WPI, Florida USA) before being digitized at 40 kHz, 16 bit, using an analogue to digital converter (NI 9205, National Instruments, TX, USA). Responses were acquired by triggered averaging, with between 40 and 100 presentations per averaged response. The VsEP was evoked by a 0.6 ms Gaussian monophasic BCV-pulse. The auditory CAP was evoked by a 0.1 ms click approximately 10–20 dB above visual detection threshold.

2.3. EVS exposure & electrical stimulation

A small incision was made between the caudal edge of the occipital bone and lambda, where a posterior craniotomy was undertaken, and the dura mater cut. A small section of cerebellum was aspirated to expose the floor of the fourth ventricle. Fluid build-up within the opening was controlled with tissue wicks adjacent to the brainstem region of interest. For brainstem stimulation, a pair of tungsten bipolar electrodes (0.61 mm diameter) coated with parylene-C insulation up to the very tips, with a 250 µm tip separation and 1.0 MΩ impedance were used (Microprobes, MD, USA).

Crossed olivocochlear bundle (COCB) stimulation was always performed prior to cochlear destruction as a control to confirm our set up was working, and to localize the lateral-medial plane of the efferent fibers for subsequent vestibular efferent stimulation. The electrodes were directed to the region of interest at the floor of the fourth ventricle using a micromanipulator and generally orientated in the naso-occipital plane under the guidance of a surgical microscope. For COCB stimulation electrodes were positioned superficially (~0.2–0.4 mm depth) at the midline, at the region most sensitive for generating eye and whisker twitches. After the confirmation of a COCB effect, the cochlea was ablated with a sharp metal pick, whilst preserving the vestibular sensory regions.

For EVS stimulation, electrode placement was based on guinea pig stereotaxic map coordinates (Rapisarda and Bacchelli, 1977; Voitenko and Marlinsky, 1993) and guinea pig EVS immunohistochemistry studies (Strutz, 1982; Motts et al., 2008). Placement of the bipolar electrodes was on the same lateral-medial plane as the COCB, and lateral of the facial nerve genu beneath the sulcus limitans, approximately 1 mm lateral of the midline. Low threshold facial twitches likely meant we were stimulating the facial nerve genu or abducens nucleus, and therefore minor dorsolateral electrode repositioning was required. Final placement of the bipolar electrodes was determined by the maximal physiological effect on the VsEP with the lowest shock level, which was always approximately 1 mm lateral of the midline, dorso-lateral of the facial nerve genu, at the sulcus limitans (Fig. 13A), consistent with the location of the vestibular efferent cell bodies in previous studies (Strutz, 1982; Shumilina et al., 1986; Motts et al., 2008). Shocks were delivered to the animal via a bi-phasic isolated current stimulator (Model DS4, Digitimer Ltd., UK). The effect of shocks on both the CAP and the VsEP were produced using two different stimulation protocols (Fig. 2). Protocol A or 'Train ES' involved presenting the CAP or VsEP stimulus shortly after a 100 ms electrical pulse train, with the following pulse stimulation parameters: 100µs biphasic pulse width, 50–400 pulses per second, 0–920 µA, 120 ms interstimulus interval. Protocol B or 'Paired ES' involved presenting the CAP or VsEP stimulus in between individual electrical pulses (Fig. 2), which were presented at rates between 1 and 250 pulses per second. The BCV-pulse delay after the initial current pulse varied between 0 and 11ms. Note that the stimulus was not presented between every shock, but rather every second shock, which

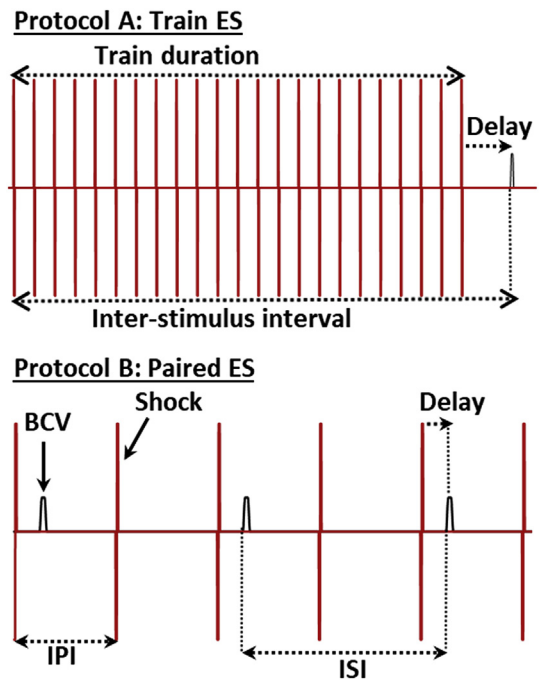

Fig. 2. An illustration of the two-different electrical stimulation (ES) paradigms used in this study. Protocol A, or 'Train ES' was used to visualize the effect of a 100 ms shock train on the VsEP evoked *after* the train. Protocol B, or 'Paired ES' was used to view changes in the VsEP evoked *during* a shock train. For the Paired ES paradigm BCV stimuli were presented every second current pulse, and a subtraction technique was used to remove the ES artifact from VsEP responses. Abbreviations: ES: Electrical stimulation, IPI: Inter-pulse interval, ISI: Inter-stimulus interval.

allowed us to record the electrical artifact with or without a response, and subtract the electrical artifact from the CAP or VsEP response waveform, leaving the averaged evoked response (Fig. 7).

2.4. Drug perfusion & EVS lesion

In selected animals, the nicotinic acetylcholine receptor antagonist Strychnine Hydrochloride (1 mM; abcam, VIC, AUS) or agonist 1,1-Dimethyl-4-phenylpiperazinium iodide (DMPP; 20 mM; Sigma Aldrich, NSW, AUS), were given with an aim to block the peripheral vestibular efferent receptors. Strychnine was delivered via intraperitoneal injection at 10 mg/kg as per previous studies (Rajan, 1988; Maison et al., 2007) To confirm the drug was passing the blood-labyrinth barrier and having a physiological effect on the nicotinic acetylcholine receptors, crossed-olivocochlear bundle fibers were stimulated at the midline floor of the fourth ventricle, whilst monitoring the level of suppression of auditory nerve CAP in 3 animals. After confirming an effect, the waveshape and absolute peak-peak amplitude of the VsEP was longitudinally monitored with and without current shocks. In 4 ears, ~0.5 ml DMPP was flooded into the intra-tympanic space, and thereafter the VsEP waveshape and peak-peak amplitude was monitored with and without current shocks for up to 4 h after drug delivery. For DMPP delivery the cochlea was ablated, providing a localized drug administration to the vestibular end-organ, to best replicate previous ex vivo bath perfusions (Holt et al., 2015).

To lesion the neurons at the site of stimulation, DC current between 500 and 730 μA was delivered to the EVS region via the stimulation electrodes, for 2 min.

2.5. Histology

At the end of experiments involving electrolytic lesions of the EVS region, animals were deeply anesthetized with 5% Isoflurane, and thereafter transcardially perfused with 0.1 M Sorenson's Buffer (pH = 7.4), followed by 4% Paraformaldehyde fixative solution. Brains were removed and stored for 24–48 h in fixative at 4 °C, followed by 30% sucrose for 72 h at the same temperature. Serial transverse sections were cut using a cryostat (Leica CM1860) at 20 μm thickness, mounted on gel-coated slides, stained with 0.5% Toluidine Blue, and cover slipped.

3. Results

3.1. The VsEP

With the cochlea intact, VsEPs could be recorded with or without acoustic masking noise (Fig. 3). Without acoustic noise, there were several waveform peaks with a latency greater than 1 ms (Fig. 3). In some instances, with masking noise (approximately 95–110 dB SPL white noise), the VsEP response was very similar to that recorded after the cochlea had been ablated (see Fig. 3A vs. 5B), and there were no artifacts within the response, which was completely abolished after death (Fig. 3B). It should be noted that the BCV stimulus did not generate a simple acceleration of the skull, but rather a brief, high-frequency oscillation (Fig. 3C), and yet regardless the VsEP is a relatively simple biphasic waveform, with

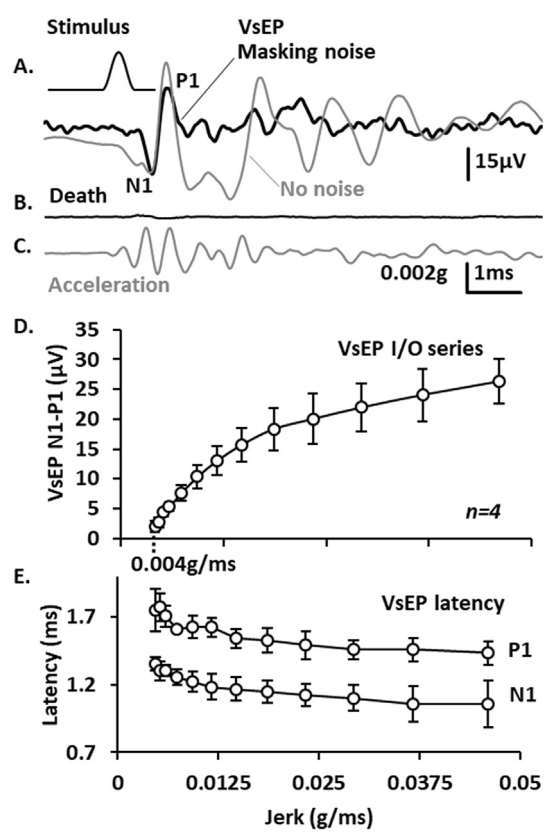

Fig. 3. A) A typical VsEP response, shown with (black) or without (grey) broadband acoustic masking noise. The BCV stimulus is shown at the top left. The latency of the VsEP N1 or P1 was measured relative to the start of the BCV pulse. B) The response following death of the animal. C) The acceleration response. Animal#726. D) A VsEP Input/Output series averaged across 4 animals. Average jerk threshold is displayed beneath the x-axis. E. VsEP N1 and P1 latencies corresponding to IO series in D. 100 averages.

an N1 and P1 peak. The VsEP amplitude increased gradually with BCV level, but when plotted against stimulus jerk (calculated from the ear-bar acceleration), the VsEP amplitude increased non-linearly (Fig. 3D; average of 4 animals), and the N1 and P1 latency (relative to the start of the BCV pulse) decreased gradually by 0.35 ms (Fig. 3E). The average VsEP jerk threshold across these 4 animals was 0.004 g/ms (Fig. 3D). Within this study, we used 0.02 g/ms BCV stimulus level to evoke a 'typical' or baseline VsEP response.

3.2. Electrical stimulation

Electrical stimulation of the EVS produced a suppression of the VsEP response, with the level of suppression dependent upon several factors such as the current strength, the delay between the current pulse and the BCV pulse, the rate of electrical stimulation, and the rate of BCV stimulation. Here, we detail the features of the VsEP suppression with electrical stimulation.

3.2.1. Effect of cochlea ablation on the VsEP suppression

The VsEP recorded with the cochlea intact (during acoustic masking noise) was suppressed by a similar magnitude to that when the cochlea was ablated (Fig. 4A and B). Note that with the cochlea intact, there was larger variability in the VsEP amplitude (Fig. 4B), due mostly to the additional noisy cochlear microphonic from the acoustic masking noise (Fig. 4B). Ablating the cochlea did not have significant effects on the ES artifact, nor the immediately following components of the electrically evoked response recorded from the facial nerve canal (Fig. 4C).

3.2.2. Train ES suppression of the VsEP

Following a 100 ms train of current pulse stimulation in the presumed EVS nucleus, the VsEP, evoked shortly after the last pulse, was suppressed. The level of VsEP suppression depended on parameters such as the shock intensity (Fig. 5A), the BCV delay after the shock (Fig. 5B–D), and the rate of the current pulses (Fig. 5C and D). Interestingly, with a lower shock rate of 50 pulses per second (pps), as compared to 300pps, there was a larger suppression of the VsEP when it was evoked shortly after the last current pulse (<4 ms). With a longer VsEP delay (>4 ms), higher current pulse rates produced a slightly larger suppression of the VsEP (Fig. 5C and D).

In addition to the immediate suppression of the VsEP following a train of current pulses, gradual accumulative effects of repetitive Train ES stimulation were observed, particularly when intense current pulses (>900 μA) were used, and these were more obvious with a longer delay (>10 ms) of the VsEP following the pulse train. An example of the accumulative effects are shown in Fig. 6, where the VsEP evoked within a Train ES stimulus was monitored over 1 h, with the current stimulation (920 μA, 300 pps) switched on or off for 5–8 min. At the onset of the current stimulation, the VsEP gradually declined in amplitude over 2–3 min, and likewise gradually increased when the electrical stimulation was switched off.

3.2.3. Paired ES suppression of the VsEP

Given the VsEP suppression occurred with low rates of electrical stimulation, and with a short delay following the last current pulse, we examined VsEP suppression using the Paired-ES protocol. An example of how the VsEP was recorded with the Paired-ES protocol is shown in Fig. 7. Current pulses produced a relatively large artifact (or response) on the facial nerve recording, which dominated the VsEP response when it was evoked 1–10 ms later. However, by subtracting the artifact obtained when no BCV stimulus was presented, we obtained a relatively 'clean' VsEP response. This was the case regardless of the level (or presence) of the electrical shocks.

With the Paired-ES protocol, VsEP suppression was dependent upon shock intensity (Fig. 8A, B & C), with more than 60% suppression above 300 μA. Increasing the current intensity had no effect on the VsEP N1 latency (Fig. 8C). Similar to the results obtained using the Train-ES protocol, the level of VsEP suppression varied with the delay between the current pulse and the BCV stimulus (Fig. 8D). The level of VsEP suppression was greatest (58%) immediately after a shock pulse (~0.5–1 ms) and decayed to zero suppression with a 10 ms delay (Fig. 8D). Factoring in a compensation for the latency shift due to changes in the BCV stimulus delay, the VsEP latency was unchanged during the suppression (Fig. 8C and D). In addition to the immediate suppressive effects of the electrical stimulation, there was a rate-dependent, accumulative decay of the VsEP suppression, which was absent at low current levels (<80pps), but present for rates >100 pps (Fig. 9A and B).

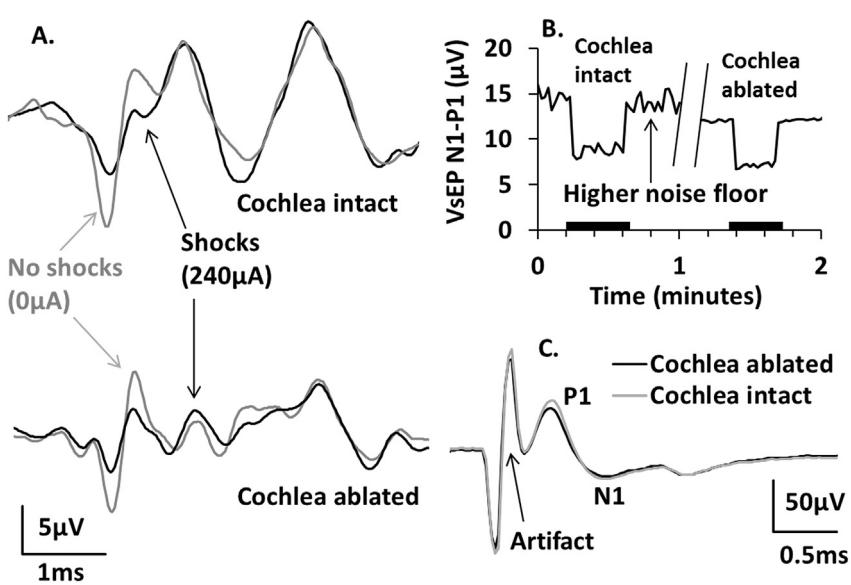

Fig. 4. A) ES suppressed the VsEP with the cochlea intact and surgically destroyed. B) VsEP pk-pk amplitudes with the cochlear intact using masking noise and after cochlea ablation. C) Artifact and components of the electrically evoked response recorded from the facial nerve canal before and after cochlear removal. Animal#1108, 100 averages.

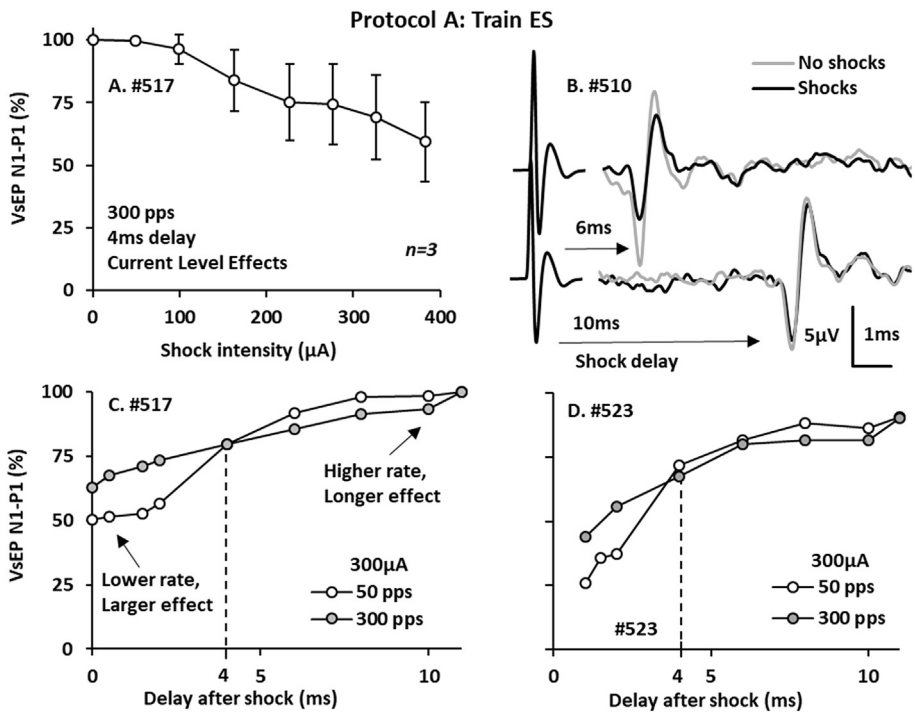

Fig. 5. A) Current level effects during Train ES presented at 300 pps with a 4 ms delay across 3 animals. B) VsEPs recorded with the cochlea ablated either during (black trace) or without (grey trace) Train ES presented at 255 µA with a 6 ms (top) and 10 ms (bottom) delay. 100 averages. Animal#510. C), D) High (300pps) vs. low (50 pps) Train ES effects on the VsEP with delay across two animals, #517 and #523.100 averages.

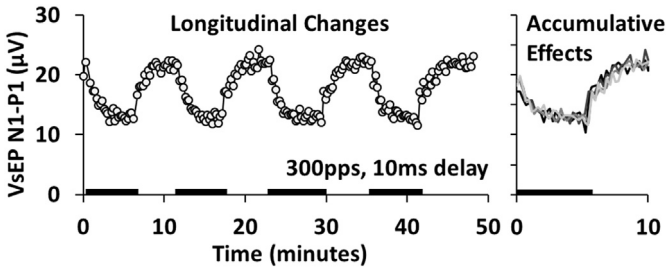

Fig. 6. Longitudinal fluctuations in the VsEP during Train ES presented at 300 pps, during high shock levels (920 µA) with a 10 ms delay (left). Turning off the shocks results in an inverse time-dependent recovery of the VsEP back to baseline, with similar kinetics. All four decay and recovery time sequences overlaid (right). 100 averages. Animal#502.

Electrical stimulation in the EVS region did not noticeably change the waveshape of the VsEP, but rather caused a simple reduction in the peak to peak amplitude (Fig. 10A and D). Without electrical stimulation, the VsEP amplitude increased non-linearly with jerk level (Fig. 10B, E). During Paired-ES, the slope of the VsEP growth function decreased, however the threshold remained constant (Fig. 10B and E). Importantly, whilst the VsEP latency decreased with increasing jerk levels (Figs. 10C, F & 11), the latency did not change with increasing levels of ES induced suppression (Fig. 11).

3.3. Electrode placement & histology

Suppression of the VsEP with electrical stimulation in the brainstem was only observed with stimulation at a small ipsilateral region at the floor of the fourth ventricle, lateral of the facial nerve genu (Fig. 12 A, B & C). Contralateral and midline stimulation at any stimulus rate or level did not affect the VsEP (Fig. 12A).

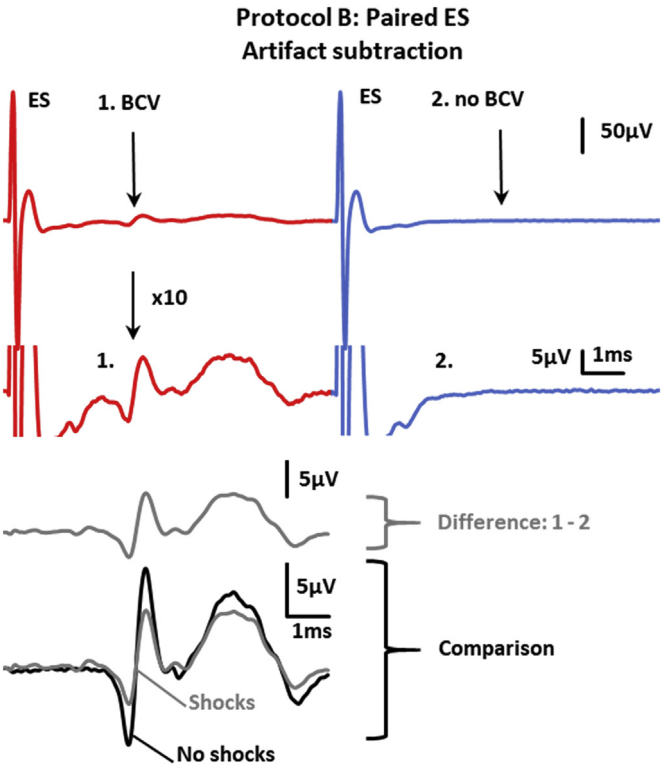

Fig. 7. Illustration of the artifact subtraction technique used in the Paired ES protocol. The response to an ES pulse with a BCV stimulus (red) was subtracted from the response of an ES pulse without a BCV stimulus (blue), leaving the VsEP without any artifact (grey). 100 averages. Animal#510. (For interpretation of the references to color in this figure legend, the reader is referred to the Web version of this article.)

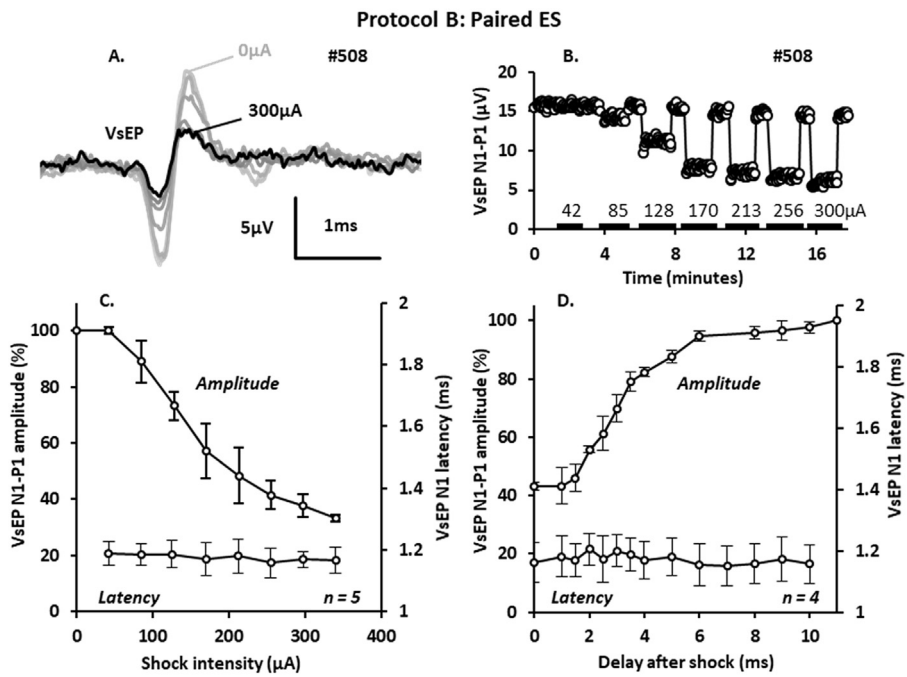

Fig. 8. A) VsEPs recorded to Paired ES shock intensities from 0 to 300 μA. B) Time chart detailing changes in VsEP N1-P1 amplitude with increasing shock intensities, corresponding to waveforms shown in A. 100 averages. Animal#508. C) Current level effects on the VsEP N1-P1 amplitude and N1 latency, across 5 animals. D) Effect of aftershock delay on the VsEP amplitude and latency, across 4 animals.

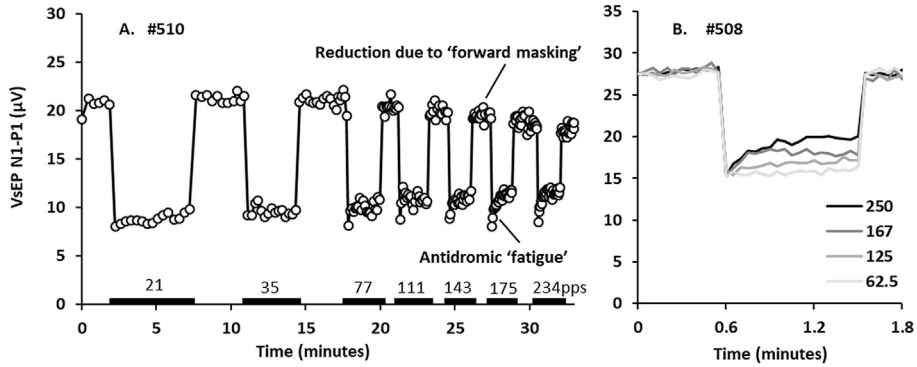

Fig. 9. Time chart demonstrating rate dependent changes in the VsEP suppression during Paired ES. A) Time chart showing the effect of increasing Paired ES shock rates on the VsEP N1-P1 amplitude. Animal#510.100 averages. B) Time sequences showing VsEP N1-P1 amplitude overlaid across four shock rates in animal #508.

Furthermore, low level (27 μA) ipsilateral stimulation, which was below the threshold for suppressing the VsEP, failed to have an effect in any animals, even when electrical stimulation was maintained for several minutes (data not shown). Minimal suppression was observed at the approximate location of the facial nerve genu and abducens nucleus, which was the most sensitive region for evoking facial and whisker twitches. Although the VsEP suppression was consistently localized to a small region across all animals, smaller effects were observed within 0.25–0.5 mm of this area (Fig. 12A, B & C). Fig. 12C shows that maximal VsEP suppression was obtained at a depth corresponding to the position of the EVS cell bodies (±0.2 mm), lateral of the facial nerve genu at the floor of the fourth ventricle.

A transverse section of the guinea pig brainstem stained with Toluidine blue indicates the position of the stimulating electrode pair (arrow), dorsolateral of the facial nerve genu (VII) (Fig. 13). This marked location corresponded to the most sensitive position for VsEP suppression in this animal (GP#630).

3.4. Effect of nAChR drugs & lesioning EVS

Prior to removal of the cochlea, suppression of a click-evoked CAP induced by electrical stimulation at the midline, using the Train-ES protocol, was observed (Fig. 14 A & 14B). Across 3 animals, electrical stimulation of the midline floor of the fourth ventricle resulted in the normalized CAP N1-P1 average amplitude being suppressed by 26.62% (±5.35). After approximately 30 min following an intraperitoneal injection of 10 mg/kg of Strychnine Hydrochloride the normalized CAP suppression reduced to 7.25% (±6.74) ($p < 0.001$, $\alpha = 0.05$, $n = 3$, Welch's *t*-test; Fig. 14A). An example of the CAP suppression with midline Train-ES is provided in Fig. 14B. This suppression or 'MOCs effect' was subsequently blocked after an I.P. injection of Strychnine (50 averages, GP#118).

Whilst Strychnine blocked the CAP ES suppression, it failed to block the 200pps Paired-ES evoked suppression of the VsEP ($p = 0.791$, $\alpha = 0.05$, $n = 5$, Student's t-test, Fig. 14A). Likewise, 10 min after 20 mM DMPP had been applied to the bulla (flooding

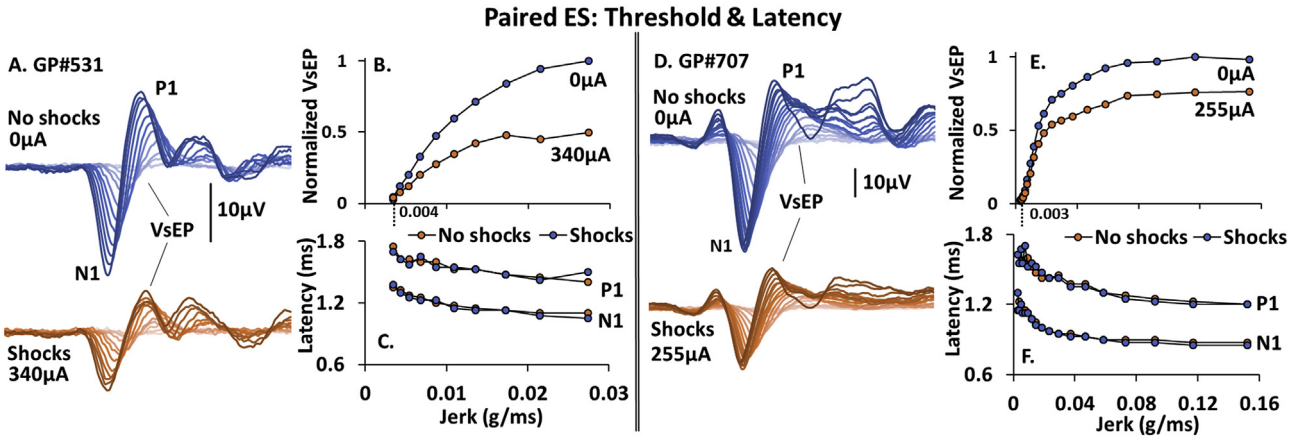

Fig. 10. A) Averaged VsEPs recorded at increasing BCV stimulus levels without (top) and during (bottom) 340 μA paired ES, in animal #531. B) VsEP I/O series corresponding to the waveforms presented in Fig. 9A. C) VsEP N1 and P1 latency corresponding to the I/O series in Fig. 9B. D) Averaged VsEPs recorded at increasing BCV stimulus levels without (top) and during (bottom) 255 μA ES, in animal #707. E) VsEP I/O series corresponding to the waveforms presented in Fig. 9D. F) VsEP N1 and P1 latency corresponding to the I/O series in Fig. 9E.

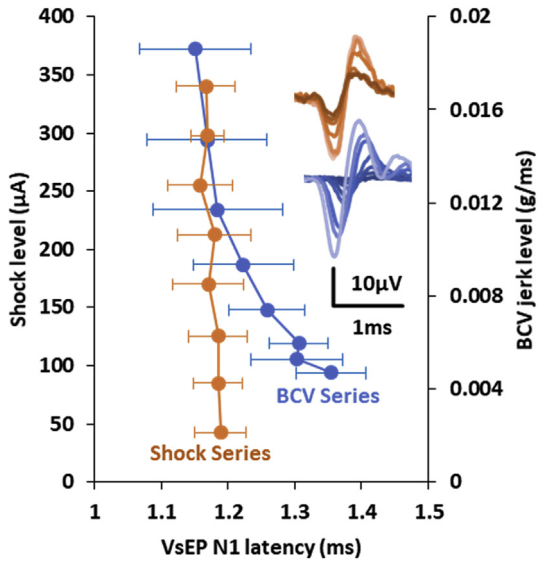

Fig. 11. Effect of increasing BCV level (blue) and ES shock intensity (red) on the VsEP N1 latency, across 4 animals. Averaged VsEP waveforms associated with changes, in two different animals. 100 averages. (For interpretation of the references to color in this figure legend, the reader is referred to the Web version of this article.)

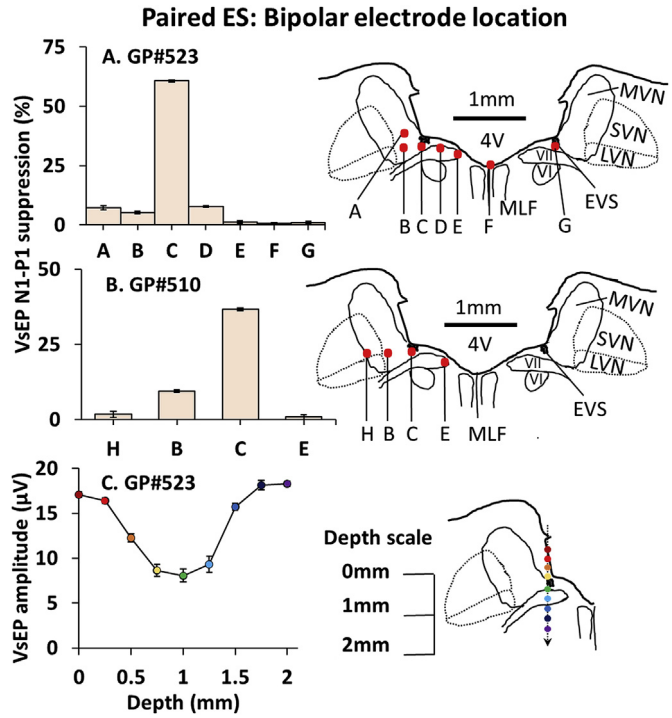

Fig. 12. Effect of Paired ES with changes in electrode placement. A), B) Level of VsEP suppression as a percentage corresponding to the approximate electrode placements (A–H) represented in the schematic diagrams, in animals, GP#523 and GP#510. C) The effect of stimulating electrode depth on the VsEP suppression, corresponding to the colored dots on the schematic diagram, in Animal GP#523. The position of the EVS is schematically represented by the cluster of black dots, dorsolateral of the facial nerve genu, under the sulcus limitans, adapted from previous immunohistochemistry studies in the guinea pig (Strutz, 1982; Shumilina et al., 1986; Motts et al., 2008).

the bulla after removal of the cochlea), there was no change in the electrically evoked suppression of the VsEP ($p = 0.079$, $\alpha = 0.05$, $n = 4$, Student's t-test, Fig. 14A).

At the end of several experiments, an electrolytic lesion was made at the EVS region, which resulted in an irreversible blockade of the suppression effects ($p < 0.001$, $\alpha = 0.05$, Welch's *t*-test, $n = 4$; Fig. 14A). In two animals, the EVS region was surgically aspirated as an alternative to electrolytic lesioning, and this also blocked the VsEP suppression, but it also caused a slight reduction in the amplitude of the P1 peak of the VsEP.

3.5. Characterization of the antidromic eCAP P1-N1

In most animals, electrical stimulation in the EVS region without BCV stimuli evoked not only an electrical artifact on the facial nerve recording, but a P1-N1 waveform immediately following the artifact, which we have termed here an electrically evoked Compound Action Potential (eCAP) P1-N1 (Fig. 15A and D). This response was not present when electrically stimulating regions just off the EVS area, even though the electrical artifact was still present. The eCAP amplitude increased non-linearly with increasing shock intensities above 80 μA (Fig. 15D and E), which was approximately the threshold for electrical suppression of the VsEP (Fig. 8C). Conversely, the electrical shock artifact increased linearly with current level (Fig. 15E). We then examined changes in the eCAP

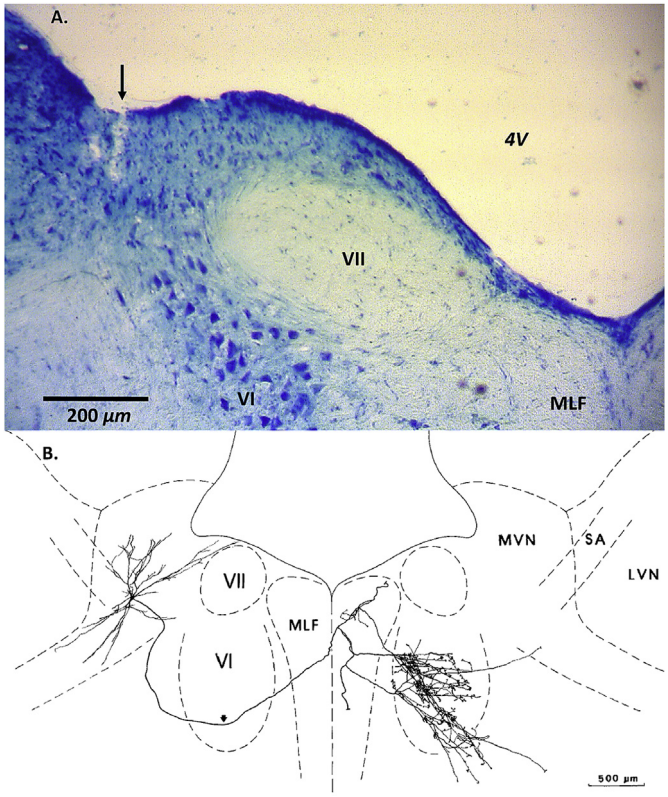

Fig. 13. A) Photograph of a transverse guinea pig brainstem section showing the position of our stimulating electrode pair at the floor of the fourth ventricle, dorso-lateral of the facial nerve genu. MLF: Medial Longitudinal Fasciculus; VI: Abducens nucleus; VII: Facial nerve genu; 4V: Fourth ventricle. Scale bar: 200 μm. Animal#630. B) A frontal section of the cat brainstem at approximately the same location as we used for efferent stimulation in the guinea pig (see A). To show the location of the efferent vestibular cells bodies with respect to the medial vestibular nucleus. One single MVN neuron has been stained by HRP and reconstructed. The dendrites of this MVN neuron extend close to and possibly even into the region of the efferent cell-bodies. Incoming axons of afferent neurons terminate on the dendrites of this MVN neuron. Given this apparent proximity, it is likely that a stimulating electrode in the area of the efferent cells will antidromically activate axons of vestibular afferent neurons. Reproduced with permission of Ohgaki et al. (1988).

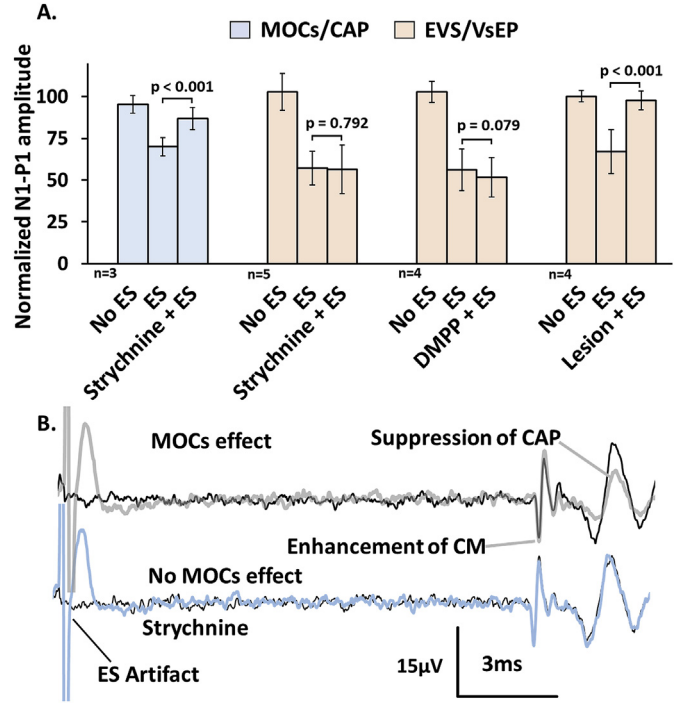

Fig. 14. A): Bar plots showing the effect of pharmacological agents (Strychnine and DMPP) and an electrolytic lesion on the normalized N1-P1 amplitude of either the CAP (blue) or VsEP (orange) across animals. B) Effect of intraperitoneal Strychnine on the MOCs mediated suppression of the acoustic CAP. GP#1108, 50 averages. (For interpretation of the references to color in this figure legend, the reader is referred to the Web version of this article.)

response with increasing stimulation rates, to observe the effect of a preceding current pulse on the eCAP. Like the electrically evoked suppression of the VsEP, the eCAP amplitude decreased when it occurred less than 10 ms following a preceding current pulse, and the level of suppression increased as the delay was further reduced (Figs. 15B and 16B).

4. Discussion

Our results show that the VsEP was suppressed by electrical stimulation in a brainstem region corresponding to the EVS cell bodies, or 'group e' (Strutz, 1982; Shumilina et al., 1986; Motts et al., 2008). A single current pulse was sufficient to suppress the VsEP amplitude by 50% when the VsEP was presented shortly after (<2 ms) the ES pulse. The level of suppression declined as the BCV stimulus was delayed from the ES pulse, such that there was little suppression with a 10 ms delay. Whilst it is tempting to suggest that the VsEP suppression may be mediated via an effect of the EVS on the sensitivity of the peripheral vestibular afferent neurons underlying the VsEP, we failed to block the suppression effect with pharmacological agents known to block vestibular efferent action in the periphery (Holt et al., 2015). Moreover, that the VsEP suppression was immediate seems at odds with the previously observed effects of electrical stimulation of the EVS on single-unit recordings (Goldberg and Fernandez, 1980), where changes in afferent firing rate were induced 10 ms after electrical stimulation. Additionally, we assume that any action of the EVS on the vestibular afferent neurons would involve, at the very least, both a transmission and a synaptic delay at the efferent-afferent synapse in the periphery, which is likely to delay any effects by 1 ms–4 ms, yet we observed suppression effects occurring with a delay shorter than this. Ultimately, as detailed below, our results suggest the suppression is due to the electrical stimulation generating antidromic action potentials in primary vestibular afferent neurons that then blocks the normal transmission in the same neurons. Goldberg and Fernandez (1980) also reported antidromic collisions in 10 out of the 27 animals, however, this occurred in only a small proportion of the population of their recorded units. It nonetheless demonstrates that electrical stimulation at the site of the mammalian EVS will result in antidromic stimulation in some proportion of the primary vestibular afferents. This antidromic effect may be more apparent when using the VsEP as a measure of afferent activity, rather than single units, because the VsEP represents the response of a larger population of afferent neurons, such as the effects observed in cochlear afferent responses observed by Brown (1994,

Brown (1994) evoked antidromic action potentials on the cochlear nerve by direct stimulation in the cochlear nucleus region of the brainstem, and measured an 'antidromic CAP (ACAP) field potential from the cochlear fluids, which appeared as an inverted version of the orthodromic CAP. Experiments performed with temporally separated pairs of either two electrical shocks, or an acoustic click and a shock, were used to determine the refractory characteristics of the auditory nerve. Results indicated that the ACAP directly interfered with the orthodromic CAP. Brown (1994) did not rule out an ACAP contribution from sources other than

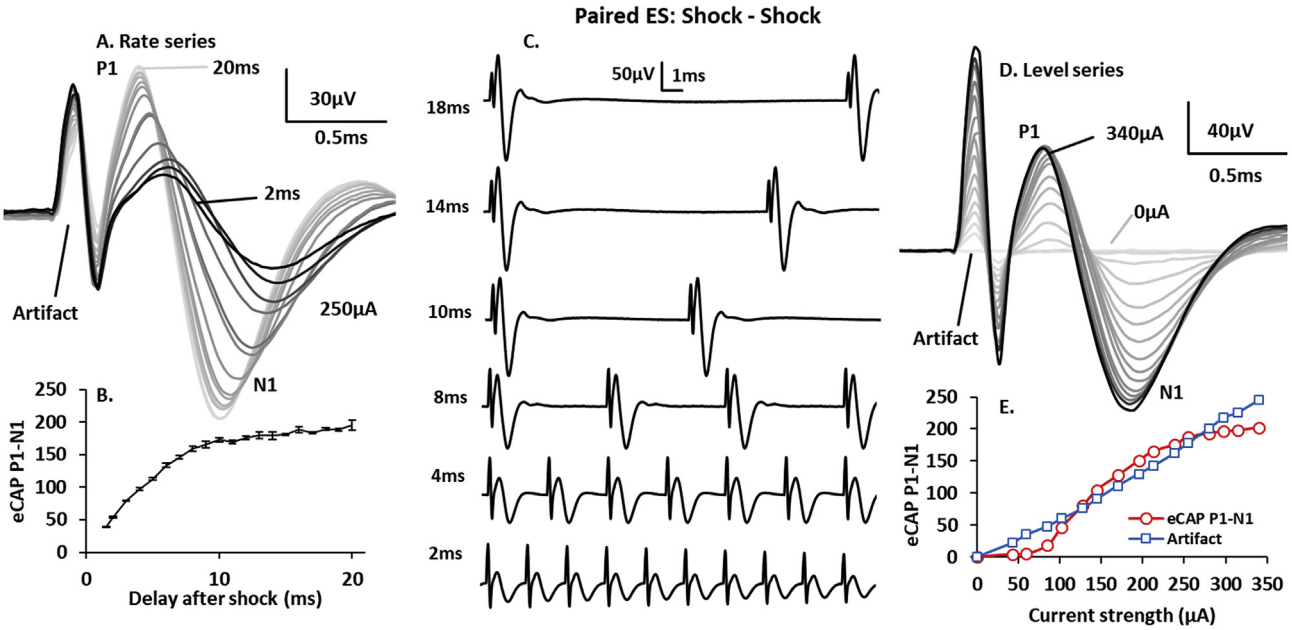

Fig. 15. A) Rate effects on the P1-N1 waveform whilst changing the inter-shock interval (20-2 ms). B) The relationship between P1-N1 amplitude and inter-shock delay (0–20 ms). Error bar standard deviation is across 3 recordings in the same animal. All recordings in Animal#602. C) Individual recordings (20 ms segments) corresponding to the effects shown in A. D) Effect of changing the ES intensity from 0 to 340 µA on the P1-N1 waveform at a 20 ms delay. E) Relationship between eCAPP1-N1 and artifact amplitude and current level.

type I auditory neurons, such as the cochlear nucleus, or even the larger diameter, lower threshold vestibular nerve fibers. There is an important distinction between Brown (1994) and our work, in that his stimulation site was at the cochlear nucleus which was distant from the cochlear efferent cell bodies at the superior olivary complex and their associated axons at the midline floor of the fourth ventricle. Conversely, our stimulating array was positioned lateral of the facial nerve genu at the EVS (Fig. 12A), which is in close proximity to the neighboring MVN (Strutz, 1982; Motts et al., 2008). Furthermore, the dendrites from the mammalian MVN, which receive primary afferent input, have been shown to extend into this lateral region of the facial nerve genu (Fig. 12B) where the EVS cell bodies innervate (Ohgaki et al., 1988).

In our experiments, the suppression of the VsEP was greatest when the VsEP was evoked shortly (<4 ms) after the electrical stimulation. With a short delay between the current pulse and the BCV, lower stimulation rates (50 pps) resulted in a greater suppression than higher rates (300 pps; Figs. 5 and 9), suggesting that the mechanism underlying the VsEP suppression adapts or fatigues with high-rate electrical stimulation, similar to mechanisms described in previous studies where there was a supposed antidromic blockade of orthodromic activity (Baertschi and Dreifuss, 1979). These effects likely reflect a reduction in the number of antidromic action potentials that are generated by the ES pulse in the brainstem, at high stimulation rates. Importantly, this decline in the level of suppression during high-rate (>100pps) ES was not affected by DMPP (Fig. 14A).

In addition to the above adaptation of the VsEP suppression during high-rate ES stimulation, during Paired-ES there was a subtle reduction in VsEP amplitude in the absence of shocks. This subtle decline was dependent on pulse rate, arising around 77pps (Fig. 9A). Given that previous studies in the squirrel monkey (Goldberg and Fernandez, 1980) and chinchilla (Marlinski et al., 2004) observed larger efferent-mediated effects on primary vestibular afferents with higher pulse rates, it is tempting to suggest that this rate-dependent reduction in VsEP amplitude, is mediated by the EVS. However, like the cochlear CAP, the VsEP does 'forward mask' (Jones et al., 2002), with increasing inter-stimulus intervals, resulting in a subtle reduction of N1-P1 amplitude. In the 'Paired-ES' protocol (Fig. 2 – Protocol B), the inter-stimulus interval (ISI) is dependent on the ES pulse rate, such that a high pulse rate results in a shorter ISI. The VsEP amplitude in the absence of ES begins to decline at 77pps (Fig. 9A), which is equivalent to an ISI of 12 ms, and is consistent with the subtle 'forward-masking' effect of the VsEP occurring independent of electrical stimulation (Jones et al., 2002). Moreover, this rate-dependent decline in VsEP amplitude without ES was not abolished after longitudinal monitoring following the local administration of 20 mM DMPP into the bulla, which has been shown to block calyx-dimorphic efferent-mediated excitation in the turtle (Holt et al., 2015).

The gradual suppression of the VsEP (Fig. 6) required intense ES shock amplitudes (>900 µA), much larger than the levels previously used to stimulate the EVS (Goldberg and Fernandez, 1980; Marlinski et al., 2004). It should be noted that this effect was only observed using high pulse rates, and when the delay between the electrical stimulation and the BCV pulse was 10 ms or greater. Moreover, this longitudinal effect was always associated with a poor 'immediate' suppression of the VsEP, suggesting that the electrode pair may not have been in the immediate vicinity of the EVS, and that the gradual suppressive effect was likely due to electrotonic spread of the current pulses to the EVS and MVN. This was confirmed in several experiments where the electrode pair was intentionally placed outside of the most sensitive area for evoking the VsEP suppression - here high current levels induced a gradual suppressive effect. Additionally, this effect persisted after DMPP and Atropine treatment, further suggesting it was not mediated by the EVS.

During the electrical stimulation induced suppression, the VsEP waveform did not change, nor did its latency shift, but rather there was a simple reduction in VsEP amplitude (Fig. 10A, D). Importantly, whilst the VsEP latency decreased with increasing BCV stimulus levels (Figs. 10C, F & 11), latency did not change with electrical induced suppression (Fig. 11). Moreover, the slope of the VsEP growth curve decreased during electrical stimulation, but response

threshold did not change (Fig. 10B, E). Had the electrical stimulation been affecting the sensitivity of the vestibular periphery (i.e. had it been affecting either hair cell or afferent conductances upstream of the spike encoder, we would assume that VsEP latency and threshold would change. Our results therefore suggest that electrical stimulation was merely acting on post-synaptic generation of the afferent action potential. Interestingly, Brown (1994) observed a small but significant decrease in the CAP latency, in addition to a large amplitude suppression, when stimulating the proximal end of the cochlear afferent nerve, which suggests that factors other than antidromic blockage of afferent responses may have occurred in that study. The exponential suppression of the VsEP amplitude as the delay between the shock and the BCV pulse are reduced (Fig. 8D) is consistent with the forward-masking or refractory characteristics of the VsEP. This is demonstrated when the electrical shock is replaced by a BCV pulse in a "BCV-BCV" stimulation paradigm (Fig. 16A). The changes in the amplitude of the VsEP in response to the second BCV pulse (Fig. 16B) show a similar relationship to that of the Paired-ES paradigm (Fig. 8D), decreasing gradually with delay. There were additional complex changes in the VsEP amplitude with the BCV-BCV protocol, which we have attributed to a complex interaction of the skull-vibration to paired BCV pulses, because the skull can vibrate for several milliseconds. That is, there were vibration-related interactions between the two BCV pulses that caused additional changes to the amplitude of the second VsEP response, that add to the forward-masking or refractory effects which dominate the reduction in the VsEP response.

Ultimately, we conclude that the VsEP suppression we have observed is likely due to antidromic suppression of afferent responses, and we have found no evidence of efferent involvement. VsEP suppression with electrical stimulation in the EVS region occurred on a timescale 10 times faster than the reported effects of electrical stimulation on the single-unit activity of otolithic irregular responses in mammals (Goldberg and Fernandez, 1980; Marlinski et al., 2004). Moreover, across all species it appears that efferent vestibular stimulation is ineffective to single shocks (Goldberg and Fernandez, 1980), which suggests there may be a neurotransmitter facilitation or post synaptic amplification mechanism involved (Holt et al., 2011). That we consistently observed VsEP suppression with low shock rates, or even single shocks, suggests the effects we have observed are not mediated via the EVS neurons. Moreover, that VsEP suppression was not eliminated after the administration of nicotinic AChR drugs further suggests the suppressive effect was not efferent-mediated. Consistent with previous studies (Desmedt, 1962; Gifford and Guinan., 1987; Rajan, 1988), Strychnine eliminated the MOC-mediated suppression of the CAP in 3 animals ($p < 0.001$), suggesting that the drug was having a physiological effect on the peripheral cholinergic receptors of the inner ear. Here, we did not extensively investigate the effects (or lack thereof) of pharmacological agents on the VsEP suppression, because there was sufficient evidence from the functional changes alone to suggest that the VsEP suppression with electrical stimulation was not being mediated by efferent neurons. Our finding that Strychnine and DMPP failed to alter the VsEP suppression provides supportive evidence that the suppression effect did not involve an efferent component.

It has also been demonstrated that EVS stimulation from both the ipsilateral and contralateral brainstem result in both irregular and regular afferent excitation (Goldberg and Fernandez., 1980; Marlinski et al., 2004), and yet we observed no changes in the VsEP with contralateral stimulation. It is plausible that electrical stimulation at the midline of the fourth ventricle could activate the EVS fibers, by the same mechanism as midline MOC stimulation, as vestibular efferent fibers cross over at the floor of the fourth ventricle with the COCB fibers (Mccue and Guinan, 1994). Since these vestibular efferent axonal fibers are myelinated, like the MOC fibers, electrical stimulation at the midline should theoretically activate this both crossed MOCS and EVS neurons, albeit at higher current levels than that used for cell body activation. Mccue and Guinan (1994) accomplished this by successfully stimulating the EVS at the midline floor of the fourth ventricle whilst monitoring acoustically responsive irregular discharging vestibular afferents in the cat. The finding that we were only able to suppress the VsEP with electrical stimulation in a very localized region of the ipsilateral brainstem further suggests it is unlikely that our results involved efferent-driven activity.

The presence of a P1-N1 eCAP response on the facial nerve canal recording, immediately after the ES artifact, further supports the suppression effects being mediated via antidromic stimulation, although theoretically this eCAP response may have represented stimulated activity of the efferent fibers. Brainstem stereotaxic maps (Rapisarda and Bacchelli, 1977; Voitenko and Marlinsky, 1993) and immunohistochemistry studies (Strutz, 1982; Shumilina et al., 1986; Motts et al., 2008) in the guinea pig demonstrate that the main EVS neurons, the 'group e', closely neighbor the vestibular nuclei. Furthermore, irregular otolithic afferents terminate in all vestibular nuclei, but are most densely populated closer towards the EVS than the periphery (Büttner-Ennever, 2000; Goldberg, 2000). This would explain the stimulation area in the brainstem, at the approximate location of the 'group e' neurons. Moreover, the histological section (Fig. 13A) provides evidence that the stimulation site was at the region associated with the EVS in the guinea pig, under the sulcus limitans, lateral of the genu of the facial nerve (Strutz, 1982; Shumilina et al., 1986; Motts et al., 2008). A horseradish peroxidase tracer study in the cat also reveals that the MVN is situated very close to the sulcus limitans, and their dendrites, which receive primary afferent input extend and innervate the brainstem location associated with our

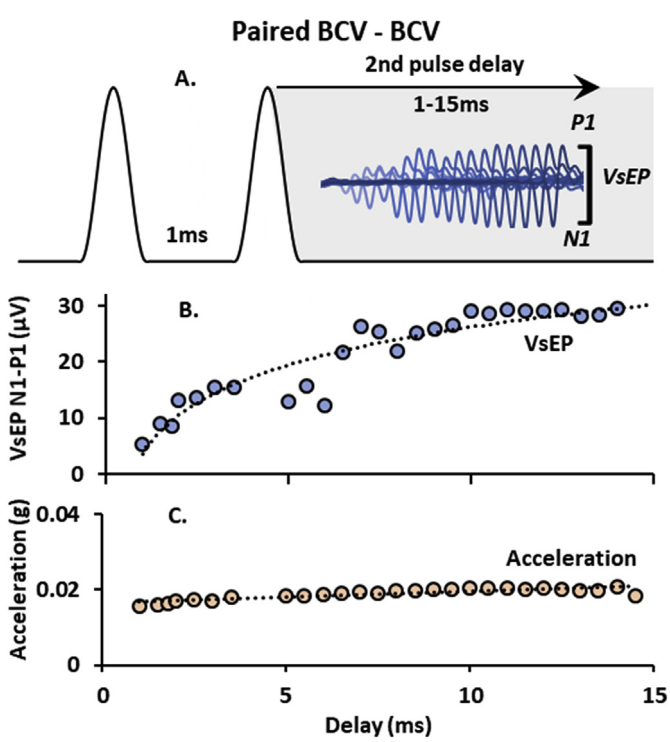

Fig. 16. A) Schematic showing the BCV – BCV pulse paradigm. B) Effect of changing the inter-pulse interval between 1 and 15ms on the VsEP N1-P1 amplitude. C) Peak-peak acceleration corresponding to interval changes in B. Animal#531.

stimulating region (Fig. 13A and B). Thus, our results can be explained by electrical shocks stimulating the utricular afferents from the proximal throughputs in the central vestibular system, causing electrically-evoked antidromic action potentials on the vestibular afferents, which collide with the orthodromic BCV-driven afferent activity that underlies the VsEP. This study provides a caveat for those aiming to investigate the function of the EVS using electrical stimulation in the midbrain, where a reduction in current stimulus intensity may be necessary to minimize antidromic spread. Our results indicate that electrical stimulation of the EVS at levels equivalent to and below those used in previous EVS studies can result in activation of the vestibular afferent nerve, and such activation may be difficult to avoid, unless electrical stimulation is limited to regions where there are EVS neurons, but no afferent fibers. Importantly, our results do not suggest that electrical stimulation of the EVS does not produce changes in the afferent response that are mediated via the efferent pathway. It is merely that in our recording montage, where we have examined the VsEP (as opposed to the single-unit response recordings performed in previous studies), any such effects are not obvious, or are at the very least masked by the much larger effect of antidromic stimulation of the afferents.

Finally, this study also provides the details on the refractory characteristics of the vestibular afferent nerve, which are similar to those reported by Stypulkowski and van den Honert (1984) and Brown (1994). This information may be of importance to the development of vestibular implants and prosthetics.

Author contributions

CP performed the experiments, analyzed the data and drafted the manuscript. DB developed the experimental hardware and software, and edited the manuscript. IC provided advice on the project. LS provided assistance with the histology.

Acknowledgements

This study was funded by The Medical Foundation of The University of Sydney, with funds raised by the Meniere's Research Fund Inc.

References

Baertschi, A.J., Dreifuss, J.-J., 1979. The antidromic compound action potential of the hypothalamo-neurohypophysial tract, a tool for assessing posterior pituitary activity in vivo. Brain Res. 171 (3), 437–451.
Bernard, C., Cochran, S.L., Precht, W., 1985. Presynaptic actions of cholinergic agents upon the hair cell-afferent fiber synapse in the vestibular labyrinth of the frog. Brain Res. 338 (2), 225–236.
Boyle, R., Highstein, S.M., 1990. Efferent vestibular system in the toadfish: action upon horizontal semicircular canal afferents. J. Neurosci. 10 (5), 1570–1582.
Boyle, R., Carey, J.P., Highstein, S.M., 1991. Morphological correlates of response dynamics and efferent stimulation in horizontal semicircular canal afferents of the toadfish. Opsanus tau. J. Neurophysiol. 66 (5), 1504–1521.
Brichta, A.M., Peterson, E.H., 1994. Functional architecture of vestibular primary afferents from the posterior semicircular canal of a turtle, Pseudemys (Trachemys) scripta elegans. J. Comp. Neurol. 344 (4), 481–507. https://doi.org/10.1002/cne.903440402.
Brichta, A.M., Goldberg, J.M., 1996. Afferent and efferent responses from morphological fiber classes in the turtle posterior crista. Ann. N. Y. Acad. Sci. 781 (1), 183–195.
Brichta, A.M., Goldberg, J.M., 2000. Responses to efferent activation and excitatory response-intensity relations of turtle posterior-crista afferents. J.Neurophysiol. 83 (3), 1224–1242.
Brown, M., 1994. The antidromic compound action potential of the auditory nerve. J.Neurophysiol. 71 (5), 1826–1834.
Büttner-Ennever, J., 2000. Overview of the vestibular system: anatomy. Neurochem. Vestib. Syst. 3–24.
Chagnaud, B.P., Banchi, R., Simmers, J., Straka, H., 2015. Spinal corollary discharge modulates motion sensing during vertebrate locomotion. Nat. Commun. 6.
Chi, F., Wang, Z., Li, K., 1999. Calcitonin gene-related peptide changes in efferent vestibular system during vestibular compensation. Zhonghua Er Bi Yan Hou Ke Za Zhi 34 (1), 11–13.
Chihara, Y., Wang, V., Brown, D.J., 2013. Evidence for the utricular origin of the vestibular short-latency-evoked potential (VsEP) to bone-conducted vibration in Guinea pig. Exp. Brain Res. 229 (2), 157–170. https://doi.org/10.1007/s00221-013-3602-5.
Cullen, K.E., Brooks, J.X., Jamali, M., Carriot, J., Massot, C., 2011. Internal models of self-motion: computations that suppress vestibular reafference in early vestibular processing. Exp. Brain Res. 210 (3–4), 377–388. https://doi.org/10.1007/s00221-011-2555-9.
Cullen, K.E., 2012. The vestibular system: multimodal integration and encoding of self-motion for motor control. Trends Neurosci. 35 (3), 185–196. https://doi.org/10.1016/j.tins.2011.12.001.
Curthoys, I.S., Kim, J., McPhedran, S.K., Camp, A.J., 2006. Bone conducted vibration selectively activates irregular primary otolithic vestibular neurons in the Guinea pig. Exp. Brain Res. 175 (2), 256–267.
Curthoys, I.S., Vulovic, V., Burgess, A.M., Sokolic, L., Goonetilleke, S.C., 2016. The response of Guinea pig primary utricular and saccular irregular neurons to bone-conducted vibration (BCV) and air-conducted sound (ACS). Hear. Res. 331, 131–143.
Desmedt, J., 1962. Auditory-evoked potentials from cochlea to cortex as influenced by activation of the efferent olivo-cochlear bundle. J. Acoust. Soc. Am. 34 (9B), 1478–1496.
Didier, A., Dupont, J., Cazals, Y., 1990. GABA immunoreactivity of calyceal nerve endings in the vestibular system of the Guinea pig. Cell Tissue Res. 260 (2), 415–419.
Galambos, R., 1956. Suppression of auditory nerve activity by stimulation of efferent fibers to cochlea. J. Neurophysiol. 19 (5), 424–437.
Gifford, M.L., Guinan Jr., J.J., 1987. Effects of electrical stimulation of medial olivocochlear neurons on ipsilateral and contralateral cochlear responses. Hear. Res. 29 (2–3), 179–194.
Goldberg, J.M., Fernandez, C., 1980. Efferent vestibular system in the squirrel monkey: anatomical location and influence on afferent activity. J. Neurophysiol. 43 (4), 986–1025.
Goldberg, J.M., 2000. Afferent diversity and the organization of central vestibular pathways. Exp. Brain Res. 130 (3), 277–297.
Highstein, S.M., Baker, R., 1985. Action of the efferent vestibular system on primary afferents in the toadfish, Opsanus tau. J.Neurophysiol. 54 (2), 370–384.
Holt, J.C., Lysakowski, A., Goldberg, J.M., 2006. Mechanisms of efferent-mediated responses in the turtle posterior crista. J. Neurosci. 26 (51), 13180–13193.
Holt, J.C., 2008. The effect of efferent stimulation on an afferent's response to sinusoidal indentation in the turtle posterior crista. In: Paper Presented at the Association for Research in Otolaryngology Midwinter Meeting Abstracts.
Holt, J.C., Lysakowski, A., Goldberg, J.M., 2011. The efferent vestibular system. In: Auditory and Vestibular Efferents. Springer, pp. 135–186.
Holt, J.C., Kewin, K., Jordan, P.M., Cameron, P., Klapczynski, M., McIntosh, J.M., Lysakowski, A., 2015. Pharmacologically distinct nicotinic acetylcholine receptors drive efferent-mediated excitation in calyx-bearing vestibular afferents. J. Neurosci. 35 (8), 3625–3643.
Holt, J.C., Jordan, P.M., Lysakowski, A., Shah, A., Barsz, K., Contini, D., 2017. Muscarinic acetylcholine receptors and M-currents underlie efferent-mediated slow excitation in calyx-bearing vestibular afferents. J. Neurosci. 37 (7), 1873–1887.
Hübner, P.P., Khan, S.I., Migliaccio, A.A., 2015. The mammalian efferent vestibular system plays a crucial role in the high-frequency response and short-term adaptation of the vestibuloocular reflex. J.Neurophysiol. 114 (6), 3154–3165.
Hübner, P.P., Khan, S.I., Migliaccio, A.A., 2017. The mammalian efferent vestibular system plays a crucial role in vestibulo-ocular reflex compensation after unilateral labyrinthectomy. J.Neurophysiol. 117 (4), 1553–1568.
Jones, S.M., Subramanian, G., Avniel, W., Guo, Y., Burkard, R.F., Jones, T.A., 2002. Stimulus and recording variables and their effects on mammalian vestibular evoked potentials. J. Neurosci. Meth. 118 (1), 23–31.
Jones, T.A., Jones, S.M., Vijayakumar, S., Brugeaud, A., Bothwell, M., Chabbert, C., 2011. The adequate stimulus for mammalian linear vestibular evoked potentials (VsEPs). Hear. Res. 280, 133–140. https://doi.org/10.1016/j.heares.2011.05.005.
Lopez, I., Juiz, J.M., Altschuler, R.A., Meza, G., 1990. Distribution of GABA-like immunoreactivity in Guinea pig vestibular cristae ampullaris. Brain Res. 530 (1), 170–175.
Luebke, A.E., Maroni, P.D., Guth, S.M., Lysakowski, A., 2005. Alpha-9 nicotinic acetylcholine receptor immunoreactivity in the rodent vestibular labyrinth. J. Comp. Neurol. 492 (3), 323–333.
Lysakowski, A., Goldberg, J.M., 1997. A regional ultrastructural analysis of the cellular and synaptic architecture in the chinchilla cristae ampullares. J. Comp. Neurol. 389 (3), 419–443.
Lysakowski, A., Singer, M., 2000. Nitric oxide synthase localized in a subpopulation of vestibular efferents with NADPH diaphorase histochemistry and nitric oxide synthase immunohistochemistry. J. Comp. Neurol. 427 (4), 508–521.
Lysakowski, A., Goldberg, J.M., 2004. Morphophysiology of the vestibular periphery. In: The Vestibular System. Springer, pp. 57–152.
Maison, S.F., Vetter, D.E., Liberman, M.C., 2007. A novel effect of cochlear efferents: in vivo response enhancement does not require α9 cholinergic receptors. J. Neurophysiol. 97 (5), 3269–3278.
Marlinski, V., Plotnik, M., Goldberg, J.M., 2004. Efferent actions in the chinchilla vestibular labyrinth. J. Assoc. Res. Otolaryngol. 5 (2), 126–143.
Mccue, M.P., Guinan, J., 1994. Influence of efferent stimulation on acoustically responsive vestibular afferents in the cat. J. Neurosci. 14 (10), 6071–6083.

Meredith, G.E., 1988. Comparative view of the central organization of afferent and efferent circuitry for the inner ear. Acta Biol. Hung. 39 (2–3), 229–249.
Morley, B.J., Lysakowski, A., Vijayakumar, S., Menapace, D., Jones, T.A., 2017. Nicotinic acetylcholine receptors regulate vestibular afferent gain and activation timing. J. Comp. Neurol. 525 (5), 1216–1233.
Motts, S., Slusarczyk, A., Sowick, C., Schofield, B., 2008. Distribution of cholinergic cells in Guinea pig brainstem. Neuroscience 154 (1), 186–195.
Ohgaki, T., Curthoys, I.S., Markham, C.H., 1988. Morphology of physiologically identified second-order vestibular neurons in cat, with intracellularly injected HRP. J. Comp. Neurol. 276 (3), 387–411.
Plotnik, M., Marlinski, V., Goldberg, J.M., 2005. Efferent-mediated fluctuations in vestibular nerve discharge: a novel, positive-feedback mechanism of efferent control. J. Assoc. Res. Otolaryngol. 6 (4), 311–323.
Popper, P., Wackym, P., 2001. Opioid peptides and receptors in the vestibular epithelia in rats. In: Paper Presented at the 31st SFN Meeting, Abstract.
Rajan, R., 1988. Electrical stimulation of cochlear efferents at the round window reduces auditory desensitization in Guinea pigs. I. Dependence on electrical stimulation parameters. Hear. Res. 36 (1), 53–73.
Rapisarda, C., Bacchelli, B., 1977. The brain of the Guinea pig in stereotaxic coordinates. Arch. Sci. Biol. 61 (1–4), 1–37.
Rennie, K., Ashmore, J., 1993. Effects of extracellular ATP on hair cells isolated from the Guinea-pig semicircular canals. Neurosci. Lett. 160 (2), 185–189.
Rossi, M.L., Prigioni, I., Valli, P., Casella, C., 1980. Activation of the efferent system in the isolated frog labyrinth: effects on the afferent EPSPs and spike discharge recorded from single fibers of the posterior nerve. Brain Res. 185 (1), 125–137.
Rossi, M.L., Martini, M., Pelucchi, B., Fesce, R., 1994. Quantal nature of synaptic transmission at the cytoneural junction in the frog labyrinth. J. Physiol. 478 (1), 17–35.
Shumilina, V.F., Preobrazhenskii, N.N., Maiskii, V.A., 1986. Efferent vestibular neurons in the Guinea pig by horseradish peroxidase and fluorochrome labeling techniques. Neurophysiology 18 (6), 513–520.
Strutz, J., 1982. The origin of efferent vestibular fibres in the Guinea pig. Acta Otolaryngol. 94 (1–6), 299–305.
Stypulkowski, P., Van den Honert, C., 1984. Physiological properties of the electrically stimulated auditory nerve. I. Compound action potential recordings. Hear. Res. 14 (3), 205–223.
Sugai, T., Yano, J., Sugitani, M., Ooyama, H., 1992. Actions of cholinergic agonists and antagonists on the efferent synapse in the frog sacculus. Hear. Res. 61 (1), 56–64.
Syeda, S., Lysakowski, A., 2001. P2X2 purinergic receptor localized in the inner ear. In: Paper presented at the Association for Research in Otolaryngology Midwinter Meeting Abstracts.
Voitenko, L., Marlinsky, V., 1993. Stereotaxic atlas of the Guinea pig brainstem. Neurophysiology 25 (1), 43–67.
Wackym, P., Popper, P., Ward, P., Micevych, P., 1991. Cell and molecular anatomy of nicotinic acetylcholine receptor subunits and calcitonin gene-related peptide in the rat vestibular system. Otolaryngol.–Head Neck Surg. Off. J. Am. Acad. Otolaryngol.-Head Neck Surg. 105 (4), 493–510.

2.3. Conclusion

Antidromic modulation of the VsEP was a highly effective way of directly modulating peripheral nerve function in the absence of hair cell and mechanical changes and provided a simple means to differentially alter peripheral vestibular nerve function. Whilst antidromic potentials in the vestibular nerve is unlikely to occur clinically, pathologies such as schwannoma's or viral infections of the VIIIth nerve are likely to result in 'isolated' changes in vestibular nerve function, independent of mechanical or hair cell changes. Later, in Chapter 5.2, we demonstrate isolated changes in the VsEP due to pharmacological manipulations.

Direct manipulation of vestibular nerve function may have future clinical utility in electrical or optical afferent stimulation. As with hearing, peripheral implants may be used to bypass inactive hair cells and stimulate vestibular afferents as a means to restore balance dysfunction. Antidromic stimulation may help identify the characteristics of peripheral vestibular afferents during electrical stimulation. Like previous studies in the cochlea that used shocks delivered to the proximal end of the cochlear nerve to understand refractory characteristics, so as to avoid multiple peripheral activation sites such as the hair cells and other peripheral afferent terminals (Brown 1994), antidromic stimulation of the vestibular afferents can provide valuable information such as refractory periods and optimal stimulation rates.

Unlike the medial olivocochlear efference, which can be electrically stimulated at the midline floor of the fourth ventricle away from the proximal end of the cochlear afferents, the EVS lies adjacent to the facial nerve genu in close proximity to the vestibular nucleus (and proximal vestibular nerve). For this reason, it may be difficult to electrically stimulate the EVS cell bodies in isolation of the proximal end of the vestibular neurons. Previous EVS stimulation studies which demonstrated changes in single vestibular afferent activity in the periphery (Goldberg and Fernandez 1980) also reported antidromic collisions, however, it is likely this effect was exaggerated in our setup by measuring a global, summed response of many afferents, in the VsEP. It is also possible that low-level current stimulated the EVS cell-bodies, but the increased spontaneous firing rate was not reflected in changes to the VsEP.

It is possible that EVS stimulation may have had some direct effect on the utricular hair cells, given that some EVS neurons synapse with type II hair cells directly (Lysakowski and Goldberg 1997, Lysakowski and Goldberg 2004). Unfortunately, in the above study we were not able to measure hair cell or mechanical responses with EVS stimulation, as this would require 'sealing' the stimulating electrodes in place in the brainstem and turning the animal over to destroy the cochlea and expose the utricle for subsequent hair cell measurements (see Chapters 3 & 4 for details). Due to the technical difficulty and inherent risk of damaging the brainstem (and efferent cell bodies) when turning the animal over, we did

not attempt to record UM responses with EVS stimulation. Although we did not directly measure hair cell responses for the above reasons, the finding that VsEP threshold and latency were unchanged, and that there were no longitudinal effects of EVS stimulation at low-modest current levels, suggests the observed effects were most likely post-synaptically mediated, downstream of the hair cells.

One of the main limitations of the VsEP, as a diagnostic marker of vestibular nerve function, is that it represents only a small population of vestibular neurons, innervating a small subset of vestibular hair cells. Previous studies have shown that the VsEP is sensitive to cranial jerk and is therefore a measure of irregular afferent activity (Jones, Lee et al. 2015). Further experimental confirmation from our laboratory demonstrating the 'jerk-sensitivity' of the VsEP can be found in Appendix 1. Overall the VsEP only provides a 'partial' measure of otolithic nerve function and does not report regular nerve activity. Future development of gross static afferent activity is needed to have a complete measure of peripheral utricular nerve function.

Moreover, previous studies in our laboratory have demonstrated the VsEP to BCV is *primarily* a utricular nerve response (Chihara, Wang et al. 2013) (for further experimental evidence see Appendix 1). It is not exactly clear why this is the case since several studies have shown that vibration activates both utricular and saccular afferents (Young, Fernández et al. 1977, Curthoys, Vulovic et al. 2016). However, afferent activation by BCV does not necessarily translate to CAP generation, which requires a high-level of neural synchrony at the stimulus onset. One possible explanation is the position of the recording wire in the facial nerve canal, near the superior branch of the vestibular nerve, which may receive greater electrical 'pick-up' and be dominated by the utricle. Additionally, delivery of the BCV stimulus in the latero-medial plane may preferentially activate utricular hair cells over saccular receptors. That the utricle lies in the horizontal plane (Dimiccoli, Girard et al. 2013) and is approximately parallel to delivery of BCV stimulation in our setup, means it is likely that this stimulation mode would produce a differential shearing between the utricular otoliths and neuroepithelium, resulting in stereocilia deflection. A previous study has demonstrated that shearing forces directed orthogonal to otolithic hair bundles are rather ineffective at producing otolith receptor excitation (Fernandez and Goldberg 1976), which may be the case with the saccular hair bundles in our experimental setup. Additionally, further studies have shown it may be possible to selectively record VsEPs from the utricle and saccule by alternating the orientation of the stimulus from latero-medial to dorso-ventral, respectively (Freeman, Plotnik et al. 1999, Jones, Jones et al. 2001). Therefore, development of a saccular (and semi-circular canal) gross nerve response may be

achieved by changing the recording location and stimulation method, which would allow a more complete measure of vestibular nerve activity.

Importantly, the VsEP provides a relatively simple method to longitudinally study utricular nerve function under various experimental manipulations. Since it is measured from a facial nerve canal wire out of the way of the utricular macula, it can be used during simultaneous recordings of hair cell and mechanical function, *in vivo.*

Chapter 3: Development of the vestibular microphonic

3.1. Introduction

To have a complete assessment of peripheral vestibular function, *in vivo*, an objective and robust measure of vestibular hair cell function is needed. The VM has featured in several studies mostly involving *ex* vivo and non-mammalian models (Huizinga, De Vries et al. 1951, Hudspeth 1982, Corey and Hudspeth 1983, Wit, Kahmann et al. 1986); however, unlike the CM, it has not progressed as a research tool. This is likely due to a lack of clarity regarding how to record or interpret the VM as it may contain contributions from the cochlea, vestibular nerve or electrical artifact components. Of the few studies which have recorded the VM, most reflect global vestibular hair cell function (Wit, Kahmann et al. 1986), and not localized hair cell activity (Corey and Hudspeth 1983). *In vivo* measurements of a localized microphonic potential, free from neural or other contamination allows a reliable measure of hair cell function and the ability to differentiate the effect of experimental manipulations resulting in loss of neural sensitivity, as originating from either hair cell or neural dysfunction. The following describes the development and characterization of this novel hair cell measurement, *in vivo.*

3.2. *In vivo* recording of the vestibular microphonic in mammals

Pastras, C. J., Curthoys, I. S., & Brown, D. J. (2017). In vivo recording of the vestibular microphonic in mammals. *Hearing research*, *354*, 38-47.

Hearing Research 354 (2017) 38–47

Contents lists available at ScienceDirect

Hearing Research

journal homepage: www.elsevier.com/locate/heares

Research Paper

In vivo recording of the vestibular microphonic in mammals

C.J. Pastras [a], I.S. Curthoys [b], D.J. Brown [a, *]

[a] The Meniere's Laboratory, Sydney Medical School, The University of Sydney, Sydney, NSW, 2050, Australia
[b] Vestibular Research Laboratory, The University of Sydney, School of Psychology, Sydney, NSW, 2050, Australia

ARTICLE INFO

Article history:
Received 9 March 2017
Received in revised form
15 June 2017
Accepted 25 July 2017
Available online 26 July 2017

Keywords:
Vestibular microphonic
Utricle
Hair cell
Guinea pig
In vivo
Bone conducted vibration

ABSTRACT

Background: The Vestibular Microphonic (VM) has only featured in a handful of publications, mostly involving non-mammalian and *ex vivo* models. The VM is the extracellular analogue of the vestibular hair cell receptor current, and offers a tool to monitor vestibular hair cell activity *in vivo*.
Objective: To characterise features of the VM measured *in vivo* in guinea pigs, using a relatively simple experimental setup.
Methods: The VM, evoked by bone-conducted vibration (BCV), was recorded from the basal surface of either the utricular or saccular macula after surgical removal of the cochlea, in 27 guinea pigs.
Results: The VM remained after vestibular nerve blockade, but was abolished following end-organ destruction or death. The VM reversed polarity as the recording electrode tracked across the utricular or saccular macula surface, or through the utricular macula. The VM could be evoked by BCV stimuli of frequencies between 100 Hz and 5 kHz, and was largest to vibrations between 600 Hz and 800 Hz. Experimental manipulations demonstrated a reduction in the VM amplitude with maculae displacement, or rupture of the utricular membrane.
Conclusions: Results mirror those obtained in previous *ex vivo* studies, and further demonstrate that vestibular hair cells are sensitive to vibrations of several kilohertz. Changes in the VM with maculae displacement or rupture suggest utricular hydrops may alter vestibular hair cell sensitivity due to either mechanical or ionic changes.

1. Introduction

The cochlear microphonic (CM) and vestibular microphonic (VM) were first reported in 1930 and 1934, respectively (Wever and Bray., 1930; Ashcroft and Hallpike., 1934). The CM has been used extensively in auditory research to study auditory physiology and pathology, increasing our understanding of the cochlear amplifier (Legan et al., 2000; Cheatham et al., 2004), endolymphatic hydrops (Kumagami et al., 1981; Brown et al., 2009), the auditory efferent system (Guinan, 1996), hearing loss due to ototoxicity (Lodhi et al., 1980; Fitzgerald et al., 1993), acoustic trauma (Patuzzi et al., 1989a,b), genetic disorders (Steel et al., 1987) and aging (Harris and Dallos, 1984; Conlee et al., 1988). Conversely, the VM has only featured in a handful of publications mostly involving non-mammalian and *ex vivo* models (Adrian et al., 1938; Zotterman, 1943; Lowenstein and Roberts., 1951; Corey and Hudspeth, 1983). Trincker (1959) was the first to report *in vivo* mammalian recordings of the VM, detailing the effects of recording location, stimulus frequency, surgical destruction, cooling and death. Later, Wit et al. (1986) reported on the VM recorded in pigeons, and Eatock et al. (1987) performed VM recordings in bullfrogs.

It is important to note the effect of recording location and end-organ preparation on the resultant VM. *Ex vivo* preparations typically secure a vestibular end-organ within an Using chamber, allowing recordings in close proximity to the hair cells (Hudspeth, 1982; Corey and Hudspeth, 1983; Eatock et al., 1987). Alternatively, *in vivo* preparations have recorded responses from the vestibular fluids, either within perilymph as a 'global' measure where nerve and hair cell responses summate (Huizinga et al., 1951; Wit et al., 1986), or much closer to the hair cells within the endolymph where the hair cell current contribution dominates the response (Rabbitt et al., 2005).

Both otolith organs, the utricle and saccule, act as highly

Abbreviations: BCV, bone conducted vibration; CM, cochlear microphonic; DC, direct current; ECG, electrocardiography; I/O, input/output; MET, mechanoelectrical transduction; VM, vestibular microphonic

* Corresponding author. Brain and Mind Centre, The University of Sydney, 100 Mallett St. Camperdown, Sydney, NSW, 2050, Australia.
E-mail address: daniel.brown@sydney.edu.au (D.J. Brown).

http://dx.doi.org/10.1016/j.heares.2017.07.015
0378-5955/© 2017 Published by Elsevier B.V.

sensitive three-dimensional linear accelerometers (Dimiccoli et al., 2013). Their non-planar and uniquely curved epithelium enables 3D-vector polarization (Curthoys et al., 1999; Jaeger et al., 2008), with both phasic and tonic vestibular pathways (Fernandez and Goldberg, 1976b). Central to these pathways are the vestibular hair cells, which are embedded in a dense gelatinous matrix, underneath the heavy otoconial layer (Kachar et al., 1990). Rotational and linear acceleration create shearing forces that displace the otoconia, resulting in apical hair bundle motion (Fernandez and Goldberg, 1976a), which alters the hair cell mechanoelectrical transduction (MET) channel conductance, and the receptor current and membrane potential (Shotwell et al., 1981). Like the CM, the VM is produced by vibration induced modulation of hair cell conductance, with the extracellular potential determined by changes in current flow through the impedance path between tissue and fluids (Corey and Hudspeth., 1983). However, whilst the CM is dominated by the hair cells local to the recording location (Patuzzi et al., 1989a,b; Cheatham et al., 2011), which are modulated in-phase for low-frequency (<1 kHz) tones, and thus can be used as a reliable estimate the MET channel gating (Patuzzi and Moleirinho, 1998), it is unclear if the same is true for *in vivo* VM recordings. That is, it is unclear whether the VM is dominated by hair cells local to the recording site, and is therefore dependent upon the orientation of the hair cells (kinocilium) at the sensory epithelium, or is rather the summated extracellular response of all vestibular hair cells (Corey and Hudspeth, 1983). Ultimately, the closer the recording electrode is to the hair cell, and the larger the extracellular impedances, the larger the hair cell response will be due to less current spread (Hudspeth, 1982).

Rabbitt et al. (2005) recorded the microphonic (in response to 0.1–20 Hz stimulation) within the SCC ampulla of toadfish, and demonstrated the entire response was generated by the SCC hair cells. The finding that there was little-to-no contribution from neurons or otolith hair cells to the response may be due to the close proximity of the recording to the SCC hair cells, or due to some aspect specific to the stimulus used in the toadfish, or that the SCC hair cells are polarized in a single orientation. There was no suggestion that otolith hair cells do not generate microphonic responses under different recording procedures, focused on stimulating the otoliths.

Here we have performed similar experiments as the *in vivo*, mammalian VM recordings performed by Trincker (1959). However, whereas Trincker primarily used air-conducted sound to stimulate the vestibular system, and maintained fluid within the vestibule following surgical destruction of the cochlea, we have used BCV stimuli to more effectively evoke the VM, while removing the cochlea and the perilymphatic fluid within the vestibule to provide a more localized recording of the electrical response from the vestibular hair cells. This is more akin to previous VM experiments performed *ex vivo* (Furukawa et al., 1972; Corey and Hudspeth., 1983; Eatock et al., 1987).

2. Materials and methods

2.1. Animal preparation & surgery

Experiments were performed on 27 adult tri-coloured guinea pigs (*Cavia porcellus*), of either sex, weighing between 200 and 500 g. All experimental procedures were approved by The University of Sydney's Animal Ethics Committee. Animals received premedication I.P. injections of 0.1 ml Atropine Sulphate (0.6 mg/ml; Apex Laboratories, NSW, Australia), and 0.05 ml of Temgesic (Buprenorphreine Hydrochloride, 324 μg/ml; Reckitt Benckiser, Auckland, NZ). Animals were anaesthetised in an induction chamber with 4.5% isoflurane, and once sedated and lacking a foot-withdrawal reflex, were transported to the surgical table to be tracheotomised and artificially ventilated with a mixture of oxygen and isoflurane (2–3%). Blood oxygen saturation and heart rate were continuously monitored, and body temperature was maintained using a custom-made heating pad, blanket, and infrared heating lamp. Animals were secured between custom-made ear-bars, on which an electromagnetically shielded audiometric BCV stimulator (B-81, Radioear corp., PA, USA) was directly attached. Also attached to the ear-bars was a 3-axis accelerometer (Dimension engineering, OH, USA), which had a pass-band between DC – 1500 Hz. A small incision was made behind the pinna to expose the bulla from the dorsal aspect. Approximately 3 mm^2 of bone was removed from the bulla, exposing the facial nerve canal and round window. A Teflon-coated AgCl recording wire (with the very tip exposed) was then passed approximately 3 mm into the facial nerve canal to record nerve responses. A schematic illustration of the experimental setup is shown in Fig. 1.

In the ventral position, tissue and musculature overlying the bulla were carefully removed, and the bulla was opened providing a clear view of the cochlea. Several electrophysiological recordings were performed from the facial nerve electrode with the cochlea intact. Thereafter, the cochlea was completely removed, along with the stapes footplate, providing a clear view into the vestibule. From this approach, the basal surface of the utricular macula (i.e. the surface beneath the receptor hair cells) along with the utricular compartment membrane and the saccular macula (with the saccular compartment typically collapsing) were clearly visible. Fluids within the vestibule and bulla were removed using tissue wicks, taking care not to touch the otolith organs. Tissue wicks were routinely replaced as they became saturated with fluid over the course of the experiment.

2.2. Physiological measures

BCV stimuli and evoked responses were generated and recorded using custom-developed LabVIEW (National Instruments, TX, USA) programs. BCV stimuli were generated using a PCIe soundcard (Xonar Essence STX II 7.1, ASUSTek Inc. China), and amplified using an audio amplifier (AA-0488, Digitech, UT, USA). Analogue responses were amplified by 80 dB, with a 1 Hz to 10 kHz band-pass filter (IsoDAM 8, WPI, Florida USA) before being digitized at 40 kHz, 16 bit, using an analogue to digital converter (NI 9205, National Instruments, TX, USA). Averaged responses were evoked by either brief, monophasic "BCV-pulses", or 40 ms sinusoidal "BCV-bursts" with frequencies between 50 Hz and 5 kHz. The stimulus rate was 50/s for the brief stimuli, and 8.3/s for the 40 ms duration stimulus.

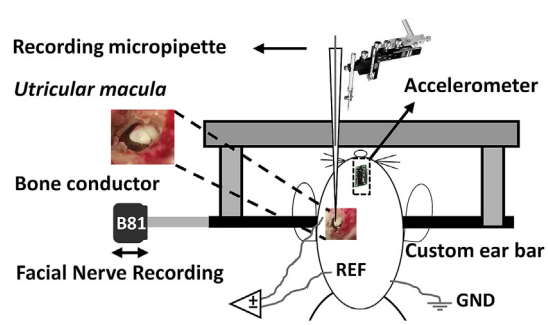

Fig. 1. Schematic diagram of our VM recording set-up using a ventral surgical approach. The animal lays supine, and was secured between custom-made ear bars, housing a B81 Bone conductor. A tri-axial accelerometer was rigidly attached to the skull vertex. The bulla was opened and the cochlea ablated, exposing the basal surface of the utricular and saccular macula. VMs were recorded from the otolithic maculae using a glass micropipette, and the facial nerve canal using an Ag/AgCl wire.

In experiments measuring the absolute peak-peak amplitude of the VM, a continuous BCV vibration stimulus was used.

2.3. Facial nerve canal & otolith recordings

Evoked electrical responses were initially recorded differentially between the facial nerve canal electrode and a neck-reference electrode. Following this, VM responses were recorded from within the vestibule using glass microelectrodes, with a tip-diameter of 4–8 μm, and housing 300 mM KCl along with an Ag/Cl recording wire. Manual micromanipulators were used to position the micropipette tip such that it was just within the small amount of fluid overlying the surface of the exposed macula within the vestibule.

3. Results

3.1. Overview

With the cochlea intact, recordings were only made from the facial nerve canal. In response to either a brief BCV-pulse, or a sinusoidal BCV-burst, the initial portion of the response had an onset latency of 0.6 ms, and consisted of a series of negative and positive peaks (Fig. 2A and B). In the case of the BCV-burst response (Fig. 2B), the later portions of the response consisted of a sinusoidal potential, with a majority of the power at the stimulus frequency (800 Hz in the example provided in Fig. 2B). Given that the BCV stimulus produced an audible sound, it seemed likely that much of this response originated from the cochlea or cochlear nerve. After removing the cochlea entirely, both the BCV-pulse and BCV-burst stimuli still evoked a response (Fig. 2C and D), with similar onset latency as observed when the cochlea was intact. Ablating the cochlea abolished much of the later components of the BCV-pulse response, however, the later components (occurring during the stimulus) became more complex and less sinusoidal, appearing more like a repetition of the initial negative/positive peaks. It should be noted that whilst the BCV-pulse stimulus was intended to evoke a brief-acceleration of the animal's skull, inherent resonance of the ear-bars and skull resulted in a more complex, damped resonant acceleration stimulus (Fig. 2C).

To investigate if these responses (post-cochlea ablation) reflected neural or hair cell activity, we applied 10 μl of 20 mg/ml Lignocaine Hydrochloride (Troy Laboratories, NSW, AUS) to the vestibule (with the cochlea removed). Prior to Lignocaine application BCV-pulses evoked a short-duration, biphasic response (Fig. 3A), and BCV-bursts evoked a repetitive response lasting as long as the stimulus, with slightly larger peaked-components at the onset and offset of the response (Fig. 3D). Responses were continuously monitored following application of the Lignocaine, where the BCV-pulse response gradually decreased in amplitude, until

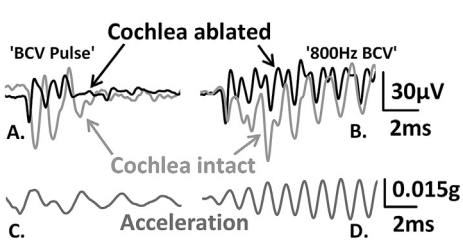

Fig. 2. A & B) 0.8 ms BCV-pulse or 800 Hz BCV-burst evoked responses recorded from the facial nerve canal. C & D) The associated skull acceleration. Both sets of responses were recorded before (grey traces) and after (black traces) cochlear ablation. Stimulus averaged (40 presentations) recordings from guinea pig GP#160722.

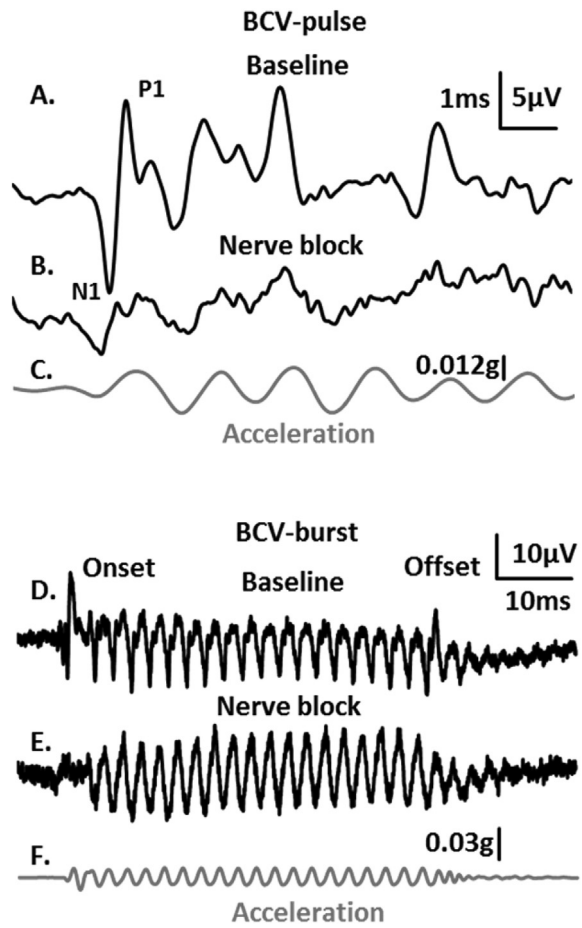

Fig. 3. BCV-pulse (0.4 ms, monophasic square wave pulse) or BCV-burst (40 ms, 400 Hz sinusoid) evoked responses recorded from the facial nerve canal after the cochlea has been ablated, measured either prior to (A & D) or following (B and E) lignocaine application to the vestibule. The skull acceleration is presented below each response (C & F). Note the acceleration was recorded with a tri-axial accelerometer with an inherent 1500 Hz low-pass filter, and that the ear-bar accelerometer does not faithfully represent the acceleration of the otolith. GP#160929.

approximately 20 min after application it had decreased in amplitude by 70% (Fig. 3B). Whilst the BCV-pulse response had diminished, the BCV-burst response remained, although the large onset and offset components had largely been abolished (Fig. 3E). It should be noted that the BCV-burst stimuli were not 'ramped' on or off, and therefore the start and end of the BCV-burst stimulus induced high-frequency acceleration components (Fig. 3F).

With the cochlea removed and the utricular macula exposed (without Lignocaine application) we could then record responses from the surface of the utricular macula. Here, BCV-burst responses were simultaneously recorded from the facial nerve canal electrode and the utricular macula electrode. Utricular responses were 20 times larger in amplitude than facial nerve responses (Fig. 4A and B). The portion of the BCV-burst response occurring during the response (i.e. not including the initial components) has been referred to here as a VM response (Fig. 4B inset). To verify that the response was an electrophysiological response of the otolith, and not an electromagnetic or movement artifact, the microelectrode was placed on the musculature just outside the bulla opening. Here, the response was either non-existent or very small (Fig. 4C).

To clearly visualize the utricular macula after cochlear ablation, it was necessary to wick the fluid (perilymph) from the vestibule. Often after placing the microelectrode onto the basal surface of the

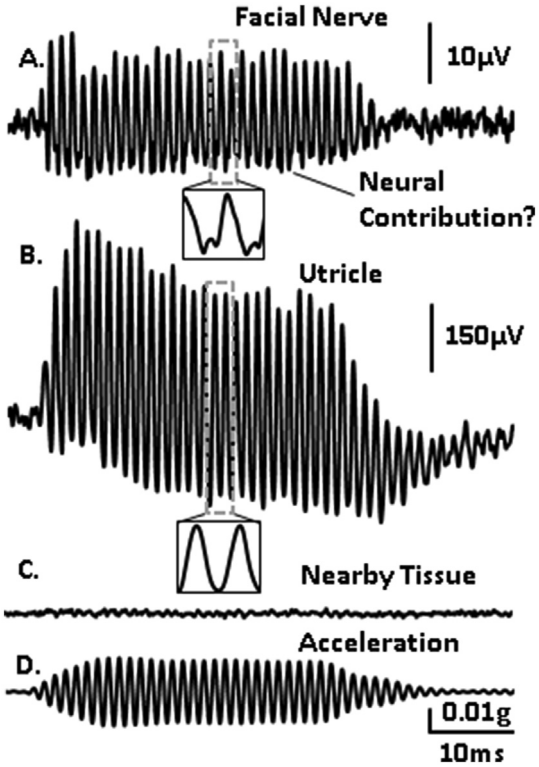

Fig. 4. VM recordings from either the facial nerve canal wire electrode (A), or the glass microelectrode placed on the basal surface of the utricular macula (B), or on the musculature outside the bulla (C). The skull acceleration (D) in response to the 800 Hz, 40 ms BCV-burst. Responses were recorded using stimulus triggered averaging (50 presentations) in animal GP#160624.

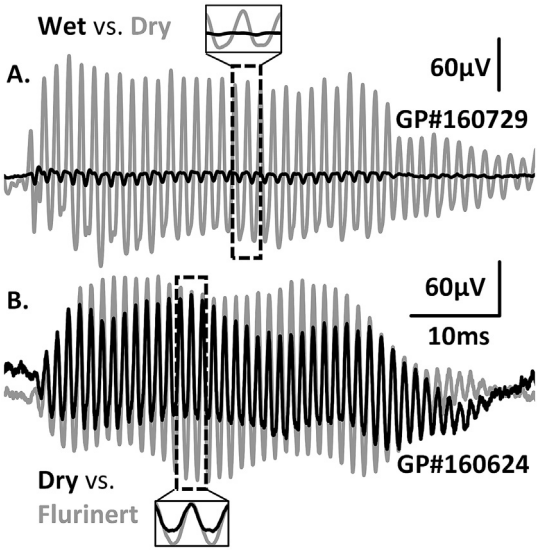

Fig. 5. A) Averaged VM responses evoked by an 800 Hz, 40 ms BCV-burst, recorded from the basal surface of the utricular macula, either with fluid build-up in the vestibule, 'Wet' (black trace) or with the fluid removed via tissue wick, 'Dry' (grey trace). GP#160729. B) Similar responses with either the fluid removed via tissue wick, 'Dry' (black trace) or with the vestibule fluid replaced by 'Fluorinert' (grey trace). Note that under 'Dry' conditions the recording environment is not dry *per se*, but only lacking a buildup of inner ear fluid within the vestibule; there is still a small layer of perilymph overlying the macula. 'Dry' vs 'Wet' is a simple distinction to describe the level of extracellular shunt impedance. GP#160624.

utricular macula the open vestibule would re-fill with fluid. This typically resulted in the VM amplitude greatly decreasing (Fig. 5A), although it was not clear if this was due to an electrical 'shorting' of the VM response recorded from the surface of the utricular macula, or if it was due to a change in the mechanical sensitivity of the utricular macula to the BCV stimulus as it became physically 'loaded' by the overlying fluid. In several animals, we replaced the perilymph in the vestibule with Fluorinert (FC-40, Sigma-Aldrich, Saint Louis, MO), which is almost twice as dense as water but is an electrical insulator. With the vestibule flooded with Fluorinert, the VM amplitude was equal to or larger than the VM recorded with most of the fluid overlying the macula removed (Fig. 5B). For the VM recordings presented hereafter, rather than placing Fluorinert into the vestibule, a tissue wick was placed permanently into the vestibule, just near the oval window niche but without touching the utricular membrane. This prevented a build-up of fluid within the vestibule such that the VM amplitude remained constant over the recording procedure.

We next investigated the effects of stimulus level on the VM. The VM evoked by relatively low-level BCV-burst stimulation closely resembled the stimulus, whereas increasing the stimulus level increased the distortion of the response, producing additional inflections on the troughs of the VM (Fig. 6A). An increase in distortion with stimulus level was not evident in the head acceleration (Fig. 6B). High level stimuli also produced VM responses with a DC offset component (Figs. 4B and 6A).

Whilst low-level BCV-burst evoked VM responses appeared relatively sinusoidal (Fig. 7A), some harmonic distortion was evident in the Fast Fourier Transform of the response (Fig. 7B; black trace). Applying Lignocaine to the vestibule abolished this distortion, leaving a sinusoidal VM response (Fig. 7A and B; grey traces).

As a final demonstration that the VM was a physiological response, it was monitored following euthanasia of an animal with a lethal injection of Lethabarb (Virbac Pty Ltd., NSW, AUS). Immediately following the animal's death (i.e. where ECG activity ceased) the VM had not changed markedly from pre-Lethabarb injection (Fig. 8A). Subsequent recordings were taken at several time points following death (Fig. 8A), showing a gradual decrease in the VM response amplitude, whereas the stimulus remained stable (Fig. 8C). Whilst the VM response did not decrease to baseline, recordings from the musculature overlying the bulla showed no evidence of an artifact response (Fig. 8B).

3.2. Recording location

As the microelectrode recording location was moved over the basal surface of the utricular macula, the VM changed phase and waveshape. There was a complete phase reversal of the response

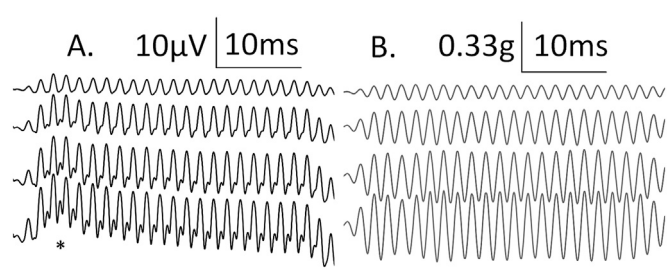

Fig. 6. Distortion of the utricular VM with increasing BCV stimulus intensity. A) Averaged VM responses recorded with the glass micropipette at the most sensitive, non-striola region of the basal surface of the utricular macula. Asterisk corresponds to the early nerve response evoked by the BCV stimulus being ramped on over a 5 ms rise time as discussed in the text. B) Corresponding acceleration of the skull. BCV stimulus: 600 Hz, 40 ms. 100 averages. GP#160624.

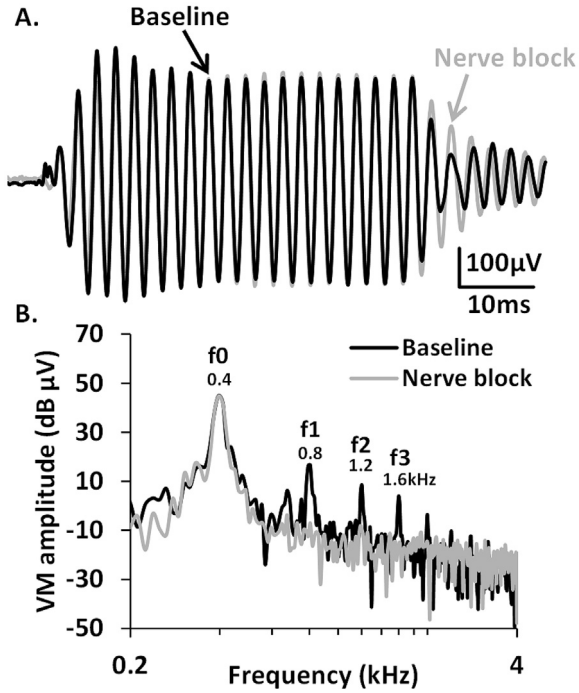

Fig. 7. Effect of neural blockade on the utricular VM. A) Superimposed averaged VM waveforms recorded to moderate level, 400 Hz BCV-bursts both before (black trace) and after (grey trace) the application of Lignocaine to the basal surface of the otolithic maculae. B) The Fast Fourier Transform of the above waveforms. f0, f1, f2, f3 = fundamental and upper harmonic components. FFT analysis was undertaken using a Hanning window centered over the entire width of the waveform in A. GP#160929.

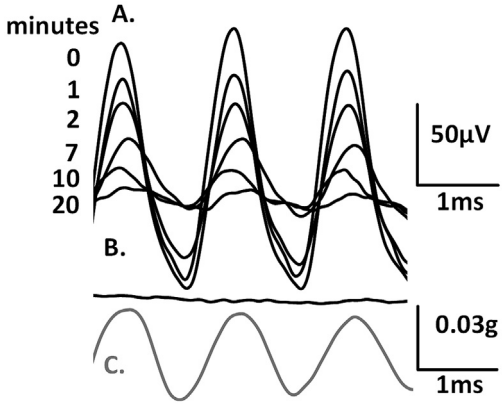

Fig. 8. A) VM waveforms recorded from the utricular surface at various intervals after death of the animal, with time points show at the left of each trace. B) Micropipette recording at the nearby musculature following death. C) Skull acceleration. Responses were recorded to 700 Hz, 40 ms BCV-burst stimuli and averaged 50 times. GP#160615.

between nearby areas of the macula, particularly either side of the dark and white regions of the utricular macula (Fig. 9A and B). The same effect occurred, to a lesser extent when recording from the saccular otoconia (Fig. 9E), however this was difficult to reproduce in all experiments as the saccular end-organ was not always accessible from the ventral approach, typically being shielded by a ridge of bone. For each of the two examples presented in Fig. 9, the grey traces are the head-acceleration.

In several experiments, we attempted to obtain a 'surface map' recording of the VM response over the utricular macula surface. To provide a more consistent recording environment whilst moving the microelectrode between recording locations, we placed

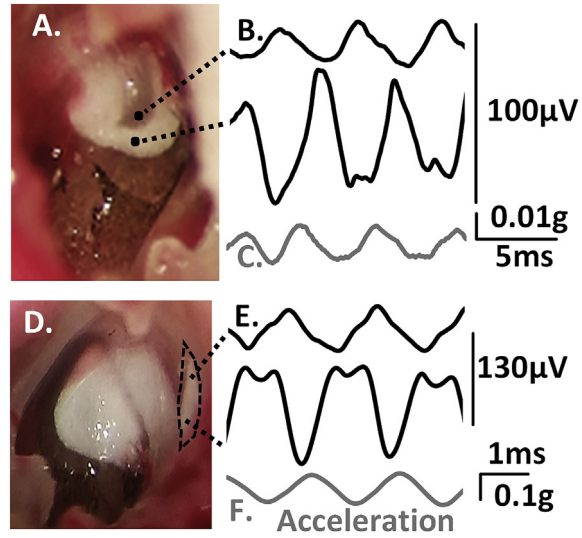

Fig. 9. A & B) The VM recorded at different locations on the utricular macula, demonstrating a polarity reversal. C) The corresponding skull acceleration. GP#160428. D & E) The VM recorded at different locations on the saccular macula. F) Skull acceleration. GP#160603.

Fluorinert in the vestibule, rather than relying on a tissue wick (which would have impeded access to some regions of the macula). Fig. 10, shows various averaged VM waveforms from one animal, with a schematic diagram of the utricular macula demonstrating the recording location of each response. The acceleration stimulus was the same for all responses. The macula outline also contains a schematic arrangement of the utricular hair cells (grey arrows), with the kinocilia of the utricular macula receptors directed inwards at the striola (grey line), and polarization vector zone (broken grey line), as reported by previous authors (Spoedlin, 1966; Dimiccoli et al., 2013). In comparison to the VM measured at the

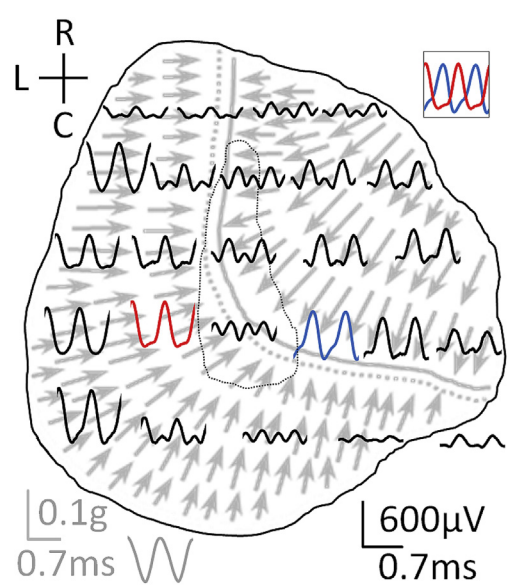

Fig. 10. Averaged VM waveforms, with only 2 cycles of the response shown, recorded from various locations on the basal surface of the utricular macula, with Fluorinert applied to the vestibule. A schematic diagram of the utricular macula is also shown, with grey arrows corresponding to the theoretical orientation of the kinocilium relative to the striola. The skull acceleration was the same for all recordings (grey trace, bottom left). Inset top right Superimposed VM responses from either side of the striola. BCV stimulus: 700 Hz, 40 ms, 100 averages. GP#160624. R = Rostral, L = Lateral.

edge of the macula, which resembled a distorted version of the stimulus, the VM measured at the central macula region, near the striola, appeared to have twice as many peaks and troughs, or double the frequency, relative to the stimulus.

3.3. Experimentally induced waveform changes

Next, we investigated if the VM inverted polarity either side of the apical/basal surface of the epithelium, the same way the CM is known to invert polarity between scala tympani and scala media. Tracking the glass micropipette through the utricular macula, from the basal to apical side, always resulted in an inversion of the VM polarity (n = 12 cochleae). In the two examples presented in Fig. 11, the VM measured from the basal surface of the macula, at an 'off-striola' region, had a similar polarity as the acceleration measured at the ear-bar. When the glass microelectrode passed through the macula (by moving the pipette tip 0.5 mm deeper), the polarity inverted. Additionally, as the micropipette was tracked through the macula, we noted a significant reduction in the amplitude of the VM, which we assumed to be related to either a mechanical displacement of the macula, or mechanical 'dampening' of the macula vibration in response to the BCV stimulus. To further investigate this, we fabricated a glass micropipette with a relatively large (20–30 μm) diameter tip that had been 'flamed' to reduce any sharp edges. Here, we could reliably push on the macula without the glass microelectrode passing through the tissue. With the microelectrode just touching the thin layer of fluid overlying the basal surface of the utricle, we step-wise advanced the electrode 300 μm using the manual micromanipulator. Pushing on the macula resulted in the VM amplitude being greatly suppressed and changing in waveshape (Fig. 12A). Retracting the microelectrode back to the initial position resulted in the VM response recovering, although the waveform did not fully recover and there appeared to be phase-changes in the response as the pipette was advanced and retracted. Fourier analysis shows the VM spectral energy shift from the fundamental harmonic frequency (800 Hz), to later harmonic components when the utricle was displaced (Fig. 12B and C).

In all experiments care was taken not to rupture or tear a hole in the utricular macula, as it was assumed that leakage of endolymph into the vestibular space may result in potassium toxicity of the otolith hair cells. To demonstrate the effect of a tear in the utricle, in one animal we measured the VM from the surface of the utricular macula, and then using the sharp tip of a glass micropipette we tore a small section of the transparent utricular membrane (i.e. not on the macula itself). This required temporarily removing the recording microelectrode, then replacing it. We tracked the amplitude of the VM over several minutes (Fig. 13). Tearing the utricular membrane immediately resulted in an 80% reduction in the VM amplitude, followed by a slight increase before eventually being completely abolished after 8 min.

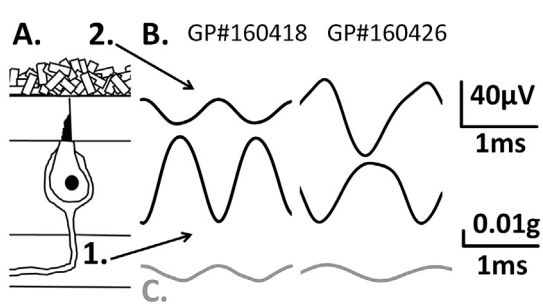

Fig. 11. The VM polarity reversal as the glass microelectrode was tracked through utricular macula. B) Averaged VM waveforms recorded at different depths correspond to the locations indicated in the schematic diagram (A) and black arrows. C) The skull acceleration. Responses are shown for two animals, GP#160418 and GP#160426.

3.4. Frequency characteristics

To determine the optimal BCV frequency for evoking the VM, we systematically varied frequency of the BCV-burst stimulus from 100 Hz to 5 kHz, and for each BCV frequency we varied the level of the stimulus from that which produced a VM just visible above the noise floor of the recording, to a level where the VM or the ear-bar acceleration waveform began to visibly distort (referred to as an I/O series). Here, we were not interested in the maximal amplitude of a VM response at a given BCV frequency (i.e. its saturation level), but rather how the VM amplitude changed with acceleration level, and frequency. To obtain this measure, the VM amplitude for each BCV frequency I/O series was plotted against the measured lateral ear-bar acceleration (Fig. 14A), and a linear trendline was approximated for each series providing a measure of the sensitivity in units of dB μV/g (Fig. 14B). The same analysis was performed for the rostral-caudal ear-bar acceleration (Fig. 14C), but not for the ventral/dorsal vibration, which was much smaller and more complex. Whilst in all animals the largest undistorted VM and ear-bar acceleration was obtained for BCV frequencies between 600 Hz and 800 Hz (Fig. 14A and B), the VM sensitivity measure was highest at 100 Hz (for both the lateral and rostro-caudal plots; Fig. 14B and C). The VM sensitivity decreased beyond 1 kHz (Fig. 14B and C), however it must be noted that the accelerometer had an inherent low-pass filter at 1.5 kHz.

4. Discussion

The BCV-evoked VM can be measured from both distal locations, such as the facial nerve canal, and from within the vestibule, close to the hair cells. This can provide a tool to study the function of the otolith hair cells during various experimental manipulations. A reliable VM measurement requires the cochlea to be removed, not only because cochlear removal provides surgical access to the otoliths, but because relatively large cochlear responses to a BCV stimulus will dominate any gross electrophysiological responses, and it may be difficult to fully suppress cochlear activity.

Whilst it does appear that a relatively low-amplitude VM can be recorded from the facial nerve canal once the cochlea is destroyed (Figs. 3E and 4A), it is likely that the VM measured here will reflect a complex, 'global' summation of various vestibular hair cell and nerve responses, because even recordings from within the vestibule are greatly altered by fluid shorting the VM response (Fig. 5).

Neural contributions to the facial nerve canal response will be particularly prevalent at the onset of a BCV response (Figs. 2A and 3A; Böhmer, 1995; Böhmer et al., 1995; Chihara et al., 2013), as jerk-sensitive hair cells and their related afferent neurons respond to BCV transients with a latency of approximately 0.6 ms corresponding to synaptic delay (Rabbitt et al., 2005). Interestingly, there seems to be little microphonic associated with transient BCV-evoked (jerk-evoked) nerve responses such as the short latency vestibular evoked response, when recorded from the facial nerve canal (Fig. 3F). This likely reflects that the facial nerve canal location provides a global recording, and that the high-gain, type I receptor hair cells account for only approximately 5–9% of the mammalian neuroepithelium (Baird et al., 1988; Desai et al., 2005), and we expect their contribution to the global VM response to be relatively small. 'Ramping' the BCV stimulus on over a few milliseconds may help reduce the neural contribution, but our results suggest that cyclic neural activity will contribute to the BCV evoked response even during the stimulus (Fig. 7B), in the same way that low-frequency sound evokes the auditory nerve neurophonic, which

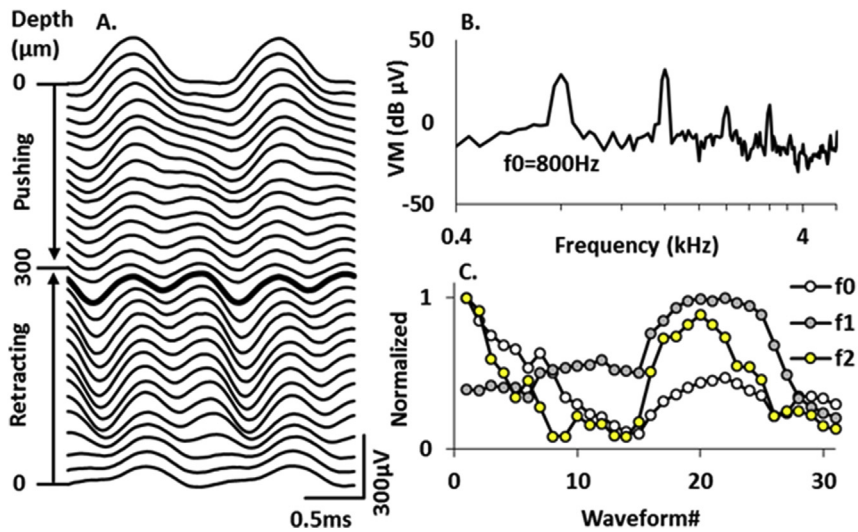

Fig. 12. The effect of utricular macula displacement on the VM response. A) Averaged VM waveforms are presented as a waterfall plot, with the position representative of the displacement of the probe used to push on the macula (shown at left). The first response was taken with the recording pipette in the fluids overlying the utricular macula. The probe depth was changed by 20 µm incremental steps. B) The Fast Fourier Transform corresponding to the indicated waveform in the waterfall plot. The selected waveform displays a 'frequency-doubling' with spectral energy at even (f2) and odd (f1, f3) harmonics indicating hair cell distortion. C. VM amplitudes (normalized to their maximal value) for each harmonic component (f0-f2) from the Fast Fourier Transform plotted against waveform# corresponding to the sequence presented in the waterfall plot A. The BCV stimulus was a 40 ms, 800 Hz sinusoid, which can be seen as the fundamental harmonic (f0) in B. GP#160622.

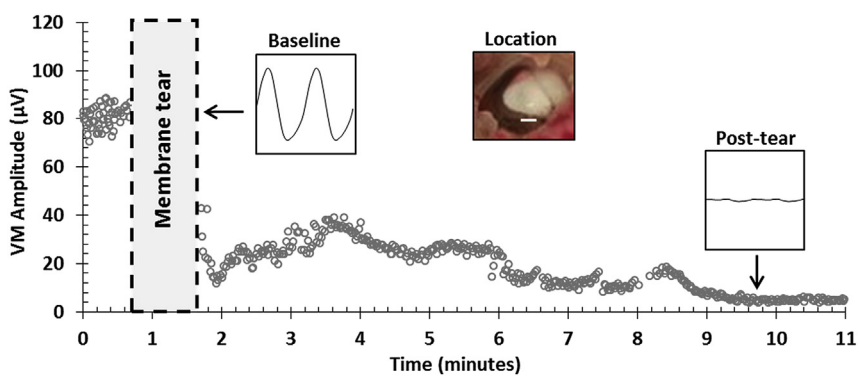

Fig. 13. Longitudinal measurement of the utricular VM amplitude, prior to, and following a tear of the utricle (white bar in 'location' inset). Example waveforms prior to and at the end of the recording series are demonstrated as inset figures. The BCV stimulus was a 700 Hz continuous vibration. GP#160819.

summates with the CM (Snyder and Schreiner, 1984; Henry, 1995). Thus ramping the stimulus may simply leave a 'smeared' neural contribution to the response at the start of a BCV-evoked response (Fig. 6A). Ultimately, the VM is most easily interpreted during the stimulus, where onset transients can be avoided. This does not isolate hair cell from neural potentials entirely, but nonetheless provides a simpler representation of the hair cell response.

To enhance the contribution of a specific subset of hair cells to the VM response, the VM should be recorded from within the vestibule, as close to the target hair cell group as possible, and using mechanisms to reduce electrical pickup from neighboring hair cells and neurons.

To the best of our knowledge the current study is the first report of an *in vivo* VM recorded using a ventral surgical approach, allowing direct access to the utricular macula. This allowed highly localized recordings from the surface of the macula, reducing the relative electrical contribution from the semicircular canals or saccule, making interpretation of the VM simpler. The highly localized nature of the VM recorded from the surface of the macula was evident in the changes in VM phase across the striola region, and as the microelectrode was passed through the macula.

The changes in the VM phase and polarity, and the VM cancellation or frequency-doubling when recorded from the central macula region, has been reported in other lateral line (Jielof et al., 1952; Krose et al., 1980) and otolithic hair cell studies (Furukawa & Ishii et al., 1967; Corey and Hudspeth, 1983). The effect is most likely due to the unique polarization of the otolithic and lateral line organs (Corey and Hudspeth, 1983), further demonstrating the VM represents the activity of the hair cells local to the recording location. Just how 'local' the recording is (i.e. what distribution of hair cells contribute to the response), is not currently clear, but most likely depends largely on the electrical impedance of the fluids overlying the utricular macula surface, given that an increase in the fluid volume within the vestibule significantly reduces the VM amplitude due to electrical shorting (Fig. 5).

The macula surface map in Fig. 10 reveals VMs of opposite phase either side of the polarization reversal line, and frequency-doubled VMs close to this line. That said, the VMs of either phase contain 'inflections' on the negative phase of the response. These inflections are most likely residual electrical contributions from hair cells on the opposite side of the line of polarity reversal, rather than neural contributions, as neural contributions would have a fixed delay

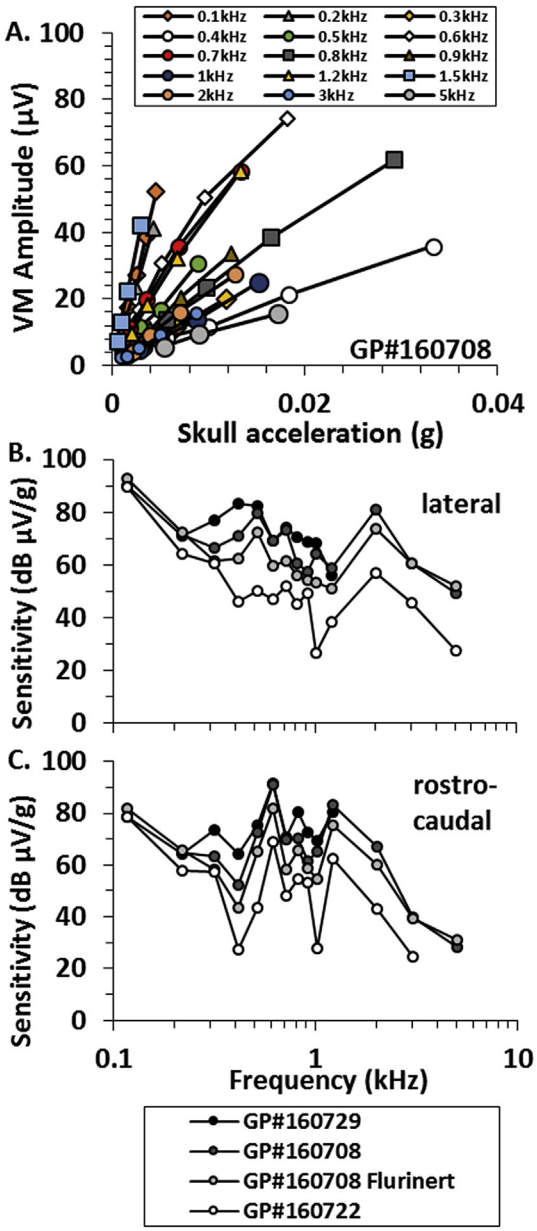

Fig. 14. A) The peak to peak amplitude of the VM (in μV), evoked by continuous BCV vibration at different frequencies and levels, plotted against the peak to peak skull acceleration (in g). The frequencies of each I/O series are shown in the legend. This series is from animal GP#160708. B) The slope (or sensitivity, presented in dB μV/g)) for each I/O series, obtained from a linear regression trendline, plotted against the BCV frequency. Here, the sensitivity was obtained from 3 different animals (animal numbers indicated at bottom of figure), and plotted against the acceleration in the lateral direction. C) The same plots as that presented in B, but for the acceleration in the rostro-caudal direction.

within the VM response rather than occurring at a fixed phase of the VM, regardless of where the response was recorded. It therefore seems that even when the VM is recorded from the surface of the macula, it may not be a purely local potential.

Ex vivo recordings from vestibular hair cells offer important insights into their biophysical processes, such as hair bundle mechanosensory function (Venturino et al., 2015; Salvi et al., 2015), selective ion channel mechanics (Corey and Hudspeth, 1979), hair cell adaptation (Cheung and Corey, 2006), and peripheral efferent vestibular hair cell control (Castellano-Munoz et al., 2010). However, there are numerous differences between an *ex vivo* and *in vivo* experimental preparation, such as differences in blood supply, neural innervation, mechanics, and extracellular fluid composition.

The ventral surgical approach developed in the present study exposes the entire basal surface of the utricular macula, permitting direct experimental manipulations of the utricle. For example, in the present study we demonstrated changes in the VM response during physical displacement the utricular macula (Fig. 12). The reduction in VM amplitude with a 100–200 μm displacement of the utricle was observed in three animal experiments. This reduction may either be due to a dampening of the utricular vibration if the glass probe tip imparts a stabilization of the macula, or it may be due to a reduction in the sensitivity of the utricular hair cells due to displacements of their stereocilia and receptor potential, much the same way displacement of cochlear hair cells reduces their sensitivity (Zwicker, 1977; Patuzzi et al., 1989a). Given that the VM waveform *per se* underwent complex changes during the displacement (Fig. 12A, B & C), that do not mimic a simple reduction in BCV level (Fig. 6), it seems more likely that the displacement induced changes were due to dampening of the macula vibration, although more evidence is required to differentiate the two effects. Regardless of the mechanism, the finding that a displacement of the utricular macula causes a reduction in the sensitivity of the utricle, which has been observed in similar studies from our laboratory (Chihara et al., 2013), suggests that pathologies such as endolymphatic hydrops, where the utricle volume is increased, may cause changes in the sensitivity of the utricle by way of a displacement of the macula rather than ionic disturbances or damage to the hair cells *per se*. However, the kinetics of endolymphatic hydrops is vastly different to the mechanical manipulations imparted on the utricular macula by our blunt micropipette, and we cannot faithfully use our results as an indication of changes that would be expected with a pathological displacement of the otolith macula.

A common theory for the mechanism whereby endolymphatic hydrops may cause a loss of vestibular sensitivity is a rupture of the membranous labyrinth (Kingma and Wit, 2009). We attempted to mimic a rupture of the utricle by manually puncturing a small hole in the utricular membrane, away from the macula. Whilst we have not obtained histological evidence of this tear, care was taken to keep it less than 0.1 mm wide, and not to disturb the nearby macula. Tearing the utricle caused a rapid and permanent decrease in the VM, which we tentatively assume is due to a mixing of the perilymph and endolymph on the basal surface of the utricular macula, causing similar effects as previously reported by Kingma and Wit (2009) who injected 150 mM KCl into the vestibule. To clarify the effect of an increase in $[K^+]$ within the vestibule on the function of the utricle, future studies will need to vary the $[K^+]$ within the vestibule whilst monitoring the VM.

Our results regarding changes in the BCV frequency demonstrate that in our recording setup, the VM can be readily evoked by vibrations between 100 Hz and 5 kHz. Higher or lower frequencies may evoke VM responses, but we would require significantly more acceleration. These results conflict with those reported by Trincker (1959), who documented VMs recorded to BCV frequencies between 300 Hz and 120 kHz. Such 'ultrasonic' VMs beyond 100 kHz seem questionable, as the otoliths do not appear to respond to frequencies higher than several kilohertz (Curthoys et al., 2006, 2012), assuming that neural activity is a fair representation of hair cell response. Curthoys et al. (2016) reported that utricular primary afferent neurons were synchronized up to 1.5 and 3 kHz, for BCV and ACS stimuli, respectively (Curthoys et al., 2016). Furthermore, *ex vivo*, bullfrog saccular microphonics were recorded at similar frequencies by probe displacement (Corey and Hudspeth, 1983). The fact that these afferent neurons are closely locked to the

stimulus cycle at this high frequency suggests that their associated stereocilia must also be mechanically responsive at these frequencies.

In our experimental set-up, the sensitivity of the VM, determined from the slope of the I/O plots, with the VM and acceleration evoked by continuous BCV vibrations rather than BCV bursts, was largest at 100 Hz. Whilst low-frequency BCV stimuli produced the steepest I/O slope, our bone-conductor was less efficient at transferring vibrations to the skull at lower frequencies, which is why only relatively small VM amplitudes are reported for BCV stimuli at 100–200 Hz (at high intensities, there was noticeable distortion of the acceleration).

Conversely, responses were insensitive at higher frequencies, with the sensitivity declining steeply above 1.5 kHz. However, the fact that our tri-axial accelerometer had a first-order low-pass filter at approximately 1.5 kHz makes estimation of the VM sensitivity above this frequency less reliable. This is also likely why the BCV-pulse acceleration response (Fig. 3C) appears as a damped resonance, with little high frequency content. It should be noted that whilst in our setup the VM sensitivity was highest at lower frequencies, this is largely dependent on where the acceleration is measured. That is, without measuring the acceleration of the utricular macula directly, which is likely to have a different frequency response than the ear-bar, we cannot define the frequency sensitivity of the guinea pig macula, which may be different in a different experimental setup. Determining the frequency response of the utricular hair cells will require a direct measurement of macula vibration, in much the same way laser interferometry or similar techniques have been applied to further our understanding of cochlear mechanics (Ren et al., 2003). Such measurements, performed *in vivo*, will potentially further our understanding of the mechanical properties of the otolith organs.

Acknowledgement

This study was funded in part by The Medical Foundation of The University of Sydney, with funds raised by the Meniere's Research Fund Inc.

References

Adrian, E., Craik, K., Sturdy, R., 1938. The electrical response of the auditory mechanism in cold-blooded vertebrates. In: Proceedings of the Royal Society of London. Series B, Biological Sciences, vol. 125 (841), pp. 435–455.
Ashcroft, D., Hallpike, C., 1934. On the function of the saccule. J. Laryngol. Otol. 49 (7), 450–460.
Baird, R., Desmadryl, G., Fernandez, C., Goldberg, J., 1988. The vestibular nerve of the chinchilla. II. Relation between afferent response properties and peripheral innervation patterns in the semicircular canals. J. Neurophysiol. 60 (1), 182–203.
Böhmer, A., 1995. Short latency vestibular evoked responses to linear acceleration stimuli in small mammals: masking effects and experimental applications. Acta Oto-Laryngologica 115 (Suppl. 520), 120–123.
Böhmer, A., Hoffman, L.F., Honrubia, V., 1995. Characterization of vestibular potentials evoked by linear acceleration pulses in the chinchilla. Otol. Neurotol. 16 (4), 498–504.
Brown, D.J., Hartsock, J.J., Gill, R.M., Fitzgerald, H.E., Salt, A.N., 2009. Estimating the operating point of the cochlear transducer using low-frequency biased distortion products. J. Acoust. Soc. Am. 125 (4), 2129–2145.
Castellano-Muñoz, M., Israel, S.H., Hudspeth, A., 2010. Efferent control of the electrical and mechanical properties of hair cells in the bullfrog's sacculus. PLoS One 5 (10), e13777.
Cheatham, M., Huynh, K., Gao, J., Zuo, J., Dallos, P., 2004. Cochlear function in Prestin knockout mice. J. Physiol. 560 (3), 821–830.
Cheatham, M.A., Naik, K., Dallos, P., 2011. Using the cochlear microphonic as a tool to evaluate cochlear function in mouse models of hearing. J. Assoc. Res. Otolaryngol. 12 (1), 113–125.
Cheung, E.L., Corey, D.P., 2006. Ca 2+ changes the force sensitivity of the hair-cell transduction channel. Biophys. J. 90 (1), 124–139.
Chihara, Y., Wang, V., Brown, D.J., 2013. Evidence for the utricular origin of the vestibular short-latency-evoked potential (VsEP) to bone-conducted vibration in Guinea pig. Exp. Brain Res. 229 (2), 157–170.
Conlee, J.W., Abdul-Baqi, K.J., McCandless, G.A., Creel, D.J., 1988. Effects of aging on normal hearing loss and noise-induced threshold shift in albino and pigmented Guinea pigs. Acta oto-laryngologica 106 (1–2), 64–70.
Corey, D., Hudspeth, A., 1979. Ionic basis of the receptor potential in a vertebrate hair cell. Nature 281 (5733), 675–677.
Corey, D., Hudspeth, A., 1983. Analysis of the microphonic potential of the bullfrog's sacculus. J. Neurosci. 3 (5), 942–961.
Curthoys, I., Betts, G., Burgess, A., MacDougall, H., Cartwright, A., Halmagyi, G., 1999. The planes of the utricular and saccular maculae of the Guinea pig. Ann. N. Y. Acad. Sci. 871 (1), 27–34.
Curthoys, I.S., Kim, J., McPhedran, S.K., Camp, A.J., 2006. Bone conducted vibration selectively activates irregular primary otolithic vestibular neurons in the Guinea pig. Exp. Brain Res. 175 (2), 256–267.
Curthoys, I.S., Vulovic, V., Burgess, A.M., Sokolic, L., Goonetilleke, S.C., 2016. The response of Guinea pig primary utricular and saccular irregular neurons to bone-conducted vibration (BCV) and air-conducted sound (ACS). Hear. Res. 331, 131–143.
Curthoys, I.S., Vulovic, V., Sokolic, L., Pogson, J., Burgess, A.M., 2012. Irregular primary otolith afferents from the Guinea pig utricular and saccular maculae respond to both bone conducted vibration and to air conducted sound. Brain Res. Bull. 89 (1), 16–21.
Desai, S.S., Zeh, C., Lysakowski, A., 2005. Comparative morphology of rodent vestibular periphery. I. Saccular and utricular maculae. J. Neurophysiol. 93 (1), 251–266.
Dimiccoli, M., Girard, B., Berthoz, A., Bennequin, D., 2013. Striola magica. A functional explanation of otolith geometry. J. Comput. Neurosci. 35 (2), 125–154.
Eatock, R., Corey, D., Hudspeth, A., 1987. Adaptation of mechanoelectrical transduction in hair cells of the bullfrog's sacculus. J. Neurosci. 7 (9), 2821–2836.
Fernandez, C., Goldberg, J.M., 1976a. Physiology of peripheral neurons innervating otolith organs of the squirrel monkey. II. Directional selectivity and force-response relations. J. Neurophysiol. 39 (5), 985–995.
Fernandez, C., Goldberg, J.M., 1976b. Physiology of peripheral neurons innervating otolith organs of the squirrel monkey. III. Response dynamics. J. Neurophysiol. 39 (5), 996–1008.
Fitzgerald, J.J., Robertson, D., Johnstone, B.M., 1993. Effects of intra-cochlear perfusion of salicylates on cochlear microphonic and other auditory responses in the Guinea pig. Hear. Res. 67 (1), 147–156.
Furukawa, T., Ishii, Y., Matsuura, S., 1972. An analysis of microphonic potentials of the sacculus of goldfish. Jpn. J. Physiol. 22 (6), 603–616.
Guinan Jr., J.J., 1996. Physiology of Olivocochlear Efferents the Cochlea. Springer, pp. 435–502.
Harris, D.M., Dallos, P., 1984. Ontogenetic changes in frequency mapping of a mammalian ear. Science 225, 741–744.
Henry, K.R., 1995. Auditory nerve neurophonic recorded from the round window of the Mongolian gerbil. Hear. Res. 90 (1), 176–184.
Hudspeth, A.J., 1982. Extracellular current flow and the site of transduction by vertebrate hair cells. J. Neurosci. 2 (1), 1–10.
Huizinga, E., De Vries, H., Vrolijk, J., 1951. Analysis of the microphonic activity of the labyrinth of the pigeon into the contributions of the various parts. Acta otolaryngologica 39 (5), 372–379.
Jaeger, R., Kondrachuk, A., Haslwanter, T., 2008. The distribution of otolith polarization vectors in mammals: comparison between model predictions and single cell recordings. Hear. Res. 239 (1), 12–19.
Jielof, R., Spoor, A., De Vries, H., 1952. The microphonic activity of the lateral line. J. Physiol. 116 (2), 137.
Kachar, B., Parakkal, M., Fex, J., 1990. Structural basis for mechanical transduction in the frog vestibular sensory apparatus: I. The otolithic membrane. Hear. Res. 45 (3), 179–190.
Kingma, C., Wit, H., 2009. Acute endolymphatic hydrops has no direct effect on the vestibular evoked potential in the Guinea pig. J. Vestib. Res. 19 (1, 2), 27–32.
Krose, A.B., Van Der Zalm, J.M., Van Den Bercken, J., 1980. Extracellular receptor potentials from the lateral-line organ of Xenopus laevis. J. Exp. Biol. 86 (1), 63–77.
Kumagami, H., Nishida, H., Moriuchi, H., 1981. Changes of the action potential, the summating potential and cochlear microphonics in experimental endolymphatic hydrops. ORL 43 (6), 314–327.
Legan, P.K., Lukashkina, V.A., Goodyear, R.J., Kössl, M., Russell, I.J., Richardson, G.P., 2000. A targeted deletion in α-tectorin reveals that the tectorial membrane is required for the gain and timing of cochlear feedback. Neuron 28 (1), 273–285.
Lodhi, S., Weiner, N.D., Mechigian, I., Schacht, J., 1980. Ototoxicity of aminoglycosides correlated with their action on monomolecular films of polyphosphoinositides. Biochem. Pharmacol. 29 (4), 597–601.
Lowenstein, O., Roberts, T., 1951. The localization and analysis of the responses to vibration from the isolated elasmobranch labyrinth. A contribution to the problem of the evolution of hearing in vertebrates. J. Physiol. 114 (4), 471.
Patuzzi, R., Moleirinho, A., 1998. Automatic monitoring of mechano-electrical transduction in the Guinea pig cochlea. Hear. Res. 125 (1), 1–16.
Patuzzi, R.B., Yates, G.K., Johnstone, B.M., 1989a. Changes in cochlear microphonic and neural sensitivity produced by acoustic trauma. Hear. Res. 39 (1–2), 189–202.
Patuzzi, R.B., Yates, G.K., Johnstone, B.M., 1989b. The origin of the low-frequency microphonic in the first cochlear turn of Guinea-pig. Hear. Res. 39 (1), 177–188.
Rabbitt, R.D., Boyle, R., Holstein, G.R., Highstein, S.M., 2005. Hair-cell versus afferent adaptation in the semicircular canals. J. Neurophysiol. 93 (1), 424–436.
Ren, T., Zou, Y., Zheng, J., Nuttall, A., Porsov, E., Matthews, S., 2003. Measurement of

basilar membrane vibration using a scanning laser interferometer. In: Paper Presented at the Biophysics of the Cochlea. From Molecules to Models.
Salvi, J.D., Maoiléidigh, D.Ó., Fabella, B.A., Tobin, M., Hudspeth, A., 2015. Control of a hair bundle's mechanosensory function by its mechanical load. Proc. Natl. Acad. Sci. 112 (9), E1000–E1009.
Shotwell, S.L., Jacobs, R., Hudspeth, A.J., 1981. Directional sensitivity of individual vertebrate hair cells to controlled deflection of their hair bundles. Ann. N. Y. Acad. Sci. 374, 1–10.
Snyder, R., Schreiner, C., 1984. The auditory neurophonic: basic properties. Hear. Res. 15 (3), 261–280.
Spoedlin, H., 1966. The Vestibular System and its Diseases. University of Pennsylvania Press, Philadelphia.
Steel, K.P., Barkway, C., Bock, G.R., 1987. Strial dysfunction in mice with cochleo-saccular abnormalities. Hear. Res. 27 (1), 11–26.
Trincker, D., 1959. Electrophysiological studies of the labyrinth of the Guinea pig. II. The changes of the DC potentials inside the ampullae of the semicircular canals during experimental cupula deviations. Ann. Otol., Rhinol., Laryngol. 68 (1), 148–152.
Venturino, A., Oda, A., Perin, P., 2015. Hair cell-type dependent expression of basolateral ion channels shapes response dynamics in the frog utricle. Front. Cell. Neurosci. 9.
Wever, E.G., Bray, C.W., 1930. Action currents in the auditory nerve in response to acoustical stimulation. Proc. Natl. Acad. Sci. 16 (5), 344–350.
Wit, H., Kahmann, H., Segenhout, J., 1986. Vestibular microphonic potentials in pigeons. Eur. Arch. Oto-Rhino-Laryngol. 243 (2), 146–150.
Zotterman, Y., 1943. The microphonic effect of teleost labyrinths and its biological significance. J. Physiol. 102 (3), 313.
Zwicker, E., 1977. Masking-period patterns produced by very-low-frequency maskers and their possible relation to basilar-membrane displacement. J. Acoust. Soc. Am. 61 (4), 1031–1040.

3.3. Conclusion

The UM[1] provides the means to simply and objectively measure utricular hair cell function using clinically relevant stimuli. It also permits the simultaneous recording of gross nerve function (the VsEP) to distinguish nerve dysfunction from sensory receptor loss, *in vivo*. One difficulty in interpreting the UM is the uncertainty regarding exactly which hair cells contribute to the response. With minimal fluid overlying the macula, the extracellular spread of the receptor current from hair cells is likely reduced greatly by the relatively high impedance of the macular epithelia[2], and we estimate, based on recordings performed across the surface of the macula, that the UM reflects the receptor current of hair cells within approximately 0.1mm from the tip of the pipette. Certainly, with fluid filling the vestibule, the UM amplitude was much smaller, and the waveform more sinusoidal, suggesting a broader electrical pick-up. This issue is less of a problem when interpreting the CM waveform recorded from the base of the cochlea, because low-frequency (~200Hz) tones are typically used to evoke the CM, and here hair cells in the entire basal turn are moving in unison. This generates a consistent CM response (Patuzzi, Yates et al. 1989, Withnell 2001, Cheatham, Naik et al. 2011) reflecting 'local' cochlear hair cell activity. Unfortunately, the utricular macular has a larger diversity of hair cells (Desai, Zeh et al. 2005), within a smaller region of epithelia, and thus more effort is needed to provide a UM response that is easily interpreted.

Recordings of the UM could potentially be improved through the use of a bipolar concentric electrode, to obtain a localized measure of hair cell activity, irrespective of how much fluid was in the vestibule. This may permit more reliable monitoring of MET channel gating analogous to the low frequency CM in the mammalian cochlea. For an example of Boltzmann analysis applied to a saturated low-frequency UM response see Appendix 1, Figure 2. Presently, with minimal fluid in the vestibule, our results are consistent with the UM being a measure of local utricular hair cell transduction. Having said that, it is likely that recordings made on or very close to the utricular polarization zone, where the dichotomous hair cell currents may partially cancel, may not be feasible, limiting UM responses to measures of hair cell function in extra-striolar regions. Measurements of hair cell function in the polarization reversal zone may require

[1] In chapter 3, the name of the response, the Vestibular Microphonic (abbreviated as VM) was kept somewhat broad, to not prematurely suggest the origin of the response, prior to our systematic investigation. Moreover, the VM was recorded from several locations, including the saccular otoconia and the facial nerve canal. For the remainder of the thesis the response is titled the Utricular Microphonic (abbreviated as the UM) describing the localized extracellular receptor potential recorded from the surface of the utricular macula.

[2] The spread of the hair cell current dipole would be larger in a low-resistance medium. Without perilymph in the vestibule, the current is 'forced' to return through the macula, limiting current spread, increasing local voltage drops.

intracellular hair cell recordings, although it is likely that such measurements may interfere with the vibration of the macular hair cells.

Whilst we have not attempted to do so, it may be possible to measure a microphonic from the semi-circular canals. Given there is no polarity reversal of semi-circular canal hair cells, it may not be necessary to drain the fluid from the canals (which would greatly interfere with their function) to obtain a localized measure of hair cell current. Previous studies have already recorded microphonic responses from the semicircular canals of non-mammalian species (Wit, Kahmann et al. 1986, Rabbitt, Boyle et al. 2005).

Finally, although BCV was the only stimulus used in this chapter, ACS can also be used to evoke UMs, however it is technically more challenging to transduce ACS to the macule when there is minimal fluid in the vestibule, and the need to preserve some of this fluid results in more electrical shorting of the UM (see Chapter 4).

Chapter 4: Measurement of utricular macula vibration

4.1. Introduction

Aside from the seminal work of von Békésy in the early 20th century (Békésy 1928, Békésy 1952, Von Békésy and Wever 1960), the first quantifiable *in vivo* measurements of the basilar membrane vibration in mammals was in 1967 by Johnstone and Boyle. Since then, numerous techniques have been used to measure the vibration of the organ of Corti in response to sound (Nuttall and Fridberger 2012). Measurements of the organ of Corti vibration, coupled with functional response measurements, have formed our understanding of cochlear sensitivity (Johnstone, Patuzzi et al. 1986, Ruggero, Robles et al. 1986, Russell and Murugasu 1997, Robles and Ruggero 2001). Moreover, these measures have been used to study auditory health and disease using experimental manipulations such as noise trauma (Patuzzi, Johnstone et al. 1984), drug administrations (Ruggero and Rich 1991) and endolymphatic hydrops (Ding, Xu et al. 2016). Importantly, they have also led to foundational discoveries such as the role of the olivocochlear efferent system (Murugasu and Russell 1996) and the cochlear active process (Rhode 1971, Patuzzi, Sellick et al. 1982, Manley 2001). By contrast, very little in the way of similar 'mechanics' research has been performed in the vestibular system. Arguably, because the cochlea is relatively easy to access surgically, particularly in experimental animals such as guinea pigs, whereas accessing the vestibular hair cells typically requires more invasive surgical strategies. Nevertheless, as seen in the previous chapter, the utricle can be accessed after removal of the cochlea, with the utricular hair cells and neurons still appearing to function quite normally (the VsEP changes little before and after cochlear removal; (Jones, Jones et al. 1997, Chihara, Wang et al. 2013)). With the entire utricular macula exposed, the possibility to measure the mechanical vibration of the utricular macula *in vivo* is presented.

There are several methods available to record mechanical responses from the inner ear such, as using the Mössbauer technique, capacitance probe, laser interferometry, velocimetry/vibrometry and Charge-couple device imaging (Ruggero and Rich 1991, Rabbitt, Boyle et al. 2010, Nuttall and Fridberger 2012). Here, we chose to use a commercial Laser Doppler Vibrometer to measure the utricular macular vibration for the first time, as it was the simplest to implement in our laboratory setup. Additionally, as LDV does not require placing any probes into the vestibule, it allowed space to perform simultaneous measurements of vestibular nerve, hair cell and mechanical function. The following manuscript demonstrates the first recordings of utricular macula mechanics, along with simultaneous functional measures in the UM and VsEP.

4.2. Dynamic response to sound and vibration of the guinea pig utricular macula, measured *in vivo* using Laser Doppler Vibrometry.

Pastras, C. J., Curthoys, I. S., & Brown, D. J. (2018). Dynamic response to sound and vibration of the guinea pig utricular macula, measured in vivo using laser Doppler vibrometry. *Hearing research*, *370*, 232-237.

Hearing Research 370 (2018) 232–237

Contents lists available at ScienceDirect

Hearing Research

journal homepage: www.elsevier.com/locate/heares

Short communication

Dynamic response to sound and vibration of the guinea pig utricular macula, measured *in vivo* using Laser Doppler Vibrometry

Christopher John Pastras [a, *], Ian S. Curthoys [b], Daniel John Brown [a]

[a] The Meniere's Laboratory, Sydney Medical School, The University of Sydney, Sydney, NSW, 2050, Australia
[b] Vestibular Research Laboratory, The University of Sydney, School of Psychology, Sydney, NSW, 2050, Australia

ARTICLE INFO

Article history:
Received 23 May 2018
Received in revised form
1 August 2018
Accepted 20 August 2018
Available online 24 August 2018

ABSTRACT

With the use of a commercially available Laser Doppler Vibrometer (LDV) we have measured the velocity of the surgically exposed utricular macula in the dorsoventral plane, in anaesthetized guinea pigs, during Air Conducted Sound (ACS) or Bone Conducted Vibration (BCV) stimulation. We have also performed simultaneous measurements of otolithic function in the form of the Utricular Microphonic (UM) and the Vestibular short-latency Evoked Potential (VsEP). Based on the level of macular vibration measured with the LDV, the UM was most sensitive to ACS and BCV between 100 and 200 Hz. The phase of the UM relative to the phase of the macular motion was relatively consistent across frequency for ACS stimulation, but varied by several cycles for BCV stimulation, suggesting a different macromechanical mode of utricular receptor activation. Moreover, unlike ACS, BCV evoked substantially distorted UM and macular vibration responses at certain frequencies, most likely due to complex resonances of the skull. Analogous to LDV studies of organ of Corti vibration, this method provides the means to study the dynamic response of the utricular macula whilst simultaneously measuring function.

1. Introduction

Whilst the mechanics of the semicircular canals are generally understood (Rabbitt et al., 1996; Iversen and Rabbitt, 2017), with the stimulus typically viewed as trans-cupula (Rabbitt et al., 2001), the same cannot be said about the otolithic organs, which can respond to head movement in almost any direction (Jaeger et al., 2008) as well as to sound and vibration above 1000 Hz (Curthoys et al., 2016).

Most of our knowledge regarding the mechanical properties of the otoliths is derived from pre-1950s *in vivo* studies, or more recent *ex-vivo* experiments, typically from non-mammalian animals (Dunlap et al., 2012). Tullio, 1929 was the first to measure the motion of the otolithic maculae using aluminum particles placed on the utricular epithelium in the pigeon, in response to ACS, suggesting that the utricular macula moved like a trampoline (Richard, 1916; Tullio, 1929). Later, De Vries used x-rays to measure the displacement of the ruff (fish) sacculus, concluding it was critically damped with a resonant frequency around 50 Hz (De Vries, 1950). Estimates of the smaller mammalian otolith were indirectly approximated using differential equations suggesting a resonant frequency around 400 Hz (Goldberg and Fernández, 1976; Fernández and Goldberg, 1976a). High speed video of *ex vivo* preparations of the turtle utricular maculae have also been used to derive otolith transfer functions and suggest the end organ functions as an accelerometer with a bandwidth between DC and its natural corner frequency, around 400 Hz (Dunlap and Grant, 2014). More recently it has been shown that guinea pig utricular and saccular afferents respond with tightly phase locked responses to frequencies of sound and vibration far above 400 Hz (Curthoys et al., 2016).

It should be emphasized that to date, no studies have directly measured the utricle's mechanical response properties *in vivo*, and our understanding of otolithic mechanics continue to rely mostly on theoretical models and numerical simulations.

From a neural response perspective, the otoliths have been viewed as low-frequency, static transducers, however, recent studies demonstrate the mammalian utricle produces mechanical and neural responses to much higher frequencies (Curthoys et al., 2016; Pastras et al., 2017). High-frequency BCV or ACS have been recently used in the clinic to evoke otolithic reflex responses (Rosengren et al., 2010), and changes in reflex tuning has been used as a diagnostic tool

* Corresponding author. Brain and Mind Centre, The University of Sydney, 100 Mallett St. Camperdown, Sydney, NSW, 2050, Australia.
E-mail address: cpas8047@uni.sydney.edu.au (C.J. Pastras).

https://doi.org/10.1016/j.heares.2018.08.005
0378-5955/

in Meniere's disease (Sandhu et al., 2012). Importantly, we currently lack a clear understanding of how or why the mechanical response properties of the utricle may be altered in pathological states, and furthermore whether there are any differences in macromechanical receptor activation of the utricle across ACS and BCV.

To better understand utricle function and mechanics we have performed simultaneous measures of utricular responses *in vivo,* in guinea pigs. The Utricular Microphonic (UM) has been measured as an indicator of hair cell function, the Vestibular short latency Evoked Potential (VsEP) has been measured as a gross indicator of neural function, and Laser Doppler Vibrometry (LDV) measurements have been used as an indicator of macular vibration. This approach is similar to numerous studies in the cochlea that have combined recordings of the cochlear microphonic, compound action potential, and basilar membrane vibration, to provide a clearer understanding of cochlear mechanics and function (Nuttall et al., 1991; Ruggero et al., 1997; Fridberger et al., 2004).

2. Methods

Experiments were performed on 17 adult tri-colored guinea pigs (*Cavia porcellus)*, of either sex weighing between 300 and 500 g. All experimental procedures were approved by The University of Sydney Animal Ethics Committee. Animals received pre-anaesthetic intraperitoneal injections of atropine sulphate (0.6 mg/ml; Apex, Aus.), and Temgesic (buprenorphreine hydrochloride, 324 μg/ml; Reckitt Benckiser, NZ) and were thereafter anaesthetized using Isoflurane (2–4%; IsoFlo). Once lacking a foot-withdrawal reflex, animals were transferred to the surgical table, tracheotomized and artificially ventilated with oxygen.

For details describing surgical access to the facial nerve canal (for VsEP recording) and utricular macula (for UM recording) see Pastras., 2017. Briefly, the cochlea was accessed from a ventral approach, and then surgically removed leaving an unobstructed view of the basal surface of the utricular macula (Fig. 1B). Reflective microbeads (40 μm diameter) were placed onto the macula surface and nearby bone. A commercial LDV (Ometron – Type 8338, Denmark) was mounted on an isolated stage, and the beam steered onto the reflective beads with the aid of a mirror (Fig. 1A). For methods detailing the recording of the UM (Fig. 1B) refer to Pastras et al., 2017, and for details on the recording of the VsEP refer to Pastras et al., 2018. Measurements of function (VsEP and UM) and mechanics (macular velocity from the LDV and skull acceleration from a 3-axis accelerometer fixed to the ear-bar) were performed simultaneously, in response to both BCV and ACS. To stimulate the utricular macula using ACS, the tympanum and ossicular chain were left intact, and a fluid pathway between the stapes foot plate and macula maintained. Controls to remove this fluid or dislodge the stapes reduced responses considerably, demonstrating the importance of this pathway for ACS stimulus coupling. The level of fluid was kept low with the use of a nearby tissue wick, such that the beads were not fully immersed, to avoid the artifact described by Cooper and Rhode (1992), where fluid surface movements introduce additional frequency shifts in the path of the LDV beam. Thus, the experimental setup involved the non-ideal situation where there was no fluid loading on the utricular macula because the vestibule was largely empty.

Stimuli and responses were generated and recorded using custom-developed LabVIEW (National Instruments, TX, USA) programs. BCV and ACS stimuli were generated using an external soundcard (SoundblasterX7, Creative Inc., Singapore). Biopotential responses were amplified and band-pass filtered (1 Hz–10 kHz; IsoDAM 8, WPI, USA) before being digitized. The VsEP was evoked by a 0.6 ms Gaussian monophasic BCV-pulse, while the UM was evoked by continuous sinusoidal BCV and ACS tones between 100 and 2000 Hz. The amplitude and phase of the UM was directly compared to measurements of the macula velocity or ear bar acceleration amplitude and phase. In an attempt to simplify interpretation and make comparison of responses evoked across frequencies simpler, the level of the BCV or ACS stimulus was adjusted at each frequency to maintain a fixed 'iso-amplitude' of either the UM or the macular vibration. The amplitude, relative phase, and Total Harmonic Distortion (THD) of each response measure was recorded from a 100 ms response window.

3. Results

Continuous ACS or BCV evoked sinusoidal UM and macular velocity responses (Fig. 1Ci and 1Cii), although the responses appeared distorted at certain frequencies, particularly for BCV stimulation. Pulsed ACS and BCV (Fig. 1D), could also be used to evoke UM and macular vibration, along with VsEP responses.

Utricular responses to continuous ACS that evoked an iso-macular vibration response close to 2 μm/s (a relatively low-level of macular vibration in our setup; Fig. 2A) evoked sinusoidal UM and utricular macula responses that had minimal distortion (Fig. 2B) across all ACS frequencies between 100 and 1000 Hz (Fig. 2A and B). For this level of macular velocity (2 μm/s across all frequencies), the UM amplitude showed a tuned response, being largest at 150 Hz, and declining with frequency (Fig. 2B). The UM phase led the macular vibration phase by close to ¼ cycle across all frequencies (Fig. 2C). Unsurprisingly, the earbar acceleration in response to ACS was almost completely absent (Fig. 2D).

In comparison to ACS, continuous BCV, which evoked macular vibration close to 2 μm/s, resulted in UM responses and macular vibration waveforms that appeared distorted at particular frequencies (Figs. 1Cii, 2E and 2F). Distortion in the UM and macular vibration coincided with distortion in the earbar acceleration, suggesting that at these frequencies the distortion was due to system distortion (i.e. of the BCV transducer and skull) and was unavoidable (Fig. 2E, F and H). Notably, for the same level of macular velocity the UM amplitude was approximately 4 times larger during BCV compared to ACS (Fig. 2B vs. 2F), however it should be noted that for ACS stimulation a fluid layer remained over the macular surface (which was not the case for BCV), which can affect the amplitude of the UM (Pastras et al., 2017).

For BCV, the UM phase was similar to the phase of the macular vibration between 100 and 200 Hz, but as frequency increased the UM gradually developed a phase-lag of up to 4 cycles at 1000 Hz (Fig. 2G).

Inter-animal comparisons of iso-macular velocity recordings indicated that the amplitude of the UM (or rather its first harmonic) was largest between 100 and 200 Hz for both ACS ($n = 3$, Fig. 2J) and BCV ($n = 7$, Fig. 2L).

To further explore the sensitivity of the utricle, the stimulus level was instead adjusted to maintain a UM amplitude close to 50 μV (an 'iso-UM' rather than 'iso-vibration' plot; Fig. 2M and O). For ACS stimulation, macular velocity was small between 100 and 300 Hz, increasing to a maximum velocity of 12 μm/s between 500 and 600 Hz. BCV stimulation produced a similar trend, inducing faster macular motion at higher frequencies (for the same UM amplitude – although again response distortion make comparisons difficult across frequency), but overall slower macular vibration was required for BCV compared to ACS to induce a 50 μV UM (Fig. 2M and O). With regards to the phase of the UM relative to the phase of the macular vibration, the trend for iso-UM plots (Fig. 2N and P) was similar to that observed with iso-vibration plots (Fig. 2C and G). That is, ACS stimulation resulted in a relatively constant phase relationship, whereas the phase relationship was more complex with BCV stimulation.

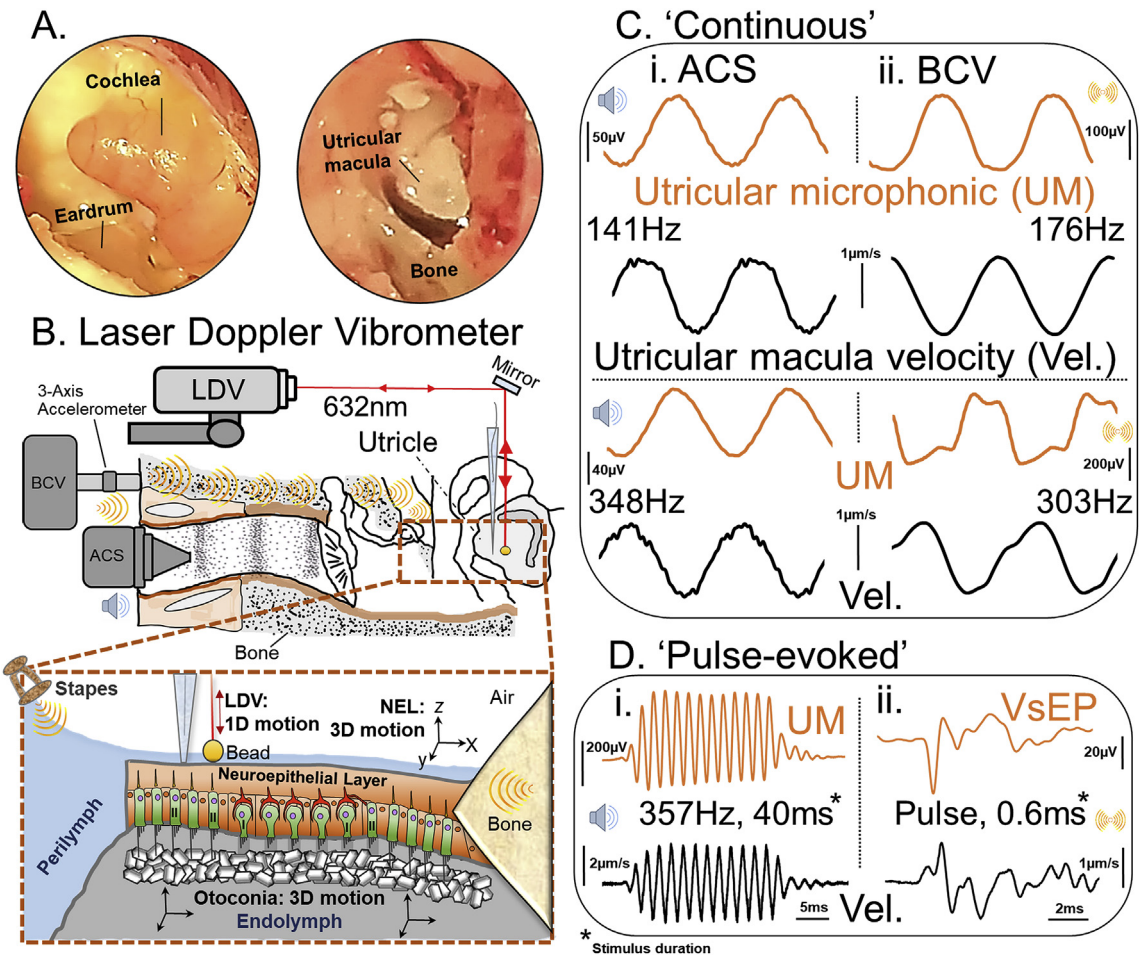

Fig. 1. A) Steps of surgical exposure of the basal surface of the utricular macula. B) Schematic of experimental setup showing simultaneous recording of the Utricular Microphonic (UM) and utricular macula velocity using Laser Doppler Vibrometry (LDV), to either Air-Conducted Sound (ACS) or Bone-Conducted Vibration (BCV), *in vivo*. Inset: Schematic cross-section showing 1D LDV relative to 3D Neuroepithelial and Otoconial motion, with simultaneous UM recordings. I: Type-I Hair cell, II: Type-II Hair cell, NEL: Neuroepithelial layer. C) Continuous i) ACS and ii) BCV evoked sinusoidal UM (orange) and macula velocity (black) recordings. Di) ACS burst evoked UM and macular velocity responses. Dii) Pulsed BCV evoked VsEP and macular velocity responses. (For interpretation of the references to color in this figure legend, the reader is referred to the Web version of this article.)

To relate utricular motion to utricular nerve function, we measured the VsEP in response to pulsed BCV over a range of levels and compared this to macular jerk to obtain a VsEP growth curve (Fig. 3).

The VsEP amplitude increased with macular jerk with a slope of 2.2 mV/g/ms below 0.015 g/ms, and with slope of just 0.2 mV/g/ms above this level. This non-linear relationship suggests the VsEP amplitude may saturate at higher levels of vibration. Notably, the latency of the VsEP decreased with increasing drive, whereas the latency of the utricular macula velocity or jerk profile did not change (Fig. 3).

4. Discussion

This is the first time both the mechanics and function of the otoliths have been recorded simultaneously in mammals, *in vivo*. We provide a simple method using a commercial LDV to monitor epithelial motion with nanometer resolution, like previous studies in cochlear mechanics (Ruggero and Rich, 1991). Recording from cochlear structures requires an unobstructed view of the site of measurement, for example, removal of the otic capsule for basilar membrane recordings (Robles et al., 1986). Similarly, exposure of the utricular macula for LDV measurements requires surgical removal of the cochlea from the ventral approach leaving the vestibular labyrinth largely dehiscent, which is likely to alter its response properties (Songer and Rosowski, 2005). Several studies that have used LDV to measure basilar membrane mechanics have 'covered' the surgical opening of the inner ear with a glass window, to reinstate a more natural cochlear state (Recio et al., 1998), noting significant changes in response properties particularly for low (<2 kHz) frequencies. To date, we have not employed such an approach in the vestibule, but it may be feasible.

It's possible that removing the vestibule fluid may alter the biological properties of the utricular hair cells similar to the effects that perilymph drainage had on basilar membrane vibration (Wilson and Johnstone, 1973). It's unclear if fluid removal in our experiments caused ionic disturbances to vestibular hair cells, potentially altering hair cell function. Mechanical amplification of hair cells has been observed in the toadfish semicircular canal (Rabbitt et al., 2010), and *ex vivo* studies in the bullfrog sacculus demonstrate that hair bundle electromechanical amplification does occur (Martin and Hudspeth, 2001), however, it is presently unknown if hair bundle electromotility exists in utricular hair cells, or if this would alter its mechanical response properties at the frequencies we have tested here. Overall, the observation that the VsEP does not change significantly after cochlear destruction (Pastras et al., 2018) suggests that vestibular hair cell function is reasonably well maintained following cochlear removal.

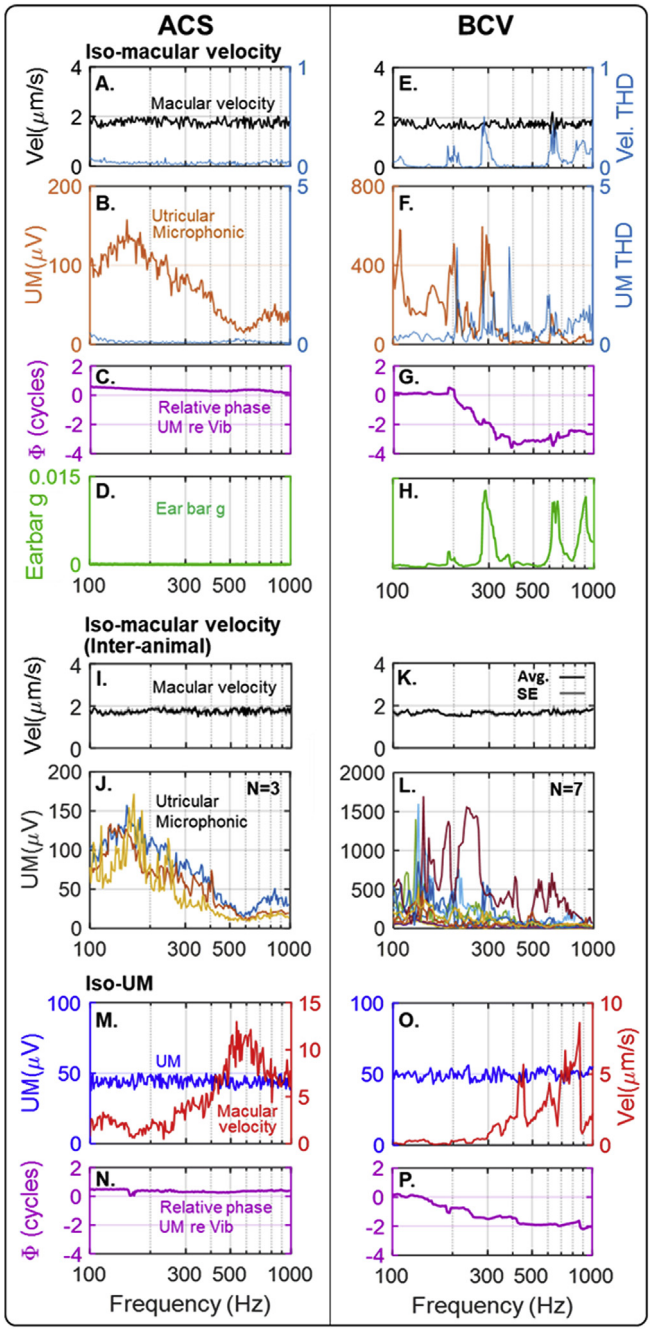

Fig. 2. Amplitude and phase frequency-responses of the UM and macular velocity to ACS (left column) and BCV (right column) stimuli. A&E) The spectral amplitude of the macular velocity and its related THD. Note that the stimulus level was automatically adjusted to maintain macular velocity near 2 μm/s across frequencies (100 Hz-1000 Hz). B&F) The spectral amplitude of the UM and its THD. C&G) The phase of the UM relative to the phase of the macular velocity. D&H) The spectral amplitude of the ear-bar acceleration (in the direction of the applied BCV force). Responses in A-H were from an example animal (GP#170829). I-L) Amplitude responses of the macular velocity (average with standard error) and individual UM plots across 3 (ACS) and 7 (BCV) animals. M – P) Amplitude and phase responses in an example animal (GP#170824) where the level of the stimulus was adjusted to maintain a constant UM amplitude, rather than a constant macular velocity.

To characterize utricular nerve sensitivity, macular vibration and the VsEP were measured simultaneously during BCV. Since the VsEP is primarily jerk-sensitive (Jones et al., 2011) we have provided levels in terms of macular jerk. Our measurements suggest VsEP thresholds to macular jerk are approximately 0.0015 g/ms.

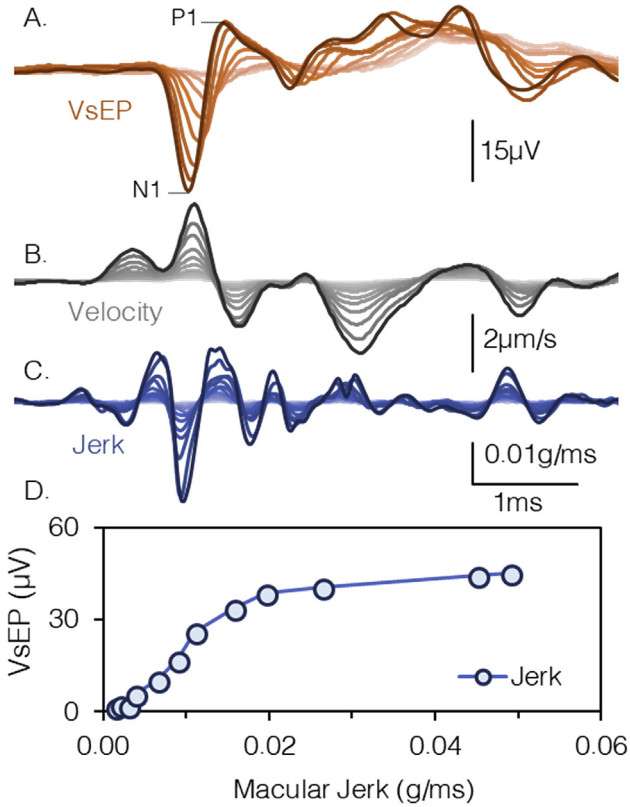

Fig. 3. A) VsEP, B) utricular macula velocity, and C) utricular macula jerk responses to increasing levels of a pulsed BCV stimulus. D). The N1–P1 amplitude of the VsEP plotted against the peak-to-peak of macular jerk. Importantly, the macular motion is measured in the transverse plane of the macula, and therefore may not accurately represent stimulation of the utricular hair cells. GP#170913.

However, it should be stressed that we are only able to measure dorsoventral ("up-down") macular vibration, and that the macular hair cells are likely to be more sensitive in the horizontal plane. Hence VsEP thresholds to macular jerk in the horizontal plane are likely to be lower than that reported here.

Regarding the appropriate stimulus for evoking utricular responses, BCV provided the simplest method of stimulating the macula. Unlike ACS stimulation, BCV did not require fluid coupling between the stapes and the macula, and thus there was less electrical shorting of the UM and no fluid interference with the LDV beam. However, at certain frequencies BCV induced UM and macular vibration responses that appeared highly distorted and decreased in peak-to-peak amplitude. Conversely, ACS stimulation produced minimal UM and macular velocity distortion, regardless of stimulus frequency. We assume that the distortion seen with BCV stimulation at certain frequencies was due to complex resonances within the skull, resulting in a complex vibration of the macula. Ultimately, if the purpose of the experiment is to monitor UM and macular vibration during experimental manipulations, BCV stimulation is sufficient to generate reliable responses, although investigators should be mindful of the frequency of the vibration, and distortion within the response. Across animals, when using an iso-vibration protocol (Fig. 2I and K), the UM was most sensitive to sound and vibration between 100 and 200 Hz (Fig. 2J and L), and generally at these frequencies there was minimal response distortion (Fig. 2F). When the stimulus level was adjusted to preserve a constant UM amplitude across stimulus frequency, the results were logically similar to that observed with iso-vibration measurements, in that again the UM was most sensitive (required the least macular

vibration) between 100 and 300 Hz.

Some researchers may be interested in how the utricular macula vibrates at different frequencies and for different stimuli. That is, it is currently unknown how the otoliths respond to high-frequency sound and vibration, which is important because it is the stimulus used in otolith reflex testing (Curthoys and Grant, 2015). Current models suggest the otoliths have complex vibrational mode changes across frequency, acting as an accelerometer below, and a seismometer above 400 Hz (Grant and Curthoys, 2017). For the purposes of exploring changes in the mechanical responses of utricular hair cells across frequency to both sound and vibration, it may be enticing to compare UM to macular vibration responses across frequency (examining phase-relationships in particular), where the UM could be used as an indicator of hair cell transduction, and the macular vibration used as a measure of mechanical drive to the cell. However, it is important to appreciate that, unlike the vibration of the organ of Corti which *primarily* moves in the transverse direction (Chen et al., 2011), the utricle has a more complex three-dimensional motion (Fernández and Goldberg, 1976c; Jaeger et al., 2008). Therefore, we cannot rely on our LDV measurements of the utricular macula as a complete indicator of the mechanical input to the utricular hair cells.

With these caveats in mind, comparisons of the phase of the UM relative to the phase of the macular vibration was used to infer macromechanical differences in receptor activation for ACS vs. BCV. Whilst the amplitude component of the frequency response of the UM was similar for ACS and BCV stimulation, (Fig. 2J and L), being most sensitive to 100–300 Hz, the UM phase response (re. the vibration phase) was markedly different between the two stimulus modes. For ACS the UM phase response was relatively 'flat' across frequency (Fig. 2C and N), whereas for BCV the UM phase significantly lagged the macular vibration above 200 Hz (Fig. 2G and P).

One possible explanation for the UM phase response difference between ACS and BCV could be that during ACS stimulation the fluid pressure wave coupling the stapes motion to the utricle primarily produces a transverse motion of the utricular macula, and thus the LDV measurement closely reflects the input to the macular hair cells, and the phase of the UM and macular vibration are therefore similar across frequency. Conversely, BCV most likely induces a more complex motion of the utricular macula, where lateral motion of the macula (not well represented by our LDV measurements) may be the dominant drive activating the hair cells, and the relationship between the UM phase and transverse and lateral motion of the macula measured by our LDV is complex and frequency dependent.

Again, it should be noted that we are currently only able to measure macular motion in the dorso-ventral plane, and therefore we have a grossly incomplete measure of the mechanical drive to the macular hair cells. For this reason, we cannot reliably use LDV measurements to compare macular responses (e.g. UM) across frequency, or for different stimuli (e.g. BCV or ACS). However, LDV measurements, in combination with neural or UM recordings, do provide the ability to differentially diagnose the basis of peripheral vestibular dysfunction, which may affect mechanical, hair cell or neural function.

In order to more accurately compare macular responses to various stimuli, we would first need a more reliable measure of the shearing between the neuroepithelial layer, and the otoconia. Recent studies in cochlear physiology have used methods such as 3D Optical coherence tomography to better understand cochlear micromechanics in 3D, and this could potentially be utilized in future vestibular research, to enable comparisons between different stimuli.

Overall, this preliminary study demonstrates that recording mammalian otolith vibration *in vivo* is possible, and that utricular macula motion (and hair cell activation) is driven by frequencies used in standard clinical VEMP tests. Importantly, for the first time, this study indicates that the macromechanical activation of the utricular macula may be different for ACS compared to BCV, which is likely to be an important consideration for current clinical reflex testing incorporating both ACS and BCV stimuli. However, given that the LDV does not provide a faithful measure of the drive to the hair cells, and that there are subtle differences between measurements of ACS and BCV evoked responses (such as the level of fluid in the vestibule, and the level of system distortion), we are presently cautious to over interpret these results as they relate to macular macromechanics.

Author contributions

C.J.P. performed the experiments, analyzed the data and wrote the manuscript. D.J.B. developed the experimental hardware and software, provided experimental assistance and edited the manuscript. I.S.C. provided advice and equipment for the project and edited the manuscript.

Acknowledgements

We thank Dr Densil Cabrera and Mr Jonothan Holmes from the University of Sydney School of Architecture, Design and Planning for supplying the Ometron Laser Doppler Vibrometer. This study was partially funded by The Medical Foundation of The University of Sydney, with funds raised by the Meniere's Research Fund Inc.

References

Cooper, N.P., Rhode, W.S., 1992. Basilar membrane mechanics in the hook region of cat and Guinea-pig cochleae: sharp tuning and nonlinearity in the absence of baseline position shifts. Hear. Res. 63 (1–2), 163–190.

Chen, F., Zha, D., Fridberger, A., Zheng, J., Choudhury, N., Jacques, S.L., Wang, R.K., Shi, X., Nuttall, A.L., 2011. A differentially amplified motion in the ear for near-threshold sound detection. Nat. Neurosci. 14 (6), 770–774. https://doi.org/10.1038/nn.2827.

Curthoys, I.S., Vulovic, V., Burgess, A.M., Sokolic, L., Goonetilleke, S.C., 2016. The response of Guinea pig primary utricular and saccular irregular neurons to bone-conducted vibration (BCV) and air-conducted sound (ACS). Hear. Res. 331, 131–143.

Curthoys, I., Grant, J., 2015. How does high-frequency sound or vibration activate vestibular receptors? Exp. Brain Res. 233 (3), 691–699.

De Vries, H., 1950. The mechanics of the labyrinth otoliths. Acta Otolaryngol. 38 (3), 262–273.

Dunlap, M.D., Spoon, C.E., Grant, J.W., 2012. Experimental measurement of utricle dynamic response. J. Vestib. Res. 22 (2), 57–68. https://doi.org/10.3233/ves-2011-0431.

Dunlap, M., Grant, J., 2014. Experimental measurement of utricle system dynamic response to inertial stimulus. J. Assoc. Res. Otolaryngol. 15 (4), 511–528.

Fernández, C., Goldberg, J.M., 1976a. Physiology of peripheral neurons innervating otolith organs of the squirrel monkey. I. Response to static tilts and to long-duration centrifugal force. J. Neurophysiol. 39 (5), 970–984.

Fernández, C., Goldberg, J.M., 1976c. Physiology of peripheral neurons innervating otolith organs of the squirrel monkey. III. Response dynamics. J. Neurophysiol. 39 (5), 996–1008.

Fridberger, A., de Monvel, J.B., Zheng, J., Hu, N., Zou, Y., Ren, T., Nuttall, A., 2004. Organ of Corti potentials and the motion of the basilar membrane. J. Neurosci. 24 (45), 10057–10063. https://doi.org/10.1523/jneurosci.2711-04.2004.

Goldberg, J.M., Fernández, C., 1976. Vestibular mechanisms. Annu. Rev. Physiol. 37 (1), 129–162.

Grant, W., Curthoys, I., 2017. Otoliths-accelerometer and seismometer; implications in vestibular evoked myogenic potential (VEMP). Hear. Res. 353, 26–35.

Iversen, M.M., Rabbitt, R.D., 2017. Wave mechanics of the vestibular semicircular canals. Biophys. J. 113 (5), 1133–1149.

Jaeger, R., Kondrachuk, A., Haslwanter, T., 2008. The distribution of otolith polarization vectors in mammals: comparison between model predictions and single cell recordings. Hear. Res. 239 (1–2), 12–19.

Jones, T.A., Jones, S.M., Vijayakumar, S., Brugeaud, A., Bothwell, M., Chabbert, C., 2011. The adequate stimulus for mammalian linear vestibular evoked potentials (VsEPs). Hear. Res. 280 (1–2), 133–140.

Martin, P., Hudspeth, A., 2001. Compressive nonlinearity in the hair bundle's active response to mechanical stimulation. Proc. Natl. Acad. Sci. Unit. States Am. 98 (25), 14386–14391.

Nuttall, A.L., Dolan, D.F., Avinash, G., 1991. Laser Doppler velocimetry of basilar membrane vibration. Hear. Res. 51 (2), 203–213.
Pastras, C.J., Curthoys, I.S., Sokolic, L., Brown, D.J., 2018. Suppression of the vestibular short-latency evoked potential by electrical stimulation of the central vestibular system. Hear. Res. 361, 23–35.
Pastras, C., Curthoys, I., Brown, D., 2017. In vivo recording of the vestibular microphonic in mammals. Hear. Res. 354, 38–47.
Rabbitt, R.D., Boyle, R., Highstein, S.M., 2010. Mechanical amplification by hair cells in the semicircular canals. Proc. Natl. Acad. Sci. Unit. States Am. 107 (8), 3864–3869.
Rabbitt, R., Highstein, S., Boyle, R., 1996. Determinants of semicircular canal afferent response dynamics in fish. Ann. N. Y. Acad. Sci. 781 (1), 213–243.
Rabbitt, R., Yamauchi, A., Boyle, R., Highstein, S., 2001. How endolymph pressure modulates semicircular canal primary afferent discharge. Ann. N. Y. Acad. Sci. 942 (1), 313–321.
Recio, A., Rich, N.C., Narayan, S.S., Ruggero, M.A., 1998. Basilar-membrane responses to clicks at the base of the chinchilla cochlea. J. Acoust. Soc. Am. 103 (4), 1972–1989.
Richard, D., 1916. Untersuchung über die Frage, ob Schallreize adäquate Reize für den Vorhofbogengangsapparat sind. Z. Biol. 66, 479–505.
Robles, L., Ruggero, M.A., Rich, N.C., 1986. Basilar membrane mechanics at the base of the chinchilla cochlea. I. Input–output functions, tuning curves, and response phases. J. Acoust. Soc. Am. 80 (5), 1364–1374.
Rosengren, S., Welgampola, M., Colebatch, J., 2010. Vestibular evoked myogenic potentials: past, present and future. Clin. Neurophysiol. 121 (5), 636–651.
Ruggero, M.A., Rich, N.C., 1991. Application of a commercially-manufactured Doppler-shift laser velocimeter to the measurement of basilar-membrane vibration. Hear. Res. 51 (2), 215–230.
Ruggero, M.A., Rich, N.C., Recio, A., Narayan, S.S., Robles, L., 1997. Basilar-membrane responses to tones at the base of the chinchilla cochlea. J. Acoust. Soc. Am. 101 (4), 2151–2163.
Sandhu, J.S., Low, R., Rea, P.A., Saunders, N.C., 2012. Altered frequency dynamics of cervical and ocular vestibular evoked myogenic potentials in patients with Ménière's disease. Otol. Neurotol. 33 (3), 444–449.
Songer, J.E., Rosowski, J.J., 2005. The effect of superior canal dehiscence on cochlear potential in response to air-conducted stimuli in chinchilla. Hear. Res. 210 (1–2), 53–62.
Tullio, P., 1929. Das Ohr und die Entstehung der Sprache und Schrift.
Wilson, J., Johnstone, J., 1973. Basilar membrane correlates of the combination tone 2f1– f2. Nature 241 (5386), 206.

4.3. Conclusion

As an initial attempt at measuring macular response mechanics, LDV provided a relatively simple method, once difficulties related to stimulus delivery had been addressed. As stated in the above study, the unfortunate aspect of this measurement is that it does not provide a reliable examination of relative vibration between the neuroepithelial layer and the otoconia, and thus results can be difficult to interpret, particularly when trying to characterize the basic properties of macular vibrational sensitivity. That said, LDV now allows simultaneous measurement of functional and mechanical hair cell recordings, alongside nerve responses, providing a 'complete' measure of utricular function, *in vivo.* Despite the issue with what the LDV measurements represent from a hair cell perspective, macular LDV measurements may be used to understand questions of MET channel gating (as will be demonstrated in Chapter 5, Figure 6 and 7). Moreover, these measurements provide a 'relative' measure of macular vibration, wherein experimentally induced changes in vibration, unrelated to changes in the stimulus itself, most likely reflect a pathological change in the macula's vibration.

Other techniques may be used to study the vibration of the utricle such as Optical Coherence Tomography (OCT), which overcome the limitations of LDV measurements, and many of these have already been applied in cochlear research (Cooper, Vavakou et al. 2018). Such measurements would ideally provide an indication of the differential vibration between the otoconia and the neuroepithelial layer, although they may not be able to provide a simultaneous measure of hair cell and neural function, which was ultimately our aim.

One aspect of our LDV measurements that we were hoping to observe was a possible active vibration component. It is unlikely that there will be an active gain process in the mammalian utricle analogous to the mammalian cochlea, as utricular hair cells do not possess voltage-dependent capacitance linked to somatic electromotility like cochlear outer hair cells (Adler, Belyantseva et al. 2003). Rather, a different mechanoamplification process may exist such as hair bundle electromotility, which has been observed in non-mammalian tetrapods, using *ex vivo* hair cell recordings (Martin and Hudspeth 1999). In order to detect such a mechanism, it may be important to develop a recording technique in close proximity to the vestibular hair bundles. Discovery of a vestibular active gain process is desirable as it may underlie peripheral end-organ mechanical tuning and sensitivity under physiologically healthy conditions, and therefore may elucidate the cause of peripheral balance dysfunction, among other things.

Chapter 5: Experimental manipulations of utricular function: examples

5.1. Introduction

Cochlear researchers have used multiple measures of peripheral auditory function to study the basis of hearing dysfunction, increasing our understanding of auditory pathologies (see Table 1). In comparison, vestibular researchers are only now starting to differentiate the cause of peripheral vestibular dysfunction at the cellular level. As an example, recent studies have focused on the experimentally induced effects of KCNQ channel disruption, to better understand the role of calyx M-currents, or efferent modulation in the vestibular periphery (Lee, Holt et al. 2017, Lee and Jones 2018). Following pharmacological disruption of the KCNQ channels, the VsEP amplitude is reduced, which could either indicate that the afferents were affected (via calyx KCNQ2-5 channels) or rather KCNQ1/KCNE1 channels in the vestibular dark cells were disrupted. Due to the lack of a technique to differentiate hair cell from neural sensitivity, the researchers were limited to performing a systematic series of experiments, requiring more complex interpretation of results. Had they had a measure of differential function at their disposal, the effects of their pharmacological agents could have been more easily resolved.

The aim of this chapter is to provide several basic examples of experimental manipulations resulting in a differential modulation of mechanical, hair cell, or neural function, and to demonstrate how the use of these novel measures can help avoid the need to make assumptions about results or perform lengthy experiments. Importantly, our aim here was NOT to explore the effects of our experimental manipulations at length. As such, we provide only examples of pilot experimental manipulations, where we have attempted to directly induce neural or hair cell dysfunction, reduce vestibular blood flow, or impose mechanical displacements of the macula, demonstrating changes in the VsEP, UM and macular vibration.

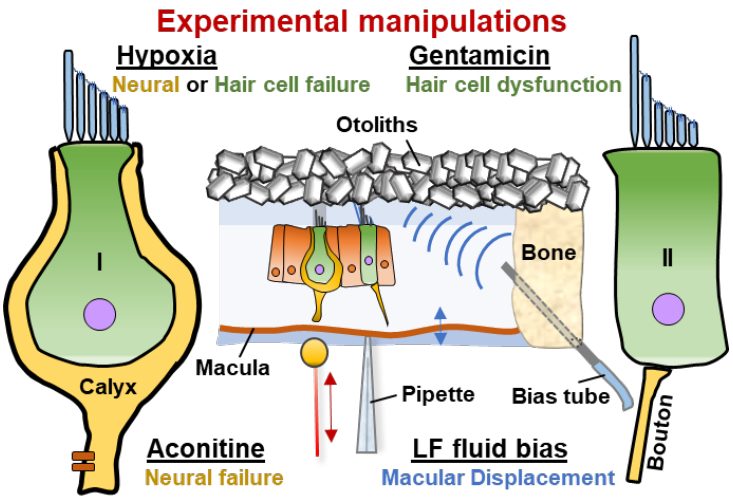

Figure 1: Like the cochlea, the utricle has various receptor subtypes that differentially affect peripheral sensitivity, such as the type-I vs. type-II hair cell and calyx (dimorphic) vs bouton neurons. Simultaneous recordings were undertaken using the VsEP as an index of irregular afferent activity, the UM as primarily a measure of local extrastriolar hair cell function and LDV as an objective measure of macular vibration. Several experimental manipulations were performed to demonstrate how peripheral utricular disorders can arise from neural (aconitine), hair cell (gentamicin), mechanical (Low-frequency bias) and global (hypoxia) changes, as a means to differentially diagnose utricular dysfunction, *in vivo*.

5.2. Neural failure

As with tetrodotoxin (Konishi and Kelsey 1968), aconitine is a potent neurotoxin that similarly interacts with voltage-gated Na^+ channels, resulting in presynaptic depolarization and action potential inhibition (Chan 2009). To provide an example of a differential diagnosis of nerve dysfunction, aconitine was added to the macula whilst simultaneously monitoring the VsEP, UM and macular vibration. Baseline recordings of all responses were monitored before 0.1ml of 20µM aconitine (in artificial perilymph) was applied to the basal surface of the utricular macula and longitudinally monitored.

Application of aconitine irreversibly abolished the VsEP over a 30-minute period, but neither the UM or macular vibration were affected (Figure 2a-f). There was a temporary reduction in the UM and LDV amplitudes following aconitine application, however these effects were most likely due to electrical shorting and disruption of the LDV pathway respectively, because they returned to their initial amplitudes immediately after wicking the excess fluid from the vestibule. With the VsEP electrode in the facial nerve canal, the response is much less affected by changes in the vestibule fluid levels. Moreover, wicking the fluid from the vestibule did not result in recovery of the VsEP after aconitine. This result, as with the results presented in Chapter 2, provided a simple example of a pharmacological manipulation that directly

suppressed neural sensitivity, but did little to hair cell or mechanical function. Without hair cell or neural measures, we would not be able to confirm that aconitine acted directly on neurons and did not have some effect (e.g. osmotic or toxic) on utricular hair cells.

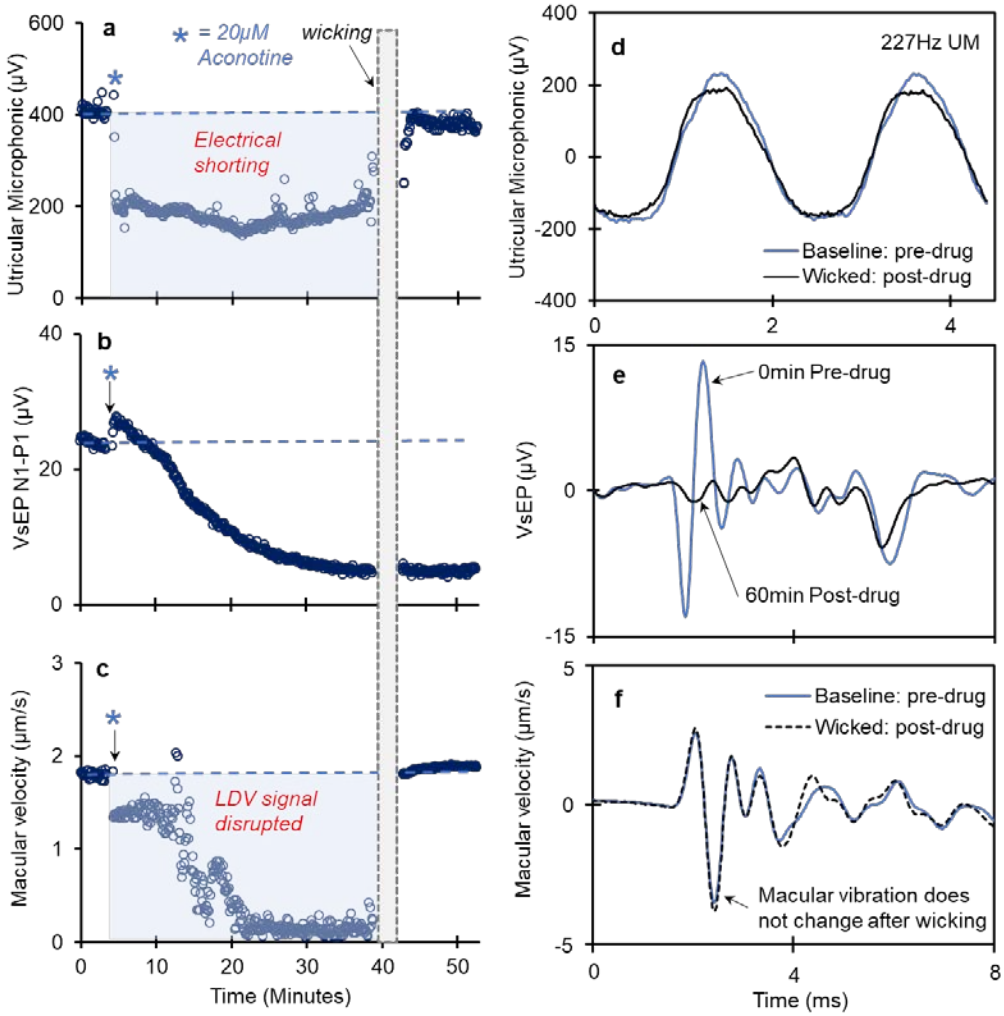

Figure 2: The effect of aconitine applied to the basal surface of the utricular macular in one representative animal, with longitudinal measurements of the UM (a & d), VsEP (b & e), and Macular velocity (c & f). GP#180522.

5.3. Hair cell failure

The antibiotic gentamicin can be 'vestibulotoxic' (Webster 1970), and is believed to gradually affect the function of type I hair cells (Hirvonen, Minor et al. 2005, Lyford-Pike, Vogelheim et al. 2007). Interestingly, previous studies in the lateral-line, saccule, semicircular canal and cochlea demonstrate aminoglycosides may have acute effects on hair cell function, causing rapid changes in the microphonic and nerve response (Wersäll and Flock 1964, Matsuura, Ikeda et al. 1971, Gallais 1979, Konishi 1979,

Kroese and van den Bercken 1980). To provide an example of an experimental manipulation affecting utricular hair cell function, gentamicin was applied locally to the macula whilst simultaneously monitoring the VsEP, UM and macular vibration, *in vivo.* In two different animals (GP#180612 & GP#180614), 50-100µl (1-2 drops) of 0.1mg/ml and 1mg/ml gentamicin sulfate (10mg/ml, ThermoFisher, NSW) in artificial perilymph was applied to the basal surface of the utricular macula. Baseline recordings were taken in both animals, and in one animal the macular velocity was recorded (Figure 3b; GP#180614) before and after drug administration to determine if gentamicin disturbed macular vibration, as previously reported in the cochlea (Ruggero and Rich 1991).

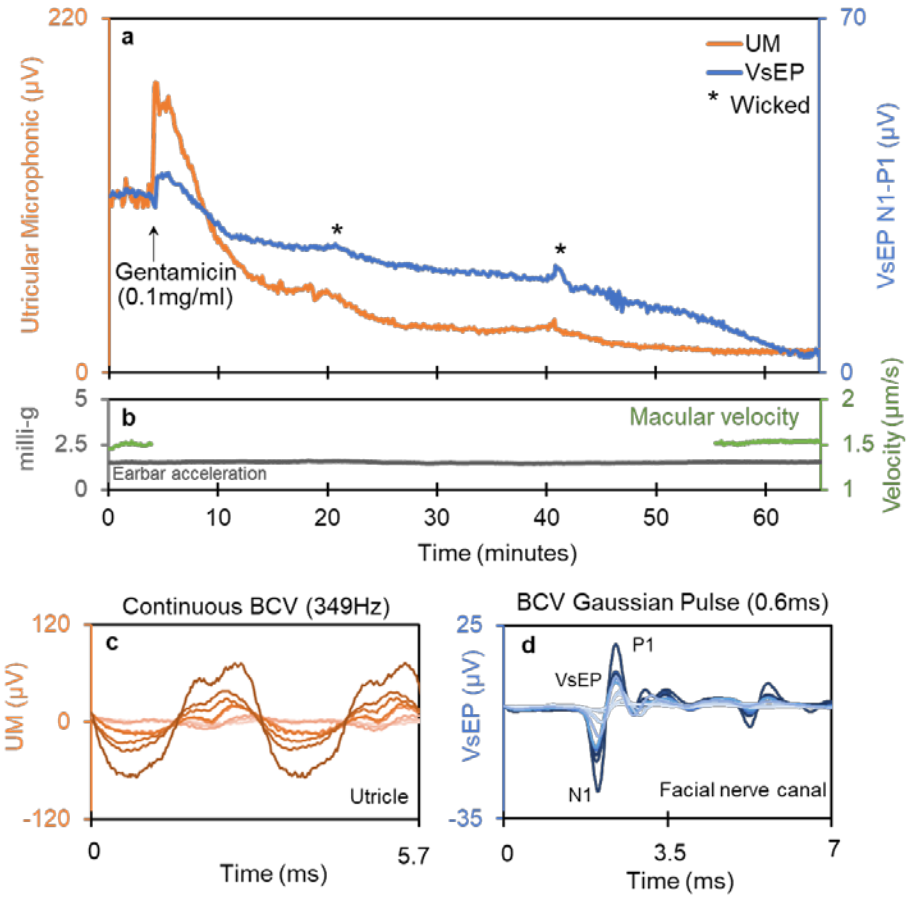

Figure 3: The effect of Gentamicin application (0.1mg/ml) to the surface of the macula, on the amplitude of the UM and VsEP (a). Macular velocity (b) was measured before gentamicin application, and after wicking it from the vestibule (velocity measurement not feasible with the excess fluid in the vestibule), showing that it, and the earbar acceleration, were unaltered during the treatment. Averaged UM (c)and VsEP (d) waveforms measured at semi-regular intervals during following the gentamicin application. GP#180614.

Both concentrations of gentamicin initially resulted in an immediate, yet transient increase in the amplitude of the UM and VsEP, possibly due to changes in the resistivity of the extracellular fluids in the vestibule following the application of fluid to the macular surface (Figure 3 and 4a). Similar effects were observed while monitoring the cochlear microphonic following perilymphatic perfusion of Neomycin in the guinea pig (Nuttall, Marques et al. 1977). Alternatively, these biphasic effects may be explained by altered potassium homeostasis, whereby K^+ channel blockade may result in an initial excitation, followed by suppression caused by an inability to adequately remove excess potassium during accumulation (Mann, Johnson et al. 2013, Yu, Guo et al. 2014). Shortly after this transient increase, 1mg/ml gentamicin resulted in both the UM and VsEP amplitudes to rapidly and irreversibly decrease (and they remained reduced after wicking the excess fluid from the vestibule). Given the decline in both the UM and VsEP (as opposed to just the VsEP with aconitine) these effects were likely mediated by a reduction in utricular hair cell transduction (Figure 4a, c and d). Compared to the higher dose of gentamicin, application of 0.1mg/ml gentamicin resulted in both the VsEP and UM decreasing, however at a slower rate (Figure 3a). Importantly, there was little to no change in the vibration of the macula (Figure 3b), demonstrating that the loss was not due to mechanical dysfunction. Interestingly, at this dose the VsEP declined less sharply than the UM (Figure 3a), which was somewhat unexpected because hair cell sensitivity should underpin neural sensitivity, and at the very least we might expect hair cell and neural responses to decrease concurrently. Whilst there are several possible explanations for this, such as the VsEP being a response of neurons synapsing with jerk-sensitive hair cells, whereas the UM is primarily a response of type II hair cells (predominantly located in the extra-striolar region), our aim here was not to explore these effects in detail. These examples demonstrate induced changes in utricular hair cell and nerve function, while leaving macular vibration unchanged. Further experiments would be needed to clarify the precise effects of locally applied gentamicin on peripheral utricular function.

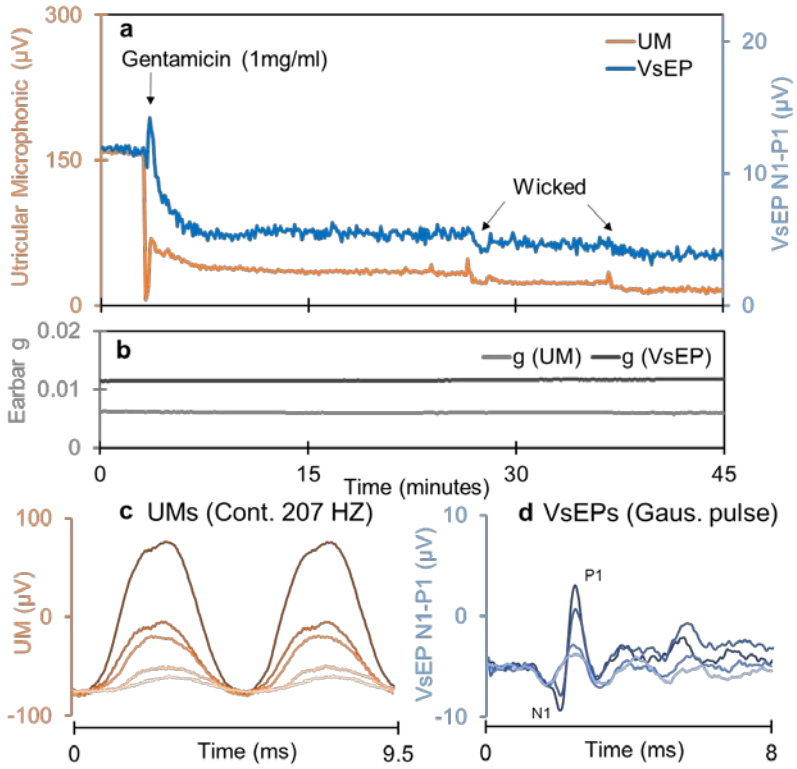

Figure 4: a) Simultaneous recordings of the UM and VsEP, following adminstration of 1mg/ml Gentamicin to the basal surface of the utrciular macula. Ear acceleration did not change during the experiment (b). Again, representative UM and VsEP waveforms over the course of the experiment are shown (c & d). GP#180612.

5.4. Changes vascular perfusion (Asphyxia)

Hypoxia or asphyxia has been used as an experimental manipulation to mimic disrupted cochlear blood supply (Misrahy, Shinabarger et al. 1958, Manley and Robertson 1976) caused by cochlear pathologies such as intense sound exposures, (Hawkins Jr 1971, Maass, Baumgärtl et al. 1976) and ototoxicity (Smith and Hawkins 1985). Hypoxia results in reduced strial blood supply, decreasing the endocochlear Potential and hair cell standing current, causing hair cell dysfunction and loss of cochlear sensitivity (Manley and Robertson 1976). Here we have used asphyxia as an experimental manipulation to alter vestibular blood flow whilst simultaneously monitoring the VsEP, UM and macular vibration.

In one animal baseline recordings were taken prior to a 3-minute asphyxia, which was initiated by clamping the animal's ventilation tubes. Approximately 1 minute after clamping the tubes, the UM began to decline, followed by the VsEP, which continued to decline at a faster rate (Figure 5a). Ventilation was re-instated 2 minutes later, where the VsEP and UM continued to decline for a short period before re-

stabilizing towards baseline (Figure 5a). Overall the VsEP amplitude declined more than the UM (40% vs. 20%) and took longer to recover (Figure 5a). Interestingly, macular velocity did not change (Figure 5b).

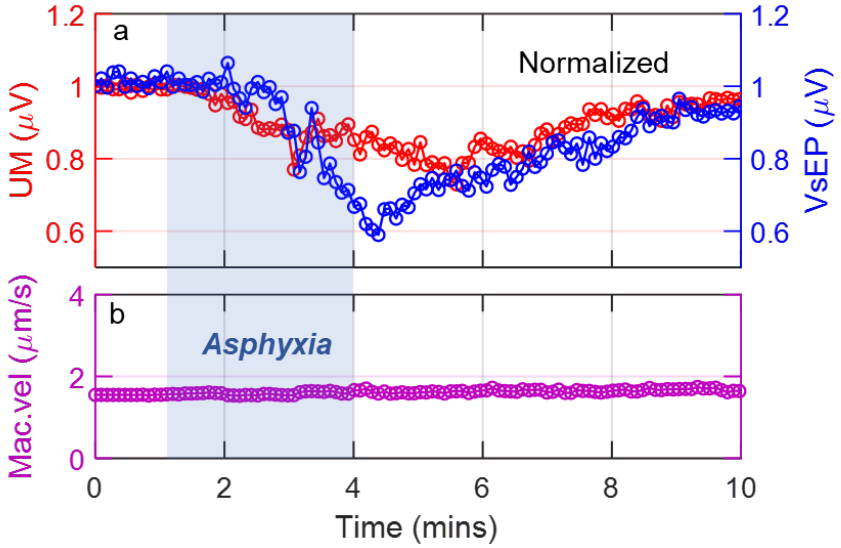

Figure 5: The effect of transient asphyxia (shaded region highlights period where the ventilation was clamped) on the UM and VsEP (a), and macular vibration (b). GP#180412.

5.5. Mechanical modulation

Since the 1950s, it has been suggested that changes in endolymphatic pressure (re. perilymph) can alter the mechanical and functional sensitivity of the cochlea (Tonndorf 1957). Experimentally, auditory researchers have used low-frequency biasing of the basilar membrane to displace hair cells and mimic pathological changes in the cochlea such as endolymphatic hydrops, to understand effects on neural, hair cell and mechanical function (Legouix 1962, Butler and Honrubia 1963, Allen, Dallos et al. 1971, Patuzzi, Sellick et al. 1984, Patuzzi, Sellick et al. 1984, Fridberger, Maarseveen et al. 1997). Similar mechanical manipulations have also taken place in the vestibular system, using techniques such as canal indentation and low-frequency focused ultrasound (Rabbitt, Boyle et al. 1995, Iversen and Rabbitt 2017, Iversen, Zhu et al. 2018). To explore the effects of displacement of the macula on nerve and hair cell activity, the utricular macular was cyclically displaced using low frequency, 10Hz, pressure applied to the vestibule, via a fluid-filled pipette sealed into the horizontal semicircular canal. A 27-gauge metal tube, coupled to a 30cm-long polyethylene tube (filled with artificial perilymph), attached to a compliant fluid-filled sac was used to deliver the low-frequency pressure. VsEP, UM and macular velocity recordings were taken before and after needle insertion to ensure this did not alter function or mechanics. At high intensities, the low frequency modulation cyclically displaced the macula, slightly, which was visible through the operating microscope.

For low-frequency biasing, the utricular macula was exposed and measurements of the VsEP, UM and utricular vibration performed as detailed previously (see Chapter 3 & 4). The UM and macular vibration were stimulated using a constant, continuous BCV stimulus between 100-300Hz, and the VsEP was evoked using a 1ms BCV pulse. The intensity of the 10Hz bias was gradually increased to a level where there was a clear modulation of the UM and VsEP, but which did not damage the utricle.

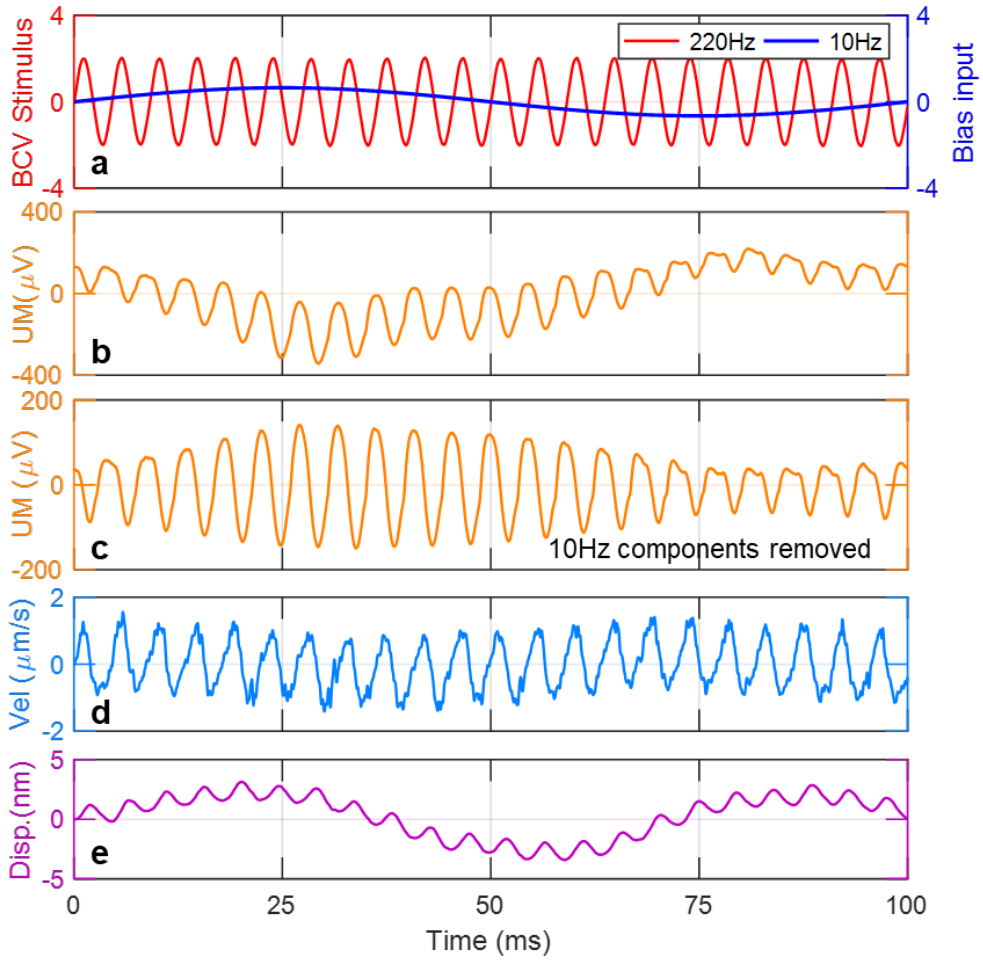

Figure 6: The effect of a 10Hz hydrostatic pressure on peripheral utricular functional and mechanical hair cell responses. a) The 220Hz BCV (red) and 10Hz bias (blue) stimulus (arbitrary units). b) The 220Hz evoked UM (an averaged waveform) during a single cycle of the 10Hz hydrostatic bias. c) The same waveform as shown in b, with 10Hz components in the response waveform removed. d) Simultaneous recordings of macular velocity. e) Macular displacement (integrated from velocity). GP#180530.

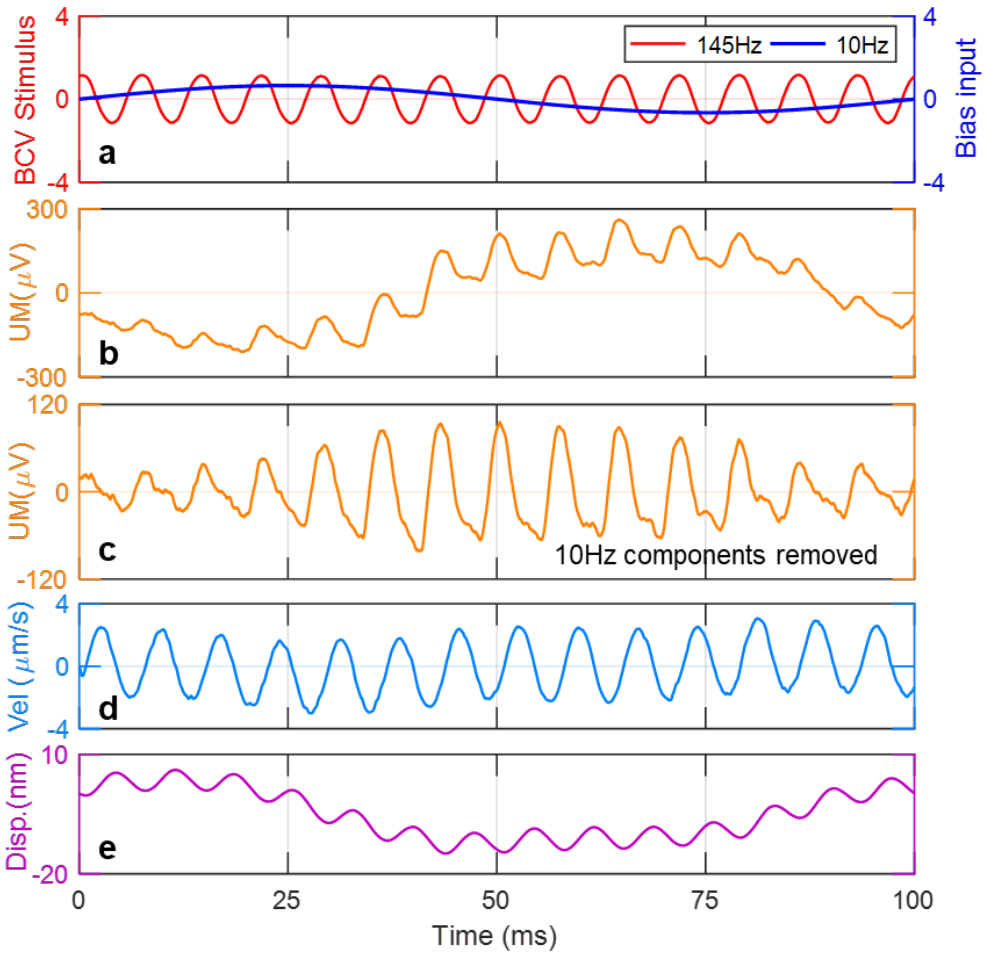

Figure 7: Duplicates of the recordings shown in Figure 6, performed in in the same animal, using a different BCV frequency. GP#180530.

In one animal (GP#180530), the 10Hz bias caused a cyclic modulation of the UM amplitude, with the UM evoked by either a 145 Hz or 220Hz BCV (Figure 6 and 7b & c). Throughout the bias the UM waveform distortion changed with the phase of the bias. To provide a clearer visualization of the UM modulation throughout the bias we have presented the averaged UM waveform (over one full bias cycle) either with or without the 10Hz component in the time waveform removed[3]. Whilst the UM response to the 145Hz or 220Hz signal was clearly modulated, there was no cyclic modulation of the macular velocity to these signals (Figure 6 and 7d), although there was evidence of a 10Hz displacement of the macula in the LDV signal, which was more evident when the LDV signal was integrated from velocity to displacement (Figure 6 and 7e).

[3] The 10Hz component was removed by performing an FFT on the time waveform, then nulling the 10Hz component, then performing an inverse FFT.

In another animal (GP#180605), the 10Hz bias resulted in a repeatable modulation of the VsEP N1-P1 amplitude (Figure 8a, b and e). Importantly, the VsEP stimulus was presented at a fixed phase relative to the 10Hz bias pressure, such that we could explore how the VsEP changed at various phases of the utricular displacement, in much the same way masker-period-patterns have been used to explore low-frequency modulation of cochlear responses (Zwicker 1977, Zwicker 1981). As a control, VsEP responses were recorded at various phases without the bias present, though this did not demonstrate any modulation, suggesting the cyclic changes in VsEP N1-P1 amplitude were mediated by the low-frequency bias (Figure 8e).

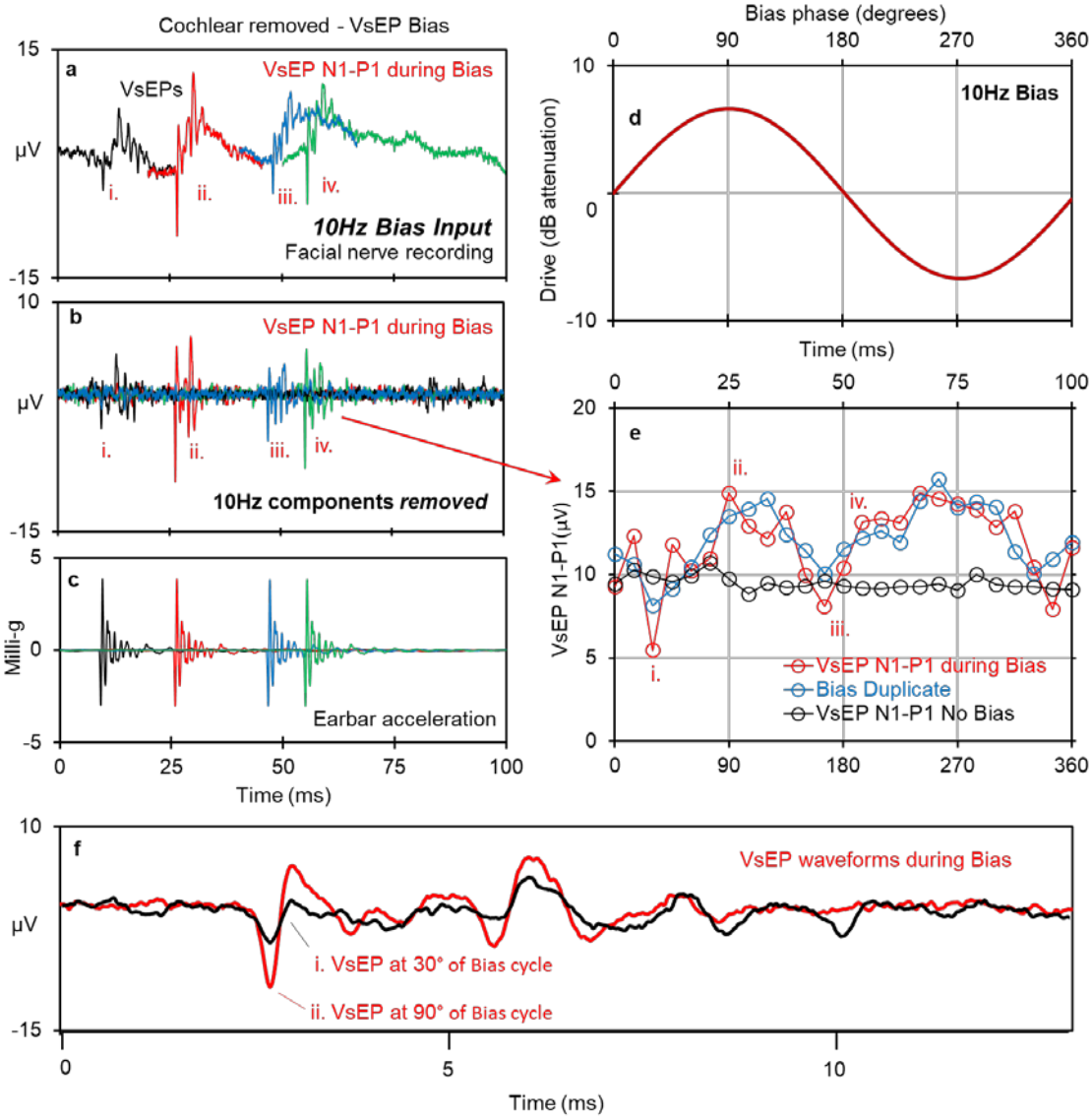

Figure 8: VsEP recordings (cochlea destroyed) during a 10Hz hydrostatic pressure bias, applied through a fluid-filled pipette in the hSCC. a) Four example VsEPs recorded at different phases of the

10Hz bias. b) The same recordings in a) with the 10Hz bias components removed, to highlight changes in the VsEP amplitude. c) Ear-bar acceleration recordings corresponding to the VsEPs in a&b). d) The 10Hz bias stimulus, and e) The N1-P1 amplitude of the VsEP, when the VsEP stimulus was presented at different phases (25 total) of the 10Hz bias (along with a duplicate) compared to no bias. f) Overlayed VsEP responses from b) corresponding to i. 30 degree and ii. 90 degree presentations of the 10Hz bias cycle, demonstrating large changes in VsEP sensitivity. GP#180605.

The effects of a low-frequency bias pressure applied to the vestibule were also explored with the cochlea intact. Here, we used a 20Hz bias, which produced an observable 'bulging' of the round window and cyclic modulation of the VsEP N1-P1 amplitude at various phases of the bias input (Figure 9a, b and e). A distorted 20Hz response was also observed during the bias, which was likely a CM response as it disappeared immediately following cochlea ablation (Figure 9a).

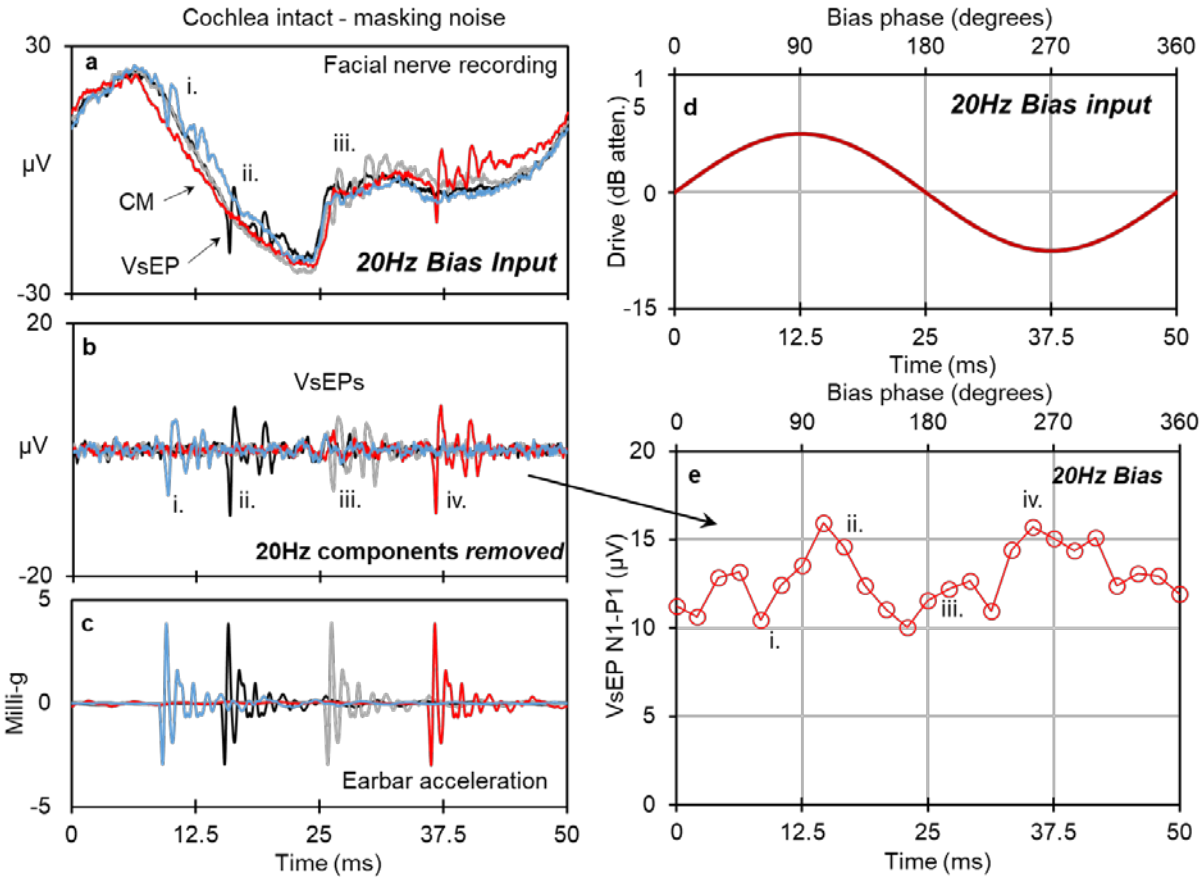

Figure 9: Duplicates of the recordings shown in Figure 8, yet with the cochlea intact, and using a 20Hz bias stimulus. GP#180605.

Importantly, ear-bar acceleration was not modulated during any of the bias recordings (Figure 8 and 9c), and removal of the 10 and 20Hz components via the inverse FFT method did not alter the VsEP

modulation, suggesting the changes in amplitude were not an artifact of the VsEP summing with the CM or other low-frequency response components arising from the bias.

These experiments are analogous to those previously undertaken in the cochlea, where low-frequency tones were used to cyclically modulate auditory hair cell and afferent responses (Zwicker 1981, Patuzzi and Sellick 1984, Patuzzi, Sellick et al. 1984, Patuzzi, Sellick et al. 1984). Biasing the position of the macula can be used to approximate what may occur in pathologies that cause mechanical or morphological changes in the utricle, such as endolymphatic hydrops. That is a given change in macular displacement can be related to a specific change in functional response amplitude, which may be used to infer about the pathophysiological mechanism of a vestibular dysfunction. Currently in the clinic, it is not clear why patients presenting with endolymphatic hydrops have enhanced VEMP responses (Maheu, Alvarado-Umanzor et al. 2017), or why patients with morphological abnormalities such as tumors or an enlarged vestibular aqueduct present with abnormally low-threshold VEMPs (Zhou and Gopen 2011). Clinicians are beginning to theorize why these changes may occur, however research is yet to validate this. Preliminary results demonstrate that the VsEP amplitude may be enhanced with macular displacement, which may help explain the enhanced VEMP amplitudes observed in some clinical studies.

5.6. Discussion

Previous chapters detailed the differential modulation of utricular nerve function (Chapter 2) and the development and characterization of novel utricular hair cell and mechanical responses (Chapter 3 and 4). This section ties these three tools together and demonstrates their effective use in studying the basis of peripheral utricular dysfunction. Importantly, these tools allow inter-subject comparisons and a detailed assessment of various disease models across animals.

A shortcoming of these simultaneous recordings is that they only provide 'partial' measures of peripheral utricular function, in that the VsEP is a gross measure of the irregular afferents, the UM is primarily an extrastriolar hair cell response, and the LDV recording only measures macular vibration in the dorso-ventral plane. If experimental manipulations affect regular and irregular receptors differentially, it may be difficult to interpret the true nature and origin of a peripheral utricular dysfunction. Moreover, if an experimental manipulation altered the function of type I hair cells, it is possible that the UM, being a response primarily from the extra-striolar region where there is an abundance of type II hair cells, would show little change. By contrast, the VsEP would be affected and we would likely conclude this drug selectively affected vestibular nerve activity directly, but in truth hair cell dysfunction may have been the root cause. Likewise, an experimental manipulation may alter the function of regular afferent activity, yet

produce no changes in the VsEP, UM or macular vibration, and thus we would incorrectly assume the experimental manipulation had no effect on peripheral utricular activity. Clearly, although the tools developed within this thesis provide an objective measure of certain aspects of peripheral vestibular function, they do not provide information related to all receptor subtypes, and investigators must be weary when interpreting results.

In regard to macular mechanics, although our 1-dimensional LDV recording only provides a partial measure of utricular macula vibration (see Chapter 4), it can still be used to study the mechanical effects of experimentally induced pathologies. That is, although we cannot use LDV measures to reliably study utricular mechanics, as we do not have a complete measure of the mechanical drive to the hair bundles. It can still be used to track the mechanical changes of the macula over time (relative to the stimulus) associated with experimental manipulations, as it is unlikely that 1-dimensional macular motion will change independently of the other 2-dimensions. The extent to which various planes of macular motion change during experimental manipulation is currently unknown and will depend upon other recording techniques such as 3-dimensional Optical Coherence Tomography (OCT) imaging.

Another issue with this approach, as mentioned in Chapter 3, is that to perform these measurements the cochlear must be removed, producing an excessively large 3rd window in the vestibular labyrinth. This is very likely to alter the fundamental response properties of the macula. For example, experiments in the toadfish have shown that a canal dehiscence alters the way SCC afferents respond to ACS via nonlinear fluid pumping (Iversen, Zhu et al. 2018). In order to avoid this, it may be possible to use other recording techniques, which may permit imaging through bone.

These example experimental manipulations demonstrate that simultaneous monitoring of nerve, hair cell and mechanical function is possible, providing the ability to study the basis of utricular dysfunction. These tools provide the means to longitudinally study an array of vestibular pathologies and associated treatments, analogous to previous work undertaken in the cochlea to understand the mechanisms behind hearing loss. However, the UM, VsEP and macular vibration only provide partial measures of functional and mechanical responses, which must be considered when interpreting results.

Chapter 6: Thesis Discussion

6.1. Clinical relevance

Although the VEMP may help identify the existence of a vestibular disorder, researchers are left to speculate the pathophysiological cause, as it may arise from a peripheral or central nerve dysfunction, or a peripheral hair cell or mechanical abnormality (Murofushi 2016, Fife, Colebatch et al. 2017). For instance, it is presently unclear why changes in VEMP tuning occur during certain pathologies such as Meniere's disease (Rauch, Zhou et al. 2004) or canal dehiscence (Manzari, Burgess et al. 2012), though this is often postulated as being due to a mechanical or morphological change.

These issues may be resolved if we had access to peripheral measures of vestibular function in humans. Unfortunately, there are several factors that preclude our ability to record the vestibular analogue of human electrocochleography. First, ACS and BCV activate cochlear receptors, producing field potentials that summate and obscure gross vestibular responses (Wit, Bleeker et al. 1981, Böhmer 1995). It may be possible to use acoustic masking noise to suppress cochlear responses (Chimento and Schreiner 1990, Biron, Freeman et al. 2002), which may then allow the recording of unadulterated peripheral vestibular responses, although the noise levels required may result in some cochlear trauma, or in a significantly 'noisy CM' that negatively influences the signal-to-noise ratio of the response. A more novel approach to reducing cochlear contributions in attempts at peripheral vestibular response recordings could involve combining continuous, sinusoidal, low-frequency BCV and ACS (with a specific phase difference) such that cochlear responses (i.e. CM) are cancelled (Lowy 1942), but the vestibular responses are not (assuming there are different pathways for ACS and BCV in the vestibular system vs. the cochlea). Alternatively, it may be possible to stimulate the vestibular system using infrasound, where the cochlear receptors are insensitive due to the middle ear transfer function, helicotrema shunt and viscous coupling of the inner ear hair cells (Moller and Pedersen 2004, Salt and Hullar 2010). However, it is unlikely this stimulation method will activate 'jerk-sensitive', irregular receptors. Rather, a 'static', regular vestibular response may be generated.

Perhaps a more pressing reason why peripheral vestibular response recordings, particularly UM, may not be possible in humans is that otolithic hair bundles have a polarity reversal (Corey and Hudspeth 1983), and their extracellular receptor currents cancel, in addition to being reduced by approximately the inverse-square of their distance from the recording location (Buzsáki, Anastassiou et al. 2012), making it difficult to measure an otolithic microphonic from an non-invasive recording montage. Previous reports

of human VsEP measurements present dubious results, with artifact and response amplitudes near the recording noise floor (Elidan, Leibner et al. 1991, Elidan, Sela et al. 1991, Rodionov, Elidan et al. 1996).

Despite being unable to measure peripheral vestibular responses in humans, clinical therapies of balance disorders continue to improve, yet measures of vestibular function in experimental animals have remained relatively stagnant. With the development of the *in vivo* recordings presented in this thesis, it may now be possible to assess the dissociative effects of various clinical treatments on peripheral vestibular function, in experimental animals. Of the therapies used to treat vestibular problems, many involve pharmacological agents that do not have clear mechanisms of action (Soto and Vega 2010). For example, the histamine (H3 receptor) antagonist, Betahistine (Van Cauwenberge and De Moor 1997) is currently used for controlling vertigo in Meniere's patients (Lacour, van de Heyning et al. 2007). However, there is no clear understanding of the differential effects on hair cell or afferent sensitivity (Soto 2001). Moreover, the most commonly used balance drug, Scopolamine (Spinks, Wasiak et al. 2007, Golding, Wesnes et al. 2018), works by antagonizing peripheral muscarinic acetylcholine (mACh) receptors (Weerts, Putcha et al. 2015). *Ex vivo* studies have shown that mACh receptors modulate type II vestibular hair cells via Big Potassium (BK) channels in mice (Guo, Wang et al. 2012) and calyx-afferent neurons via slow-mediated efferent excitation in turtles (Holt, Jordan et al. 2017). However, it is not yet clear how these individual results translate to cohesive, mammalian vestibular functioning. Simultaneous measures of the UM, VsEP and macular vibration may help resolve these questions, and provide a better mechanistic understanding of vestibular treatments.

6.2. General discussion

One of the prominent advantages of these differential recordings (the VsEP, UM and macular vibration), is an ability to investigate the tuning characteristics of otolithic afferents and hair cells to clinically relevant stimuli. Our results support previous findings that the VsEP is sensitive to cranial jerk (Jones, Jones et al. 2011, Jones, Lee et al. 2015), and additionally show that the VsEP is also sensitive to macular jerk (see Appendix 1). Importantly, this suggests that there is no VsEP kinematic transfer function from the skull to the macula. Results also indicate there is at least an order of magnitude of vibrational loss from the ear-bar to the macula, which may be used to quantify the level of macular vibration re. VsEP sensitivity based on ear-bar measurements.

UM recordings also demonstrate that otolithic hair cells are physiologically active up to several kilohertz to both BCV and ACS. However, unlike the VsEP the UM appeared to be tuned to low-frequency stimuli when controlling for macular vibration (at least in our experimental setup) and was more sensitive

to macular displacement over other kinematic components (see Appendix 1). One reason for this discrepancy may be that jerk-sensitive irregular afferents are not constrained by their pre-synaptic hair cell response properties. However, it is more likely that the UM does not reflect striolar, type I hair cell function, which supplies the irregularly discharging afferents. Like the inner hair cells of the cochlea, the freestanding type I hair cells of the striolar may be viscously-coupled, whereas the longer, type-II extrastriolar hair cells embedded in the otoconia are likely displacement sensitive like the cochlear outer hair cells (Patuzzi and Yates 1986). This may explain the different functional response properties of the VsEP and the UM.

As has been inferred from CM recordings using Boltzmann analysis (Patuzzi and Moleirinho 1998), researchers may be interested in using the UM as a tool to monitor the level and asymmetry of MET channel transduction in utricular hair cells during experimental manipulations (see appendix 1). However, caution is advised if LDV measurements are to be used as an indicator of the input or drive to the hair bundle, because as stated previously, our LDV measurements are not a reliable indicator of the stereocilia deflection. Nevertheless, analysis of the UM waveform can likely provide valuable information regarding hair cell transduction in such experiments.

One such experiment was demonstrated in Chapter 5, where we used a 10Hz hydraulic pressure to mechanically displace the macula and modulate a 200Hz-evoked UM waveform. As the macula was displaced, the UM saturation varied, suggesting that the MET channel gating was being cyclically biased. This is akin to experiments involving infrasound modulation of the CM (Salt et al., 2013), which indicated, through Boltzmann analysis of the CM waveform, that hair cell transduction may not be governed by a simple MET channel mechanism but may include various adaptive mechanisms.

Aside from studying the transduction properties of utricular hair cells, there remains a need to have a better understanding of the dynamic features of otolith mechanics. The mechanics of the cochlea is well studied (Robles and Ruggero 2001, Nuttall, Ricci et al. 2018), and research continues to reveal complex vibrational properties of the organ of Corti such as radial shearing (Lee, Raphael et al. 2016) and longitudinal funneling (Cooper, Vavakou et al. 2018). By comparison, the exact way the macular vibrates to sound and vibration is unknown. Results from Chapter 4 suggest (albeit superficially) that ACS likely displaces the macular as a unit, whereas BCV results in a more complex dynamic response of the utricle. It has been suggested that the macular has a complex vibrational 'wobble' and vibrational modes change with frequency (Land 2018). One way to test this theory is to compare macular vibration phases at different positions across the macula. If the phases differ the macular likely has a complex vibrational

pattern, like a 'wobble'. This may allow characterization of the basic vibrational properties of the otoliths, having clinical relevance to vestibular functional testing and changes in otolith tuning with pathology.

Whilst this thesis has concerned measurements of the utricle only, it may be possible, through additional new surgical and technical approaches, to obtain differential responses of the saccule and SCCs. Localized saccular microphonics have already been recorded (see Chapter 3), and it seems technically possible to record SCC microphonics by altering the stimulus and recording location (Trincker and Partsch 1959, Wit, Kahmann et al. 1986, Rabbitt, Boyle et al. 2005). Moreover, it seems possible to record saccular and SCC LDV measurements by changing the surgical approach and laser beam exposure. However, it is not immediately clear how to record a saccular or SCC evoked VsEP, given that BCV produces a utricular evoked VsEP (Chihara, Wang et al. 2013). As a means to selectively stimulating vestibular end-organs, it may be possible to use a localized stimulation method such as focused ultraviolet light (Azimzadeh, Fabella et al. 2018), or low-intensity focused-ultrasound (LiFU) (Iversen, Christensen et al. 2017). The response of isolated vestibular hair cells to UV light appears to be mediated by the heating effects of UV, although the heat can apparently be localized to a very small location and may provide a means to selectively stimulate different sub-populations of hair cells. LiFU has been shown to create non-linear acoustic radiation forces that activate otolithic primary afferent neurons in the toadfish (Iversen, Christensen et al. 2017). Of interest is how this unique stimulus differentially activates the otolithic hair cells, neurons and macular to produce otolithic function, *in vivo*.

6.4. Future directions and final comment

The availability of the VsEP, UM and macular vibration measures provides the ability to study the fundamentals of peripheral vestibular function, dysfunction, and to explore relevant clinical therapies. As with the development of any new research tool, several new potential research projects immediately spring to mind, and several of these are presented below. Future projects could use simultaneous measures of the VsEP, UM and macular vibration:

1) **to explore the fundamental properties of utricular macula vibration in response to ACS and BCV,**
2) **in animal models of altered EVS activity, to explore if the EVS primarily alters hair cell or neural function,**
3) **following noise, blast or impact trauma,**
4) **during galvanic stimulation, to determine its relative impact on hair cells and neurons,**

5) **following vestibular implant surgery, to explore residual hair cell function following implantation.**

Moreover, just as cochlear evoked responses continue to be developed, we need to further develop objective measures of vestibular function, including saccular and canal function, and responses specific to the various hair cell types. Given the ease of VsEP, UM and macular vibration measurements, we anticipate a rapid expansion of experimental research using these *in vivo* tools in the near future.

References not featured in published material

Adler, H. J., I. A. Belyantseva, R. C. Merritt, Jr., G. I. Frolenkov, G. W. Dougherty and B. Kachar (2003). "Expression of prestin, a membrane motor protein, in the mammalian auditory and vestibular periphery." Hear Res **184**(1-2): 27-40.

Allen, G. W., P. Dallos, S. Sakamoto and T. Homma (1971). "Cochlear microphonic potential in cats: effects of perilymphatic pressure." Archives of Otolaryngology **93**(4): 388-396.

Azimzadeh, J. B., B. A. Fabella and A. Hudspeth (2018). Stimulation of hair cells with ultraviolet light. AIP Conference Proceedings, AIP Publishing.

Békésy, G. (1928). "Zur Theorie des Hörens; die Schwingungsform der Basilarmembran." Phys. Zeits **29**: 793-810.

Békésy, G. v. (1952). "Direct Observation of the Vibrations of the Cochlear Partition Under a Microscope." Acta Oto-Laryngologica **42**(3): 197-201.

Biron, A., S. Freeman, J. Y. Sichel and H. Sohmer (2002). "The effect of noise exposure in the presence of canal fenestration on the amplitude of short-latency vestibular evoked potentials." Arch Otolaryngol Head Neck Surg **128**(5): 544-548.

Böhmer, A. (1995). "Short latency vestibular evoked responses to linear acceleration stimuli in small mammals: masking effects and experimental applications." Acta Oto-Laryngologica **115**(sup520): 120-123.

Bremer, H. G., J. C. De Groot, H. Versnel and S. F. Klis (2012). "Combined administration of kanamycin and furosemide does not result in loss of vestibular function in Guinea pigs." Audiology and Neurotology **17**(1): 25-38.

Brown, D., Y. Chihara and Y. Wang (2013). "Changes in utricular function during artificial endolymph injections in guinea pigs." Hearing research **304**: 70-76.

Brown, D. J., Y. Chihara, I. S. Curthoys, Y. Wang and M. Bos (2013). "Changes in cochlear function during acute endolymphatic hydrops development in guinea pigs." Hearing research **296**: 96-106.

Brown, D. J., C. J. Pastras and I. S. Curthoys (2017). "Electrophysiological Measurements of Peripheral Vestibular Function—A Review of Electrovestibulography." Frontiers in systems neuroscience **11**: 34.

Brown, M. (1994). "The antidromic compound action potential of the auditory nerve." Journal of neurophysiology **71**(5): 1826-1834.

Butler, R. A. and V. Honrubia (1963). "Responses of cochlear potentials to changes in hydrostatic pressure." The Journal of the Acoustical Society of America **35**(8): 1188-1192.

Buzsáki, G., C. A. Anastassiou and C. Koch (2012). "The origin of extracellular fields and currents—EEG, ECoG, LFP and spikes." Nature reviews neuroscience **13**(6): 407.

Chan, T. Y. (2009). "Aconite poisoning." Clinical Toxicology **47**(4): 279-285.

Cheatham, M. A., K. Naik and P. Dallos (2011). "Using the Cochlear Microphonic as a Tool to Evaluate Cochlear Function in Mouse Models of Hearing." JARO: Journal of the Association for Research in Otolaryngology **12**(1): 113-125.

Chihara, Y., V. Wang and D. J. Brown (2013). "Evidence for the utricular origin of the vestibular short-latency-evoked potential (VsEP) to bone-conducted vibration in guinea pig." Exp Brain Res **229**(2): 157-170.

Chimento, T. and C. Schreiner (1990). "Selectively eliminating cochlear microphonic contamination from the frequency-following response." Electroencephalography and clinical neurophysiology **75**(1): 88-96.

Cooper, N. P., A. Vavakou and M. van der Heijden (2018). "Vibration hotspots reveal longitudinal funneling of sound-evoked motion in the mammalian cochlea." Nature Communications **9**(1): 3054.

Corey, D. P. and A. J. Hudspeth (1983). "Analysis of the microphonic potential of the bullfrog's sacculus." J Neurosci **3**(5): 942-961.

Curthoys, I. S., J. Kim, S. K. McPhedran and A. J. Camp (2006). "Bone conducted vibration selectively activates irregular primary otolithic vestibular neurons in the guinea pig." Experimental brain research **175**(2): 256-267.

Curthoys, I. S. and V. Vulovic (2011). "Vestibular primary afferent responses to sound and vibration in the guinea pig." Experimental Brain Research **210**(3-4): 347-352.

Curthoys, I. S., V. Vulovic, A. M. Burgess, L. Sokolic and S. C. Goonetilleke (2016). "The response of guinea pig primary utricular and saccular irregular neurons to bone-conducted vibration (BCV) and air-conducted sound (ACS)." Hearing research **331**: 131-143.

Davis, H., B. H. Deatherage, D. H. Eldredge and C. A. Smith (1958). "SUMMATING POTENTIALS OF THE COCHLEA." American Journal of Physiology **195**(2): 251-261.

Deatherage, B. H., D. H. Eldredge and H. Davis (1959). "LATENCY OF ACTION POTENTIALS IN THE COCHLEA OF GUINEA-PIG." Journal of the Acoustical Society of America **31**(1): 122-123.

Desai, S. S., C. Zeh and A. Lysakowski (2005). "Comparative morphology of rodent vestibular periphery. I. Saccular and utricular maculae." J Neurophysiol **93**(1): 251-266.

Dimiccoli, M., B. Girard, A. Berthoz and D. Bennequin (2013). "Striola magica. A functional explanation of otolith geometry." Journal of computational neuroscience **35**(2): 125-154.

Ding, C. R., X. D. Xu, X. W. Wang, X. H. Jia, X. Cheng, X. Liu, L. Yang, B. S. Tong, F. L. Chi and D. D. Ren (2016). "Effect of Endolymphatic Hydrops on Sound Transmission in Live Guinea Pigs Measured with a Laser Doppler Vibrometer." Neural Plast **2016**: 8648297.

Elidan, J., E. Leibner, S. Freeman, M. Sela, M. Nitzan and H. Sohmer (1991). "Short and middle latency vestibular evoked responses to acceleration in man." Electroencephalogr Clin Neurophysiol **80**(2): 140-145.

Elidan, J., M. Sela, E. Liebner and H. Sohmer (1991). "Short latency vestibular evoked response to angular acceleration impulse in human beings." Otolaryngol Head Neck Surg **105**(3): 353-359.

Evans, E. and T. Borerwe (1982). "Ototoxic effects of salicylates on the responses of single cochlear nerve fibres and on cochlear potentials." British journal of audiology **16**(2): 101-108.

Fernandez, C. and J. M. Goldberg (1976). "Physiology of peripheral neurons innervating otolith organs of the squirrel monkey. II. Directional selectivity and force-response relations." Journal of neurophysiology **39**(5): 985-995.

Fife, T. D., J. G. Colebatch, K. A. Kerber, K. Brantberg, M. Strupp, H. Lee, M. F. Walker, E. Ashman, J. Fletcher, B. Callaghan and D. S. Gloss, 2nd (2017). "Practice guideline: Cervical and ocular vestibular evoked myogenic potential testing: Report of the Guideline Development, Dissemination, and Implementation Subcommittee of the American Academy of Neurology." Neurology **89**(22): 2288-2296.

Fitzgerald, J. J., D. Robertson and B. M. Johnstone (1993). "Effects of intra-cochlear perfusion of salicylates on cochlear microphonic and other auditory responses in the guinea pig." Hearing research **67**(1-2): 147-156.

Freeman, S., M. Plotnik, J. Elidan and H. Sohmer (1999). "Development of short latency vestibular evoked potentials in the neonatal rat." Hear Res **137**(1-2): 51-58.

Fridberger, A., J. T. P. v. Maarseveen, E. Scarfone, M. Ulfendahl, B. Flock and Å. Flock (1997). "Pressure-induced basilar membrane position shifts and the stimulus-evoked potentials in the low-frequency region of the guinea pig cochlea." Acta physiologica scandinavica **161**(2): 239-252.

Fromm, B., C. Nylen and Y. Zotterman (1935). "Studies in the mechanism of the Wever and Bray effect." Acta oto-laryngologica **22**(3): 477-486.

Gallais, A. (1979). "Comparative study of the influence of aminoglycoside antibiotics on the activity of the horizontal semicircular canal in the frog." Acta oto-laryngologica **88**(1-6): 88-96.

Goldberg, J. M. and C. Fernandez (1980). "Efferent vestibular system in the squirrel monkey: anatomical location and influence on afferent activity." J Neurophysiol **43**(4): 986-1025.

Golding, J. F., K. A. Wesnes and B. R. Leaker (2018). "The effects of the selective muscarinic M3 receptor antagonist darifenacin, and of hyoscine (scopolamine), on motion sickness, skin conductance & cognitive function." Br J Clin Pharmacol **84**(7): 1535-1543.

Guo, C.-K., Y. Wang, T. Zhou, H. Yu, W.-J. Zhang and W.-J. Kong (2012). "M2 muscarinic ACh receptors sensitive BK channels mediate cholinergic inhibition of type II vestibular hair cells." Hearing research **285**(1-2): 13-19.

Hawkins Jr, J. E. (1971). "The role of vasoconstriction in noise-induced hearing loss." Annals of Otology, Rhinology & Laryngology **80**(6): 903-913.

Hirvonen, T. P., L. B. Minor, T. E. Hullar and J. P. Carey (2005). "Effects of intratympanic gentamicin on vestibular afferents and hair cells in the chinchilla." Journal of neurophysiology **93**(2): 643-655.

Holt, J. C., P. M. Jordan, A. Lysakowski, A. Shah, K. Barsz and D. Contini (2017). "Muscarinic acetylcholine receptors and M-currents underlie efferent-mediated slow excitation in calyx-bearing vestibular afferents." Journal of Neuroscience **37**(7): 1873-1887.

Holt, J. C., K. Kewin, P. M. Jordan, P. Cameron, M. Klapczynski, J. M. McIntosh, P. A. Crooks, L. P. Dwoskin and A. Lysakowski (2015). "Pharmacologically Distinct Nicotinic Acetylcholine Receptors Drive Efferent-Mediated Excitation in Calyx-Bearing Vestibular Afferents." The Journal of Neuroscience **35**(8): 3625-3643.

Hsu, W. C., J. D. Wang, J. H. Lue, A. S. Day and Y. H. Young (2008). "Physiological and morphological assessment of the saccule in Guinea pigs after noise exposure." Arch Otolaryngol Head Neck Surg **134**(10): 1099-1106.

Hubner, P. P., S. I. Khan and A. A. Migliaccio (2017). "The mammalian efferent vestibular system plays a crucial role in vestibulo-ocular reflex compensation after unilateral labyrinthectomy." Journal of Neurophysiology **117**(4): 1553-1568.

Hudspeth, A. (1982). "Extracellular current flow and the site of transduction by vertebrate hair cells." Journal of Neuroscience **2**(1): 1-10.

Huizinga, E., H. De Vries and J. Vrolijk (1951). "Analysis of the Microphonic Activity of the Labyrinth of the Pigeon into the Contributions of the Various Parts." Acta oto-laryngologica **39**(5): 372-379.

Iversen, M., H. Zhu, W. Zhou, C. Della Santina, J. Carey and R. Rabbitt (2018). "Sound abnormally stimulates the vestibular system in canal dehiscence syndrome by generating pathological fluid-mechanical waves." Scientific reports **8**.

Iversen, M. M., D. A. Christensen, D. L. Parker, H. A. Holman, J. Chen, M. J. Frerck and R. D. Rabbitt (2017). "Low-intensity ultrasound activates vestibular otolith organs through acoustic radiation force." J Acoust Soc Am **141**(6): 4209.

Iversen, M. M. and R. D. Rabbitt (2017). "Wave Mechanics of the Vestibular Semicircular Canals." Biophysical journal **113**(5): 1133-1149.

Johnstone, B. and A. Boyle (1967). "Basilar membrane vibration examined with the Mössbauer technique." Science **158**(3799): 389-390.

Johnstone, B., R. Patuzzi and G. Yates (1986). "Basilar membrane measurements and the travelling wave." Hearing research **22**(1-3): 147-153.

Jones, S. M., L. C. Erway, K. R. Johnson, H. Yu and T. A. Jones (2004). "Gravity receptor function in mice with graded otoconial deficiencies." Hear Res **191**(1-2): 34-40.

Jones, S. M., T. A. Jones, P. L. Bell and M. J. Taylor (2001). "Compound gravity receptor polarization vectors evidenced by linear vestibular evoked potentials." Hear Res **154**(1-2): 54-61.

Jones, S. M., T. A. Jones and R. Shukla (1997). "Short latency vestibular evoked potentials in the Japanese quail (Coturnix coturnix japonica)." Journal of Comparative Physiology A **180**(6): 631-638.

Jones, S. M., G. Subramanian, W. Avniel, Y. Q. Guo, R. F. Burkard and T. A. Jones (2002). "Stimulus and recording variables and their effects on mammalian vestibular evoked potentials." Journal of Neuroscience Methods **118**(1): 23-31.

Jones, T. A., S. M. Jones, S. Vijayakumar, A. Brugeaud, M. Bothwell and C. Chabbert (2011). "The adequate stimulus for mammalian linear vestibular evoked potentials (VsEPs)." Hearing research **280**(1-2): 133-140.

Jones, T. A., C. Lee and G. C. Gaines (2015). "On the high frequency transfer of mechanical stimuli from the surface of the head to the macular neuroepithelium of the mouse." Journal of the Association for Research in Otolaryngology **16**(2): 189-204.

Kemp, D. T. (1978). "Stimulated acoustic emissions from within the human auditory system." The Journal of the Acoustical Society of America **64**(5): 1386-1391.

Killian, M. J. P., S. F. L. Klis and G. F. Smoorenburg (1994). "ADAPTATION IN THE COMPOUND ACTION-POTENTIAL RESPONSE OF THE GUINEA-PIG 8TH NERVE TO ELECTRIC-STIMULATION." Hearing Research **81**(1-2): 66-82.

Kingma, C. M. and H. P. Wit (2009). "Acute endolymphatic hydrops has no direct effect on the vestibular evoked potential in the guinea pig." Journal of Vestibular Research-Equilibrium & Orientation **19**(1-2): 27-32.

Kingma, C. M. and H. P. Wit (2010). "The effect of changes in perilymphatic K+ on the vestibular evoked potential in the guinea pig." Eur Arch Otorhinolaryngol **267**(11): 1679-1684.

Kohllöffel, L. (1972). "A study of basilar membrane vibrations III. The basilar membrane frequency response curve in the living guinea pig." Acta Acustica united with Acustica **27**(2): 82-89.

Konishi, T. (1979). "Effects of local application of ototoxic antibiotics on cochlear potentials in guinea pigs." Acta oto-laryngologica **88**(1-6): 41-46.

Konishi, T. and E. Kelsey (1968). "Effect of tetrodotoxin and procaine on cochlear potentials." The Journal of the Acoustical Society of America **43**(3): 471-480.

Kroese, A. B. and J. van den Bercken (1980). "Dual action of ototoxic antibiotics on sensory hair cells." Nature **283**(5745): 395.

Lacour, M., P. H. van de Heyning, M. Novotny and B. Tighilet (2007). "Betahistine in the treatment of Ménière's disease." Neuropsychiatric Disease and Treatment **3**(4): 429-440.

Land, Z. D., Julian; Curthoys, Ian; Grant, Wally (2018). Utricle Finite Element model; Implications at VEMPs Stimulation Frequencies. Association for Research in Otolaryngology, Manchester Grant Hyatt, San Diego, California.

Lee, C., J. C. Holt and T. A. Jones (2017). "Effect of M-current modulation on mammalian vestibular responses to transient head motion." Journal of neurophysiology **118**(6): 2991-3006.

Lee, C. and T. A. Jones (2018). "Effects of Ketamine Compared with Urethane Anesthesia on Vestibular Sensory Evoked Potentials and Systemic Physiology in Mice." Journal of the American Association for Laboratory Animal Science **57**(3): 268-277.

Lee, H. Y., P. D. Raphael, J. Park, A. K. Ellerbee, B. E. Applegate and J. S. Oghalai (2015). "Noninvasive in vivo imaging reveals differences between tectorial membrane and basilar membrane traveling waves in the mouse cochlea." Proceedings of the National Academy of Sciences **112**(10): 3128-3133.

Lee, H. Y., P. D. Raphael, A. Xia, J. Kim, N. Grillet, B. E. Applegate, A. K. E. Bowden and J. S. Oghalai (2016). "Two-dimensional cochlear micromechanics measured in vivo demonstrate radial tuning within the mouse organ of Corti." Journal of Neuroscience **36**(31): 8160-8173.

Legouix, J. P. (1962). "Changes in the cochlear microphonic of the guinea pig produced by mechanical factors in the inner ear." The Journal of the Acoustical Society of America **34**(9B): 1504-1508.

LePage, E. L. (1989). "Functional role of the olivo-cochlear bundle: a motor unit control system in the mammalian cochlea." Hearing research **38**(3): 177-198.

Liberman, M. C. and S. G. Kujawa (2017). "Cochlear synaptopathy in acquired sensorineural hearing loss: manifestations and mechanisms." Hearing research **349**: 138-147.

Lowy, K. (1942). "Cancellation of the Electrical Cochlear Response with Air-and Bone-Conducted Sound." The Journal of the Acoustical Society of America **14**(2): 156-158.

Lyford-Pike, S., C. Vogelheim, E. Chu, C. C. Della Santina and J. P. Carey (2007). "Gentamicin is primarily localized in vestibular type I hair cells after intratympanic administration." Journal of the Association for Research in Otolaryngology **8**(4): 497-508.

Lysakowski, A. and J. M. Goldberg (1997). "A regional ultrastructural analysis of the cellular and synaptic architecture in the chinchilla cristae ampullares." Journal of Comparative Neurology **389**(3): 419-443.

Lysakowski, A. and J. M. Goldberg (2004). Morphophysiology of the vestibular periphery. The vestibular system, Springer**:** 57-152.

Maass, B., H. Baumgärtl and D. W. Lübbers (1976). "Lokale pO2- und pH2-Messungen mit Nadelelektroden zum Studium der Sauerstoffversorgung und Mikrozirkulation des Innenohres." Archives of oto-rhino-laryngology **214**(2): 109-124.

Maheu, M., J. M. Alvarado-Umanzor, A. Delcenserie and F. Champoux (2017). "The Clinical Utility of Vestibular-Evoked Myogenic Potentials in the Diagnosis of Ménière's Disease." Frontiers in Neurology **8**: 415.

Manley, G. A. (2001). "Evidence for an active process and a cochlear amplifier in nonmammals." Journal of Neurophysiology **86**(2): 541-549.

Manley, G. A. and D. Robertson (1976). "Analysis of spontaneous activity of auditory neurones in the spiral ganglion of the guinea-pig cochlea." The Journal of physiology **258**(2): 323-336.

Mann, S. E., M. Johnson, F. L. Meredith and K. J. Rennie (2013). "Inhibition of K+ currents in type I vestibular hair cells by gentamicin and neomycin." Audiology and Neurotology **18**(5): 317-326.

Manzari, L., A. M. Burgess, L. A. McGarvie and I. S. Curthoys (2012). "Ocular and cervical vestibular evoked myogenic potentials to 500 Hz fz bone-conducted vibration in superior semicircular canal dehiscence." Ear Hear **33**(4): 508-520.

Marlinski, V., M. Plotnik and J. M. Goldberg (2004). "Efferent actions in the chinchilla vestibular labyrinth." Journal of the Association for Research in Otolaryngology **5**(2): 126-143.

Martin, P. and A. Hudspeth (1999). "Active hair-bundle movements can amplify a hair cell's response to oscillatory mechanical stimuli." Proceedings of the National Academy of Sciences **96**(25): 14306-14311.

Matsuura, S., K. Ikeda and T. Furukawa (1971). "Effects of streptomycin, kanamycin, quinine, and other drugs on the microphonic potentials of goldfish sacculus." The Japanese journal of physiology **21**(5): 579-590.

Misrahy, G., E. Shinabarger and J. Arnold (1958). "Changes in cochlear endolymphatic oxygen availability, action potential, and microphonics during and following asphyxia, hypoxia, and exposure to loud sounds." The Journal of the Acoustical Society of America **30**(8): 701-704.

Moller, H. and C. Pedersen (2004). "Hearing at low and infrasonic frequencies." Noise and Health **6**(23): 37-57.

Murofushi, T. (2016). "Clinical application of vestibular evoked myogenic potential (VEMP)." Auris Nasus Larynx **43**(4): 367-376.

Murugasu, E. and I. J. Russell (1996). "The effect of efferent stimulation on basilar membrane displacement in the basal turn of the guinea pig cochlea." J Neurosci **16**(1): 325-332.

Nuttall, A., D. Marques and M. Lawrence (1977). "Effects of perilymphatic perfusion with neomycin on the cochlear microphonic potential in the guinea pig." Acta oto-laryngologica **83**(1-6): 393-400.

Nuttall, A. L. and A. Fridberger (2012). "Instrumentation for studies of cochlear mechanics: from von Bekesy forward." Hear Res **293**(1-2): 3-11.

Nuttall, A. L. and A. Fridberger (2012). "Instrumentation for studies of cochlear mechanics: from von Békésy forward." Hearing research **293**(1-2): 3-11.

Nuttall, A. L., A. J. Ricci, G. Burwood, J. M. Harte, S. Stenfelt, P. Cayé-Thomasen, T. Ren, S. Ramamoorthy, Y. Zhang and T. Wilson (2018). "A mechanoelectrical mechanism for detection of sound envelopes in the hearing organ." Nature Communications **9**(1): 4175.

Oei, M. L., H. M. Segenhout, F. Dijk, I. Stokroos, J. J. van der Want and F. W. Albers (2004). "Functional and anatomic alterations in the gentamicin-damaged vestibular system in the guinea pig." Otol Neurotol **25**(1): 57-64.

Ozdamar, O. (1979). "DISTRIBUTION OF ABR (AUDITORY-BRAINSTEM-RESPONSE) COMPONENTS TO MONAURAL CLICKS IN THE GUINEA-PIGS." Journal of the Acoustical Society of America **65**: S85-S85.

Parthasarathy, A. and S. G. Kujawa (2018). "Synaptopathy in the Aging Cochlea: Characterizing Early-Neural Deficits in Auditory Temporal Envelope Processing." J Neurosci **38**(32): 7108-7119.

Patuzzi, R., B. M. Johnstone and P. M. Sellick (1984). "The alteration of the vibration of the basilar membrane produced by loud sound." Hear Res **13**(1): 99-100.

Patuzzi, R. and A. Moleirinho (1998). "Automatic monitoring of mechano-electrical transduction in the guinea pig cochlea." Hearing Research **125**(1-2): 1-16.

Patuzzi, R. and P. Sellick (1984). "The modulation of the sensitivity of the mammalian cochlea by low frequency tones. II. Inner hair cell receptor potentials." Hearing research **13**(1): 9-18.

Patuzzi, R., P. Sellick and B. Johnstone (1984). "The modulation of the sensitivity of the mammalian cochlea by low frequency tones. I. Primary afferent activity." Hearing research **13**(1): 1-8.

Patuzzi, R., P. Sellick and B. Johnstone (1984). "The modulation of the sensitivity of the mammalian cochlea by low frequency tones. III. Basilar membrane motion." Hearing research **13**(1): 19-27.

Patuzzi, R., P. M. Sellick and B. M. Johnstone (1982). "Cochlear drainage and basilar membrane tuning." J Acoust Soc Am **72**(3): 1064-1065.

Patuzzi, R. and G. Yates (1986). "Velocity and displacement coupling of mammalian inner hair cells and the mechanical resonance of the free-standing stereocilia." ORL **48**(2): 81-86.

Patuzzi, R. B., G. K. Yates and B. M. Johnstone (1989). "CHANGES IN COCHLEAR MICROPHONIC AND NEURAL SENSITIVITY PRODUCED BY ACOUSTIC TRAUMA." Hearing Research **39**(1-2): 189-202.

Patuzzi, R. B., G. K. Yates and B. M. Johnstone (1989). "THE ORIGIN OF THE LOW-FREQUENCY MICROPHONIC IN THE 1ST COCHLEAR TURN OF GUINEA-PIG." Hearing Research **39**(1-2): 177-188.

Rabbitt, R., R. Boyle and S. Highstein (1995). "Mechanical indentation of the vestibular labyrinth and its relationship to head rotation in the toadfish, Opsanus tau." Journal of neurophysiology **73**(6): 2237-2260.

Rabbitt, R. D., R. Boyle and S. M. Highstein (2010). "Mechanical amplification by hair cells in the semicircular canals." Proceedings of the National Academy of Sciences **107**(8): 3864-3869.

Rabbitt, R. D., R. Boyle, G. R. Holstein and S. M. Highstein (2005). "Hair-cell versus afferent adaptation in the semicircular canals." Journal of Neurophysiology **93**(1): 424-436.

Rauch, S. D., G. Zhou, S. G. Kujawa, J. J. Guinan and B. S. Herrmann (2004). "Vestibular evoked myogenic potentials show altered tuning in patients with Meniere's disease." Otology & Neurotology **25**(3): 333-338.

Rhode, W. S. (1971). "Observations of the vibration of the basilar membrane in squirrel monkeys using the Mössbauer technique." The Journal of the Acoustical Society of America **49**(4B): 1218-1231.

Robles, L. and M. A. Ruggero (2001). "Mechanics of the mammalian cochlea." Physiological reviews **81**(3): 1305-1352.

Rodionov, V., J. Elidan, M. Sela, M. Nitzan and H. Sohmer (1996). "Vertical plane short and middle latency vestibular evoked potentials in humans." Ann Otol Rhinol Laryngol **105**(1): 43-48.

Ruggero, M. A. and N. C. Rich (1991). "Application of a commercially-manufactured Doppler-shift laser velocimeter to the measurement of basilar-membrane vibration." Hearing research **51**(2): 215-230.

Ruggero, M. A. and N. C. Rich (1991). "Furosemide Alters Organ of Corti Mechanics: Evidence for Feedback of Outer Hair Cells upon the Basilar Membrane." The Journal of neuroscience : the official journal of the Society for Neuroscience **11**(4): 1057-1067.

Ruggero, M. A., L. Robles and N. C. Rich (1986). "Basilar membrane mechanics at the base of the chinchilla cochlea. II. Responses to low-frequency tones and relationship to microphonics and spike initiation in the VIII nerve." J Acoust Soc Am **80**(5): 1375-1383.

Russell, I. J. and E. Murugasu (1997). "Medial efferent inhibition suppresses basilar membrane responses to near characteristic frequency tones of moderate to high intensities." The Journal of the Acoustical Society of America **102**(3): 1734-1738.

Salt, A. N. and T. E. Hullar (2010). "Responses of the ear to low frequency sounds, infrasound and wind turbines." Hearing research **268**(1-2): 12-21.

Salt, A. N., I. Melichar and R. Thalmann (1987). "Mechanisms of endocochlear potential generation by stria vascularis." Laryngoscope **97**(8 Pt 1): 984-991.

Sheppard, A., S. Hayes, G.-D. Chen, M. Ralli and R. Salvi (2014). "Review of salicylate-induced hearing loss, neurotoxicity, tinnitus and neuropathophysiology." Acta Otorhinolaryngologica Italica **34**(2): 79.

Smith, D. I. and J. E. Hawkins (1985). "Effects of noise and quinine on the vessels of the stria vascularis: an image analysis study." American journal of otolaryngology **6**(4): 280-289.

Sohmer, H., J. Elidan, M. Plotnik, S. Freeman, R. Sockalingam, Z. Berkowitz and M. Mager (1999). "Effect of noise on the vestibular system - Vestibular evoked potential studies in rats." Noise Health **2**(5): 41-52.

Soto, E. and R. Vega (2010). "Neuropharmacology of Vestibular System Disorders." Current Neuropharmacology **8**(1): 26-40.

Soto, H. C. P. V. C. B. R. V. E. (2001). "Betahistine Produces Post-synaptic Inhibition of the Excitability of the Primary Afferent Neurons in the Vestibular Endorgans." Acta Oto-Laryngologica **121**(543): 19-24.

Spinks, A. B., J. Wasiak, E. V. Villanueva and V. Bernath (2007). "Scopolamine (hyoscine) for preventing and treating motion sickness." Cochrane Database Syst Rev(3): Cd002851.

Stewart, C. E., A. C. Kanicki, R. A. Altschuler and W. M. King (2018). "Vestibular short-latency evoked potential abolished by low-frequency noise exposure in rats." J Neurophysiol **119**(2): 662-667.

Stypulkowski, P. H. (1990). "Mechanisms of salicylate ototoxicity." Hearing research **46**(1-2): 113-145.

Tasaki, I. and C. Fernandez (1951). "EFFECT OF DIRECT CURRENT UPON THE COCHLEAR MICROPHONIC AND ACTION POTENTIAL OF THE GUINEA PIG." American Journal of Physiology **167**(3): 831-831.

Tonndorf, J. (1957). "Fluid motion in cochlear models." The Journal of the Acoustical Society of America **29**(5): 558-568.

Trincker, D. and C. Partsch (1959). "Electrophysiological studies of the labyrinth of the guinea pig. III. The AC potentials (microphonics) from the vestibular apparatus." The Annals of otology, rhinology, and laryngology **68**(1): 153-158.

Van Cauwenberge, P. B. and S. E. De Moor (1997). "Physiopathology of H3-receptors and pharmacology of betahistine." Acta Otolaryngol Suppl **526**: 43-46.

Von Békésy, G. and E. G. Wever (1960). Experiments in hearing, McGraw-Hill New York.

Webster, J. (1970). "Ototoxicity of Gentamicin. Histological and functional results in the cat." Trans Am Acad Ophthalmol Otolaryngl **74**: 1155-1165.

Webster, W. R. and L. M. Aitkin (1971). "EVOKED POTENTIAL AND SINGLE UNIT STUDIES OF NEURAL MECHANISMS UNDERLYING EFFECTS OF REPETITIVE STIMULATION IN AUDITORY PATHWAY." Electroencephalography and Clinical Neurophysiology **31**(6): 581-+.

Weerts, A. P., L. Putcha, S. W. Hoag, E. Hallgren, A. Van Ombergen, P. H. Van de Heyning and F. L. Wuyts (2015). "Intranasal scopolamine affects the semicircular canals centrally and peripherally." Journal of Applied Physiology **119**(3): 213-218.

Weinberger, N. M., L. M. Kitzes and D. A. Goodman (1970). "SOME CHARACTERISTICS OF AUDITORY NEUROPHONIC." Experientia **26**(1): 46-+.

Wersäll, J. and A. Flock (1964). "Suppression and restoration of the microphonic output from the lateral line organ after local application of streptomycin." Life sciences (1962) **3**: 1151.

Wever, E. G. and C. W. Bray (1930). "Action currents in the auditory nerve in response to acoustical stimulation." Proceedings of the National Academy of Sciences **16**(5): 344-350.

Wilson, J. and J. Johnstone (1975). "Basilar membrane and middle− ear vibration in guinea pig measured by capacitive probe." The Journal of the Acoustical Society of America **57**(3): 705-723.

Wit, H., J. Bleeker and J. Segenhout (1981). "Vestibular and cochlear responses to acoustic transients: some properties of whole-nerve action potentials in pigeons." Acta oto-laryngologica **92**(1-6): 409-422.

Wit, H. P., H. F. Kahmann and J. M. Segenhout (1986). "VESTIBULAR MICROPHONIC POTENTIALS IN PIGEONS." Archives of Oto-Rhino-Laryngology **243**(2): 146-150.

Withnell, R. H. (2001). "Brief report: the cochlear microphonic as an indication of outer hair cell function." Ear and hearing **22**(1): 75-77.

Young, E. D., C. Fernández and J. M. Goldberg (1977). "Responses of Squirrel Monkey Vestibular Neurons to Audio-Frequency Sound and Head Vibration." Acta Oto-Laryngologica **84**(1-6): 352-360.

Yu, H., C.-K. Guo, Y. Wang, T. Zhou and W.-J. Kong (2014). "Gentamicin blocks the ACh-induced BK current in guinea pig type II vestibular hair cells by competing with Ca2+ at the L-type calcium channel." International journal of molecular sciences **15**(4): 6757-6771.

Zhou, G. and Q. Gopen (2011). "Characteristics of vestibular evoked myogenic potentials in children with enlarged vestibular aqueduct." Laryngoscope **121**(1): 220-225.

Zwicker, E. (1977). "Masking-period patterns produced by very-low-frequency maskers and their possible relation to basilar-membrane displacement." The Journal of the Acoustical Society of America **61**(4): 1031-1040.

Zwicker, E. (1981). "Masking-period patterns and cochlear acoustical responses." Hearing research **4**(2): 195-202.

Appendix 1

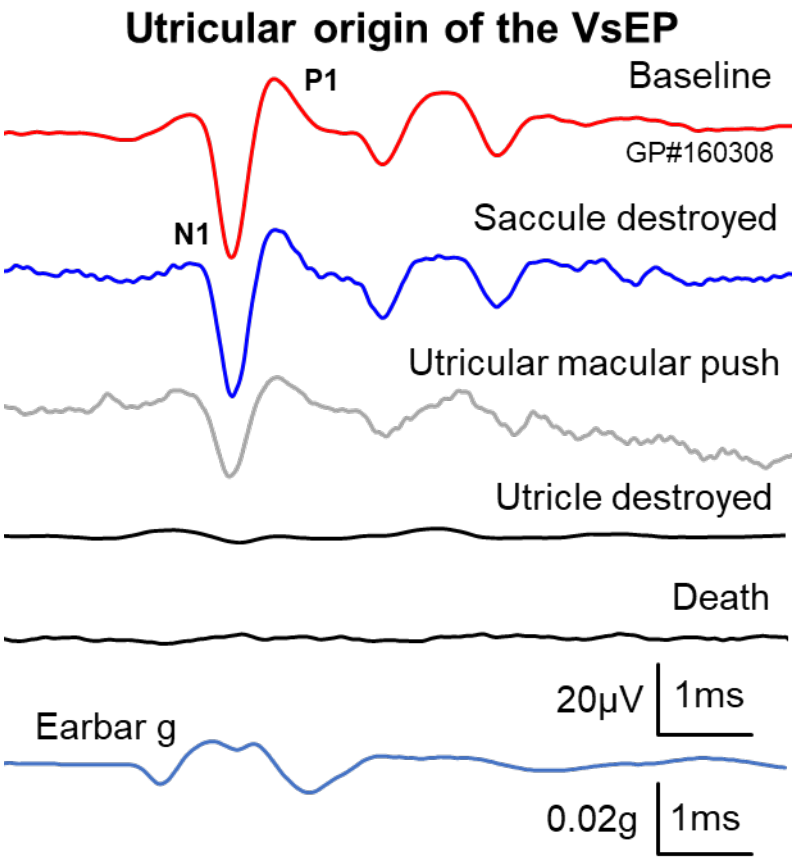

Figure 1: Evidence of the utricular origin of the VsEP in our experimental setup. Saccular destruction (blue) did not alter the VsEP, whereas directly pressing on the utricle (grey) with a blunt pipette immediately reduced the response. Surgical ablation of the utricle immediately irreversibly abolished the VsEP.

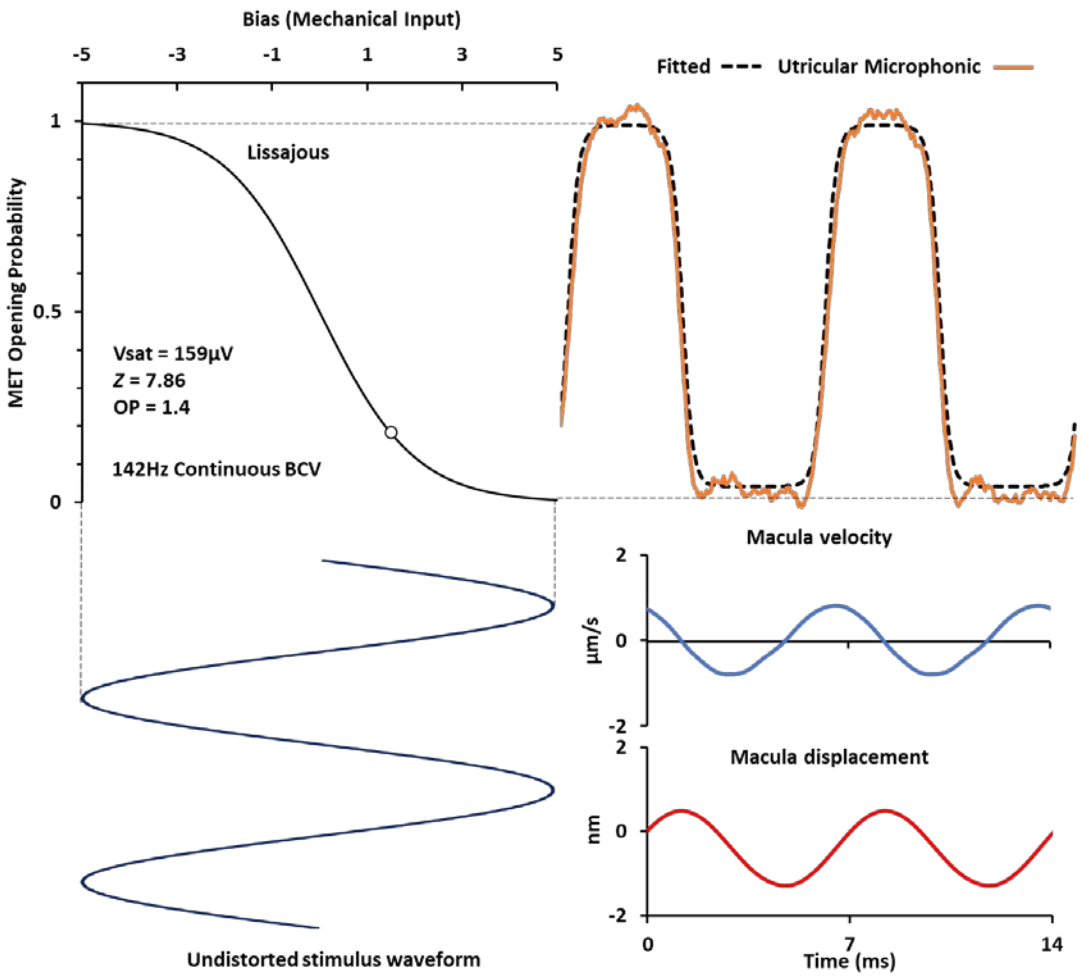

Figure 2: An example of Boltzmann analysis performed on a saturated UM response, evoked by a 142Hz continuous BCV, with simultaneous macular velocity measurements. The Boltzmann fit predicts utricular MET channels are 98% saturated, which corresponds to a dorso-ventral macula displacement of 2nm. Ultimately, our macular velocity recording only provides a partial measure of the mechanical drive to the utricular hair cells, and therefore we cannot use our LDV measure to quantify the mechanical sensitivity during MET channel gating. The equation used for the Boltzmann-fit was: $Vum \approx Vsat/[1 + \mathrm{EXP}(Z.\sin(2\pi\omega t) + OP)$.

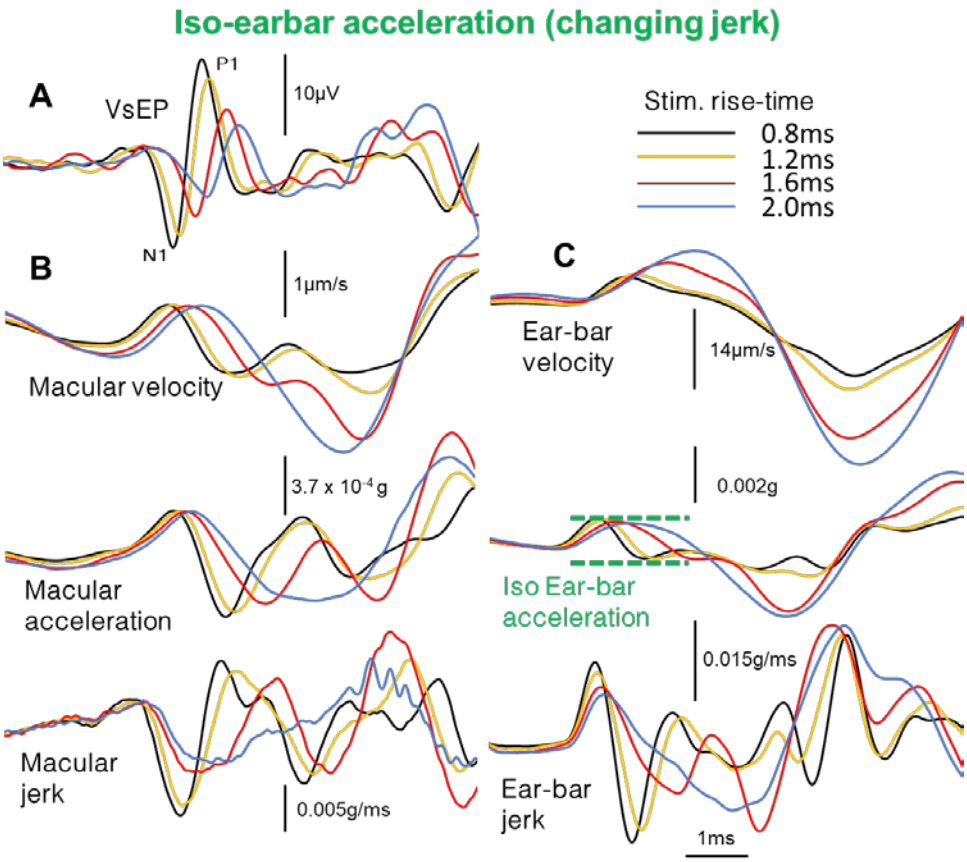

Figure 3: The effect of changing peak-peak ear-bar jerk on the VsEP. This was achieved by maintaining an iso-earbar acceleration whilst changing the stimulus length (rise-time). A. Averaged VsEP waveforms recorded during a 4ms monophasic BCV pulse at different stimulus rise-times, B. Simultaneous macular velocity, and its derivatives, macular acceleration and jerk. C. Simultaneous ear-bar velocity, and its derivatives, ear-bar acceleration and jerk. Note, ear-bar acceleration was monitored and the stimulus was adjusted manually to achieve an 'iso ear-bar acceleration'. Results demonstrate the VsEP is sensitive to changes in ear-bar and macular jerk. GP#180412.

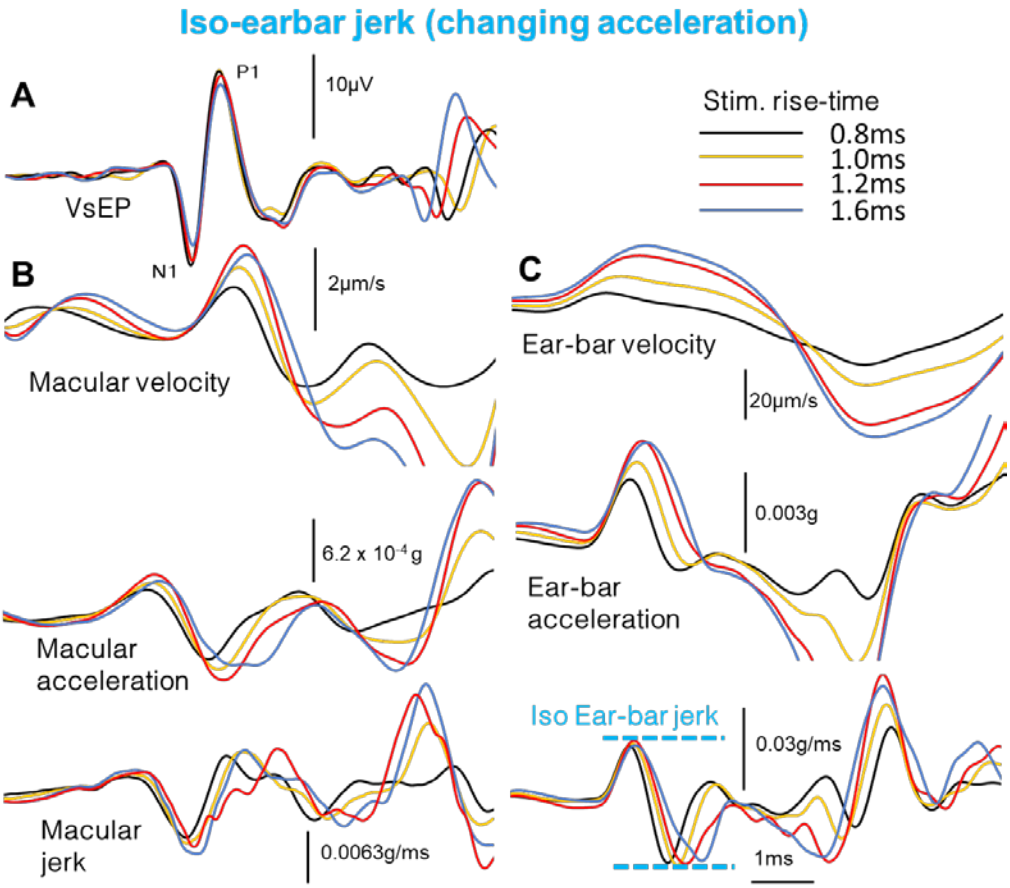

Figure 4: The effect of changing pk-pk ear-bar acceleration on the VsEP. This was achieved by maintaining an iso-earbar jerk whilst changing the stimulus length (rise-time). A. Averaged VsEP waveforms recorded during a 4ms monophasic BCV pulse at different stimulus rise-times, B. Simultaneous macular velocity, and its derivatives, macular acceleration and jerk. C. Simultaneous ear-bar velocity, and its derivatives, ear-bar acceleration and jerk. Note, ear-bar jerk was monitored and the stimulus was adjusted manually to achieve an 'iso ear-bar jerk' across the 4 stimulus rise-times. GP#180412.

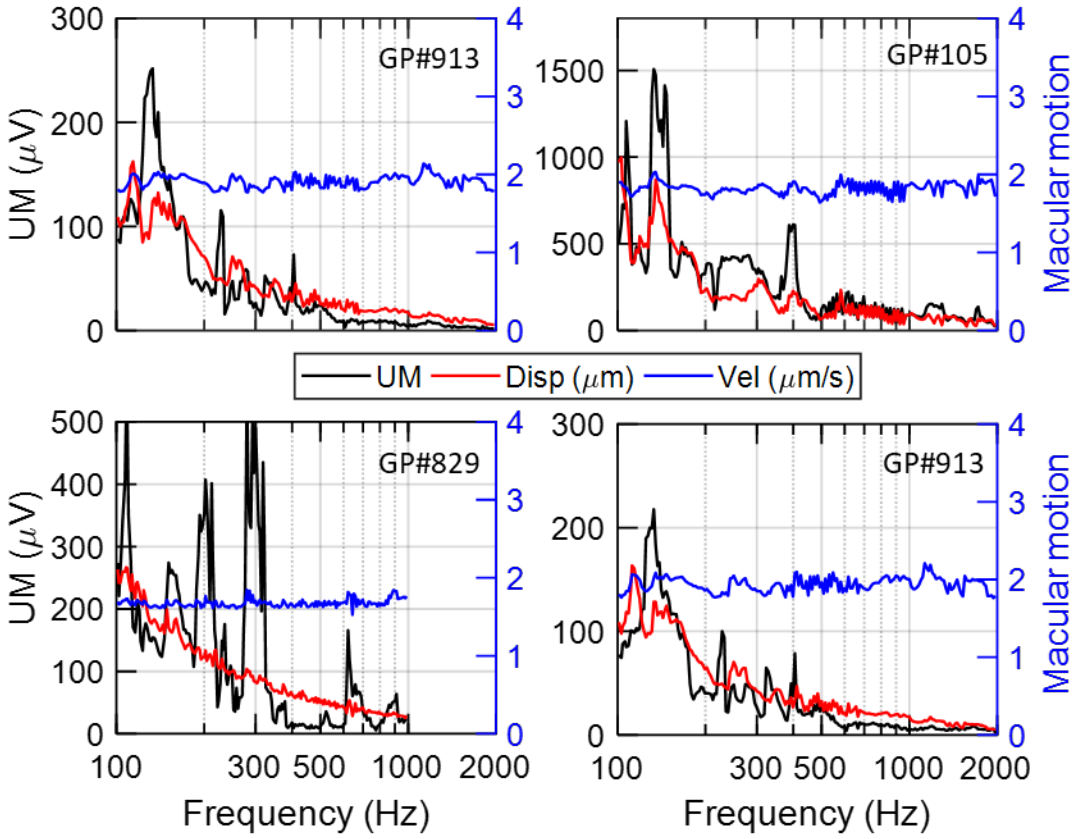

Figure 5: The amplitude of the UM, evoked by different frequency BCV stimuli (100 to 2000Hz), at a level that evoked a consistent macular velocity (~2µm/s). The recordings (presented here) were repeated in 3 separate animals (GP#170829, 170913, 171005). Results suggest the UM is more sensitive to macular displacement than macular velocity.

Appendix 2

General LDV Specifications

Name	*Ometron* Commercial Laser Doppler Vibrometer – Type 8338
Frequency range	0.5 Hz – 22 kHz
Dynamic range	>90 dB over full bandwidth
High–pass filter	100Hz on/off -3dB analogue, 3rd order Butterworth, 60 dB/dec)
Low–pass filter	FIR filter cut-off at 1kHz, 5kHz or 22kHz, roll-off >120 dB/dec
Calibration accuracy	± 1%
Output impedance	50Ω
Propagation delay	1.2ms
Power	11-14.5V DC, max. 1A
Sensitivity	5 - 125mms^{-1} ; upto 500mm/s (p-p) over 3 ranges
RMS	≤0.02µm/s/√Hz
Dimensions	299mm (11.7”) x 148mm (5.8”) x 83mm (3.2”)
Weight	3.5kg (7.71 lb.)
Laser	< 1mW output power, safety class II, He-Ne visible 632.8 nm laser (red)
Optical system	1. Fixed focus lens: 238mm (9.3 “) 2. Variable focus lens: 90mm (3.5”) - 30m (1180”)

Figure 1: The Commercial Ometron Laser Doppler Vibrometer used to record macular vibration measurements

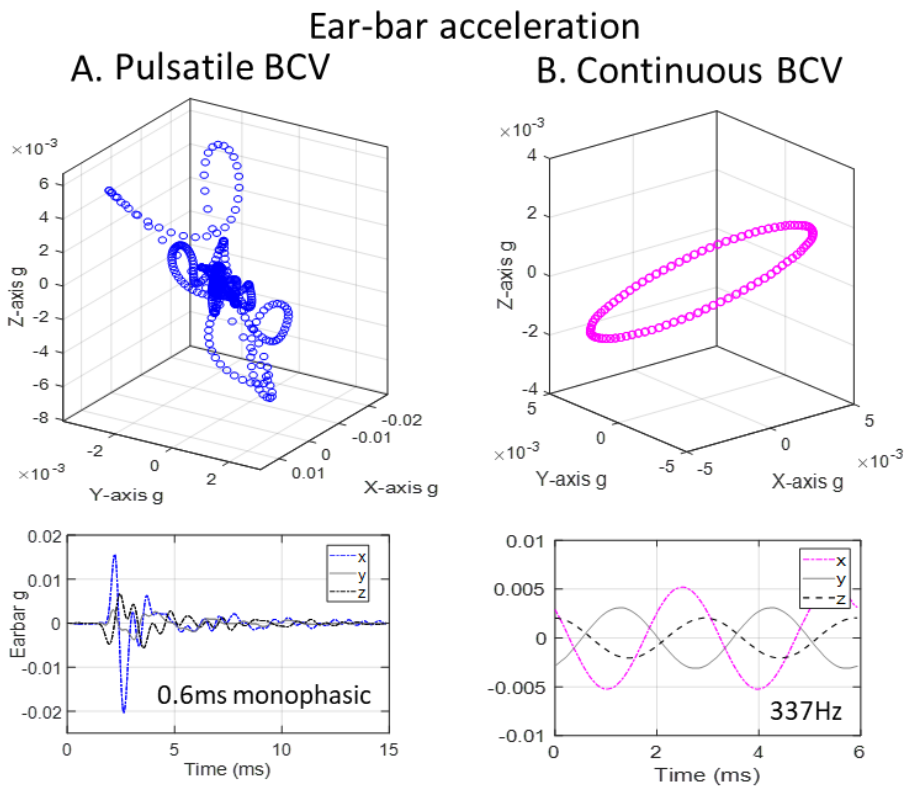

Figure 2: Comparison of the 3-axis acceleration profile recorded from the ear-bar during A. pulsatile and B. continuous BCV stimulation. GP#170811.

Appendix 3

Brown, D. J., Pastras, C. J., & Curthoys, I. S. (2017). Electrophysiological Measurements of Peripheral Vestibular Function—A Review of Electrovestibulography. *Frontiers in systems neuroscience*, *11*, 34.

frontiers in Systems Neuroscience

REVIEW
published: 31 May 2017
doi: 10.3389/fnsys.2017.00034

Electrophysiological Measurements of Peripheral Vestibular Function—A Review of Electrovestibulography

Daniel J. Brown[1]*, *Christopher J. Pastras*[1] *and Ian S. Curthoys*[2]

[1]*Neurotology Laboratory, Sydney Medical School, The University of Sydney, Sydney, NSW, Australia,* [2]*Department of Psychology, The University of Sydney, Sydney, NSW, Australia*

Electrocochleography (EcochG), incorporating the Cochlear Microphonic (CM), the Summating Potential (SP), and the cochlear Compound Action Potential (CAP), has been used to study cochlear function in humans and experimental animals since the 1930s, providing a simple objective tool to assess both hair cell (HC) and nerve sensitivity. The vestibular equivalent of ECochG, termed here *Electrovestibulography* (EVestG), incorporates responses of the vestibular HCs and nerve. Few research groups have utilized EVestG to study vestibular function. Arguably, this is because stimulating the cochlea in isolation with sound is a trivial matter, whereas stimulating the vestibular system in isolation requires significantly more technical effort. That is, the vestibular system is sensitive to both high-level sound and bone-conducted vibrations, but so is the cochlea, and gross electrical responses of the inner ear to such stimuli can be difficult to interpret. Fortunately, several simple techniques can be employed to isolate vestibular electrical responses. Here, we review the literature underpinning gross vestibular nerve and HC responses, and we discuss the nomenclature used in this field. We also discuss techniques for recording EVestG in experimental animals and humans and highlight how EVestG is furthering our understanding of the vestibular system.

Keywords: vestibular, VSEP, electrovestibulography, electrocochleography, microphonic

OPEN ACCESS

Edited by:
Jeffery Lichtenhan, Washington University in St. Louis, United States

Reviewed by:
Larry Hoffman, University of California, Los Angeles, United States
John Carey, Johns Hopkins University, United States
Timothy A. Jones, University of Nebraska Lincoln, United States

***Correspondence:**
Daniel J. Brown
daniel.brown@sydney.edu.au

Received: *23 February 2017*
Accepted: *05 May 2017*
Published: *31 May 2017*

Citation:
Brown DJ, Pastras CJ and Curthoys IS (2017) Electrophysiological Measurements of Peripheral Vestibular Function—A Review of Electrovestibulography. Front. Syst. Neurosci. 11:34. doi: 10.3389/fnsys.2017.00034

ELECTROVESTIBULOGRAPHY BACKGROUND

The history of Electrocochleography (ECochG) as a technique for recording cochlear field potentials is well established (Eggermont, 2017), beginning with Wever and Bray's (1930) recordings of the Cochlear Microphonic (CM) in response to air conducted sound (ACS) stimuli in cats, and the 8th nerve compound action potential (CAP) response shortly after by Fromm et al. (1935). Predominantly, ECochG is used to objectively monitor cochlear sensitivity to ACS in animal experiments. During the 1970s, ECochG evolved as a clinical tool for diagnosing 8th nerve schwannomas, for monitoring 8th nerve function during surgery, and for diagnosing endolymphatic hydrops, where the ratio of the Summating Potential (SP) to CAP ratio was of primary interest (Gibson et al., 1977). More recently, variants of ECochG have been used to monitor 8th nerve and hair cell (HC) function during cochlear implantation using the electrically evoked CAP (Scott et al., 2016), or have used the acoustically evoked auditory nerve neurophonic (Lichtenhan et al., 2014; Koka et al., 2017; Rampp et al., 2017) or the CM (Campbell et al., 2016) during surgery. It should be made clear that ECochG is not the name of a response *per se* (the response is the CM, CAP, ANN or SP), but rather the *process* of monitoring electrical potentials

from excitable cochlear cells. Today, there is a decreasing reliance of ECochG in the clinical setting (Hornibrook et al., 2016), with the Auditory Brainstem Response (ABR; and variants of) and otoacoustic emissions primarily being used to objectively monitor patient hearing and an increasing reliance on diagnostic imaging.

Whilst ECochG is an established tool in hearing research, there is less appreciation for the vestibular analog of ECochG, which has been infrequently termed Electrovestibulography (EVestG; Charlet de Sauvage et al., 1990; Lithgow, 2012). EVestG may be considered the process of measuring electrical responses of the peripheral vestibular system. Analogous to the CM and CAP or ABR in ECochG, EVestG responses consist of both vestibular HC and vestibular nerve field potentials. Fluctuations in the extracellular potential due to movement induced changes in the vestibular HC conductance and receptor current has been termed the "Vestibular Microphonic" (VM), whereas the vestibular afferent nerve response (or central vestibular neuron response) to movement has been termed the short-latency Vestibular Evoked Potential (VsEP). This review article will focus on the VM and VsEP, as fundamental EVestG components.

EVestG has not been extensively used by inner ear researchers. That is, although the VM and the VsEP have been characterized, they are used far less often and rarely compared to their cochlear counterparts. A simple PubMed search for "vestibular VsEP" returns a list of just 49 publications, whereas a search for "cochlear CAP" or "cochlear CM" returns a list of 570 and 930 publications respectively[1]. Moreover, Electrocochleography is an established term, with more than 4000 publications listed on Pubmed, whereas the term Electrovestibulography has only been used in 20 publications, 18 of which were from the same research group. Some of this discrepancy may be due to variation in the nomenclature of these responses.

Over the last 20 years, the term Electrovestibulography has only been used to describe a recent controversial response that forms part of a patented recording technique (Lithgow, 2006, 2012). Here, Lithgow (2006) claim that the stochastically occurring field potential of the vestibular nerve can be extracted from the biological noise measured from the ear canal (i.e., this is not a stimulus evoked response *per se*). The authors use a signal analysis process to localize any stochastically occurring field potentials that have characteristics resembling the VsEP, occurring within the raw electrical recording from the ear canal. They then average these asynchronous field potentials, somewhat similar to the methods involving spike-triggered averaging (Kiang et al., 1976). To obtain a response that is dominated by vestibular activity, they accelerate the subject in a given direction for approximately 1 s. By subtracting the averaged field potential recorded during movement, from that without movement, the resulting difference waveform theoretically resembles a response of stimulated vestibular neurones. At present, there is only weak evidence to support the claim that such a response faithfully represents the activity of vestibular neurones, and other clinical or experimental researchers have not adopted the technique. Furthermore, the technique requires a complex system capable of performing a controlled acceleration of a person many times, synchronized with the recording condition. Fortunately, researchers have demonstrated much simpler techniques for objectively measuring peripheral vestibular function, via the VM and VsEP. Most of these studies have been performed in experimental animals, with a limited number of human studies.

[1]No attempt has been made to perform a validated systematic review, but the large discrepancy in the numbers do not warrant such an approach.

RESPONSE NOMENCLATURE

Prior to reviewing how EVestG and ECochG measurements compare, there is perhaps a need to revisit, or clarify some of the terminology used in this field. Inner ear evoked responses, and more broadly electrophysiological responses, are rife with inappropriate nomenclature, although it would be impractical to alter their use today because they have been used for several decades. Nevertheless, it is necessary to have a clear understanding of how the electrical activity of excitable cells relate to extracellular potentials (Bressler, 2011; Buzsáki et al., 2012). A brief description of the major cochleovestibular electrophysiological responses, and stimulus "typically" used to evoke them is listed in **Table 1**.

These responses are all field potentials, generated by a subset of cells, evoked by a given ACS or bone conducted vibration (BCV) stimulus, whose response waveform differs with recording location and stimulus protocol. Unfortunately, most ACS or BCV stimuli will evoke a response from multiple cell-types (e.g., cochlear or vestibular neurons or HCs). For example, the CAP and VsEP can both be measured with electrodes in or near the inner ear, evoked by a BCV stimulus. Therefore, researchers might employ a technique, such as using moderate level transient ACS stimuli, with a low stimulation rate (e.g., 11/s), to maximize the contribution of the cochlear nerve to the field potential, and we may call this technique ECochG. EVestG is the technique of recording field potentials that predominantly reflect vestibular nerve or vestibular HC activity. Specifically, EVestG responses include the VM and the VsEP.

However, even the VM and VsEP may contain responses from different cell types. As discussed later, the VM may originate from either semicircular canal (SCC), utricular, or saccular HCs, and the VsEP may either reflect the compound activity of the 8th nerve, or central vestibular activity. It could be argued, for the purpose of consistency and to avoid confusion, that the VM should ideally be separated into SCC microphonic, utricular microphonic, or saccular microphonic, and that the VsEP recorded from the periphery should be re-termed the vestibular nerve CAP (as opposed to the cochlear nerve CAP), and that the VsEP recorded from the scalp should be re-termed the vestibular brainstem response. However, within this review we will continue to use the commonly accepted more general terminology, explicitly defining the recording location and origin of the response where appropriate.

TABLE 1 | Common cochlear and vestibular electrophysiological activity used to objectively measure inner ear function.

Response	Stimulus	Latency (ms)	Source	Origin
Unitary potential	Spont.	N/A	Neuron(s)	The spontaneous field potential of a single neuron, or collection of neurons, measured distant to the cell. Requires special recording techniques to extract it from noise.
Neural noise or neurophonic	Spont. or ACS	N/A	Nerve	The ensemble electrical activity related to stochastic or cyclic activity of the 8th nerve.
Compound action potential (CAP)	**ACS**	**~1**	**Nerve**	**The compound summation of synchronously occurring unitary potentials.**
Cochlear microphonic (CM)	**ACS**	**<0.1**	**Hair cells**	**The field potential generated by hair cells. Typically recorded from the cochlear fluids.**
Summating potential (SP)	**ACS**	**<0.1**	**Hair cells**	**The charge imbalance (i.e., asymmetry) of the hair cell field potential, which is obtained by removing the symmetric components of the CM (either by stimulus inversion and averaging, or low-pass filtering).**
Auditory brainstem response (ABR)	ACS	1–7	Nerve/ Brainstem	The compound summation of synchronously occurring neural activity in the auditory brainstem.
eCAP	Current	0–0.5	Nerve	An electrically evoked CAP
Middle and long latency response	ACS	10–500	Cortex	The compound summation of synchronously occurring neural activity in the auditory cortex.
Post-auricular muscle response	ACS	12–20	Myocytes	A compound summation of the electrical response of the post-auricular muscle.
Frequency following response	ACS	N/A	Nerve/ Brainstem	The ensemble electrical activity related to cyclic activity of the auditory brainstem.
Vestibular short latency evoked potential (VsEP)	**BCV**	**0.5**	**Nerve/ Brainstem**	**The compound summation of synchronously occurring neural activity of the vestibular nerve and brainstem.**
Vestibular microphonic (VM)	**BCV**	**<0.1**	**Hair cell**	**The field potential generated by hair cells. Typically recorded from the vestibule fluids.**
Vestibular evoked myogenic potential (VEMP)	BCV	10–20	Myocytes	A compound summation of the electrical activity of the extra-ocular or sternocleidomastoid muscles.

Also provided is the typical stimulus for each response (Spont., Spontaneous; ACS, Air Conducted Sound; BCV, Bone Conducted Vibration, N/A, not applicable), and a brief explanation of the origin of each activity. Highlighted responses refer to those typically forming parts of ECochG and EVestG responses. The latency refers to the time after the onset of the stimulus, where the stimulus is evoked by the onset of a stimulus.

THE VM AND VsEP

Arguably, the greatest obstacle with performing EVestG measures and using them as a faithful measure of peripheral vestibular function is that both ACS and BCV stimuli can evoke cochlear field potentials (i.e., CM and CAP), which are an order of magnitude larger than vestibular responses, and will summate with the VsEP or VM. Selectively destroying the cochlea, which does not abolish the VsEP or VM, or destroying the vestibule, which does abolish them, provides clear evidence that these responses originate from vestibular sources. Researchers wishing to use EVestG without destroying the inner ear either need to suppress cochlear responses, or record responses at a location where cochlear activity is not present, or use a stimulus that does not stimulate the cochlea. There are a number of technical considerations when measuring EVestG responses, and a clear understanding of recording techniques is necessary when using EVestG as an objective measure of peripheral (or central) vestibular function.

EVestG BCV Stimuli

Some form of transient or cyclic translation or rotation of the skull is commonly used to evoke the VsEP and VM. Often, this stimulus is transmitted to the head via an electromagnetic transducer or "modal shaker", rigidly attached to the head. Whether the stimulus is a pulsed, cyclic, or angular translation of the head, here we consider all forms of head movement to be BCV stimuli. Other forms of vestibular stimulation include ACS, manual force applied to the head, or even force directly applied to the HC stereocilia, although this last method requires surgical exposure of the inner ear.

For the purposes of reproducibility and interpretation, it is necessary to measure the stimulus delivered to the vestibular system. Ideally, researchers could measure the movement of the vestibular end-organ directly (as has been performed in cochlear mechanics studies; Sellick et al., 1982; Chen et al., 2007), however this is impractical in most scenarios because the vestibular system is housed deep inside the inner ear. The next best, albeit indirect, option is to measure the movement of the skull, which can be achieved by rigidly attaching an accelerometer to the bone, skin, or to the modal shaker directly. However, with these indirect methods, the property of vibration through the skull needs to be considered.

The mechanical properties of BCV are complex, because the skull consists of rigid and compliable bone, combined with soft tissue and fluids. Additionally, the skull is segmented

and separated by sutures, and has complex resonance features (Håkansson et al., 1994). Various attempts have been made to model and measure the properties of vibration transmission through the head, primarily in humans, and primarily aimed at understanding BCV hearing (Stenfelt, 2015, 2016). For the human head at least, the skull *approximately* moves as a rigid structure for BCV below 400 Hz (Stenfelt and Goode, 2005), as a resonant structure between 400 Hz to 2 kHz (Håkansson et al., 1994), and as a wave-propagating structure above 2 kHz (Stenfelt, 2015). These parameters solely relate to the propagation of vibration through the bone, and do not include the additional compliance of soft tissues like skin, or the fluid dynamics of the inner ear known to play a role in HCs stimulation (Sohmer et al., 2000; Sohmer and Freeman, 2004; Stenfelt, 2015). Moreover, there is little information regarding BCV through experimental animal heads, which will have vastly different mechanical properties to that of human skulls. Ultimately, it should be made clear that, particularly for pulsed or cyclic (>100 Hz) BCV in experimental animals, that movements measured on or near the skull are unlikely to faithfully represent the vibration of the vestibular HCs. Moreover, particularly for high-frequency (>400 Hz) BCV, the head movement is likely to differ when measured at different locations (Durrant and Hyre, 1993). Without a standard BCV measurement technique, it can be difficult to compare head movements between studies. Thus, whilst researchers can directly measure otolith sensitivity to different BCV frequencies, caution should be taken when interpreting the response properties of the end-organ itself, particularly when the BCV stimulus is delivered to the head at different locations and under different conditions.

At one level, ACS stimulation of the vestibular system may be easier to interpret, because the bulk of the energy is transmitted through the ear canal where sound levels can be measured as a standard, and a great deal of work has been done on ACS transmission through the middle-ear (Ravicz et al., 2010). The frequency response of ACS stimulation of the otolith neurons closely resembles middle-ear transmission frequency response, although there are differences in the sensitivity of the different vestibular end-organs. How ACS stimulates the vestibular system is less clear, although it presumably involves fluid pressure waves inducing displacements of the vestibular HCs or their stereocilia. The problem with ACS stimulation for EVestG measurements however, is that cochlear HCs are 100 dB more sensitive to ACS than vestibular HCs, and relatively large ECochG responses will be present in ACS evoked field potential recordings.

VM Recordings

The VM was first reported just 8 years after the CM in 1938, albeit in an *ex vivo* preparation (Adrian et al., 1938; Zotterman, 1943; Lowenstein and Roberts, 1951; Wever and Vernon, 1956). Since then, the VM has been recorded *in vivo* in zebrafish (Trapani and Nicolson, 2010; Yao et al., 2016), toadfish (Rabbitt et al., 1995), bullfrogs (Eatock et al., 1987), pigeons (De Vries and Vrolijk, 1953; Wit et al., 1986, 1990), and guinea pigs (Trincker and Partsch, 1959). The VM reflects changes in the receptor current through the mechano-electrical transduction channels located on the stereocilia of the vestibular HCs, which are displaced due to inertial drag, resulting from a shearing force that displaces the otoconia or cupula (Fernández and Goldberg, 1976).

Ex Vivo VM

Much of our knowledge regarding the properties of HCs comes from *ex vivo* recordings of the VM from bullfrog otolithic HCs (Corey and Hudspeth, 1983; Azimzadeh and Salvi, 2017). Here, the otolithic maccula (most studies have used the sacculus) is extracted and placed between perilymph/endolymph filled baths in an Ussing chamber (**Figure 1A**; from Corey and Hudspeth, 1983), with a region of the epithelia exposed to both baths. Vibration is directly applied to the macula, or overlying otolithic membrane (OM), via a stiff probe (**Figures 1A,B**). Recording the bath potential provides a global measure of the VM generated from the HCs exposed to both baths (i.e., a summed response of all HCs), or alternatively intracellular potentials can be recorded with glass microelectrodes. VM recordings have been made with either the OM intact (**Figure 1C**), partially removed so as to only stimulate HCs with stereocilia of a particular orientation (**Figure 1D**), or totally removed. Removing the OM uncouples hair bundle motions from neighboring HCs, and has substantial effects on their excitability and sensitivity (Benser et al., 1993; Dierkes et al., 2008; Fredrickson-Hemsing et al., 2012; Ó Maoiléidigh et al., 2012). With the otolith membrane intact and all HCs are stimulated, the global VM will exhibit a response with twice the frequency of the vibration stimulus (**Figures 1C,E**). This is because HCs of both polarities are stimulated (Flock, 1965; Corey and Hudspeth, 1983). When only HCs on one side of the line of polarity reversal (Li et al., 2008) are stimulated the VM is cyclic, following the vibration stimulus (**Figures 1D,E**), although it will saturate at high stimulus levels (Hudspeth and Corey, 1977; Corey and Hudspeth, 1983).

Several other studies have examined the microphonic from the SCC HCs using an *ex vivo* preparation (De Vries and Bleeker, 1949; Van Eyck, 1951a,b,c; Masetto et al., 1995; Botta et al., 1998; Rabbitt et al., 2005). Here, the polarity of mechanical sensitivity is the same for all hair bundle stereocilia, such that mechanical displacements of the cupula either increases the conductance of all SCC HCs, or decreases it. This results in an asymmetrically distorted microphonic, which can be recorded some distance from the cristae in the vestibular fluids (Botta et al., 1998).

In Vivo VM

Few studies over the last 50 years have recorded the VM *in vivo*. This is arguably because evoking the VM requires low-frequency (10–1000 Hz) stimulation, which induces hair bundle displacements (Huizinga and Van Der Meulen, 1951; Trincker and Partsch, 1959; Bleeker et al., 1980; Wit et al., 1981, 1990), yet this will evoke a CM that will dominate the inner ear fluid potentials. That is, compared to VM responses, the CM is large (1–2 millivolts in the perilymph, and several times larger in endolymph; Honrubia et al., 1973) because there is a large electrochemical driving potential for the receptor current through cochlear HCs of +150mV (involving a +90 mV electrogenic potential on the apical

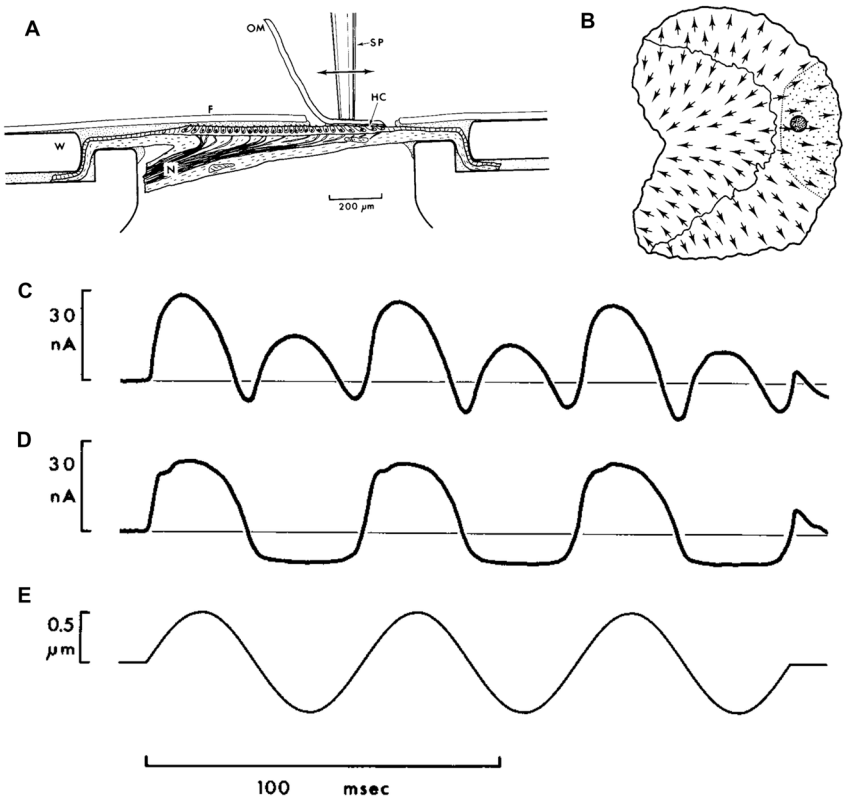

FIGURE 1 | (A) *Ex vivo* Vestibular Microphonic (VM) recordings from a bullfrog's saccular maccula. The macula has been extracted and placed between two fluid-filled baths, sealed with a washer (W) in an Ussing-chamber format. A thin plastic film (F) isolates a region of the macula exposed to the bath. The fluid potential between the baths is used to provide a measure of the VM. The macula is vibrated via a stimulating probe (SP) directly attached to the otolithic membrane (OM), which is either intact, or partially removed from the macula such that it only adheres to hair cells (HCs) of a single orientation. **(B)** A schematic illustrating of the saccular macula, with arrows indicating HCs polarities, and highlighting the location of the probe (dark shaded circle) and the area where the OM remains intact (shaded region on right of macula). **(C)** The VM response with the OM covering all HCs, demonstrating a response with twice the frequency of the vibration stimulus. **(D)** The saturated VM response, with the OM peeled back so that only HCs of a single orientation were stimulated. **(E)** The 16.5 Hz vibration stimulus. Reproduced with permission from Corey and Hudspeth (1983).

surface, and a transmembrane potential of −60 mV; Davis, 1965), whereas the driving potential for the receptor current through HCs in the SCCs, utricle or saccule is most likely to be closer to +65 mV due to a much lower endolymphatic potential (Schmidt, 1963; Ono and Tachibana, 1990; He et al., 1997). Additionally, the CM is large because the polarization of HCs stereocilia sensitivity, within a given region of the cochlea, are aligned in the same direction (Russell, 1983), and cochlea scalae are separated by an epithelium with an electrical impedance of 40–50 kOhm (Johnstone et al., 1966). Conversely, the otolith HCs microphonic will cancel in the fluids due to opposite polarity of HCs either side of the line of polarity reversal, which generates microphonic potentials in the fluids which are 180° out of phase (Corey and Hudspeth, 1983). Furthermore, vestibular HCs are either supported by bone-anchored epithelia, or in the case of the utricle, suspended on a membrane which most likely has an electrical impedance close to 13 kOhm, and therefore the circuit potential related to vestibular HC stimulation will be comparatively low.

Most *in vivo* studies of the VM have necessarily abolished cochlear function prior to monitoring the VM, and have measured the VM within the inner ear fluids (Adrian et al., 1938; Wever and Vernon, 1956; Trincker and Partsch, 1959; Wit et al., 1981, 1986, 1990). Only a few studies, mostly using fish, have recorded the VM without destroying the cochlea (Zotterman, 1943; Furukawa and Ishii, 1967; Fay and Popper, 1974; Rabbitt et al., 2005; Sisneros, 2007; Yao et al., 2016). VM recordings in fish, particularly zebrafish, are emerging as a powerful tool for studying inner ear developmental biology (Trapani and Nicolson, 2010; Yao et al., 2016). Here, both the lateral line organ and the inner ear (the otic capsule) will respond to alternating pressures and generate microphonic potentials, and differentiating the source of the VM (i.e., explicitly which HCs generate the VM), will be complex due to the small size of the organ.

De Vries and Bleeker (1949) and Van Eyck (1949) were the first to measure VM *in vivo*, from the SCCs of pigeons. De Vries and Vrolijk (1953), used sinusoidal tympanic membrane displacements to evoke SCC microphonics in pigeons after the

cochlea and otoliths had been destroyed. The otoliths were destroyed because they too were stimulated by displacement of the tympanic membrane, and the otolith responses contaminated the SCC responses. Here, the VM was recorded both in the vestibule, and in the SCC after a small hole had been made in the canal wall, which was shown to induce the Tullio effect and enhance SCC responses. Ultimately, the VM from the SCCs demonstrated phase relationships which supported Ewald's laws, demonstrating highly nonlinear microphonic potentials, where each SCC was maximally stimulated for fluid motion in a given direction. Later Wit et al. (1986) used ACS stimuli, with a SCC fenestration and cochlear extirpation, to evoke VM responses in pigeons (**Figure 2**). Increasing the level of the stimulus resulted in the response frequency doubling, similar to that obtained with *ex vivo* experiments where the whole otolith was stimulated (**Figure 1C**), suggesting that additional vestibular HCs were being recruited with high level ACS, which had a response phase difference of 180°. No attempt was made to separate the response components.

Trincker and Partsch (1959) performed arguably the most extensive *in vivo* assessment of the VM in mammals, using guinea pigs, and stimulated microphonic potentials from the SCCs, utricle, and saccule, using both BCV and ACS tones, after the cochlea was completely destroyed. Recordings were performed with electrodes within the cochlear fluids, within the SCCs, or within the ampulla. Selective ablation of each end organ was used to confirm the specific origin of the microphonic. VM responses from all vestibular end organs were evoked with sinusoidal stimuli of frequencies between 300 Hz and 120 kHz. Given that CM responses are known to be evoked in mammals by sinusoidal stimuli up to 30 kHz (Cheatham et al., 2011), it seems highly unlikely that either cochlear or vestibular microphonic responses would have been evoked by the ultrasonic stimuli by Trincker and Partsch, and suggests that potentially some of the ultrasonic responses in their study may have included an artifact component.

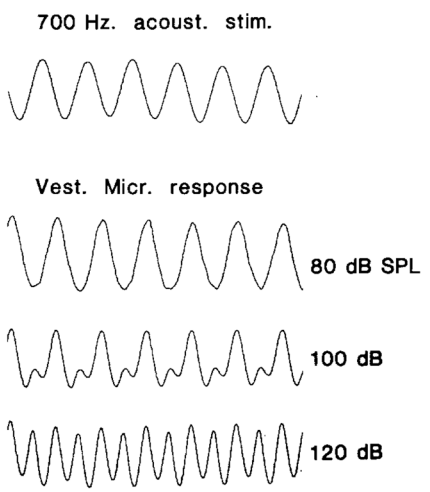

FIGURE 2 | Scala tympani recordings of the VM recordings in pigeons, in response to a 700 Hz air conducted sound (ACS) tone (upper trace) after cochlear extirpation and semicircular canal (SCC) fenestration. At low sound levels, the VM (lower three traces) is a slightly distorted sinusoid, and as the stimulus level increases, so does the distortion, generating a response whose frequency is twice that of the stimulus. Reproduced with permission from Wit et al. (1986).

Ultimately, whilst much research continues to utilize *ex vivo* measurements of vestibular HCs function, there is a need to substantiate the use of such *ex vivo* preparations as a reliable measure of the *in vivo* properties of vestibular HCs. Certainly for cochlear research, the CM remains a mainstay of experimental research measures, and has been used to support and further our understanding of the properties of HCs transduction, derived from intracellular receptor potential measurements (Patuzzi and Sellick, 1983; Patuzzi et al., 1989). For example, the *in vivo* CM has been used to demonstrate the underlying HCs related cause of many forms of sensorineural hearing loss (Patuzzi et al., 1989), which may have otherwise been attributed to neural dysfunction. Unfortunately, there has been little work done to establish techniques for measuring the VM *in vivo*, and most *in vivo* animal studies of the vestibular system are limited to measuring single-unit afferent responses (Fernández and Goldberg, 1976; Curthoys et al., 2006; Curthoys and Vulovic, 2011), single cell receptor potentials (Rabbitt et al., 2005), and VsEP responses (see below). Thus, our understanding of the origin of many forms of vestibular dysfunction may be lacking, as we have not utilized methods that may separate vestibular HCs from neural dysfunction. VM recordings offer an opportunity to perform simple recordings of vestibular HCs sensitivity *in vivo*, and may demonstrate changes that drive or differ from neural dysfunction.

VsEP Recordings

The VsEP was arguably first demonstrated in 1949 in pigeons (De Vries and Bleeker, 1949). The VsEP has been further demonstrated in pigeon (Wit et al., 1981), chicken (Jones and Pedersen, 1989; Jones and Jones, 1996, 2000; Nazareth and Jones, 1998), canary (Jones S. M. et al., 1998), quail (Jones et al., 1997), mouse (Jones and Jones, 1999; Jones et al., 2006), rat (Lange, 1988; Plotnik et al., 1999a,b), chinchilla (Böhmer, 1995; Böhmer et al., 1995; Plotnik et al., 2005), guinea pig (Cazals et al., 1987; Jones and Jones, 1999; Oei et al., 2001; Kingma and Wit, 2010; Brown et al., 2013; Chihara et al., 2013; Bremer et al., 2014), rhesus monkey (Böhmer et al., 1983) cat (Elidan et al., 1987a,b; Böhmer, 1995), and human (Elidan et al., 1991a,b; Knox et al., 1993; Pyykkö et al., 1995; Rodionov et al., 1996; Loose et al., 2002). The VsEP has predominantly been evoked by a brief (2 ms) "linear" BCV pulse stimulus, with the response evoked by skull jerk rather than acceleration (Jones T. A. et al., 2011). It has mostly been recorded in experimental animals with a non-inverting electrode placed at the vertex, or within the facial nerve canal. The VsEP reflects the compound field potential of vestibular neurons (either peripheral or central), firing synchronously to the onset of a motion.

It is important to note that there are various VsEP recording procedures, and as a result, responses can reflect activity from different sources. Some recording protocols use linear-BCV pulses, whereas others use rapid head rotations. Moreover, the location of the recording electrodes significantly determines the

VsEP waveform. The non-inverting VsEP recording electrode has been placed at various locations including the vertex (Elidan et al., 1982; Jones, 1992; Bremer et al., 2014), at different sub-cranial locations (Jones et al., 2002), within the vestibular nucleus (Cazals et al., 1987), within the facial nerve canal (Böhmer, 1995; Kingma and Wit, 2009; Bremer et al., 2012; Chihara et al., 2013), or on the round window (Aran et al., 1980). The inverting electrode is typically placed subcutaneously at a relatively non-responsive area such as the pinna or mastoid, and the ground (or common) electrode is placed at a distal location on the body, such as the neck. The characteristics of these different VsEPs, such as latency, waveform, and stimulus related phenomena also change with recording protocol. Importantly, all responses have short latencies (starting 1 ms to 2 ms) and remain after cochlear extirpation, but are abolished by damage of the vestibule or 8th nerve, or death (Jones and Jones, 1999). Moreover, the response is abolished via the application of neural blockers such as tetrodotoxin (Weisleder et al., 1990; Jones, 1992; Jones and Jones, 1999; Chihara et al., 2013), demonstrating that the VsEP is a neurogenic response. Any new VsEP recording protocol should first demonstrate that the response reflects the activity of the vestibular nerve.

Central vs. Peripheral VsEPs

The majority of VsEP studies have recorded the response with the non-inverting electrode placed subcutaneously at the vertex, or sub-cranially at different locations overlying the cortex. Here, responses typically start with a small (~0.5–1 μV) P1 peak (**Figure 3A**; which corresponds to the initial peak in facial nerve recordings; (Aran et al., 1980; Jones, 1992; Nazareth and Jones, 1998), and a series of slightly larger positive and negative peaks thereafter (Elidan et al., 1987a; Jones and Pedersen, 1989; Jones and Jones, 1999; Plotnik et al., 1999b; Bremer et al., 2014). This VsEP primarily reflects the response of various vestibular brainstem nuclei and nerves (Nazareth and Jones, 1998), much the same way the ABR reflects central auditory neuron responses (**Figure 3B**). Importantly, ACS evoked ABR responses are suppressed by acoustic forward-masking noise (**Figure 3B**), whereas BCV evoked VsEP responses are not (**Figure 3A**).

VsEP recordings performed with the non-inverting electrode within the cochlea or facial nerve canal will appear similar in waveshape to the cochlear CAP, with an initial negative and positive peak (with amplitudes between 20 μV and 100 μV), termed N1 and P1, with a few smaller peaks thereafter (Böhmer, 1995; Bremer et al., 2012; Chihara et al., 2013); **Figure 4A**). That said, other studies have suggested that VsEPs recorded within the facial nerve begin with a large positive peak (Oei et al., 2001; Kingma and Wit, 2009), and appear similar to an inverted version of a cochlear CAP. Regardless of the polarity of the first VsEP peak, this activity primarily reflects the compound field potential of the vestibular nerve.

VsEP Stimulus

The most widely utilized stimulus for evoking the VsEP involves delivering a rapid, linear-BCV impulse to the skull, in a naso-occipital direction, transduced by a large electrodynamic shaker bolted or clamped to the skull (**Figure 5A**). This theoretically permits a controlled, rapid push-pull of the

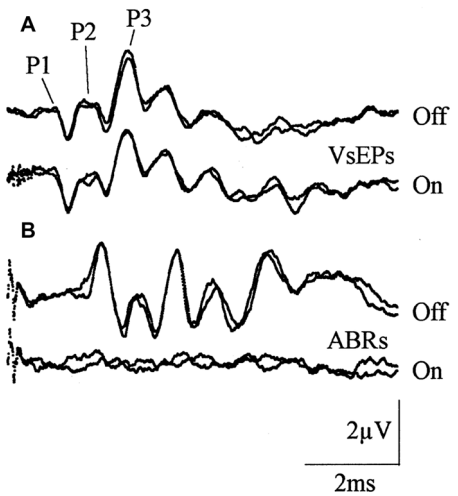

FIGURE 3 | Vestibular evoked potential (VsEP) responses recorded from sub-cranial vertex electrodes in mice. (A) VsEP responses evoked by a 2 ms bone conducted vibration (BCV) jerk pulse, with and without forward acoustic masking, which does not alter the response. **(B)** Auditory brainstem response (ABR) responses with and without forward masking, demonstrating that ABR responses are forward masked. Reproduced with permission from Jones and Jones (1999).

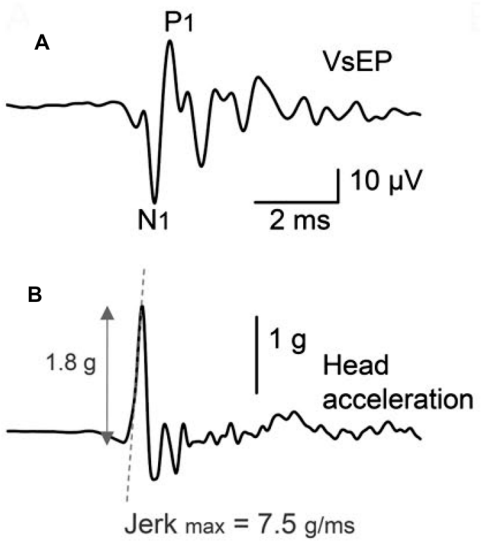

FIGURE 4 | (A) Facial nerve canal recordings of the VsEP in an anesthetized guinea pig, in response to a brief, linear BCV click. Recordings were performed with the cochlea intact, and in the presence of continuous ACS masking noise. The VsEP consists of an initial negative peak (N1) and positive peak (P1), and a series of smaller peaks thereafter. **(B)** The acceleration of the skull, where the stimulus was designed to produce minimal oscillation of the head. Reproduced with permission from Chihara et al. (2013).

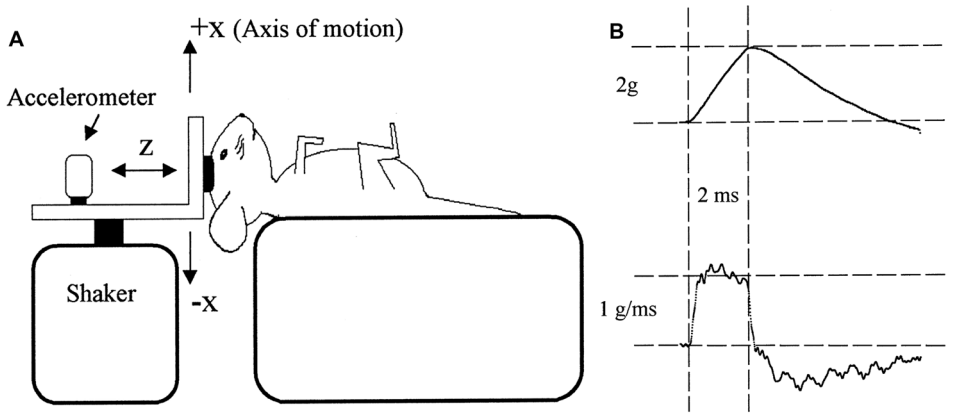

FIGURE 5 | (A) The typical experimental setup used to evoke VsEP responses in animals. An electrodynamic modal shaker is attached to the animal's skull via a screw or clamp. The acceleration is measured on the modal shaker connector. **(B)** Acceleration pulses rise gradually over 2 ms, producing a monophasic 2 ms jerk of the head. Reproduced with permission from Jones and Jones (1999).

animal's entire head (with <100 μm displacement) in the naso-occipital direction. An extensive examination of the appropriate parameters for evoking the VsEP in mice and rats using this setup has been performed by Jones et al. (Jones and Jones, 1999; Jones et al., 2002; Jones T. A. et al., 2011). Here, it has been suggested that a rapid acceleration of the head, producing a 1 ms to 4 ms pulsed "jerk" (the derivative of acceleration; **Figure 5B**) is ideal for evoking the VsEP. Indeed, the level of BCV jerk, rather than the level of acceleration, velocity, or displacement, appears to be the main factor determining the amplitude of the VsEP response, and suggests the VsEP is a response of the primary afferents that innervate otolith jerk-sensitive HCs (Jones T. A. et al., 1998; Jones T. A. et al., 2011). Jones T. A. et al. (2011) also suggest that an ideal duration of the linear BCV jerk pulse is approximately 2 ms, which preferentially stimulates the vestibular system, with less cochlear activation. Most studies have demonstrated a reliable VsEP in response to a linear BCV stimulation between 0.5 g and 8 g, or 0.1 g/ms to 6 g/ms.

It should be noted that a 2 ms duration jerk pulse requires an acceleration pulse that increases from zero, peaks at 2 ms, and slowly declines thereafter (**Figure 5B**). The head velocity change will peak several milliseconds after the onset of the movement, and the peak displacement will occur several milliseconds after that (typically well after the VsEP has occurred). Such a movement of the head can be difficult to produce (particularly for larger heads), but may be necessary to maximally stimulate the jerk-sensitive HCs of the otoliths with minimal cochlear stimulation. Importantly, the head acceleration in this setup is measured on the mechanism attached to the shaker and skull, which arguably may not faithfully represent the acceleration of the vestibular system (Jones et al., 2015). That is, the otolith acceleration may be more complex than that recorded elsewhere in the system, given that the skull can compress and resonate in a complex manner in response to BCV pulses (Durrant and Hyre, 1993), and viscous forces act on the otolith organs (Jones et al., 2015). Moreover, it is not clear how much inter-aural or rostro-caudal movement of the skull is induced by a BCV pulse applied directly to the vertex in a naso-occipital direction.

Other studies have utilized a linear BCV pulse without necessarily controlling for jerk, and most often recording the VsEP from the facial nerve canal (Böhmer, 1995; Kingma and Wit, 2009, 2010; Brown et al., 2013; Chihara et al., 2013). These later studies have all utilized simultaneous acoustic masking to suppress ECochG responses evoked by the BCV click stimulus. Importantly, click-like BCV stimulation can induce a highly synchronized response of the vestibular afferents (**Figure 6**; Curthoys et al., 2006), where typically only one spike is initiated by the BCV pulse, but the latency of this spike relative to the peak skull acceleration may vary slightly (by 0.2 ms to 0.5 ms) between afferent neurons. This latency variability is most likely related to the indirect nature of measuring skull acceleration as a means of interpreting the displacement of otolith HCs, although it may also demonstrate variability in the response of different HCs to a given vibration of the vestibular end-organ. Regardless of this slight variability, single-unit recordings suggest that the histogram of afferent responses to a BCV-click should be highly synchronized, and therefore the VsEP response should provide a faithful representation of the vestibular nerve field potential. This raises a question—what are the later peaks in the VsEP recorded from the facial nerve canal (**Figure 4A**)? Are they derived from brainstem activity, or are they a result of a complex resonance of the skull producing multiple successive VsEP responses, or are they the result of different vestibular afferent nerve responses to the BCV stimulus?

Chihara et al. (2013) attempted to determine if the later peaks were the result of a skull-resonance, evoking multiple vestibular nerve responses. Here, we (the experiments were performed in the author's laboratory) used an audiometric bone conductor rigidly attached to the skull of a guinea pig, with an accelerometer placed nearby on the skull, to deliver a brief linear-BCV stimulus that resulted in an acceleration profile that had minimal later peaks or resonant features (**Figure 4B**). Acoustic masking was used to suppress cochlear responses. This

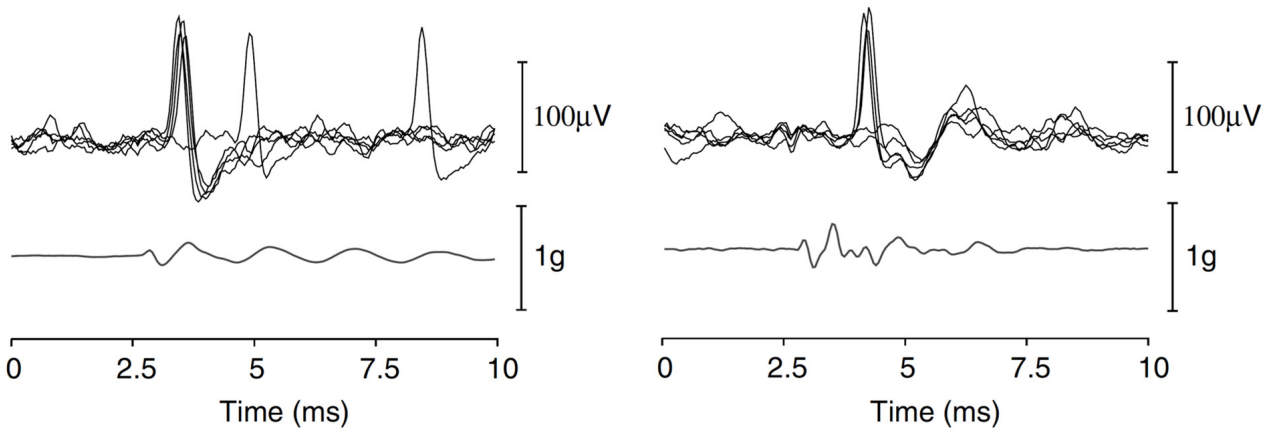

FIGURE 6 | Repeated single-unit responses from two pitch-static sensitive otolith afferent neurones, evoked by a BCV click (acceleration shown below the unit responses). Reproduced with permission from Curthoys et al. (2006).

approach reduced some, but not all of the later components in the VsEP response. Again, it should be realized that skull acceleration responses, particularly at high frequencies, are unlikely to represent the vibration of the end-organ. We have now abandoned this approach, and instead simply deliver brief (0.2–4 ms) monophasic pulses to the bone conductor, which is attached to the ear-bar (Brown et al., 2016). The later peaks in the VsEP responses remain, but we have so far been unable to clarify their origin.

Regardless of the exact vibration of the vestibule, using variants of this setup, several studies have demonstrated that the linear-BCV evoked VsEP is a response of otolith organs. That is, the VsEP remains after cochlear extirpation, or SCC plugging, but is abolished after death (Jones and Jones, 1999; Plotnik et al., 1999b). Moreover, selective otolith destruction abolishes the linear VsEP (Chihara et al., 2013), and otoconia deficient mice have absent or reduced VsEP responses (Jones et al., 1999, 2004). A few studies (Freeman et al., 1999a; Plotnik et al., 1999a) have attempted to stimulate selected vestibular end-organs with pulsed BCV applied in either the naso-occipital, dorso-ventral, or inter-aural directions (along with rotatory pulses), and found similar VsEP response waveforms evoked by all stimuli, but with different response amplitudes. Moreover, Jones et al. (2001) demonstrated in chickens that the initial directional polarity of the linear BCV (relative to the vestibular system), particularly for inter-aural directed stimuli, significantly alters the response waveform. It is not clear if such selective linear BCV stimulation permits a selective activation of the different vestibular end-organs, but this result highlights that that the VsEP is, at least partly, directionally sensitive.

Whilst the linear-BCV evoked VsEP is believed to originate from otolith afferent neurons, several studies have suggested that different stimuli, such as a rapid rotation of the head may generate a SCC afferent VsEP response (Elidan et al., 1982, 1987b; Li et al., 1993; Freeman et al., 1999b; Sohmer et al., 1999). Other studies have used brief low-frequency sinusoidal ACS tones, with fenestration of a given SCC canal, to stimulate a nerve response from the SCC (Wit et al., 1981; Curthoys, 2017). Some studies have suggested that high-intensity ACS can stimulate SCC afferent neurons (Zhu et al., 2014), whereas others have suggested that it does not (Curthoys et al., 2006; Curthoys, 2017). Certainly, it would seem that the otoliths are far more sensitive to transient ACS or BCV than the SCCs. Ultimately, the majority of VsEP studies that have performed additional experimental measures to investigate the origin of the VsEP response, such as selective end-organ ablation, have used a linear-BCV stimulus, and currently more evidence is required to demonstrate that a VsEP can be evoked via a stimulus designed to selectively, or preferentially activate the SCCs afferent neurons.

Reducing Artifacts and Cochlear Contributions

There are several potential pitfalls that need to be considered when recording EVestG responses. First, most EVestG responses are evoked using BCV stimuli generated by an electrodynamic shaker. This can produce a significant amount of electromagnetic radiation, which should be prevented from radiating to the electrodes using standard techniques such as shielded or twisted cables, and electrical and magnetic shielding of the shaker with grounded MU-metal shielding (Ford et al., 2004). Moreover, BCV of the head can produce significant electrode movement artifact, although electrode stabilization techniques can be of benefit (Comert and Hyttinen, 2015). Using alternating polarity (i.e., reverse direction) BCV stimulation can attenuate much of the artifact in VsEP measurements, but this should only be employed if the VsEP has the same waveshape and latency for either polarity stimuli, otherwise responses may partially cancel. Jones et al. (2002) demonstrated that the VsEP amplitude changed slightly with stimulus polarity, but the latency did not,[2] and therefore alternating polarity responses could be

[2]It should be noted that Jones et al. (2002) were able to push and pull the skull, and that under different stimulus conditions, there may be a difference in the latency of the VsEP due to a difference in the BCV transduction.

averaged together to minimize any electrical or movement artifact, with minimal changes to the VsEP waveshape. Both Plotnik et al. (1997) and Jones et al. (2002) demonstrated that the amplitude of the VsEP decreased by up to 15% with increasing stimulus presentation rates, suggesting that an ideal rate should be around 16 per second, which is similar to the ideal repetition rate used for ECochG responses (Eggermont, 1974).

In order to suppress ECochG responses from VsEP recordings, most studies have utilized broad-band acoustic masking noise. This is often necessary because transient BCV stimuli can produce an acoustic click that is transmitted to the cochlea either as an ACS or through direct BCV (Puria and Rosowski, 2012). Acoustic masking noise can either be presented simultaneously with BCV stimulus (Böhmer, 1995; Jones and Jones, 1999; Oei et al., 2001; Chihara et al., 2013), or it can be silenced immediately prior to it (Jones T. A. et al., 2011; King et al., 2017),where forward-masking effects are sufficient to suppress any cochlear responses (Verschooten et al., 2012). It's not clear if the primary purpose for silencing the masking noise just prior to the BCV stimulus is because the masking noise itself generates CM or electrical artifact, which can contaminate the VsEP response, or if it is believed that the acoustic masking noise may directly interfere with the BCV stimulation of the vestibular system. Several studies have suggested that high levels of noise (>110 dB SPL) can reduce the linear-VsEP amplitude (Böhmer, 1995; Sohmer et al., 1999), particularly if there is a fenestration of the SCC (Wit et al., 1981; Biron et al., 2002). This suggests that the otolith jerk-responsive HCs may be sensitive to high levels of ACS, as is known from single-unit recordings (Curthoys and Vulovic, 2011), and studies have demonstrated that loud noise exposure can produce a permanent reduction in the VsEP (Biron et al., 2002), although this conflicts with previous studies (Sohmer et al., 1999). Nevertheless, moderate continuous or forward-masking acoustic noise most likely provides an adequate suppression of cochlear activity, without overly attenuating otolith responses. Interestingly, Jones and Jones (1999) and Jones et al. (2002) suggest that VsEP responses, recorded with sub-cranial electrodes, are often unaffected by forward masking noise, suggesting that there is little contamination from ABR. This likely reflects the fact that they use a stimulus designed to maximize jerk stimulation of the otoliths, whilst minimizing cochlear stimulation.

Lastly, whilst several studies have demonstrated that the VsEP is a response of peripheral and central vestibular neurones (Nazareth and Jones, 1998; Jones and Jones, 1999; Jones et al., 2002), some studies have suggested that the VsEP measured within the inner ear can contain components that reflect vestibular *HCs* activity (Wit et al., 1986, 1990). This raises the possibility that there may be an SP-like component of the VsEP when it is measured close to the vestibular HCs. Moreover, it suggests that it may be possible to measure vestibular HCs responses, such as VM, from electrode montages that enable recording of both vestibular nerve and HCs activity.

Interpretation of the VsEP

A concern with interpreting VsEP responses is the uncertainty of which vestibular end-organs contribute to the response. That is, BCV stimuli can induce neural responses from all vestibular end-organs, despite primarily activating otolithic irregular afferent neurons (Curthoys et al., 2006). Whilst researchers have attempted to use the direction of the applied BCV to activate selected vestibular HCs, it is unlikely that this circumvents the complex 3-dimensional vibration of the inner ear and the complex transduction pathways (Stenfelt, 2015, 2016; Chhan et al., 2016). Mechanical engineers are well aware of the complexity of interpreting the vibrational response of a structure via its "impulse response". An alternative method involves measuring the "steady-state" or continuous vibrational response, where the complexities of the impulse response have dissipated. For the vestibular system, this would involve measuring its response to a continuous sinusoidal linear (or rotatory) BCV stimulus, which should provide a stimulation of the vestibule that is easier to interpret, and would provide a response that could be more readily compared to single-unit recordings obtained during sinusoidal BCV (Curthoys et al., 2006; Curthoys and Vulovic, 2011). Indeed, a few studies have demonstrated that a continuous sinusoidal stimulus can evoke both a sinusoidal VM (Wit et al., 1986) and cyclic neural responses (Wit et al., 1981, 1986 **Figure 7**). These responses are reminiscent of the auditory nerve neurophonic, used to assess low-frequency sensitivity of the cochlea during a tone (Henry, 1995; Lichtenhan et al., 2014). It may therefore be possible to use sinusoidal ACS or BCV to evoke vestibular neurophonic, and this may provide a means to obtain responses from vestibular neurones which are most sensitive to vibration in a specific direction. Meanwhile, the VsEP obtained using impulse stimuli should assume that the VsEP is "mostly" a response of the afferent neurons synapsing with the jerk-sensitive HCs in the otoliths, with some potential contributions from all vestibular end-organs (see "VsEP Stimulus" Section).

Whilst it may be tempting to use static tilts to probe the origin of the VsEP response, the issue of static head position during VsEP measurements is one which still needs to be resolved. Plotnik et al. (1999a) suggested that, in addtion to changes related to stimulus delivery direction, VsEP responses were altered by the static orientation of the head, suggesting that gravity may alter the sensitivity of the jerk-sensitive HCs. This contrasts with a lack of static head-orientation changes in similar measures otolith function in humans (Kastanioudakis et al., 2016).

Encouragingly, for researchers using the VsEP as a measure of peripheral vestibular function in longitudinal studies, Honaker et al. (2015) demonstrated that the VsEP amplitude and threshold do not change significantly across repeated recordings, which includes repositioning of electrodes (at fixed/standardized positions). Thus, as long as the delivery of the BCV stimulus is consistent between successive recording sessions, the VsEP should provide a sensitive measure of changes in peripheral vestibular sensitivity. It should be noted that response variability will also depend on the signal-to-noise ratio of the response, which greatly depends on the number of averages. For the VsEP measured at the vertex, the response is typically averaged

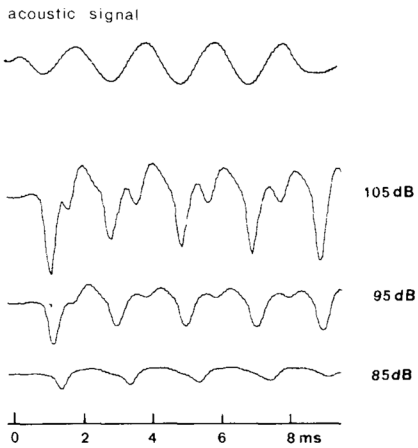

FIGURE 7 | Vestibular nerve responses, measured from a scala tympani electrode in pigeons, after cochlear extirpation and SCC fenestration, evoked by a 500 Hz ACS toneburst (upper trace) of sound levels between 85 dB SPL and 105 dB SPL. It is thought that these responses reflect a neurophonic of the vestibular nerve. Reproduced with permission from Wit et al. (1981).

of over 200 times, due to the low signal-to-noise ratio (Jones et al., 2002). To reduce variability in the responses due to the noise-floor of the recording, responses can be band-pass filtered between 300 kHz and 10 kHz (Jones et al., 2002), although these filter settings were obtained for VsEP responses recorded at the vertex, and may differ for VsEP responses measured in the periphery.

An important factor to consider when monitoring VsEP responses during an intervention, is how to assess changes. Previously, many studies have monitored the peak-to-peak amplitude of the response, however because the later peaks in the VsEP reflect central responses, they may be altered without an equivalent change in the 8th nerve's sensitivity, resulting in changes in the VsEP waveform (Jones et al., 2000; Morley et al., 2017). Therefore, VsEP thresholds should ideally be used to assess changes in the sensitivity of the irregular otolith afferents, although changes in the VsEP waveform, such as changes in inter peak intervals and peak latencies, may provide additional information. That said, the source of the later peaks in VsEP responses recorded from the vertex is not as well defined as the origin in the later peaks in ABR responses (Kaga et al., 1997), although several studies have used electrical source analysis to localize VsEP activity (Todd et al., 2014, 2017).

One final issue to consider is the potential influence of anesthetics on EVestG responses (Gaines and Jones, 2013). Although anesthesia is known to suppress certain cortical activity, there seems to be little difference in the VsEP measured at the vertex, between anesthetized and awake animals, other than a suppression of a late (>7 ms) component, which may potentially reflect cortical vestibular activity (Jones, 1992). Nonetheless, it is possible that different anesthetics may induce changes in the VsEP response, particularly of the later, central components.

HUMAN EVestG RECORDINGS

Other than the recent controversial asynchronous-EVestG responses recorded on the tympanum in humans (Lithgow, 2006; Lithgow et al., 2008; Dastgheib et al., 2016), several studies have reported on VsEP responses measured in humans, with virtually no human VM recordings. Elidan et al. (1991b), and Rodionov et al. (1996) recorded small (0.5 μV peak to peak) short latency potentials from the forehead (with a mastoid inverting electrode), in response to rapid angular rotations of the head (10,000°/s^2). Similarly, Pyykkö et al. (1995) measured small VsEP responses evoked by brief linear BCV stimulation in people. Both short-latency (starting 2 ms to 3 ms) and larger middle-latency (starting 8 ms to 10 ms) responses were observed in these studies, and it was suggested that the first positive peak of the short-latency responses reflected activity of the peripheral vestibular nerve. The responses were not present in cadaver heads, or subjects with bilateral vestibular loss, but they were present in deaf subjects. These rotationally evoked human responses were compared to the VsEP responses measured in cats using a similar stimulus and measurement protocol (Li et al., 1993), and were believed to reflect responses of the SCC afferents and central vestibular neurons. Knox et al. (1993) recorded similar short latency vestibular responses to rapid whole-body linear accelerations, measured between the forehead and mastoid, and suggested the early components of their responses reflected the activity of the peripheral vestibular nerve from otolith neurons. Ultimately, each of these human VsEP displayed a poor signal-to-noise ratio, and required an elaborate setup to produce controlled acceleration of the head, which induced significant artifact.

de Waele et al. (2001) electrically stimulated the 8th nerve in 11 patients undergoing vestibular nerve section for Meniere's disease, and recorded evoked responses occurring 3–5 ms after stimulation, with 30 subcutaneous electrodes placed on the scalp. Electrical source analysis was used to localize the response activity to various regions of the brain, including an early component localized to the region of the vestibular nucleus. This study supported the theory that vestibular information is processed in spatially distributed central pathways, rather than at a focal cortical region (Cullen, 2016). It should be noted that de Waele et al. (2001) suggested their electrically evoked response reflected the activity of central vestibular neurones only, and that the activity of the peripheral vestibular system, including the 8th nerve, was not represented in the response.

More recently, several studies have suggested that vestibular responses, termed VsEPs, to loud (>100 dB SPL), low frequency (e.g., 500 Hz) acoustic tone bursts can be recorded with electrodes placed at the vertex (Todd et al., 2003, 2014; McNerney et al., 2011). Certainly it has been shown that the human vestibular system, particularly the otoliths, is sensitive to acoustic tones (Chihara et al., 2009; Murofushi et al., 2010). Moreover, the origin of these short latency scalp potentials were localized to various brain regions known to be related to central vestibular pathways (Todd et al., 2003, 2014). However, like the responses reported by de Waele et al. (2001), no components were localized to the peripheral vestibular system, such as the 8th nerve. Here, it

appears that human scalp VsEP responses are similar to the later components observed in experimental animal VsEPs (Nazareth and Jones, 1998). Moreover, recent human scalp VsEP recordings have demonstrated that the amplitude of components of this response can be modulated by head and eye position (Todd et al., 2017), which reflects their central origin. Thus, caution should be taken when using human VsEP responses as an estimate of peripheral vestibular function, because like vestibular reflex responses, central vestibular activity may not faithfully reflect the sensitivity of the peripheral vestibular system.

Here we ask the question, what is the advantage of EVestG as a measure of vestibular sensitivity compared to several reflex measures of vestibular function clinically (Curthoys, 2012; Colebatch et al., 2016). For experimental animal researchers the answer is clear—it can be difficult, but not impossible, to measure vestibular reflexes in anesthetized animals because central reflex pathways and myogenic activity is heavily suppressed (Vulovic and Curthoys, 2011). Experimental animal research has traditionally relied on objective measures of vestibular activity, such as single-unit recordings or gross HCs and nerve responses. However, the modulation of vestibular reflexes highlights an additional need to develop objective measures of peripheral vestibular function in humans. These responses, whilst typically robust and incorporating only three or four neurons in the reflex pathway, can adapt and may be modulated by central mechanisms (Mantokoudis et al., 2016). Thus, the clinical diagnosis of vestibular disorders would likely benefit from measures of peripheral vestibular function, similar to how ECochG has been used in the diagnosis of several inner ear disorders, such as Meniere's disease, 8th nerve schwannomas, auditory neuropathy, and sudden sensorineural hearing loss (see Eggermont, 2017).

UTILITY OF EVestG IN RESEARCH

Increasingly, the linear BCV evoked VsEP is being used in experimental animals to improve our understanding of both fundamental and pathological peripheral vestibular function. The VsEP has been studied in animal models of otoconia deficiencies (Jones et al., 1999, 2004; Zhao et al., 2008), aging (Mock et al., 2011; Vijayakumar et al., 2015), hyper-gravity (Jones et al., 2000), gentamicin treatment (Perez et al., 2000; Bremer et al., 2014; King et al., 2017), endolymphatic hydrops (Kingma and Wit, 2009, 2010; Chihara et al., 2013), diuretic effects (Bremer et al., 2012), anesthetics (Gaines and Jones, 2013), pharmacological agents (Irons-Brown and Jones, 2004), inner ear genetic disorders (Jones S. M. et al., 2011; Lee et al., 2013; Robertson et al., 2008; Mathur et al., 2015), and noise trauma (Sohmer et al., 1999; Biron et al., 2002). More recently, studies have demonstrated abnormal VsEP responses in knockout mice lacking nicotinic acetylcholine receptors (Morley et al., 2017), which are expressed at the peripheral vestibular efferent synapse (Holt et al., 2015), on vestibular HCs (Simmons and Morley, 2011), and within peripheral and central vestibular neurons (Happe and Morley, 1998). Additionally, there is an increasing interest in utilizing EVestG as a means to uncover the functional role of the vestibular efferent system, in much the same way the cochlear CAP and CM have been used to study the functional role of the olivocochlear efferent neurones (Gifford and Guinan, 1987; Elgueda et al., 2011; Lichtenhan et al., 2016).

Importantly, it should be recognized that the VsEP provides only a limited measure of peripheral vestibular function. That is, research suggests that the BCV evoked VsEP is primarily a response of the neurons innervating jerk-sensitive HCs on the otoliths. The corollary of this is that the VsEP does *not* provide a measure of neurones innervating static-sensitive HCs, such as those in the extra-striola regions, or the SCCs, and moreover it does not provide a measure of HCs function. Therefore, the VsEP should not be used as a measure of overall vestibular sensitivity. Experimental manipulations or pathologies that alter the function of extra-striola or SCC HCs, are unlikely to produce significant changes in the VsEP. There are several pathologies that affect SCC but not otolith function (e.g., Meniere's disease; McGarvie et al., 2015), or affect the superior nerve (which innervates the SCC and most of the utricle; Curthoys et al., 2009), but not inferior nerve (e.g., superior vestibular neuritis; Curthoys et al., 2011). Moreover, the VsEP is a neural response, and should not be used as a definitive indicator of vestibular HCs function. Auditory neuropathy spectrum disorder is an example pathology of a pathology which affects peripheral nerve but not HCs function (Stuermer et al., 2015; Kim et al., 2016). Lastly, precisely which HCs and neurones are responsible for generating the VsEP is still not entirely clear. That is, whilst evidence points towards the VsEP being a response of jerk-sensitive HCs/neurons, this may need further clarification, particularly given that different forms of BCV stimulation, in different experimental animals, may stimulate various the sub-sets of the peripheral vestibular system.

As studies continue to demonstrate changes in the VsEP due to genetic abnormalities or pharmacological treatments, with little or no change in tissue morphology (Lee et al., 2013; King et al., 2017; Morley et al., 2017), there may be a need to differentiate the cause of the functional loss as either HCs or neural dysfunction, and it is here that VM may be employed. When recorded from the inner ear fluids, the VM is a "global" response from all vestibular HCs types, because all vestibular HCs respond to low-frequency stimulation, and the extracellular potentials will summate in the fluids. Such a global VM measure is of limited use as a measure of peripheral vestibular function. However, it may be possible to obtain a "local" VM measure from specific HCs, if the VM is recorded with glass micropipettes localized in close proximity to the HCs (Pastras et al., under review). Currently, there is a need to further develop techniques for measuring vestibular HCs receptor potentials or currents *in vivo*.

Lastly, there are few studies monitoring evoked EVestG responses in humans. One area in which both ECochG and EVestG are rapidly developing is as an intraoperative monitor of inner ear function during inner ear surgeries such as the insertion of cochlear and vestibular implants (Frijns et al., 2002; Campbell et al., 2015, 2016; Scott et al., 2016). Like the electrically evoked

CAP (eCAP) component of "neural response telemetry", the electrically evoked VsEP (vestibular eCAP, or eVsEP) represents the electrically evoked response of the vestibular nerve (Nie et al., 2011). As the vestibular implant continues to be developed for chronic vestibular disorders, the eVsEP is likely to play an important role in the surgical positioning of the implant electrodes within the vestibular system, and objectively assessing the implants efficacy over time, as a supplement to monitoring the electrically evoked vestibular reflex responses when patients are awake.

CONCLUSION

Foremost, EVestG presents a simple tool to monitor vestibular function in animal experiments. Currently, VsEPs are the most prevalent EVestG responses measured in experimental research, and the test setup and protocol developed by Jones and Jones (1999), for use in mice and rats, largely dominate the field. Gradually more research laboratories, such as ours, are incorporating VsEP measurements, and experience suggests that it is vital to have a clear understanding of the potential pitfalls of EVestG measurements. That is not to suggest new EVestG techniques cannot be developed to suit individual research needs, and certainly we anticipate that EVestG measurement techniques will evolve much the same way new ECochG techniques are being developed. Particularly, techniques for measuring both the VM and the VsEP simultaneously (Wit et al., 1981, 1986), as in the case of the cochlear CAP and CM, are likely to help address several key "unknowns" in vestibular research, such as the role the vestibular efferents play (Morley et al., 2017).

Human EVestG responses haven't shown much promise to date; either because they are exceptionally small compared to the noise floor, or because they have been entirely superseded by a host of vestibular reflex tests that permits a rapid assessment of the peripheral vestibular system, with minimal central processing. It's unlikely that EVestG could be monitored from the tympanum or round-window, as is the case with ECochG, but certainly as the vestibular implant continues to develop, researchers may be able to leverage the proximity of the electrodes to the vestibular nerve to obtain clear vestibular responses in humans.

Finally, just as there are a host of terms given to differential ECochG measures, new terminology should be developed for EVestG responses, either drawing on comparative terms that have been applied to cochlear responses, or being based more on the logical appreciation of what the response represents. However, given the overlap between cochlear and vestibular research, it would seem more appropriate to utilize terminology that has already been developed for cochlear responses.

AUTHOR CONTRIBUTIONS

DJB developed the review and wrote the manuscript. ISC and CJP edited the manuscript, and provided additional input to the content.

FUNDING

Dr. Brown is funded in part by a Garnett Passe and Rodney Williams Memorial Foundation, Senior Principal Research Fellowship, and by the Sydney Medical School Foundation—Meniere's Research Fund, with charitable donations raised by the Meniere's Research Fund Inc.

REFERENCES

Adrian, E. D., Craik, K. J. W., and Sturdy, R. S. (1938). The electrical response of the auditory mechanism in cold-blooded vertebrates. *Proc. R. Soc. B Biol. Sci.* 125, 435–455. doi: 10.1098/rspb.1938.0036

Aran, J. M., Cazals, Y., Charlet de Sauvage, R., Guilhaume, A., and Erre, J. P. (1980). Electrophysiological monitoring of the cochlea during and after total destruction of the organ of corti. *Acta Otolaryngol.* 89, 376–383. doi: 10.3109/00016488009127151

Azimzadeh, J. B., and Salvi, J. D. (2017). Physiological preparation of hair cells from the sacculus of the american bullfrog (*Rana catesbeiana*). *J. Vis. Exp.* 121:e55380. doi: 10.3791/55380

Benser, M. E., Issa, N. P., and Hudspeth, A. J. (1993). Hair-bundle stiffness dominates the elastic reactance to otolithic-membrane shear. *Hear. Res.* 68, 243–252. doi: 10.1016/0378-5955(93)90128-n

Biron, A., Freeman, S., Sichel, J. Y., and Sohmer, H. (2002). The effect of noise exposure in the presence of canal fenestration on the amplitude of short-latency vestibular evoked potentials. *Arch Otolaryngol. Head Neck Surg.* 128, 544–548. doi: 10.1001/archotol.128.5.544

Bleeker, J. D., Wit, H. P., and Segenhout, J. H. (1980). Evidence for sound perception with the labyrinth. *Acta Otolaryngol.* 89, 76–84. doi: 10.3109/00016488009127112

Böhmer, A. (1995). Short latency vestibular evoked responses to linear acceleration stimuli in small mammals: masking effects and experimental applications. *Acta Otolaryngol. Suppl.* 520, 120–123. doi: 10.3109/00016489509125206

Böhmer, A., Henn, V., and Lehmann, D. (1983). Vestibular evoked potentials in the awake rhesus monkey. *Adv. Otorhinolaryngol.* 30, 54–57. doi: 10.1159/000407611

Böhmer, A., Hoffman, L. F., and Honrubia, V. (1995). Characterization of vestibular potentials evoked by linear acceleration pulses in the chinchilla. *Am. J. Otol.* 16, 498–504.

Botta, L., Mira, E., Valli, S., Perin, P., Zucca, G., and Valli, P. (1998). Effects of betahistine on vestibular receptors of the frog. *Acta Otolaryngol.* 118, 519–523. doi: 10.1080/00016489850154658

Bremer, H. G., de Groot, J. C., Versnel, H., and Klis, S. F. (2012). Combined administration of kanamycin and furosemide does not result in loss of vestibular function in Guinea pigs. *Audiol. Neurootol.* 17, 25–38. doi: 10.1159/000327256

Bremer, H. G., Versnel, H., Hendriksen, F. G., Topsakal, V., Grolman, W., and Klis, S. F. (2014). Does vestibular end-organ function recover after gentamicin-induced trauma in Guinea pigs? *Audiol. Neurootol.* 19, 135–150. doi: 10.1159/000357587

Bressler, S. L. (2011). "Event-related potentials of the cerebral cortex," in *Electrophysiological Recording Techniques*, eds R. P. Vertes and R. W. Jr. Stackman (Totowa, NJ: Humana Press), 169–190.

Brown, D. J., Chihara, Y., and Wang, Y. (2013). Changes in utricular function during artificial endolymph injections in guinea pigs. *Hear. Res.* 304, 70–76. doi: 10.1016/j.heares.2013.05.011

Brown, D. J., Mukherjee, P., Pastras, C. J., Gibson, W. P., and Curthoys, I. S. (2016). Sensitivity of the cochlear nerve to acoustic and electrical stimulation months after a vestibular labyrinthectomy in guinea pigs. *Hear. Res.* 335, 18–24. doi: 10.1016/j.heares.2016.01.017

Buzsáki, G., Anastassiou, C. A., and Koch, C. (2012). The origin of extracellular fields and currents—EEG, ECoG, LFP and spikes. *Nat. Rev. Neurosci.* 13, 407–420. doi: 10.1038/nrn3241

Campbell, L., Kaicer, A., Briggs, R., and O'Leary, S. (2015). Cochlear response telemetry: intracochlear electrocochleography via cochlear implant neural response telemetry pilot study results. *Otol. Neurotol.* 36, 399–405. doi: 10.1097/MAO.0000000000000678

Campbell, L., Kaicer, A., Sly, D., Iseli, C., Wei, B., Briggs, R., et al. (2016). Intraoperative real-time cochlear response telemetry predicts hearing preservation in cochlear implantation. *Otol. Neurotol.* 37, 332–338. doi: 10.1097/MAO.0000000000000972

Cazals, Y., Erre, J. P., and Aurousseau, C. (1987). Eighth nerve auditory evoked responses recorded at the base of the vestibular nucleus in the guinea pig. *Hear. Res.* 31, 93–97. doi: 10.1016/0378-5955(87)90216-4

Charlet de Sauvage, R., Dolivet, G., Erre, J. P., and Aran, J. M. (1990). Electrovestibulography in experimental animals. *Physiologist* 33, S117–S118.

Cheatham, M. A., Naik, K., and Dallos, P. (2011). Using the cochlear microphonic as a tool to evaluate cochlear function in mouse models of hearing. *J. Assoc. Res. Otolaryngol.* 12, 113–125. doi: 10.1007/s10162-010-0240-5

Chen, F., Choudhury, N., Zheng, J., Matthews, S., Nutall, A. L., and Jacques, S. L. (2007). *In vivo* imaging and low-coherence interferometry of organ of Corti vibration. *J. Biomed. Opt.* 12:021006. doi: 10.1117/1.2717134

Chhan, D., Bowers, P., McKinnon, M. L., and Rosowski, J. J. (2016). Middle-ear and inner-ear contribution to bone conduction in chinchilla: the development of Carhart's notch. *Hear. Res.* 340, 144–152. doi: 10.1016/j.heares.2016.02.015

Chihara, Y., Iwasaki, S., Fujimoto, C., Ushio, M., Yamasoba, T., and Murofushi, T. (2009). Frequency tuning properties of ocular vestibular evoked myogenic potentials. *Neuroreport* 20, 1491–1495. doi: 10.1097/WNR.0b013e328332 9b4a

Chihara, Y., Wang, V., and Brown, D. J. (2013). Evidence for the utricular origin of the vestibular short-latency-evoked potential (VsEP) to bone-conducted vibration in guinea pig. *Exp. Brain Res.* 229, 157–170. doi: 10.1007/s00221-013-3602-5

Colebatch, J. G., Rosengren, S. M., and Welgampola, M. S. (2016). Vestibular-evoked myogenic potentials. *Handb. Clin. Neurol.* 137, 133–155. doi: 10.1016/B978-0-444-63437-5.00010-8

Comert, A., and Hyttinen, J. (2015). Investigating the possible effect of electrode support structure on motion artifact in wearable bioelectric signal monitoring. *Biomed. Eng. Online* 14:44. doi: 10.1186/s12938-015-0044-2

Corey, D. P., and Hudspeth, A. J. (1983). Analysis of the microphonic potential of the bullfrog's sacculus. *J. Neurosci.* 3, 942–961.

Cullen, K. E. (2016). Physiology of central pathways. *Handb. Clin. Neurol.* 137, 17–40. doi: 10.1016/B978-0-444-63437-5.00002-9

Curthoys, I. S. (2012). The interpretation of clinical tests of peripheral vestibular function. *Laryngoscope* 122, 1342–1352. doi: 10.1002/lary.23258

Curthoys, I. S. (2017). The new vestibular stimuli: sound and vibration-anatomical, physiological and clinical evidence. *Exp. Brain Res.* 235, 957–972. doi: 10.1007/s00221-017-4874-y

Curthoys, I. S., Iwasaki, S., Chihara, Y., Ushio, M., McGarvie, L. A., and Burgess, A. M. (2011). The ocular vestibular-evoked myogenic potential to air-conducted sound; probable superior vestibular nerve origin. *Clin. Neurophysiol.* 122, 611–616. doi: 10.1016/j.clinph.2010.07.018

Curthoys, I. S., Kim, J., McPhedran, S. K., and Camp, A. J. (2006). Bone conducted vibration selectively activates irregular primary otolithic vestibular neurons in the guinea pig. *Exp. Brain Res.* 175, 256–267. doi: 10.1007/s00221-006-0544-1

Curthoys, I. S., Manzari, L., Smulders, Y. E., and Burgess, A. M. (2009). A review of the scientific basis and practical application of a new test of utricular function—ocular vestibular-evoked myogenic potentials to bone-conducted vibration. *Acta Otorhinolaryngol. Ital.* 29, 179–186.

Curthoys, I. S., and Vulovic, V. (2011). Vestibular primary afferent responses to sound and vibration in the guinea pig. *Exp. Brain Res.* 210, 347–352. doi: 10.1007/s00221-010-2499-5

Dastgheib, Z. A., Lithgow, B., Blakley, B., and Moussavi, Z. (2016). A new diagnostic vestibular evoked response. *Ann. Biomed. Eng.* 44, 1672–1684. doi: 10.1007/s10439-015-1441-1

Davis, H. (1965). A model for transducer action in the cochlea. *Cold Spring Harb. Symp. Quant. Biol.* 30, 181–190.

De Vries, H., and Bleeker, J. D. (1949). The microphonic activity of the labyrinth of the pigeon; the response of the cristae in the semicircular canals. *Acta Otolaryngol.* 37, 298–306. doi: 10.3109/00016484909120248

De Vries, H., and Vrolijk, J. M. (1953). Phase relations between the microphonic crista effect of the three semi-circular canals, the cochlear microphonics and the motion of the stapes. *Acta Otolaryngol.* 43, 80–89. doi: 10.3109/00016485309119820

de Waele, C., Baudonniere, P. M., Lepecq, J. C., Tran Ba Huy, P., and Vidal, P. P. (2001). Vestibular projections in the human cortex. *Exp. Brain Res.* 141, 541–551. doi: 10.1007/s00221-001-0894-7

Dierkes, K., Lindner, B., and Julicher, F. (2008). Enhancement of sensitivity gain and frequency tuning by coupling of active hair bundles. *Proc. Natl. Acad. Sci. U S A* 105, 18669–18674. doi: 10.1073/pnas.0805752105

Durrant, J. D., and Hyre, R. (1993). Observations on temporal aspects of bone-conduction clicks: real head measurements. *J. Am. Acad. Audiol.* 4, 213–219.

Eatock, R. A., Corey, D. P., and Hudspeth, A. J. (1987). Adaptation of mechanoelectrical transduction in hair cells of the bullfrog's sacculus. *J. Neurosci.* 7, 2821–2836.

Eggermont, J. J. (1974). Basic principles for electrocochleography. *Acta Otolaryngol. Suppl.* 316, 7–16. doi: 10.1080/16512251.1974.11675742

Eggermont, J. J. (2017). Ups and downs in 75 years of electrocochleography. *Front. Syst. Neurosci.* 11:2. doi: 10.3389/fnsys.2017.00002

Elgueda, D., Delano, P. H., and Robles, L. (2011). Effects of electrical stimulation of olivocochlear fibers in cochlear potentials in the chinchilla. *J. Assoc. Res. Otolaryngol.* 12, 317–327. doi: 10.1007/s10162-011-0260-9

Elidan, J., Langhofer, L., and Honrubia, V. (1987a). The neural generators of the vestibular evoked response. *Brain Res.* 423, 385–390. doi: 10.1016/0006-8993(87)90868-7

Elidan, J., Langhofer, L., and Honrubia, V. (1987b). Recording of short-latency vestibular evoked potentials induced by acceleration impulses in experimental animals: current status of the method and its applications. *Electroencephalogr. Clin. Neurophysiol.* 68, 58–69. doi: 10.1016/0168-5597(87)90070-0

Elidan, J., Leibner, E., Freeman, S., Sela, M., Nitzan, M., and Sohmer, H. (1991a). Short and middle latency vestibular evoked responses to acceleration in man. *Electroencephalogr. Clin. Neurophysiol.* 80, 140–145. doi: 10.1016/0168-5597(91)90151-m

Elidan, J., Sela, M., Liebner, E., and Sohmer, H. (1991b). Short latency vestibular evoked response to angular acceleration impulse in human beings. *Otolaryngol. Head Neck Surg.* 105, 353–359. doi: 10.1177/019459989110500302

Elidan, J., Sohmer, H., and Nizan, M. (1982). Recording of short latency vestibular evoked potentials to acceleration in rats by means of skin electrodes. *Electroencephalogr. Clin. Neurophysiol.* 53, 501–505. doi: 10.1016/0013-4694(82)90062-1

Fay, R. R., and Popper, A. N. (1974). Acoustic stimulation of the ear of the goldfish *(Carassius auratus)*. *J. Exp. Biol.* 61, 243–260.

Fernández, C., and Goldberg, J. M. (1976). Physiology of peripheral neurons innervating otolith organs of the squirrel monkey. III. Response dynamics. *J. Neurophysiol.* 39, 996–1008.

Flock, A. (1965). Transducing mechanisms in the lateral line canal organ receptors. *Cold Spring Harb. Symp. Quant. Biol.* 30, 133–145. doi: 10.1101/SQB.1965.030.01.016

Ford, M. R., Sands, S., and Lew, H. L. (2004). Overview of artifact reduction and removal in evoked potential and event-related potential recordings. *Phys. Med. Rehabil. Clin. N. Am.* 15, 1–17. doi: 10.1016/s1047-9651(03)00125-6

Fredrickson-Hemsing, L., Strimbu, C. E., Roongthumskul, Y., and Bozovic, D. (2012). Dynamics of freely oscillating and coupled hair cell bundles under mechanical deflection. *Biophys. J.* 102, 1785–1792. doi: 10.1016/j.bpj.2012.03.017

Freeman, S., Plotnik, M., Elidan, J., Rosen, L. J., and Sohmer, H. (1999a). Effect of white noise "masking" on vestibular evoked potentials recorded using different stimulus modalities. *Acta Otolaryngol.* 119, 311–315. doi: 10.1080/00016489950181305

Freeman, S., Plotnik, M., Elidan, J., and Sohmer, H. (1999b). Development of short latency vestibular evoked potentials in the neonatal rat. *Hear. Res.* 137, 51–58. doi: 10.1016/s0378-5955(99)00137-9

Frijns, J. H., Briaire, J. J., de Laat, J. A., and Grote, J. J. (2002). Initial evaluation of the Clarion CII cochlear implant: speech perception and neural response imaging. *Ear Hear.* 23, 184–197. doi: 10.1097/00003446-200206000-00003

Fromm, B., Nylen, C. O., and Zottermann, Y. (1935). Studies in the mechanism of the weber and bray effect. *Acta Otolaryngol.* 22, 477–486. doi: 10.3109/00016483509118125

Furukawa, T., and Ishii, Y. (1967). Neurophysiological studies on hearing in goldfish. *J. Neurophysiol.* 30, 1377–1403.

Gaines, G. C., and Jones, T. A. (2013). Effects of acute administration of ketorolac on mammalian vestibular sensory evoked potentials. *J. Am. Assoc. Lab. Anim. Sci.* 52, 57–62.

Gibson, W. P., Moffat, D. A., and Ramsden, R. T. (1977). Clinical electrocochleography in the diagnosis and management of Meneère's disorder. *Audiology* 16, 389–401. doi: 10.3109/00206097709071852

Gifford, M. L., and Guinan, J. J. Jr. (1987). Effects of electrical stimulation of medial olivocochlear neurons on ipsilateral and contralateral cochlear responses. *Hear. Res.* 29, 179–194. doi: 10.1016/0378-5955(87)90166-3

Håkansson, B., Brandt, A., Carlsson, P., and Tjellström, A. (1994). Resonance frequencies of the human skull *in vivo*. *J. Acoust. Soc. Am.* 95, 1474–1481. doi: 10.1121/1.408535

Happe, H. K., and Morley, B. J. (1998). Nicotinic acetylcholine receptors in rat cochlear nucleus: [^{125}I]-alpha-bungarotoxin receptor autoradiography and in situ hybridization of alpha 7 nAChR subunit mRNA. *J. Comp. Neurol.* 397, 163–180. doi: 10.1002/(SICI)1096-9861(19980727)397:2<163::AID-CNE2>3.0.CO;2-Z

He, D., Chen, Z., and Zhou, W. (1997). The ampullar endolymhatic potential in the guinea pigs. *Zhongguo Ying Yong Sheng Li Xue Za Zhi* 13, 246–248.

Henry, K. R. (1995). Auditory nerve neurophonic recorded from the round window of the Mongolian gerbil. *Hear. Res.* 90, 176–184. doi: 10.1016/0378-5955(95)00162-6

Holt, J. C., Kewin, K., Jordan, P. M., Cameron, P., Klapczynski, M., McIntosh, J. M., et al. (2015). Pharmacologically distinct nicotinic acetylcholine receptors drive efferent-mediated excitation in calyx-bearing vestibular afferents. *J. Neurosci.* 35, 3625–3643. doi: 10.1523/JNEUROSCI.3388-14.2015

Honaker, J. A., Lee, C., Criter, R. E., and Jones, T. A. (2015). Test-retest reliability of the vestibular sensory-evoked potential (VsEP) in C57BL/6J mice. *J. Am. Acad. Audiol.* 26, 59–67. doi: 10.3766/jaaa.26.1.7

Honrubia, V., Strelioff, D., and Ward, P. H. (1973). A quantitative study of cochlear potentials along the scala media of the guinea pig. *J. Acoust. Soc. Am.* 54, 600–609. doi: 10.1121/1.1913639

Hornibrook, J., Bird, P., Flook, E., and O'Beirne, G. A. (2016). Electrocochleography for the diagnosis of meniere's disease: the wrong stimulus. *Otol Neurotol.* 37, 1677–1678. doi: 10.1097/MAO.0000000000001206

Hudspeth, A. J., and Corey, D. P. (1977). Sensitivity, polarity and conductance change in the response of vertebrate hair cells to controlled mechanical stimuli. *Proc. Natl. Acad. Sci. U S A* 74, 2407–2411. doi: 10.1073/pnas.74.6.2407

Huizinga, E., and Van Der Meulen, P. (1951). Vestibular rotatory and optokinetic reactions in the pigeon. *Ann. Otol. Rhinol. Laryngol.* 60, 927–947. doi: 10.1177/000348945106000403

Irons-Brown, S. R., and Jones, T. A. (2004). Effects of selected pharmacological agents on avian auditory and vestibular compound action potentials. *Hear. Res.* 195, 54–66. doi: 10.1016/j.heares.2004.02.011

Johnstone, B. M., Johnstone, J. R., and Pugsley, I. D. (1966). Membrane resistance in endolymphatic walls of the first turn of the guinea-pig cochlea. *J. Acoust. Soc. Am.* 40, 1398–1404. doi: 10.1121/1.1910239

Jones, T. A. (1992). Vestibular short latency responses to pulsed linear acceleration in unanesthetized animals. *Electroencephalogr. Clin. Neurophysiol.* 82, 377–386. doi: 10.1016/0013-4694(92)90007-5

Jones, S. M., Erway, L. C., Bergstrom, R. A., Schimenti, J. C., and Jones, T. A. (1999). Vestibular responses to linear acceleration are absent in otoconia-deficient C57BL/6JEi-het mice. *Hear. Res.* 135, 56–60. doi: 10.1016/s0378-5955(99)00090-8

Jones, S. M., Erway, L. C., Johnson, K. R., Yu, H., and Jones, T. A. (2004). Gravity receptor function in mice with graded otoconial deficiencies. *Hear. Res.* 191, 34–40. doi: 10.1016/j.heares.2004.01.008

Jones, S. M., and Jones, T. A. (1996). Short latency vestibular evoked potentials in the chicken embryo. *J. Vestib. Res.* 6, 71–83. doi: 10.1016/0957-4271(95)02008-X

Jones, T. A., and Jones, S. M. (1999). Short latency compound action potentials from mammalian gravity receptor organs. *Hear. Res.* 136, 75–85. doi: 10.1016/s0378-5955(99)00110-0

Jones, S. M., and Jones, T. A. (2000). Ontogeny of vestibular compound action potentials in the domestic chicken. *J. Assoc. Res. Otolaryngol.* 1, 232–242. doi: 10.1007/s101620010026

Jones, S. M., Jones, T. A., Bell, P. L., and Taylor, M. J. (2001). Compound gravity receptor polarization vectors evidenced by linear vestibular evoked potentials. *Hear. Res.* 154, 54–61. doi: 10.1016/S0378-5955(01)00216-7

Jones, T. A., Jones, S. M., and Colbert, S. (1998). The adequate stimulus for avian short latency vestibular responses to linear translation. *J. Vestib. Res.* 8, 253–272. doi: 10.1016/S0957-4271(97)00072-4

Jones, S. M., Jones, T. A., Johnson, K. R., Yu, H., Erway, L. C., and Zheng, Q. Y. (2006). A comparison of vestibular and auditory phenotypes in inbred mouse strains. *Brain Res.* 1091, 40–46. doi: 10.1016/j.brainres.2006.01.066

Jones, S. M., Jones, T. A., and Shukla, R. (1997). Short latency vestibular evoked potentials in the Japanese quail *(Coturnix coturnix japonica)*. *J. Comp. Physiol. A* 180, 631–638. doi: 10.1007/s003590050079

Jones, T. A., Jones, S. M., Vijayakumar, S., Brugeaud, A., Bothwell, M., and Chabbert, C. (2011). The adequate stimulus for mammalian linear vestibular evoked potentials (VsEPs). *Hear. Res.* 280, 133–140. doi: 10.1016/j.heares.2011.05.005

Jones, T. A., Lee, C., Gaines, G. C., and Grant, J. W. (2015). On the high frequency transfer of mechanical stimuli from the surface of the head to the macular neuroepithelium of the mouse. *J. Assoc. Res. Otolaryngol.* 16, 189–204. doi: 10.1007/s10162-014-0501-9

Jones, T. A., and Pedersen, T. L. (1989). Short latency vestibular responses to pulsed linear acceleration. *Am. J. Otolaryngol.* 10, 327–335. doi: 10.1016/0196-0709(89)90108-7

Jones, S. M., Robertson, N. G., Given, S., Giersch, A. B., Liberman, M. C., and Morton, C. C. (2011). Hearing and vestibular deficits in the Coch$^{-/-}$ null mouse model: comparison to the Coch$^{G88E/G88E}$ mouse and to DFNA9 hearing and balance disorder. *Hear. Res.* 272, 42–48. doi: 10.1016/j.heares.2010.11.002

Jones, S. M., Ryals, B. M., and Colbert, S. (1998). Vestibular function in Belgian Waterslager canaries *(Serinus canarius)*. *Hear. Res.* 121, 161–169. doi: 10.1016/s0378-5955(98)00074-4

Jones, S. M., Subramanian, G., Avniel, W., Guo, Y., Burkard, R. F., and Jones, T. A. (2002). Stimulus and recording variables and their effects on mammalian vestibular evoked potentials. *J. Neurosci. Methods* 118, 23–31. doi: 10.1016/s0165-0270(02)00125-5

Jones, S. M., Warren, L. E., Shukla, R., Browning, A., Fuller, C. A., and Jones, T. A. (2000). The effects of hypergravity and substrate vibration on vestibular function in developing chickens. *J. Gravit. Physiol.* 7, 31–44.

Kaga, K., Shinoda, Y., and Suzuki, J. I. (1997). Origin of auditory brainstem responses in cats: whole brainstem mapping and a lesion and HRP study of the inferior colliculus. *Acta Otolaryngol.* 117, 197–201. doi: 10.3109/00016489709117768

Kastanioudakis, I., Saravakos, P., Leontis, T., Balatsouras, D. G., and Ziavra, N. (2016). Ocular vestibular-evoked myogenic potentials using air-conducted sound: test parameters and normative data in healthy children; effect of body position on threshold. *Eur. Arch. Otorhinolaryngol.* 273, 2385–2394. doi: 10.1007/s00405-015-3800-9

Kiang, N. Y. S., Moxon, E. C., and Kahn, A. R. (1976). "The relationship of gross potentials recorded from the cochlea to single unit activity in the auditory nerve," in *Electrocochleography*, eds R. J. Ruben, C. Elberling and G. Salomon (Baltimore: University Park Press), 95–115.

Kim, S. H., Choi, H. S., Han, Y. E., and Choi, B. Y. (2016). Diverse etiologies manifesting auditory neuropathy characteristics from infants with profound hearing loss and clinical implications. *Int. J. Pediatr. Otorhinolaryngol.* 86, 63–67. doi: 10.1016/j.ijporl.2016.04.013

King, E. B., Shepherd, R. K., Brown, D. J., and Fallon, J. B. (2017). Gentamicin applied to the oval window suppresses vestibular function in guinea pigs. *J. Assoc. Res. Otolaryngol.* 18, 291–299. doi: 10.1007/s10162-016-0609-1

Kingma, C. M., and Wit, H. P. (2009). Acute endolymphatic hydrops has no direct effect on the vestibular evoked potential in the guinea pig. *J. Vestib. Res.* 19, 27–32. doi: 10.3233/VES-2009-0341

Kingma, C. M., and Wit, H. P. (2010). The effect of changes in perilymphatic K^+ on the vestibular evoked potential in the guinea pig. *Eur. Arch. Otorhinolaryngol.* 267, 1679–1684. doi: 10.1007/s00405-010-1298-8

Knox, G. W., Isaacs, J., Woodard, D., Johnson, L., and Jordan, D. (1993). Short latency vestibular evoked potentials. *Otolaryngol. Head Neck Surg.* 108, 265–269. doi: 10.1177/019459989310800310

Koka, K., Saoji, A. A., and Litvak, L. M. (2017). Electrocochleography in cochlear implant recipients with residual hearing: comparison with audiometric thresholds. *Ear Hear.* 38, e161–e167. doi: 10.1097/AUD.0000000000000385

Lange, M. E. (1988). *Far-Field Recordings of Vestibular Responses in Mammals.* Lincoln, NE: University of Nebraska.

Lee, S. I., Conrad, T., Jones, S. M., Lagziel, A., Starost, M. F., Belyantseva, I. A., et al. (2013). A null mutation of mouse Kcna10 causes significant vestibular and mild hearing dysfunction. *Hear. Res.* 300, 1–9. doi: 10.1016/j.heares.2013.02.009

Li, G., Elidan, J., and Sohmer, H. (1993). The contribution of the lateral semicircular canal to the short latency vestibular evoked potentials in cat. *Electroencephalogr. Clin. Neurophysiol.* 88, 225–228. doi: 10.1016/0168-5597(93)90007-c

Li, A., Xue, J., and Peterson, E. H. (2008). Architecture of the mouse utricle: macular organization and hair bundle heights. *J. Neurophysiol.* 99, 718–733. doi: 10.1152/jn.00831.2007

Lichtenhan, J. T., Hartsock, J. J., Gill, R. M., Guinan, J. J. Jr., and Salt, A. N. (2014). The auditory nerve overlapped waveform (ANOW) originates in the cochlear apex. *J. Assoc. Res. Otolaryngol.* 15, 395–411. doi: 10.1007/s10162-014-0447-y

Lichtenhan, J. T., Wilson, U. S., Hancock, K. E., and Guinan, J. J. Jr. (2016). Medial olivocochlear efferent reflex inhibition of human cochlear nerve responses. *Hear. Res.* 333, 216–224. doi: 10.1016/j.heares.2015.09.001

Lithgow, B. J. (2006). A neural event process. AU patent application PCT/AU2005/001330. 01.09.2005.

Lithgow, B. J. (2012). A methodology for detecting field potentials from the external ear canal: NEER and EVestG. *Ann. Biomed. Eng.* 40, 1835–1850. doi: 10.1007/s10439-012-0526-3

Lithgow, B. J., Garrett, A., and Heibert, D. (2008). EVestG: a measure for Meniere's disease. *Conf. Proc. IEEE Eng. Med. Biol. Soc.* 2008, 4162–4165. doi: 10.1109/IEMBS.2008.4650126

Loose, R., Probst, T., Tucha, O., Bablok, E., Aschenbrenner, S., and Lange, K. W. (2002). Vestibular evoked potentials from the vertical semicircular canals in humans evoked by roll-axis rotation in microgravity and under 1-G. *Behav. Brain Res.* 134, 131–137. doi: 10.1016/s0166-4328(01)00462-4

Lowenstein, O., and Roberts, T. D. (1951). The localization and analysis of the responses to vibration from the isolated elasmobranch labyrinth; a contribution to the problem of the evolution of hearing in vertebrates. *J. Physiol.* 114, 471–489. doi: 10.1113/jphysiol.1951.sp004638

Mantokoudis, G., Saber Tehrani, A. S., Wong, A. L., Agrawal, Y., Wenzel, A., and Carey, J. P. (2016). Adaptation and compensation of vestibular responses following superior canal dehiscence surgery. *Otol. Neurotol.* 37, 1399–1405. doi: 10.1097/MAO.0000000000001196

Masetto, S., Perin, P., Botta, L., Zucca, G., and Valli, P. (1995). Mechanisms for sensory adaptation in frog vestibular organs. *Neuroreport* 7, 230–232. doi: 10.1097/00001756-199512290-00055

Mathur, P. D., Vijayakumar, S., Vashist, D., Jones, S. M., Jones, T. A., and Yang, J. (2015). A study of whirlin isoforms in the mouse vestibular system suggests potential vestibular dysfunction in DFNB31-deficient patients. *Hum. Mol. Genet.* 24, 7017–7030. doi: 10.1093/hmg/ddv403

McGarvie, L. A., Curthoys, I. S., MacDougall, H. G., and Halmagyi, G. M. (2015). What does the dissociation between the results of video head impulse versus caloric testing reveal about the vestibular dysfunction in Meniere's disease? *Acta Otolaryngol.* 135, 859–865. doi: 10.3109/00016489.2015.1015606

McNerney, K. M., Lockwood, A. H., Coad, M. L., Wack, D. S., and Burkard, R. F. (2011). Use of 64-channel electroencephalography to study neural otolith-evoked responses. *J. Am. Acad. Audiol.* 22, 143–155. doi: 10.3766/jaaa.22.3.3

Mock, B., Jones, T. A., and Jones, S. M. (2011). Gravity receptor aging in the CBA/CaJ strain: a comparison to auditory aging. *J. Assoc. Res. Otolaryngol.* 12, 173–183. doi: 10.1007/s10162-010-0247-y

Morley, B. J., Lysakowski, A., Vijayakumar, S., Menapace, D., and Jones, T. A. (2017). Nicotinic acetylcholine receptors regulate vestibular afferent gain and activation timing. *J. Comp. Neurol.* 525, 1216–1233. doi: 10.1002/cne.24131

Murofushi, T., Wakayama, K., and Chihara, Y. (2010). oVEMP to air-conducted tones reflects functions of different vestibular populations from cVEMP? *Eur. Arch. Otorhinolaryngol.* 267, 995–996. doi: 10.1007/s00405-010-1246-7

Nazareth, A. M., and Jones, T. A. (1998). Central and peripheral components of short latency vestibular responses in the chicken. *J. Vestib. Res.* 8, 233–252. doi: 10.1016/S0957-4271(97)00076-1

Nie, K., Bierer, S. M., Ling, L., Oxford, T., Rubinstein, J. T., and Phillips, J. O. (2011). Characterization of the electrically evoked compound action potential of the vestibular nerve. *Otol. Neurotol.* 32, 88–97. doi: 10.1097/mao.0b013e3181f6ca45

Oei, M. L., Segenhout, J. M., Wit, H. P., and Albers, F. W. (2001). The vestibular evoked response to linear, alternating, acceleration pulses without acoustic masking as a parameter of vestibular function. *Acta Otolaryngol.* 121, 62–67. doi: 10.1080/000164801300006290

Ono, T., and Tachibana, M. (1990). Origin of the endolymphatic DC potential in the cochlea and ampulla of the guinea pig. *Eur. Arch. Otorhinolaryngol.* 248, 99–101. doi: 10.1007/bf00240229

Ó Maoiléidigh, D., Nicola, E. M., and Hudspeth, A. J. (2012). The diverse effects of mechanical loading on active hair bundles. *Proc. Natl. Acad. Sci. U S A* 109, 1943–1948. doi: 10.1073/pnas.1120298109

Patuzzi, R., and Sellick, P. M. (1983). A comparison between basilar membrane and inner hair cell receptor potential input-output functions in the guinea pig cochlea. *J. Acoust. Soc. Am.* 74, 1734–1741. doi: 10.1121/1.390282

Patuzzi, R. B., Yates, G. K., and Johnstone, B. M. (1989). Outer hair cell receptor current and sensorineural hearing loss. *Hear. Res.* 42, 47–72. doi: 10.1016/0378-5955(89)90117-2

Perez, R., Freeman, S., Sohmer, H., and Sichel, J. Y. (2000). Vestibular and cochlear ototoxicity of topical antiseptics assessed by evoked potentials. *Laryngoscope* 110, 1522–1527. doi: 10.1097/00005537-200009000-00021

Plotnik, M., Elidan, J., Mager, M., and Sohmer, H. (1997). Short latency vestibular evoked potentials (VsEPs) to linear acceleration impulses in rats. *Electroencephalogr. Clin. Neurophysiol.* 104, 522–530. doi: 10.1016/s0168-5597(97)00062-2

Plotnik, M., Freeman, S., Sohmer, H., and Elidan, J. (1999a). The effect of head orientation on the vestibular evoked potentials to linear acceleration impulses in rats. *Am. J. Otol.* 20, 735–740.

Plotnik, M., Sichel, J. Y., Elidan, J., Honrubia, V., and Sohmer, H. (1999b). Origins of the short latency vestibular evoked potentials (VsEPs) to linear acceleration impulses. *Am. J. Otol.* 20, 238–243.

Plotnik, M., Marlinski, V., and Goldberg, J. M. (2005). Efferent-mediated fluctuations in vestibular nerve discharge: a novel, positive-feedback mechanism of efferent control. *J. Assoc. Res. Otolaryngol.* 6, 311–323. doi: 10.1007/s10162-005-0010-y

Puria, S., and Rosowski, J. J. (2012). Bekesy's contributions to our present understanding of sound conduction to the inner ear. *Hear. Res.* 293, 21–30. doi: 10.1016/j.heares.2012.05.004

Pyykkö, I., Aalto, H., Grönfors, T., Starck, J., and Ishizaki, H. (1995). Vestibular evoked responses in man: methodological aspects. *Acta Otolaryngol. Suppl.* 520, 117–119. doi: 10.3109/00016489509125205

Rabbitt, R. D., Boyle, R., and Highstein, S. M. (1995). Mechanical indentation of the vestibular labyrinth and its relationship to head rotation in the toadfish, Opsanus tau. *J. Neurophysiol.* 73, 2237–2260.

Rabbitt, R. D., Boyle, R., Holstein, G. R., and Highstein, S. M. (2005). Hair-cell versus afferent adaptation in the semicircular canals. *J. Neurophysiol.* 93, 424–436. doi: 10.1152/jn.00426.2004

Rampp, S., Rahne, T., Plontke, S. K., Strauss, C., and Prell, J. (2017). (Intraoperative monitoring of cochlear nerve function during cerebello-pontine angle surgery). *HNO* 65, 413–418. doi: 10.1007/s00106-016-0262-3

Ravicz, M. E., Slama, M. C., and Rosowski, J. J. (2010). Middle-ear pressure gain and cochlear partition differential pressure in chinchilla. *Hear. Res.* 263, 16–25. doi: 10.1016/j.heares.2009.11.014

Robertson, N. G., Jones, S. M., Sivakumaran, T. A., Giersch, A. B., Jurado, S. A., Call, L. M., et al. (2008). A targeted Coch missense mutation: a knock-in mouse model for DFNA9 late-onset hearing loss and vestibular dysfunction. *Hum. Mol. Genet.* 17, 3426–3434. doi: 10.1093/hmg/ddn236

Rodionov, V., Elidan, J., Sela, M., Nitzan, M., and Sohmer, H. (1996). Vertical plane short and middle latency vestibular evoked potentials in humans. *Ann. Otol. Rhinol. Laryngol.* 105, 43–48. doi: 10.1177/000348949610500107

Russell, I. J. (1983). Origin of the receptor potential in inner hair cells of the mammalian cochlea—evidence for Davis′ theory. *Nature* 301, 334–336. doi: 10.1038/301334a0

Schmidt, R. S. (1963). Types of endolymphatic potentials. *Comp. Biochem. Physiol.* 10, 83–87. doi: 10.1016/0010-406x(63)90105-1

Scott, W. C., Giardina, C. K., Pappa, A. K., Fontenot, T. E., Anderson, M. L., Dillon, M. T., et al. (2016). The compound action potential in subjects receiving a cochlear implant. *Otol. Neurotol.* 37, 1654–1661. doi: 10.1097/MAO.0000000000001224

Sellick, P. M., Patuzzi, R., and Johnstone, B. M. (1982). Measurement of basilar membrane motion in the guinea pig using the Mössbauer technique. *J. Acoust. Soc. Am.* 72, 131–141. doi: 10.1121/1.387996

Simmons, D. D., and Morley, B. J. (2011). Spatial and temporal expression patterns of nicotinic acetylcholine alpha9 and alpha10 subunits in the embryonic and early postnatal inner ear. *Neuroscience* 194, 326–336. doi: 10.1016/j.neuroscience.2011.08.005

Sisneros, J. A. (2007). Saccular potentials of the vocal plainfin midshipman fish, Porichthys notatus. *J. Comp. Physiol. A Neuroethol. Sens. Neural. Behav. Physiol.* 193, 413–424. doi: 10.1007/s00359-006-0195-5

Sohmer, H., Elidan, J., Plotnik, M., Freeman, S., Sockalingam, R., Berkowitz, Z., et al. (1999). Effect of noise on the vestibular system—vestibular evoked potential studies in rats. *Noise Health* 2, 41–52.

Sohmer, H., and Freeman, S. (2004). Further evidence for a fluid pathway during bone conduction auditory stimulation. *Hear. Res.* 193, 105–110. doi: 10.1016/j.heares.2004.03.015

Sohmer, H., Freeman, S., Geal-Dor, M., Adelman, C., and Savion, I. (2000). Bone conduction experiments in humans—a fluid pathway from bone to ear. *Hear. Res.* 146, 81–88. doi: 10.1016/s0378-5955(00)00099-x

Stenfelt, S. (2015). Inner ear contribution to bone conduction hearing in the human. *Hear. Res.* 329, 41–51. doi: 10.1016/j.heares.2014.12.003

Stenfelt, S. (2016). Model predictions for bone conduction perception in the human. *Hear. Res.* 340, 135–143. doi: 10.1016/j.heares.2015.10.014

Stenfelt, S., and Goode, R. L. (2005). Bone-conducted sound: physiological and clinical aspects. *Otol. Neurotol.* 26, 1245–1261. doi: 10.1097/01.mao.0000187236.10842.d5

Stuermer, K. J., Beutner, D., Foerst, A., Hahn, M., Lang-Roth, R., and Walger, M. (2015). Electrocochleography in children with auditory synaptopathy/neuropathy: diagnostic findings and characteristic parameters. *Int. J. Pediatr. Otorhinolaryngol.* 79, 139–145. doi: 10.1016/j.ijporl.2014.11.025

Todd, N. P., Govender, S., and Colebatch, J. G. (2017). The inion response revisited: evidence for a possible cerebellar contribution to vestibular evoked potentials produced by air conducted sound stimulation. *J. Neurophysiol.* 117, 1000–1013. doi: 10.1152/jn.00545.2016

Todd, N. P., Paillard, A. C., Kluk, K., Whittle, E., and Colebatch, J. G. (2014). Source analysis of short and long latency vestibular-evoked potentials (VsEPs) produced by left vs. right ear air-conducted 500 Hz tone pips. *Hear. Res.* 312, 91–102. doi: 10.1016/j.heares.2014.03.006

Todd, N. P., Rosengren, S. M., and Colebatch, J. G. (2003). A short latency vestibular evoked potential (VsEP) produced by bone-conducted acoustic stimulation. *J. Acoust. Soc. Am.* 114, 3264–3272. doi: 10.1121/1.1628249

Trapani, J. G., and Nicolson, T. (2010). Physiological recordings from zebrafish lateral-line hair cells and afferent neurons. *Methods Cell Biol.* 100, 219–231. doi: 10.1016/B978-0-12-384892-5.00008-6

Trincker, D., and Partsch, C. J. (1959). Electrophysiological studies of the labyrinth of the guinea pig. III. The AC potentials (microphonics) from the vestibular apparatus. *Ann. Otol. Rhinol. Laryngol.* 68, 153–158. doi: 10.1177/000348945906800113

Van Eyck, M. (1949). Potentiels microphoniques dérivés des ampoules des canaux semi-circulaires chez le pigeon. *Arch. Int. Physiol. Biochim.* 57, 102–105.

Van Eyck, M. (1951a). Cochlear and ampullar potentials of the pigeon. *Arch. Int. Physiol.* 58, 476–477.

Van Eyck, M. (1951b). Microphonic potentials derived from semicircular canal ampullae and Ewald's law. *Arch. Int. Physiol.* 59, 236–238.

Van Eyck, M. (1951c). Recent research on the electrophysiology of the vestibular apparatus in the pigeon. *Ned. Tijdschr. Geneeskd.* 95:98.

Verschooten, E., Robles, L., Kovac, D., and Joris, P. X. (2012). Auditory nerve frequency tuning measured with forward-masked compound action potentials. *J. Assoc. Res. Otolaryngol.* 13, 799–817. doi: 10.1007/s10162-012-0346-z

Vijayakumar, S., Lever, T. E., Pierce, J., Zhao, X., Bergstrom, D., Lundberg, Y. W., et al. (2015). Vestibular dysfunction, altered macular structure and trait localization in A/J inbred mice. *Mamm. Genome* 26, 154–172. doi: 10.1007/s00335-015-9556-0

Vulovic, V., and Curthoys, I. S. (2011). Bone conducted vibration activates the vestibulo-ocular reflex in the guinea pig. *Brain Res. Bull.* 86, 74–81. doi: 10.1016/j.brainresbull.2011.06.013

Weisleder, P., Jones, T. A., and Rubel, E. W. (1990). Peripheral generators of the vestibular evoked potentials (VsEPs) in the chick. *Electroencephalogr. Clin. Neurophysiol.* 76, 362–369. doi: 10.1016/0013-4694(90)90037-k

Wever, E. G., and Bray, C. W. (1930). Action currents in the auditory nerve in response to acoustical stimulation. *Proc. Natl. Acad. Sci. U S A* 16, 344–350. doi: 10.1073/pnas.16.5.344

Wever, E. G., and Vernon, J. A. (1956). The sensitivity of the turtle's ear as shown by its electrical potentials. *Proc. Natl. Acad. Sci. U S A* 42, 213–220. doi: 10.1073/pnas.42.4.213

Wit, H. P., Bleeker, J. D., and Segenhout, J. H. (1981). Vestibular and cochlear responses to acoustic transients. Some properties of whole-nerve action potentials in pigeons. *Acta Otolaryngol.* 92, 409–422. doi: 10.3109/00016488109133280

Wit, H. P., Kahmann, H. F., and Segenhout, J. M. (1986). Vestibular microphonic potentials in pigeons. *Arch. Otorhinolaryngol.* 243, 146–150. doi: 10.1007/bf00453769

Wit, H. P., Spoelstra, H. A., and Segenhout, J. M. (1990). Bárány's theory is right, but incomplete. An experimental study in pigeons. *Acta Otolaryngol.* 110, 1–6. doi: 10.3109/00016489009122507

Yao, Q., DeSmidt, A. A., Tekin, M., Liu, X., and Lu, Z. (2016). Hearing assessment in zebrafish during the first week postfertilization. *Zebrafish* 13, 79–86. doi: 10.1089/zeb.2015.1166

Zhao, X., Jones, S. M., Yamoah, E. N., and Lundberg, Y. W. (2008). Otoconin-90 deletion leads to imbalance but normal hearing: a comparison with other otoconia mutants. *Neuroscience* 153, 289–299. doi: 10.1016/j.neuroscience.2008.01.055

Zhu, H., Tang, X., Wei, W., Maklad, A., Mustain, W., Rabbitt, R., et al. (2014). Input-output functions of vestibular afferent responses to air-conducted clicks in rats. *J. Assoc. Res. Otolaryngol.* 15, 73–86. doi: 10.1007/s10162-013-0428-6

Zotterman, Y. (1943). The microphonic effect of teleost labyrinths and its biological significance. *J. Physiol.* 102, 313–318. doi: 10.1113/jphysiol.1943.sp004037

Conflict of Interest Statement: The authors declare that the research was conducted in the absence of any commercial or financial relationships that could be construed as a potential conflict of interest.

Appendix 4

Curthoys, I. S., Grant, J. W., Burgess, A. M., Pastras, C. J., Brown, D. J., & Manzari, L. (2018). Otolithic Receptor Mechanisms for Vestibular-Evoked Myogenic Potentials: A Review. *Frontiers in neurology*, *9*.

frontiers in Neurology

REVIEW
published: 25 May 2018
doi: 10.3389/fneur.2018.00366

Otolithic Receptor Mechanisms for Vestibular-Evoked Myogenic Potentials: A Review

Ian S. Curthoys[1], J. Wally Grant[2], Ann M. Burgess[1], Chris J. Pastras[3], Daniel J. Brown[3] and Leonardo Manzari[4]*

[1] Vestibular Research Laboratory, School of Psychology, The University of Sydney, Sydney, NSW, Australia, [2] Department of Biomedical Engineering and Mechanics, VA Tech, Blacksburg, VA, United States, [3] The Menière's Laboratory, Sydney Medical School, The University of Sydney, Sydney, NSW, Australia, [4] MSA ENT Academy Center, Cassino, Italy

Air-conducted sound and bone-conduced vibration activate otolithic receptors and afferent neurons in both the utricular and saccular maculae, and trigger small electromyographic (EMG) responses [called vestibular-evoked myogenic potentials (VEMPs)] in various muscle groups throughout the body. The use of these VEMPs for clinical assessment of human otolithic function is built on the following logical steps: (1) that high-frequency sound and vibration at clinically effective stimulus levels activate otolithic receptors and afferents, rather than semicircular canal afferents, (2) that there is differential anatomical projection of otolith afferents to eye muscles and neck muscles, and (3) that isolated stimulation of the utricular macula induces short latency responses in eye muscles, and that isolated stimulation of the saccular macula induces short latency responses in neck motoneurons. Evidence supports these logical steps, and so VEMPs are increasingly being used for clinical assessment of otolith function, even differential evaluation of utricular and saccular function. The proposal, originally put forward by Curthoys in 2010, is now accepted: that the ocular vestibular-evoked myogenic potential reflects predominantly contralateral utricular function and the cervical vestibular-evoked myogenic potential reflects predominantly ipsilateral saccular function. So VEMPs can provide differential tests of utricular and saccular function, not because of stimulus selectivity for either of the two maculae, but by measuring responses which are predominantly determined by the differential neural projection of utricular as opposed to saccular neural information to various muscle groups. The major question which this review addresses is how the otolithic sensory system, with such a high density otoconial layer, can be activated by individual cycles of sound and vibration and show such tight locking of the timing of action potentials of single primary otolithic afferents to a particular phase angle of the stimulus cycle even at frequencies far above 1,000 Hz. The new explanation is that it is due to the otoliths acting as seismometers at high frequencies and accelerometers at low frequencies. VEMPs are an otolith-dominated response, but in a particular clinical condition, semicircular canal dehiscence, semicircular canal receptors are also activated by sound and vibration, and act to enhance the otolith-dominated VEMP responses.

Keywords: vestibular, utricular, saccular, vestibular-evoked myogenic potential, cervical vestibular-evoked myogenic potential, ocular vestibular-evoked myogenic potential, sound, vibration

OPEN ACCESS

Edited by:
Brian D. Corneil, University of Western Ontario, Canada

Reviewed by:
Mathieu Beraneck, UMR8119 Centre de neurophysique, physiologie, pathologie, France
Erin Gillikin Piker, James Madison University, United States

****Correspondence:***
Ian S. Curthoys
ian.curthoys@sydney.edu.au

Specialty section:
This article was submitted to Neuro-Otology, a section of the journal Frontiers in Neurology

Received: *26 March 2018*
Accepted: *07 May 2018*
Published: *25 May 2018*

Citation:
Curthoys IS, Grant JW, Burgess AM, Pastras CJ, Brown DJ and Manzari L (2018) Otolithic Receptor Mechanisms for Vestibular-Evoked Myogenic Potentials: A Review. Front. Neurol. 9:366. doi: 10.3389/fneur.2018.00366

PREFACE

In the last 5 years, there has been a very rapid growth of knowledge concerning vestibular-evoked myogenic potentials (VEMPs) and their physiological basis (1, 2). This includes new understanding of how sound and vibration activate otolithic receptors. The present review seeks to provide a concise comprehensive overview, as accurate as we can make it at May 2018, of the basic physiological mechanisms underlying VEMPs.

INTRODUCTION

Before the 1990s, the usual way to probe the function of the otoliths was to measure responses, such as eye movements or perception, to maintained or low-frequency linear acceleration stimuli provided by sleds or centrifuges or tilting chairs (3–8). Such tests were clinically impractical because of the small, variable, unreliable responses, as well as safety issues in delivering the stimuli. Since then there has been a major change: now surface electrodes on the skin are being used to record myogenic potentials in response to sound and vibration to probe otolith function, simply, quickly, reliably, and safely. These are called vestibular-evoked myogenic potentials (VEMPs). It is now clear that because of extensive indirect projections of vestibular neurons there are a host of VEMPs throughout the body (9, 10), with the two most frequently studied being the cervical vestibular-evoked myogenic potential [cVEMP—recorded from above the tensed sternocleidomastoid muscle (SCM)] and the ocular vestibular-evoked myogenic potential (oVEMP—recorded from above the inferior oblique as the patient looks up) (11–14) (see **Figure 1**).

The primary question is: are VEMP responses to sound (ACS) or bone-conducted vibration (BCV) really due to vestibular activation, since obviously sound and vibration stimulate cochlear receptors? That question was answered by showing the presence of VEMPs in patients without hearing but with vestibular function, and the absence of VEMPs in patients with hearing but without vestibular function after systemic gentamicin (11, 13, 17). These data show conclusively that VEMP tests are vestibular and not cochlear, and that evidence is supported by physiological research showing primary otolithic neurons are activated by sound and vibration. However, the next major question is how sound and vibration activate otolithic receptors and afferents, and that is the main focus of this review—the physiological basis for using these myogenic potentials to index otolith function, and the rationale for using these tests to test utricular or saccular function differentially.

The traditional view of the otoliths has been that they are flat sheets of tissue (called maculae—**Figure 2**) in which there are embedded thousands of receptor hair cells with their hair bundles projecting into the gelatinous otoconial layer (OL) covered by crystals of dense otoconia [specific gravity of 2.73—similar to granite (18)]. In the human, there are around 33,000 receptors in each utricular macula and 18,000 in each saccular macula, with about 5,000 utricular afferents and 4,000 saccular afferents (19, 20). The stimulus for causing vestibular hair cell transduction is deflection of the hair bundle with respect to the cell body of the receptor in the neuroepithelial layer (NEL) of the macula or crista. The traditional view is that the otoliths are stimulated by linear accelerations (such as head tilt) because the linear acceleration drags the otoconia and so deflects the hair bundles of the otolithic receptors (21) (**Figures 2B–E**). Because of the high density of the otoconia, the otoliths have been regarded as a sensory system responsive to static tilts and fairly low frequencies of linear acceleration—up to a few hundred Hertz [e.g., Ref. (21–26)].

Physiological evidence shows the otoliths do respond to maintained tilts and low-frequency linear accelerations, and here, we call this the accelerometer mode of otolith operation. But there is now abundant evidence that some otolithic receptors and afferents can be activated by air-conducted sound (ACS) and BCV up to frequencies of thousands of Hertz. This is shown by neural recordings of otolithic afferents with irregular resting discharge in squirrel monkey, cat, rat, and guinea pig (28–41). This neural evidence of otolithic activation by high frequencies is the foundation on which VEMPs to ACS and BCV are used to test otolith function.

The maculae are (moderately) curved structures (**Figure 2**) (42). The receptor cells, embedded in the neurepithelium of the maculae, fall into two types: amphora-shaped type I receptors or cylindrical type II receptors, and these two types are intermingled across the maculae (43, 44). Otolithic receptors are activated by hair bundle deflection toward the longest cilium (the kinocilium), and so each receptor has a preferred direction which is termed its morphological polarization. The receptors have opposite morphological polarization on either side of a dividing line now called "the line of polarity reversal" (**Figure 2**).

The receptors in a band (called the striola) straddling the line of polarity reversal are especially important—they have short stiff cilia with tenuous attachment to the otoconial membrane (27, 45), and there is a greater concentration of type I receptors in the striola (44, 46). The type I receptor cell bodies are enveloped by the calyx ending of afferents with irregular resting discharge (31, 47, 48). It appears that the attachment of the hair bundles of striolar receptors to the overlying otoconial membrane is tenuous (27, 49, 50). Extracellular recordings from primary otolithic afferents with irregular resting discharge have shown that these afferents are sensitive to sound and vibration, and histological tracing has shown these afferents contact type I receptors at the striola (31, 33).

Songer and Eatock (51) used intracellular recording from isolated type I otolithic receptors and showed that mammalian type I receptors could respond to displacements at frequencies of hundreds of Hertz (and probably higher). The size of these displacements is small, but only small displacements are needed since individual vestibular receptors are almost as sensitive as individual cochlear receptors. Using intracellular recordings

Abbreviations: ABR, auditory brainstem response; ACS, air-conducted sound; BCV, bone-conducted vibration; Fz, the midline of forehead at the hairline; IO, inferior oblique eye muscle; VEMP, vestibular-evoked myogenic potential; cVEMP, cervical vestibular-evoked myogenic potential; oVEMP, ocular vestibular-evoked myogenic potential; OL, otoconial layer; NEL, neuroepithelial layer; SCD, semicircular canal dehiscence; n10, the negative potential of the oVEMP at about 10 ms latency; SCM, sternocleidomastoid muscle; SPL, sound pressure level.

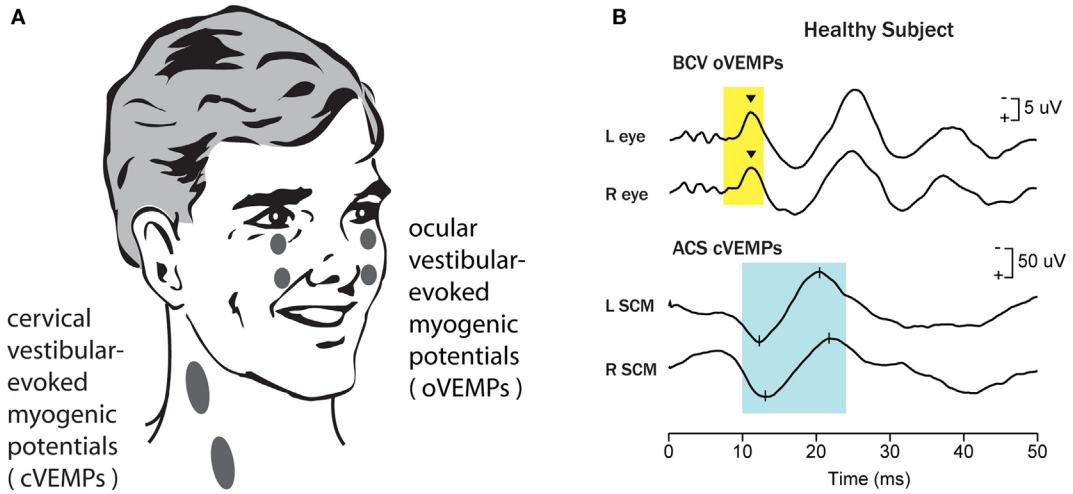

FIGURE 1 | Vestibular-evoked myogenic potentials (VEMPs). There are a host of VEMPs since vestibular input projects indirectly to many muscle groups. The two VEMPs which have received the most attention are cervical vestibular-evoked myogenic potentials (cVEMPs) and ocular vestibular-evoked myogenic potentials (oVEMPs). cVEMPs are recorded by surface electromyographic (EMG) electrodes over the tensed sternocleidomastoid muscles (SCMs) (11). The cVEMP consists of a short latency (13 ms from onset to peak) positive (i.e., inhibitory) EMG potential in response to high-intensity air-conducted sound (ACS) or bone-conducted vibration (BCV) (15). oVEMPs consist of a small (5–10 μV) negative (i.e., excitatory) potential recorded by surface electrodes on the skin beneath the eyes from the inferior oblique in response to BCV or ACS (12, 13). To record the oVEMP, the subject must be looking up. **(A)** Electrode placement for oVEMPs and cVEMPs; the ground electrode (not shown) is typically on the chin or sternum. **(B)** [Reprinted from Iwasaki et al. (16) © 2009, with permission from Elsevier.] Typical oVEMP and cVEMP traces for a healthy subject: the magnitude of the n10 response is approximately equal beneath both eyes for the oVEMP, and similarly the magnitude of the p13–n23 response is approximately equal in both SCMs for the cVEMP.

from individual receptors stimulated by hair bundle deflection, Geleoc et al. (52) have shown that isolated vestibular receptors have similar thresholds for hair bundle displacement as cochlear receptors—deflections of the receptor hair bundles of around 10 nm generate intracellular potentials in both cochlear and vestibular receptors.

Throughout both utricular and saccular maculae, there are receptors (probably cylindrical type II receptors) with long cilia projecting into the otolithic membrane (45). Afferent neurons with regular resting discharge make extensive contacts with extrastriolar type I and II receptors (47), but guinea pig otolithic afferents with regular resting discharge do not respond to ACS and BCV at reasonable levels [2 *g* peak to peak max or 130 dB sound pressure level (SPL) (31)].

Extracellular recordings of single primary otolithic afferents with irregular resting discharge show that they have a stimulus-locked increase in firing rate to ACS or BCV stimulation up to frequencies of thousands of Hertz (31) (**Figure 3**). The threshold as a function of frequency is very different for ACS vs BCV. For ACS, the lowest thresholds are at around 90 dB SPL at 1,000 Hz, with cells still responding with relatively low thresholds to 2,000 and 3,000 Hz ACS stimuli. For BCV, the lowest threshold is around 0.02 *g* at frequencies from 100 to 500 Hz. For BCV frequencies above 750 Hz, there is a very steep increase in threshold beyond 750 Hz, so that few neurons are activated by BCV at 2,000 Hz (even at 2 *g* peak to peak). At lower frequencies such as 500 and 750 Hz, BCV is a much more effective and reliable stimulus than ACS—the threshold for single neurons to BCV is around 0.02 *g* peak to peak, which is around the level for auditory brainstem response (ABR) threshold, whereas vestibular neural thresholds for ACS are at levels about 70 dB above ABR threshold (29, 31).

PHASE LOCKING

The exact response of these primary otolithic irregular neurons to BCV and ACS reveals a vital principle in the mechanism of transduction of high frequencies. For all neurons activated by ACS or BCV, the neurons do not fire an action potential on every single cycle, but the moment when the neuron fires is locked to a narrow band of phase angles of the stimulus waveform (**Figure 4**) (31, 38, 53). This is true up to very high frequencies even >3,000 Hz. For individual afferents, the measured optimum phase angle systematically changes with frequency for both ACS and BCV, reflecting the latency of the afferent. Also the optimum phase angle for an individual afferent neuron at a given frequency is not constant but varies from neuron to neuron (38, 53).

The phenomenon of phase locking shows that for both BCV and ACS, every single cycle of the sine wave stimulus is the effective stimulus for the afferent (31), even up to frequencies of 3,000 Hz where the duration of an individual cycle is so short (0.3 ms). It means that the receptors are being displaced at this very high frequency (3,000 times/s in this example), but when they fire is tightly locked to a particular phase angle of the sine wave stimulus even at this high frequency (38). Phase locking is very well established for cochlear receptors and afferents—the action potentials in cochlear afferent neurons are locked to each displacement of the basilar membrane. Phase locking of cochlear afferents is recognized as being a major code for the transmission

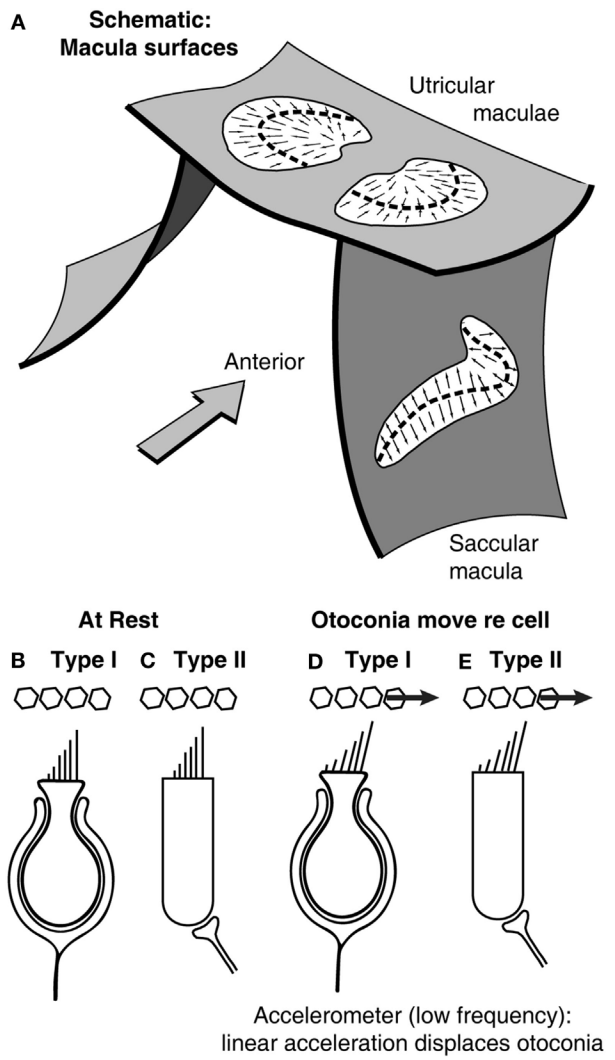

FIGURE 2 | **(A)** Schematic representation of the plates of otolithic receptors (the utricular and saccular maculae). The arrows show the preferred polarization of hair cell receptors across the maculae. The dashed lines are lines of polarity reversal (lpr). The striola refers to a band of receptors on either side of the lpr (27). Schematics of type I **(B,D)** and type II receptors **(C,E)** show how linear acceleration acts on otoliths and so deflects the hair bundles of individual receptors.

of auditory frequency information (54, 55), see Fettiplace (56) for a recent excellent review. It is now clear that phase locking applies to otolithic neurons with very tight locking to particular phase angles up to high frequencies. This may be due to the fact that irregular afferents are excellent detectors of change in stimulation (jerk detectors) (31, 38).

How can such an apparently sluggish system as the otoliths with such dense otoconia exhibit phase locking to stimulus frequencies of thousands of Hertz? One answer comes from recording the vestibular microphonic, which shows that mammalian utricular receptors are activated at such high frequencies (57, 58). The vestibular microphonic is a field potential to sound or vibration and is a direct electrophysiological indicator of otolithic receptor hair cell function. The vestibular microphonic has been recorded *in vivo* in anesthetized guinea pigs by electrodes piercing the underside of the utricular macula with a glass microelectrode and then measuring the vestibular microphonic to BCV or ACS stimuli of varying frequency and amplitude (**Figure 5**) (57). Most importantly, in these animals, the cochlea has been completely removed, so there is no contribution from the cochlear microphonic. The recent paper (57) gives the evidence that the vestibular microphonic is a field potential due to otolithic receptor hair cell activation—reporting all the correct controls—such as chemically silencing afferent neurons and showing that the vestibular microphonic remains, and conversely chemically silencing the receptors and showing that the vestibular microphonic disappears, leading to the conclusion that the vestibular microphonic is a field potential generated by otolithic hair cells (utricular hair cells in this case) (**Figure 5**). The vestibular microphonic (strictly the utricular microphonic) has been recorded up to frequencies of 3,000 Hz. Those results complement the results from single neuron recordings: mammalian utricular receptors really do respond to very high frequencies (up to 3,000 Hz), far above what the otoliths are usually thought to be capable of transducing. But how? The simple answer is that the macula moves.

Many years ago, Tullio used fine aluminum particles on the surface of the utricular macula to demonstrate visually that sound caused rabbit utricular macula to move (60). We have confirmed Tullio's results by using laser Doppler vibrometry to measure the velocity of guinea pig utricular macula movement during ACS and BCV stimulation. A tiny glass bead was placed on the exposed underside of the utricular macula and a laser beam aimed at it. The Doppler shift in the wavelength of the reflected beam during BCV or ACS stimulation (59) confirms that the macula is moving and gives the macula velocity. These measures show that both ACS and BCV cause the macula to move as Tullio had reported, and at frequencies up to 3,000 Hz. The actual displacements are small—nanometers—but the results of Geleoc et al. (52) show how very sensitive vestibular receptors are, so that deflections of the macula of nanometers can activate vestibular receptors.

Irregular otolithic afferents respond to the time rate of change of acceleration (jerk) rather than to acceleration itself. That jerk sensitivity has been demonstrated in otolithic evoked potentials (61) to pulses of linear acceleration. That jerk sensitivity adds to the puzzle—now this "sluggish" system not only transduces maintained linear accelerations but also this evidence shows it really does respond to extremely fast stimuli. The puzzle to be explained is that the one sensory system is responding over a large range of frequencies—from DC up to 3,000 Hz. How could high frequencies of BCV cause macula and hair bundle displacements at 3,000 Hz, given the very large specific gravity of the otoconia and the viscosity of the otolithic membrane?

Grant and Curthoys (62) have put forward a model of the otoliths which addresses that question. The model holds that there are two modes of otolithic operation: the traditional accelerometer mode and the new seismometer mode. At low frequencies of BCV, the otoconia move relative to the skull, while the macula stays stationary, and so the hair bundles of the receptor cells

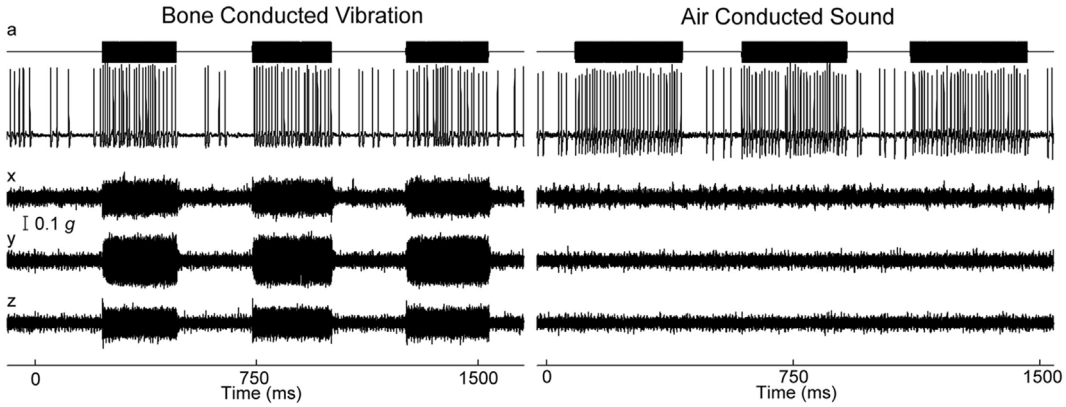

FIGURE 3 | Time series of firing of an irregular otolith neuron during stimulation by bone-conducted vibration (BCV) and air-conducted sound (ACS) at 500 Hz—both stimuli cause stimulus-locked activation. The top trace (a) shows the command voltage indicating when the stimulus is on. The second trace shows the extracellular recording. The three bottom traces (*x, y, z*) show the triaxial accelerometer recording of the stimulus. The *left panel* is an example of BCV stimulation and the *right* of ACS stimulation of the same neuron. Note the scale of stimulus intensity in *g* at the left margin between traces *x* and *y*. Reprinted by permission from Springer Nature, Curthoys and Vulovic (29), © 2011.

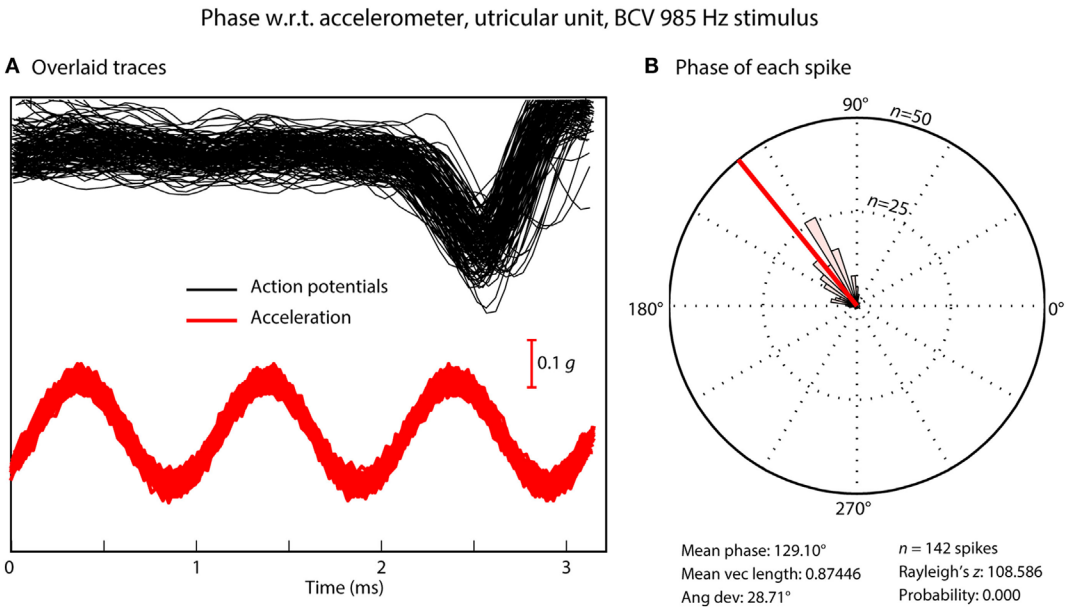

FIGURE 4 | **(A)** Time series of action potentials in response to a bone-conducted vibration stimulus (shown by the red acceleration trace). Traces which contain a spike of neural firing are aligned using the timing of the stimulus pulse. **(B)** Circular histogram (rose plot) of the phase of each spike; the small and large concentric circles represent $n = 25$ and $n = 50$ spikes, respectively. The Rayleigh test of circular uniformity was performed on the 142 spikes, and was significant ($p < 0.001$), showing that the time when an afferent is activated is phase locked to the stimulus. Here, the neuron misses many cycles **(A)**, as can be seen from the value of the action potentials which contain no spikes in the cycles preceding each instance of firing, but the time when the neuron fires is locked to a narrow band of phase angles of the stimulus **(B)**. Clearly each individual cycle of the stimulus is acting to activate the receptor/afferent.

are deflected (**Figure 6**). This is the "traditional" accelerometer mode of operation. In the accelerometer mode, the otoconia move relative to the macula, while the macula is accelerated with the skull motion. At high frequencies, the system operates in the seismometer mode: the otoconia remain at rest (due to their inertia) while the macula is in motion, again producing a relative displacement between the otoconia and macula. In both cases, there is relative motion between the otoconia and macula, displacing hair bundles. We explain this in more detail below.

Otoliths are biological–mechanical sensors that measure the acceleration of the head in the plane of the otolith. The acceleration that is measured is the vector sum of gravity and the inertial acceleration and is called the gravitoinertial acceleration, but is generally just referred to as the head acceleration. The otolith

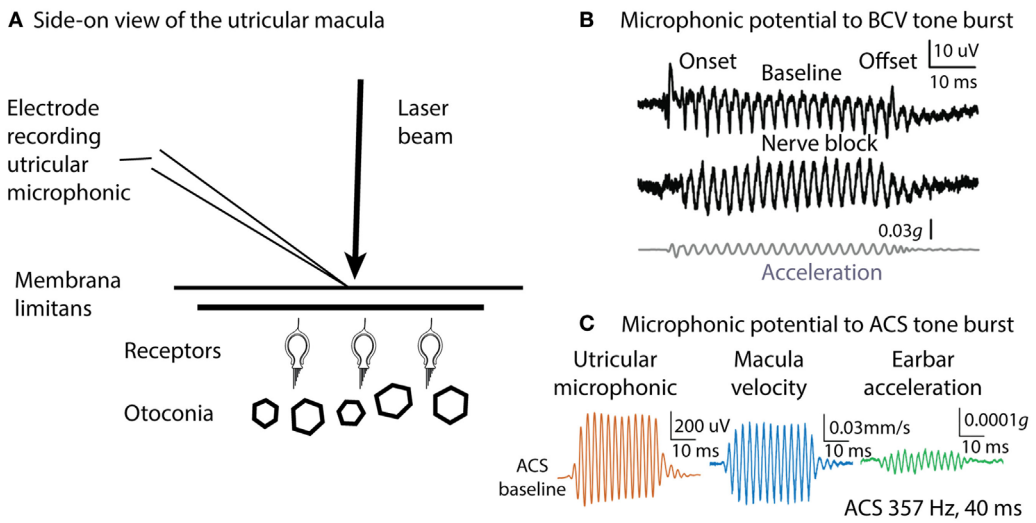

FIGURE 5 | Microphonic recording and laser Doppler measurement of macula movement, showing the relation between the vestibular microphonic and the velocity of macula movement during bone-conducted vibration (BCV) or air-conducted sound (ACS) stimulation. A microelectrode on the surface of the utricular macula **(A)** records a microphonic potential from the utricular receptors in response to BCV **(B)** or to ACS **(C)**. There is no contribution from the cochlea since it has been completely ablated. **(B)** Vestibular microphonic responses to a BCV tone burst (40 ms, 400 Hz sinusoid) prior (top trace) and following (middle trace) lignocaine application to the vestibule to block the vestibular nerve. The microphonic remains after lignocaine injection showing it is a receptor field potential. Bottom trace: the BCV stimulus; the linear acceleration as recorded by a triaxial linear accelerometer on the ear bar. **(C)** Laser Doppler vibrometry. A laser beam is projected onto a reflective glass bead on the macula and the Doppler shift of the wavelength of the reflected beam shows the velocity of macula movement during BCV or ACS stimulation. Panel **(C)** shows the simultaneous measurement of vestibular microphonic and macula velocity. **(B)** Reprinted from Pastras et al. (57), © 2017, with permission from Elsevier. Panel **(C)** is from Pastras et al. (59).

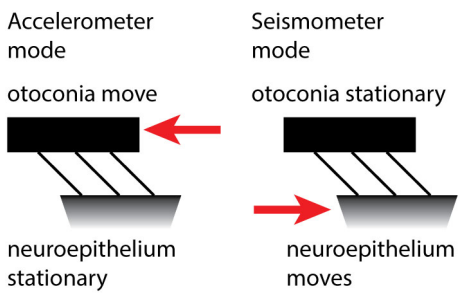

FIGURE 6 | The accelerometer–seismometer model of otolith operation holds that at low frequencies *(left)* the otoconia move relative to the macula, but at high frequencies *(right)* the otoconia remain stationary while the macula moves. In both cases, the hair bundles are deflected and the receptors are activated.

acceleration value is a measurement of the relative displacement between the otolithic membrane and the NEL. This displacement measurement is made by the hair cells in the NEL and reported to the brain *via* the otolithic afferents.

Static or low-frequency linear acceleration causes the otoconia to move relative to the NEL of the utricular macula. During a maintained head tilt (a DC stimulus), the linear acceleration of gravity acts on the otoconia and displaces the otoconia relative to the NEL, so the hair bundles of the otolithic receptor hair cells (both type I and type II receptors) are deflected relative to their cell bodies and a neural signal is transmitted to the brain *via* the otolithic afferents, signaling that linear acceleration has occurred. This is the "traditional" accelerometer mode of otolith operation.

If a high-frequency vibration (e.g., 2,000 Hz) is applied to the skull, it causes the NEL to move at the same 2,000 Hz frequency. But because of their mass, the otoconia remain stationary. The consequence is that again the hair bundles will be deflected and action potentials will be propagated in otolithic afferent neurons. This is the seismometer mode of otolith operation. The difference is that in the first (accelerometer) mode, the otoconia move relative to the skull and in the second (seismometer) mode, the macula moves relative to the skull. In both modes, the otoconia and macula move with respect to each other, so the hair bundles of the receptors are displaced relative to the cell body. In this way, linear acceleration and high-frequency vibration can both stimulate the otolithic receptors.

Neurons cannot fire at such high rates (2,000 spikes/s), but at all frequencies the hair bundles of the receptors are deflected and activated once per cycle, and the neural evidence shows that when the afferent neurons fire, the action potentials show phase locking to the individual cycles of the stimulus at both low and high frequencies.

Given the usual stimulus strength used in VEMP testing to BCV, we estimate that the magnitude of these deflections is probably in the 50–80 nm range. With such small deflections, it is only the type I hair cells in the striolar region, that are stimulated. These type I hair cells are stiff (45) due to their large number of stereocilia and are stimulated with these small

displacements seen in the high-frequency seismometer mode stimulus. The type II hair cells are less stiff and require larger deflections for stimulation. Afferents with regular resting discharge receive input predominantly from type II receptors, but are not activated by high-frequency BCV or ACS at the levels tested experimentally.

The model is essentially the result of application of engineering principles for the design of accelerometers and seismometers, to the otoliths. Importantly, engineering analysis shows that the one system can operate both as an accelerometer and as a seismometer. On this "accelerometer–seismometer" model, the one sensory system, the otoliths, transduces both low-frequency (even DC) linear accelerations and also very high-frequency stimuli. The empirical evidence that this happens comes from recordings of single otolithic afferents to a wide range of frequencies varying from 37 to 2,000 Hz (31) and showing that the one afferent is activated by stimuli across such a large frequency range, and from measuring (and modeling) the stimulus thresholds needed to activate the neuron across this large range.

Commercial accelerometers have an undamped natural frequency in the 10–20 kHz range and seismometers in the 5–10 Hz range. Otoliths have undamped natural frequencies in between these frequencies, which allows them to operate in both modes (accelerometer and seismometer) over the frequency ranges that have been shown to activate otoliths. It is the unique undamped natural frequency that allows the otoliths to make the transition over the two operating modes.

While this model accounts for the fact that receptor hair bundles can be displaced at various frequencies, we need to drill down into the micromechanics of hair bundle deflection to answer the final question: exactly how do the hair bundle deflections occur for both BCV and ACS stimuli? This comes down to what happens at the interface between the receptor cilia and the otolithic membrane during stimulation.

At the striola the short, stiff hair bundles of the receptors project into holes in the otolithic membrane (49, 50, 63–65). So any wall motion of the holes in the column filament-gel layer structure of the otolithic membrane will produce endolymph fluid motion within the hole. In the striolar region, the hair cell bundles are only weakly attached at the top of the kinocilium (27), or not attached at all and are free standing (49). This fluid motion within the hole produces a drag force on the bundle, causing it to deflect. The fluid environment is so viscously dominated (Reynold's numbers—the ratio of inertial to viscous forces of 10^{-3}–10^{-2}) that bundles move instantaneously with any fluid movement. In other words, this coupling of fluid motion to hair bundle is so strong that the hair bundle displacement follows the fluid displacement almost exactly. The viscous dominated environment results in bundle displacement matching fluid displacement almost exactly, so fluid displacement is synonymous with hair bundle displacement. This account would also apply to receptor activation by ACS, since the vibrometry shows that the utricular macula moves during high-frequency ACS as well as during BCV. In sum, we suggest that the actual stimulus causing hair bundle deflection is the fluid displacement around the cilia of the type I receptors (see **Box 1**).

BOX 1 | Transduction model of Grant and Curthoys (62).

1. The otolithic system is underdamped. The transition from accelerometer mode to seismometer mode would not take place if the system were not underdamped.
2. The transition from accelerometer to seismometer takes place at the system undamped natural frequency (estimated to be around 600 Hz for humans).
3. In the accelerometer mode, head acceleration causes the otoconial layer (OL) to lag behind the neuroepithelial layer (NEL), producing a relative displacement between NEL and OL. This relative displacement deflects receptor hair bundles which activates the receptors.
4. In the seismometer mode at high frequencies, the OL remains at rest due to its inertia and the NEL is in motion, again producing relative displacement between the two layers and so again activating receptors.
5. Using vestibular-evoked myogenic potential (VEMP) test frequencies and acceleration magnitudes, we estimate the relative displacement between the two layers is around 50–80 nm. This displacement is small but sufficient to stimulate the short, stiff, loosely attached type I hair cell bundles in the striolar regions, while not large enough to activate extrastriolar type II hair bundles.
6. The model has implications for clinical testing: the ideal stimulus for otoliths and thus VEMPs is one with a very rapid rise time since the otolithic receptors are jerk detectors. That agrees with animal experimental (61) and clinical data (98) (see below) that short rise times are optimal for eliciting ocular vestibular-evoked myogenic potentials. Modeling of the neural data (62) indicates 750 Hz is probably the optimum frequency for testing VEMPs.

PHYSIOLOGY RELEVANT FOR CLINICAL TESTING

Suzuki et al. electrically stimulated the utricular nerve in cats and showed it caused eye movements with torsional, vertical, and horizontal components (66). We reasoned that if 500 Hz BCV is a specific otolithic stimulus, it should generate a similar pattern of eye movements to those reported by Suzuki et al., and Vulovic and Curthoys (67) showed that brief 500 Hz BCV pulses of the skull of an alert guinea pig generated eye movements with horizontal vertical and torsional components similar to those Suzuki et al. found (**Figure 7**). These eye movements are due to vestibular as opposed to cochlear activation, because after intratympanic injection of gentamicin to the guinea pig, a procedure which selectively kills vestibular type I receptor cells (68, 69), the BCV evoked eye movements disappear but the indicator of cochlear function, the ABR response, remains (67).

Do these conclusions apply to human otolith-induced eye movements? In some healthy subjects (without any symptoms of superior canal dehiscence) we used fast high resolution video recording to record eye movements, and found that brief bursts of 500 Hz BCV of one mastoid delivered by a small clinical bone oscillator (Radioear B-71) caused small but systematic and reliable stimulus-locked eye movement responses with horizontal, vertical, and torsional components (**Figure 7**) at a short latency of about 20 ms or less (70). In these experiments, the subjects were biting on a bite-bar during the BCV stimulation to minimize head rotation and so minimize semicircular canal stimulation. Prior to such eye movements there would be electromyographic (EMG) potentials in the ocular muscles to cause the eye movement

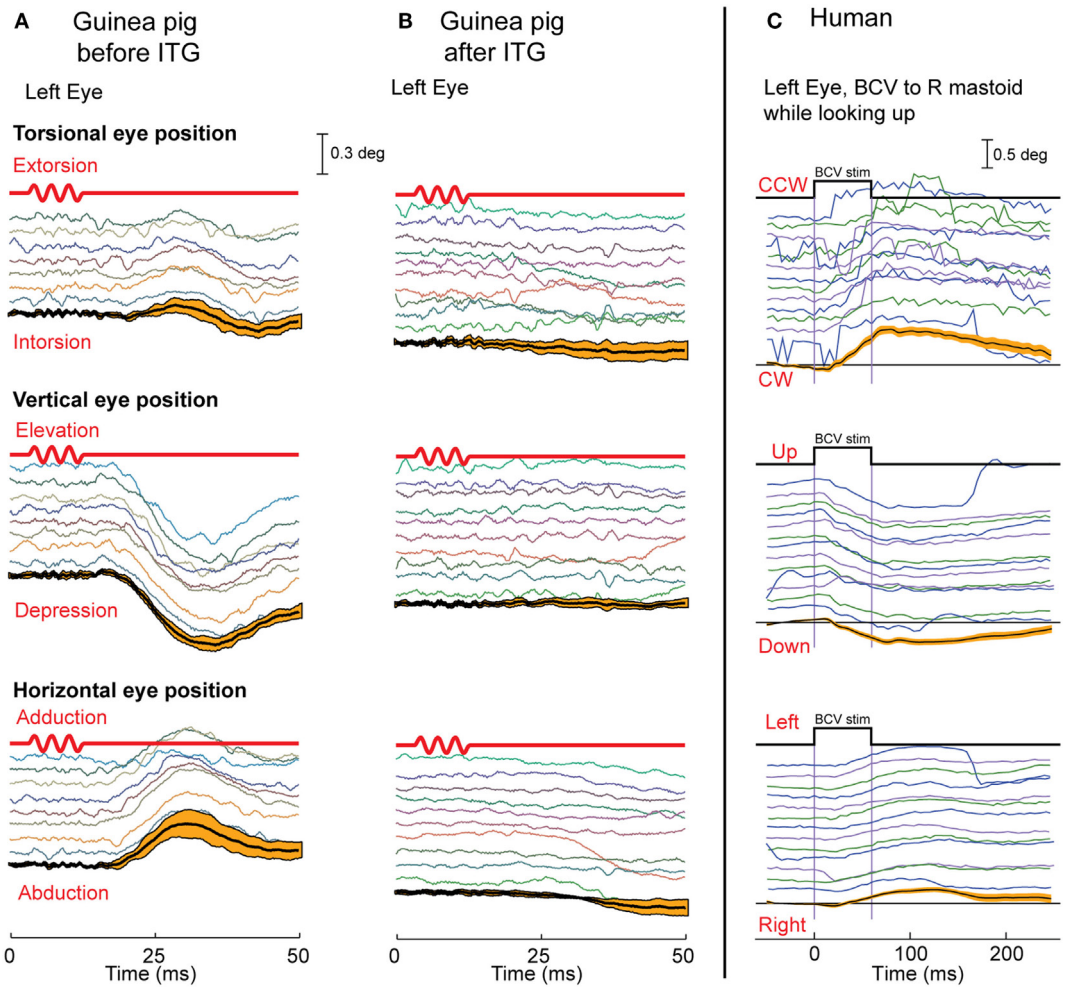

FIGURE 7 | The eye movements in guinea pigs **(A,B)** and humans **(C)** in response to bone-conducted vibration (BCV). Each panel shows time series of torsional, vertical, and horizontal components of eye position in response to repeated tone bursts of 500 Hz BCV; below the traces are the mean and 95% confidence intervals *(orange bars)* calculated over responses to multiple stimuli. **(A,B)** The first line in red is the command voltage for the 500 Hz BCV stimulus. The eye movements in guinea pigs are eliminated **(B)** by intratympanic gentamicin which selectively attacks type I receptors. In humans **(C)**, a small vibration applied to the mastoid (start and end time shown by the top black trace) elicits stimulus-locked torsional, vertical, and horizontal eye movements. **(A,B)** Reprinted from Vulovic and Curthoys (67), © 2011, with permission from Elsevier.

response, and it is these potentials in eye muscles which are recorded in VEMPs.

Air-conducted sound and BCV both activate both utricular and saccular afferents (29, 31, 33). Saccular afferents in guinea pigs do have a lower threshold to ACS than utricular afferents. But afferents from both maculae respond to both ACS and BCV (30, 31, 33). So how then is it possible to differentially assess utricular as opposed to saccular function? Curthoys put forward the original idea that the differential assessment of utricular and saccular function can come from the largely differential neural projections of these two systems (71). Physiology shows that short latency saccular projections to inferior oblique are weak, whereas saccular projections to neck and spinal motoneurons are strong (72). The work of Suzuki et al. (66) had shown that utricular projections to inferior oblique are strong, so Curthoys suggested that measuring the contralateral oVEMP—from the inferior oblique eye muscles—largely reflects the activation of contralateral utricular afferents by either ACS or BCV. Saccular projection to ipsilateral neck motoneurons is strong, so it was suggested that measuring the ipsilateral cVEMP from stretched neck muscles shows largely ipsilateral saccular function (71) (**Figure 8**). In this way, VEMPs can provide tests of utricular and saccular function not because of stimuli which selectively activate one or other of the two maculae, but by measuring responses which are predominantly determined by the differential neural projection of utricular as opposed to saccular projections to various muscle groups (**Figure 8**). This suggestion caused considerable controversy at the time (73, 74); however, data from patients with partial unilateral vestibular

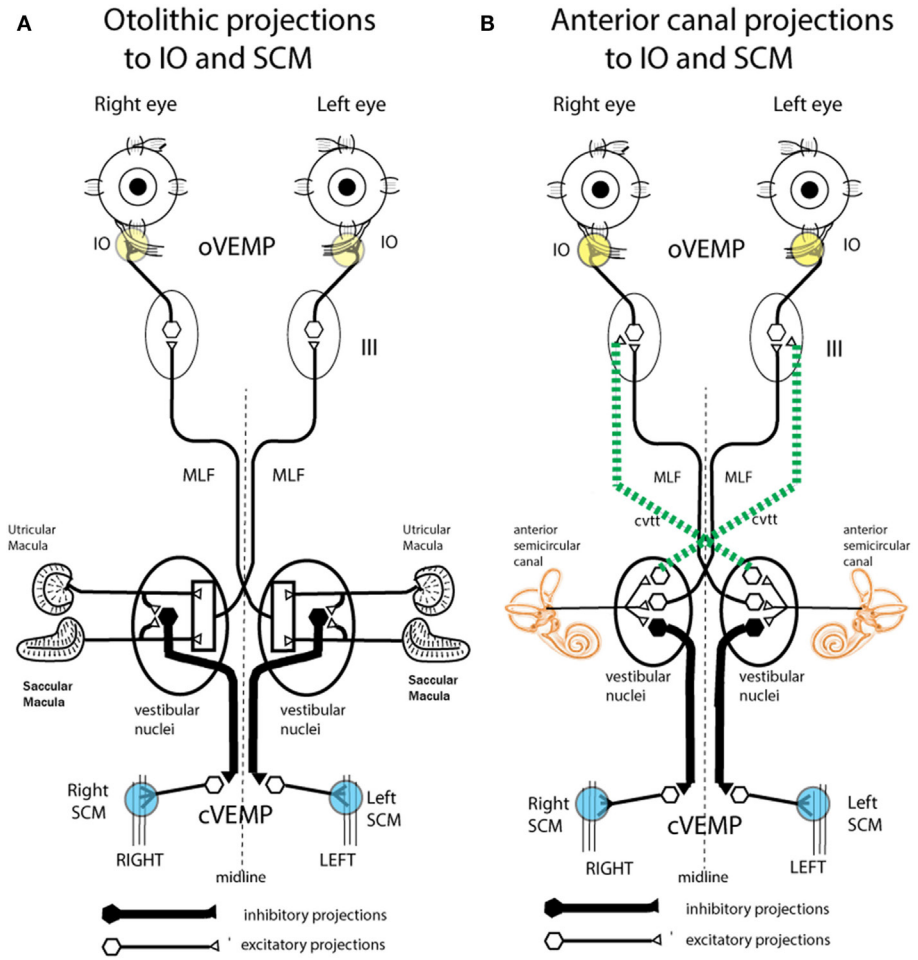

FIGURE 8 | Schematic representations of the major neural projections from vestibular receptors to the eye muscles and the neck muscles. **(A)** The otolithic projections to inferior oblique eye muscle (IO) and sternocleidomastoid muscle (SCM). **(B)** The analogous projections of the anterior semicircular canal neurons to the IO and SCM (72). Stimulation in animals with intact labyrinths causes the neural connections shown on the left panel to be activated. However, after a semicircular canal dehiscence (SCD), the anterior semicircular canals are also activated by sound and vibration, so the neural projections on the right come into play. The green dotted lines represent the projection from the anterior canal neurons in the vestibular nucleus to the contralateral third nerve nucleus *via* the crossed ventral-tegmental track. It appears that it is this combination of otolithic and canal afferent activation which in part results in the enhanced ocular vestibular-evoked myogenic potential (oVEMP) and cervical vestibular-evoked myogenic potential (cVEMP) responses after SCD. **(A)** Reprinted by permission from John Wiley and Sons, Curthoys et al. (80), © 2011. **(B)** Reprinted by permission from Springer Nature, Curthoys (81), © 2017.

neuritis have provided evidence confirming those suggestions. In response to ACS or BCV some patients show *selective* loss of the contralateral oVEMP n10, but preservation of the ipsilateral cVEMP p13–n23 (75, 76). Other patients show the converse: symmetrical oVEMPs but asymmetrical cVEMPs: the ipsilateral cVEMP is reduced or eliminated, yet the oVEMP is not detectably affected (77). The logical consequence of that dissociation is that the two responses, oVEMP and cVEMP, must be generated from different sense organs—because to the same stimulus one response is affected, the other is not. Since the utricular afferents travel in the superior nerve and project to contralateral inferior oblique, it is most likely the utricular afferents which are affected. In light of these results, the Curthoys (71, 74) suggestion is now accepted: "Ocular vestibular evoked potentials are mainly dependent on utricular pathway function" [(78), p. 1843] and "The oVEMP originates predominantly from utricular afferents" [(79), p. 1051].

The stimulus frequency usually used for clinical testing of VEMPs is 500 Hz, and that frequency causes fairly selective activation of otolithic irregular neurons: at 500 Hz semicircular canal afferents with irregular resting discharge are not usually activated by sound or vibration in animals with normally encased bony labyrinths, at least up to BCV stimulus levels of 2 *g* or 130 dB SPL ACS (28, 31). Carey et al. reported that to elicit phase locking in irregular canal afferents in the chinchilla with a normally encased labyrinth required an extremely high intensity (135 dB SPL) (82). We have confirmed that result in guinea pigs (81, 83). Regular canal and otolith afferents are not

activated usually by physiological levels of ACS and BCV. Higher level stimuli may cause them to be activated, but such levels are not clinically realistic. So usually there is little or no contribution from regular or irregular semicircular canal afferents during VEMP testing. That is changed in patients with a thinning—a dehiscence or window (fenestra or SCD) of the bony wall of the semicircular canal, who show very large VEMP potentials (discussed below).

The physiological results show that an SCD changes the neural response. After making an opening into the bony wall of the anterior canal, the procedure resulted in phase-locked activation of irregular canal afferents at a much lower intensity (96 dB SPL) than with the labyrinth encased (135 dB SPL) (82). These SCD-enhanced vestibular neural responses are consistent with the results from patients with a CT-verified SCD who show enhanced VEMPs to sound and vibration and nystagmus in the plane of the dehiscent canal during maintained tonal stimulation (84). However, it should be emphasized that both the neural and clinical results are variable; not all patients with CT-verified SCD develop the same classic symptoms, and there is considerable variability in the neural results (85). This is not surprising since the fenestra varies from patient to patient in humans and animals, and many other factors have the potential for influencing the results, such as collapse of the membranous duct (86).

The definitive evidence about the neural response in SCD comes from the response of individual neurons where the same neuron was recorded both before and after the SCD and in some cases after resealing the SCD (**Figure 9**). After SCD, guinea pig irregular semicircular canal afferents, previously unresponsive to ACS or BCV in animals with fully encased labyrinths, respond vigorously with low threshold to the same stimulus magnitude which was ineffective before SCD (83, 87). Maintained sound or vibration results in a maintained high firing rate in irregular anterior canal neurons. This has been confirmed by Iversen et al. (88), who also confirmed the report by Curthoys and Grant (53) that an SCD causes a slow change in firing of regular canal afferents to maintained sound. This change in neural firing corresponds to the cupula deflection caused by endolymph movement due to the SCD causing an impedance pumping type of action. Such a high firing rate would cause a maintained nystagmus in human patients (the Tullio phenomenon) (81). Nystagmus caused by such phase-locked activation in human patients would be expected to have abrupt onset and offset, as in fact happens in some patients in the clinical test called vibration-induced nystagmus (89).

Why should an SCD cause semicircular canal neurons previously unaffected by ACS or BCV now to respond to ACS and BCV? The SCD is a third window and so ACS and BCV cause larger fluid displacement in the duct (90, 91), and irregular canal afferents synapsing on type I receptors at the crest of the crista (43, 92, 93) are activated by these fluid displacements (83). Although similar structurally and physiologically to otolith type I receptors, canal type I receptors are not usually activated by ACS or BCV, because the sealed bony wall of the canal limits the amplitude of the sound-induced or vibration-induced fluid displacement in the canal. We reasoned that after an SCD, the increased fluid displacement is sufficient to deflect the short stiff cilia of type I semicircular canal receptors on the crista, and so irregular canal afferents would show phase-locked activation after SCD to both ACS and BCV, and in humans, canal neurons would thus contribute to the VEMP response as was found (83).

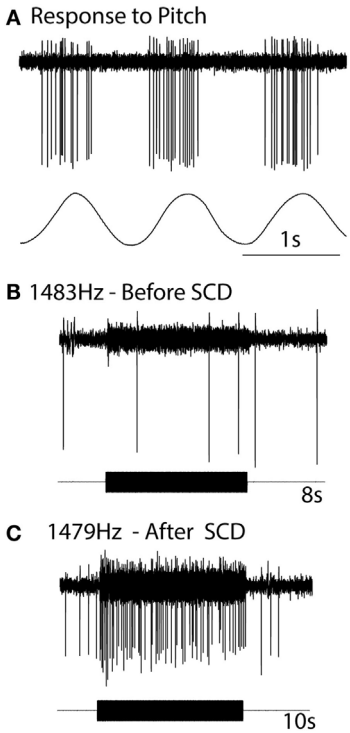

FIGURE 9 | The response of the one anterior canal neuron to high-frequency air-conducted sound (ACS), before and after a small dehiscence in the bony wall of the anterior canal. **(A)** The response of the neuron to pitch angular acceleration identifies the neuron as being an anterior canal afferent. **(B)** Before semicircular canal dehiscence (SCD), an 8 s burst of 1,483 Hz ACS has no effect on the neural response. **(C)** After SCD, a 10 s burst of an ACS of 1,479 Hz causes strong activation. Resealing the SCD causes that enhanced response to disappear. Reprinted by permission from Springer Nature, Curthoys (81), © 2017.

Such an outcome in human SCD patients would result in lower VEMP thresholds, as is observed. In addition, irregular anterior canal neurons project to contralateral inferior oblique, and so after SCD these neurons would now contribute to and enhance the oVEMP n10 response in the contralateral inferior oblique after SCD (**Figure 10**). Also by virtue of their ipsilateral (inhibitory) projection to SCM (72) (**Figure 8**), the activity of these canal afferents would enhance the cVEMP over the ipsilateral SCM.

In summary, the physiological evidence predicts the enhanced VEMP response seen after SCD. Patients with CT-verified SCD show VEMPs in response to very high-frequency stimulation which is ineffective in healthy subjects with intact bony

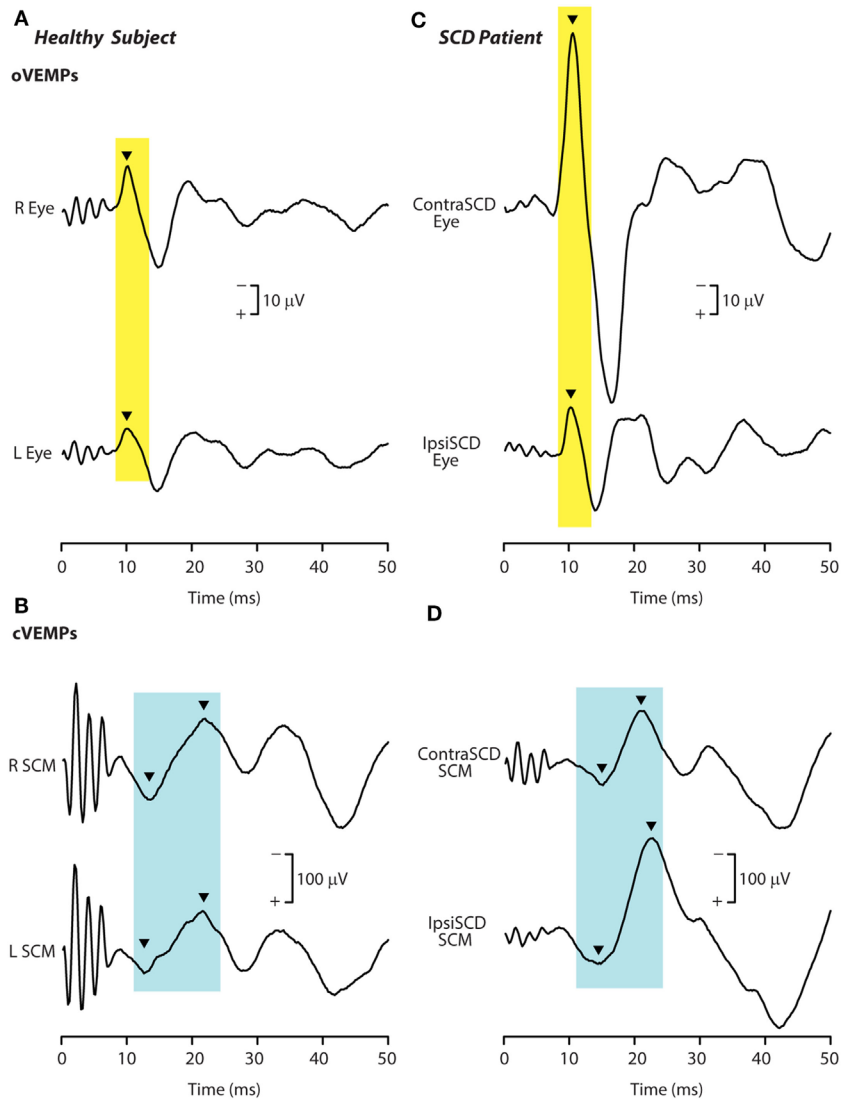

FIGURE 10 | Recordings of ocular vestibular-evoked myogenic potentials (oVEMPs) **(A,C)** and cervical vestibular-evoked myogenic potentials (cVEMPs) **(B,D)** to 500 Hz bone-conducted vibration (BCV) from a healthy subject **(A,B)** and a patient with semicircular canal dehiscence (SCD) **(C,D)**. In each record, the stimulus onset occurred at time 0. In the healthy subject, BCV at the midline of forehead at the hairline (Fz) causes symmetric oVEMP beneath both eyes, with approximately equal amplitude oVEMP n10 components (arrowheads). By contrast, the same Fz stimulus causes an asymmetric n10 component of the oVEMP response in the patient: the oVEMP n10 recorded from beneath the contralesional eye is much larger than the oVEMP n10 recorded from beneath the ipsilesional eye, and is also much larger than seen in the healthy subject. In response to BCV at Fz, both subjects show clear cVEMP p13–n23 [arrowheads in **(B,D)**]. The response in the ipsilesional sternocleidomastoid muscle (SCM) in the patient is larger than in the patient's contralesional SCM, but the asymmetry is not as great as in the same patient's oVEMP traces. The cVEMP responses of the normal subject are more symmetrical than in the SCD patient. Reprinted by permission from Wolters Kluwer Health, Inc.: Manzari et al. (94), © 2012.

labyrinth (95): a single VEMP test using 4,000 or 8,000 Hz elicits clear oVEMPs in such patients. Patients may have trouble even hearing the 8,000 Hz stimulus, which produces clear oVEMP n10 (95).

Afferents from other canals would probably not be affected by the SCD in one canal because after SCD the enhanced fluid displacement is apparently mainly directed to the canal with the new "third window." This is in accord with what is usually found with human patients—the nystagmus produced by sound usually aligns with the canal in which the fenestra is located (96).

So how is an oVEMP n10 in human subjects to ACS or BCV normally caused? Probably the most effective otolithic stimulus is a light tap with a tendon hammer to the skull at the midline of forehead at the hairline, because that is a high-jerk stimulus (97), and that pulse of jerk would be expected to cause simultaneous activation in many otolithic irregular afferents. We know it is the very onset of the stimulus which is effective in generating human

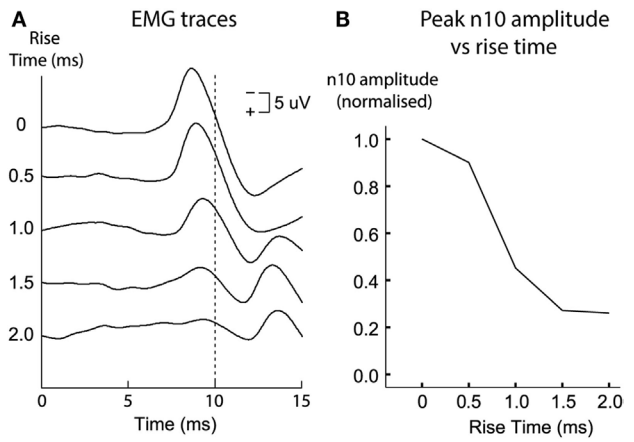

FIGURE 11 | Ocular vestibular-evoked myogenic potential (oVEMP) responses [**(A)** time series for each stimulus type; **(B)** amplitudes of the n10 peak] from a subject receiving 500 Hz bone-conducted vibration stimuli at the midline of forehead at the hairline. Tone bursts of varying rise times (ramps) were presented in random order. The size of the n10 component of the oVEMP depends on the rise-time of the tone burst stimulus: increasing the rise time causes a systematic reduction of the n10 amplitude. This is quantified in panel **(B)**, where n10 amplitude is plotted against rise-time. Reprinted by permission from Wolters Kluwer Health, Inc.: Burgess et al. (98), © 2013.

oVEMP n10. Using very short rise-times (ramps) increases the magnitude of the oVEMP n10 (98) (**Figure 11**). Also, if a long duration 500 Hz stimulus is used and then its duration progressively reduced, the size of the oVEMP n10 for a stimulus duration of 2 ms is about the same as for a stimulus lasting 10 ms (99). The paradoxical aspect is that such a short stimulus sounds (and feels) pathetically weak, but the EMG measures show it is just as effective at eliciting an oVEMP n10 response as a long duration 10 ms stimulus (99) which subjectively appears to be a much stronger stimulus. Both results point to the very onset of the stimulus as being of great importance in determining the size of the oVEMP n10.

The widespread use of these tests together with the use of the video head impulse test of the function of all the semicircular canals has refined vestibular diagnosis of peripheral vestibular disorders. It is now clear that some patients have normal semicircular canal function bilaterally but total loss of otolith function unilaterally—as shown by reduced or absent oVEMP and cVEMP from one labyrinth. Even with unilateral loss of just the utricular macula with completely normal canal function and normal saccular function (100). These selective deficits support the contention that any individual sense organ of the vestibular labyrinth can exhibit dysfunction while the remainder of the labyrinth functions normally.

There is strong physiological evidence underpinning the initial step of VEMP—the activation of vestibular receptors by sound or vibration. The extensive projection of vestibular nuclei allow for many VEMP to be recorded. These with very short latency (cVEMPs and oVEMPs) have been favored for clinical evaluation of otolithic function (see **Box 2** for summary).

BOX 2 | Summary.

- There are two kinds of otolithic receptor hair cells—amphora-shaped type I receptors and barrel-shaped type II receptors—and they are intermingled across the utricular and saccular maculae. There is a special band of receptors called the striola, on both the utricular macula and the saccular macula, where there is an increased concentration of receptors with short stiff cilia and poor attachment to the overlying otolithic membrane.
- Afferent neurons from the striolae form calyx synapses on type I receptors and have irregular resting discharge. It is these afferents which are activated by both sound and vibration. In animals with normally encased bony labyrinths, neurons with regular resting discharge are not activated by ACS or bone-conducted vibration (BCV) up to the maximum levels which were used.
- Bone-conducted vibration is a much more effective and reliable stimulus—vestibular neural thresholds to BCV are around the level for auditory brainstem response (ABR) threshold, whereas vestibular neural thresholds for ACS are around 70 dB above ABR threshold.
- The action potentials in the irregular afferents activated by sound and vibration are phase-locked to a particular band of phase angles of the stimulus waveform, up to frequencies well above 1,000 Hz for both ACS and BCV. In order to elicit this tight phase locking, each cycle of the waveform is the effective stimulus—each cycle is deflecting the hair bundles of the receptors.
- Grant and Curthoys (62) have suggested that the utricular macula operates both as an accelerometer at low frequencies and as a seismometer at high frequencies. On this model, at low frequencies the otoconia move relative to the receptor cell body (accelerometer mode), but at high frequencies the otoconia are stationary and the receptors move relative to the otoconia (seismometer mode).
- In both cases, the hair bundles are deflected relative to the cell body, so the receptors are activated both at low (accelerometer) and at high (seismometer) frequencies. That is confirmed by recording of the field potential of the utricular receptor hair cells—the utricular microphonic—which shows that utricular receptors are activated by the BCV stimulus up to high frequencies. It is stressed that the vestibular microphonic occurs without any input from the cochlea.
- Direct measures of utricular macula movement show that the macula moves up and down during vibration stimulation (and sound) up to frequencies of thousands of Hertz. The movements are very small, but *in vitro* studies (52) have shown that individual vestibular receptors have thresholds of nanometers of displacement, similar to the thresholds of cochlear receptors.
- In this way, 500 Hz mastoid vibration activates otolithic receptors and results in eye movements with horizontal, vertical, and torsional components, in human subjects consistent with utricular nerve activation at such high frequencies.
- Surface electrodes over muscle groups can record the electromyographic potentials evoked by abrupt simulation by ACS and BCV, and thus these vestibular evoked myogenic potentials (VEMPs) are being used in the clinic to indicate otolithic function.
- Because of the largely differential projection of the utricular macula to eye muscles and of the saccular macula to neck muscles, it has been possible to index predominantly utricular function by measuring the ocular vestibular-evoked myogenic potential by surface electrodes beneath the eyes as the subject looks up. Surface electrodes over tensed neck muscles record the cervical vestibular-evoked myogenic potential which indexes predominantly saccular function.

AUTHOR CONTRIBUTIONS

IC wrote the paper. JG wrote the section about the accelerometer–seismometer model. AB contributed to the section about clinical evidence. CP and DB contributed to the section about vestibular microphonics and vibrometry. LM contributed to the section about clinical evidence. All authors reviewed the text of the final paper.

ACKNOWLEDGMENTS

Much of the work reported here has been supported by the Garnett Passe and Rodney Williams Memorial Foundation, and we are very grateful for their continued support, and also for the support of the National Health and Medical Research Council of Australia.

FUNDING

IC receives funding from a Conjoint Grant from the Garnett Passe and Rodney Williams Memorial Foundation: this grant funds the salary of AB. DB is in receipt of a Senior Research Fellowship from the Garnett Passe and Rodney Williams Memorial Foundation.

REFERENCES

1. Weber KP, Rosengren SM. Clinical utility of ocular vestibular-evoked myogenic potentials (oVEMPs). *Curr Neurol Neurosci Rep* (2015) 15:22. doi:10.1007/s11910-015-0548-y
2. Dlugaiczyk J. Ocular vestibular evoked myogenic potentials: where are we now? *Otol Neurotol* (2017) 38:E513–21. doi:10.1097/MAO.0000000000001478
3. Clark B, Graybiel A. Perception of the postural vertical in normals and subjects with labyrinthine defects. *J Exp Psychol* (1963) 65:490–4. doi:10.1037/h0045606
4. Diamond SG, Markham CH, Furuya N. Binocular counter-rolling during sustained body tilt in normal humans and in a patient with unilateral vestibular nerve-section. *Ann Otol Rhinol Laryngol* (1982) 91:225–9. doi:10.1177/000348948209100222
5. Graybiel A. Oculogravic illusion. *AMA Arch Ophthalmol* (1952) 48:605–15. doi:10.1001/archopht.1952.00920010616007
6. Lichtenberg BK, Young LR, Arrott AP. Human ocular counter-rolling induced by varying linear accelerations. *Exp Brain Res* (1982) 48:127–36. doi:10.1007/BF00239580
7. Miller EF, Fregly AR, Graybiel A. Visual horizontal-perception in relation to otolith-function. *Am J Psychol* (1968) 81:488–96. doi:10.2307/1421053
8. Schone H. On the role of gravity in human spatial orientation. *Aerosp Med* (1964) 35:764–72.
9. Rudisill HE, Hain TC. Lower extremity myogenic potentials evoked by acoustic stimuli in healthy adults. *Otol Neurotol* (2008) 29:688–92. doi:10.1097/MAO.0b013e3181730377
10. Cherchi M, Bellinaso NP, Card K, Covington A, Krumpe A, Pfeifer MS, et al. Sound evoked triceps myogenic potentials. *Otol Neurotol* (2009) 30:545–50. doi:10.1097/MAO.0b013e31819d89eb
11. Colebatch JG, Halmagyi GM, Skuse NF. Myogenic potentials generated by a click-evoked vestibulocollic reflex. *J Neurol Neurosurg Psychiatry* (1994) 57:190–7. doi:10.1136/jnnp.57.2.190
12. Rosengren SM, Todd NPM, Colebatch JG. Vestibular-evoked extraocular potentials produced by stimulation with bone-conducted sound. *Clin Neurophysiol* (2005) 116:1938–48. doi:10.1016/j.clinph.2005.03.019
13. Iwasaki S, McGarvie LA, Halmagyi GM, Burgess AM, Kim J, Colebatch JG, et al. Head taps evoke a crossed vestibulo-ocular reflex. *Neurology* (2007) 68:1227–9. doi:10.1212/01.wnl.0000259064.80564.21
14. Todd NP, Rosengren SM, Aw ST, Colebatch JG. Ocular vestibular evoked myogenic potentials (OVEMPs) produced by air- and bone-conducted sound. *Clin Neurophysiol* (2007) 118:381–90. doi:10.1016/j.clinph.2006.09.025
15. Halmagyi GM, Yavor RA, Colebatch JG. Tapping the head activates the vestibular system: a new use for the clinical reflex hammer. *Neurology* (1995) 45:1927–9. doi:10.1212/WNL.45.10.1927
16. Iwasaki S, Chihara Y, Smulders YE, Burgess AM, Halmagyi GM, Curthoys IS, et al. The role of the superior vestibular nerve in generating ocular vestibular-evoked myogenic potentials to bone conducted vibration at Fz. *Clin Neurophysiol* (2009) 120:588–93. doi:10.1016/j.clinph.2008.12.036
17. Colebatch JG, Halmagyi GM. Vestibular evoked potentials in human neck muscles before and after unilateral vestibular deafferentation. *Neurology* (1992) 42:1635–6. doi:10.1212/WNL.42.8.1635
18. Maqsood A, Anis-ur-Rehman M, Gul IH. Chemical composition, density, specific gravity, apparent porosity, and thermal transport properties of volcanic rocks in the temperature range 253 to 333 K. *J Chem Eng Data* (2003) 48:1310–4. doi:10.1021/je034077p
19. Lopez I, Ishiyama G, Tang Y, Frank M, Baloh RW, Ishiyama A. Estimation of the number of nerve fibers in the human vestibular endorgans using unbiased stereology and immunohistochemistry. *J Neurosci Methods* (2005) 145:37–46. doi:10.1016/j.jneumeth.2004.11.024
20. Bergström B. Morphology of the vestibular nerve. III. Analysis of the calibers of the myelinated vestibular nerve fibers in man at various ages. *Acta Otolaryngol* (1973) 76:331–8. doi:10.3109/00016487309121518
21. Baloh RW, Honrubia V. *Clinical Neurophysiology of the Vestibular System*. 2nd ed. Philadelphia, PA: F. A. Davis (1990).
22. DeVries H. The mechanics of the labyrinth otoliths. *Acta Otolaryngol* (1950) 38:262–73. doi:10.3109/00016485009118384
23. Grant W, Best W. Otolith-organ mechanics – lumped parameter model and dynamic-response. *Aviat Space Environ Med* (1987) 58:970–6.
24. Cotton JR, Grant JW. A finite element method for mechanical response of hair cell ciliary bundles. *J Biomech Eng* (2000) 122:44–50. doi:10.1115/1.429626
25. Dunlap MD, Grant JW. Experimental measurement of utricle system dynamic response to inertial stimulus. *J Assoc Res Otolaryngol* (2014) 15:511–28. doi:10.1007/s10162-014-0456-x
26. Grant JW, Best WA, Lonigro R. Governing equations of motion for the otolith organs and their response to a step change in velocity of the skull. *J Biomech Eng* (1984) 106:302–8. doi:10.1115/1.3138498
27. Lindeman HH. Studies on the morphology of the sensory regions of the vestibular apparatus with 45 figures. *Ergeb Anat Entwicklungsgesch* (1969) 42:1–113.
28. Curthoys IS, Kim J, McPhedran SK, Camp AJ. Bone conducted vibration selectively activates irregular primary otolithic vestibular neurons in the guinea pig. *Exp Brain Res* (2006) 175:256–67. doi:10.1007/s00221-006-0544-1
29. Curthoys IS, Vulovic V. Vestibular primary afferent responses to sound and vibration in the guinea pig. *Exp Brain Res* (2011) 210:347–52. doi:10.1007/s00221-010-2499-5
30. Curthoys IS, Vulovic V, Burgess AM, Manzari L, Sokolic L, Pogson J, et al. Neural basis of new clinical vestibular tests: otolithic neural responses to sound and vibration. *Clin Exp Pharmacol Physiol* (2014) 41:371–80. doi:10.1111/1440-1681.12222
31. Curthoys IS, Vulovic V, Burgess AM, Sokolic L, Goonetilleke SC. The response of guinea pig primary utricular and saccular irregular neurons to bone-conducted vibration (BCV) and air-conducted sound (ACS). *Hear Res* (2016) 331:131–43. doi:10.1016/j.heares.2015.10.019
32. Curthoys IS, Vulovic V, Pogson J, Sokolic L. Responses of guinea pig primary vestibular afferents to low frequency (50-100 Hz) bone conducted vibration (BCV) – the neural basis of vibration induced nystagmus. *Program No 57406 2012 Neuroscience Meeting Planner [Online]*. New Orleans, LA: Society for Neuroscience (2013).
33. Curthoys IS, Vulovic V, Sokolic L, Pogson J, Burgess AM. Irregular primary otolith afferents from the guinea pig utricular and saccular maculae respond to both bone conducted vibration and to air conducted sound. *Brain Res Bull* (2012) 89:16–21. doi:10.1016/j.brainresbull.2012.07.007
34. Fernandez C, Goldberg JM. Physiology of peripheral neurons innervating otolith organs of the squirrel monkey. I. Response to static tilts and to long-duration centrifugal force. *J Neurophysiol* (1976) 39:970–84. doi:10.1152/jn.1976.39.5.970
35. McCue MP, Guinan JJ Jr. Acoustically responsive fibers in the vestibular nerve of the cat. *J Neurosci* (1994) 14:6058–70. doi:10.1523/JNEUROSCI.14-10-06058.1994
36. McCue MP, Guinan JJ Jr. Sound-evoked activity in primary afferent neurons of a mammalian vestibular system. *Am J Otol* (1997) 18:355–60.
37. Murofushi T, Curthoys IS, Topple AN, Colebatch JG, Halmagyi GM. Responses of guinea pig primary vestibular neurons to clicks. *Exp Brain Res* (1995) 103:174–8. doi:10.1007/BF00241975
38. Young ED, Fernandez C, Goldberg JM. Responses of squirrel monkey vestibular neurons to audio-frequency sound and head vibration. *Acta Otolaryngol* (1977) 84:352–60. doi:10.3109/00016487709123977

39. Zhu H, Tang X, Wei W, Maklad A, Mustain W, Rabbitt R, et al. Input-output functions of vestibular afferent responses to air-conducted clicks in rats. *J Assoc Res Otolaryngol* (2014) 15:73–86. doi:10.1007/s10162-013-0428-6
40. Zhu H, Tang X, Wei W, Mustain W, Xu Y, Zhou W. Click-evoked responses in vestibular afferents in rats. *J Neurophysiol* (2011) 106:754–63. doi:10.1152/jn.00003.2011
41. Curthoys IS, MacDougall HG, Vidal PP, de Waele C. Sustained and transient vestibular systems: a physiological basis for interpreting vestibular function. *Front Neurol* (2017) 8:117. doi:10.3389/fneur.2017.00117
42. Uzun-Coruhlu H, Curthoys IS, Jones AS. Attachment of the utricular and saccular maculae to the temporal bone. *Hear Res* (2007) 233:77–85. doi:10.1016/j.heares.2007.07.008
43. Desai SS, Zeh C, Lysakowski A. Comparative morphology of rodent vestibular periphery. I. Saccular and utricular maculae. *J Neurophysiol* (2005) 93:251–66. doi:10.1152/jn.00746.2003
44. Watanuki K, Schuknecht HF. A morphological study of human vestibular sensory epithelia. *Arch Otolaryngol* (1976) 102:583–8. doi:10.1001/archotol.1976.00780150051001
45. Spoon C, Grant W. Biomechanics of hair cell kinocilia: experimental measurement of kinocilium shaft stiffness and base rotational stiffness with Euler-Bernoulli and Timoshenko beam analysis. *J Exp Biol* (2011) 214:862–70. doi:10.1242/jeb.051151
46. Watanuki K, Meyer zum Gottesberge A. Morphological observations of the sensory epithelium of the macula sacculi and utriculi in the guinea pig. *Arch Klin Exp Ohren Nasen Kehlkopfheilkd* (1971) 200:136–44. doi:10.1007/BF00418197
47. Fernandez C, Goldberg JM, Baird RA. The vestibular nerve of the chinchilla. III. Peripheral innervation patterns in the utricular macula. *J Neurophysiol* (1990) 63:767–80. doi:10.1152/jn.1990.63.4.767
48. Goldberg JM, Desmadryl G, Baird RA, Fernandez C. The vestibular nerve of the chinchilla. IV. Discharge properties of utricular afferents. *J Neurophysiol* (1990) 63:781–90. doi:10.1152/jn.1990.63.4.781
49. Lim DJ. Morphological and physiological correlates in cochlear and vestibular sensory epithelia. *Scan Electron Microsc* (1976) 2:269–76.
50. Lim DJ. Fine morphology of the otoconial membrane and its relationship to the sensory epithelium. *Scan Electron Microsc* (1979) 3:929–38.
51. Songer JE, Eatock RA. Tuning and timing in mammalian type I hair cells and calyceal synapses. *J Neurosci* (2013) 33:3706–24. doi:10.1523/JNEUROSCI.4067-12.2013
52. Geleoc GSG, Lennan GWT, Richardson GP, Kros CJ. A quantitative comparison of mechanoelectrical transduction in vestibular and auditory hair cells of neonatal mice. *Proc Biol Sci* (1997) 264:611–21. doi:10.1098/rspb.1997.0087
53. Curthoys IS, Grant JW. In what way is an air conducted sound an otolithic stimulus? PS-927. *Abstr Assoc Res Otolaryngol* (2016) 39:568.
54. Palmer AR, Russell IJ. Phase-locking in the cochlear nerve of the guinea-pig and its relation to the receptor potential of inner hair-cells. *Hear Res* (1986) 24:1–15. doi:10.1016/0378-5955(86)90002-X
55. Rose JE, Brugge JF, Anderson DJ, Hind JE. Phase-locked response to low-frequency tones in single auditory nerve fibers of the squirrel monkey. *J Neurophysiol* (1967) 30:769–93. doi:10.1152/jn.1967.30.4.769
56. Fettiplace R. Hair cell transduction, tuning, and synaptic transmission in the mammalian cochlea. *Compr Physiol* (2017) 7:1197–227. doi:10.1002/cphy.c160049
57. Pastras CJ, Curthoys IS, Brown DJ. In vivo recording of the vestibular microphonic in mammals. *Hear Res* (2017) 354:38–47. doi:10.1016/j.heares.2017.07.015
58. Brown DJ, Pastras CJ, Curthoys IS. Electrophysiological measurements of peripheral vestibular function – a review of electrovestibulography. *Front Syst Neurosci* (2017) 11:34. doi:10.3389/fnsys.2017.00034
59. Pastras C, Curthoys IS, Brown D. Dynamic response and sensitivity of the utricular macula, measured in vivo using laser Doppler vibrometry in guinea pigs. PS547. *Abstr Assoc Res Otolaryngol* (2018) 41:342.
60. Tullio P. *L'orecchio*. Bologna: L. Capelli Editore (1928).
61. Jones TA, Jones SM, Vijayakumar S, Brugeaud A, Bothwell M, Chabbert C. The adequate stimulus for mammalian linear vestibular evoked potentials (VsEPs). *Hear Res* (2011) 280:133–40. doi:10.1016/j.heares.2011.05.005
62. Grant W, Curthoys I. Otoliths – accelerometer and seismometer; implications in vestibular evoked myogenic potential (VEMP). *Hear Res* (2017) 353:26–35. doi:10.1016/j.heares.2017.07.012
63. Lim DJ. Vestibular sensory organs – scanning electron microscopic investigation. *Arch Otolaryngol* (1971) 94:69–76. doi:10.1001/archotol.1971.00770070105013
64. Lim DJ, Anniko M. Developmental morphology of the mouse inner ear. A scanning electron microscopic observation. *Acta Otolaryngol Suppl* (1985) 422:1–69. doi:10.3109/00016488509121766
65. Lim DJ, Lane WC. Vestibular sensory epithelia – a scanning electron microscopic observation. *Arch Otolaryngol* (1969) 90:283–92. doi:10.1001/archotol.1969.00770030285007
66. Suzuki JI, Tokumasu K, Goto K. Eye movements from single utricular nerve stimulation in the cat. *Acta Otolaryngol* (1969) 68:350–62. doi:10.3109/00016486909121573
67. Vulovic V, Curthoys IS. Bone conducted vibration activates the vestibulo-ocular reflex in the guinea pig. *Brain Res Bull* (2011) 86:74–81. doi:10.1016/j.brainresbull.2011.06.013
68. Lyford-Pike S, Vogelheim C, Chu E, Della Santina CC, Carey JP. Gentamicin is primarily localized in vestibular type I hair cells after intratympanic administration. *J Assoc Res Otolaryngol* (2007) 8:497–508. doi:10.1007/s10162-007-0093-8
69. Lue J-H, Day A-S, Cheng P-W, Young Y-H. Vestibular evoked myogenic potentials are heavily dependent on type I hair cell activity of the saccular macula in guinea pigs. *Audiol Neurootol* (2009) 14:59–66. doi:10.1159/000156701
70. Cornell ED, Burgess AM, MacDougall HG, Curthoys IS. Bone conducted vibration to the mastoid produces horizontal, vertical and torsional eye movements. *J Vestib Res* (2015) 25:91–6. doi:10.3233/VES-150550
71. Curthoys IS. A critical review of the neurophysiological evidence underlying clinical vestibular testing using sound, vibration and galvanic stimuli. *Clin Neurophysiol* (2010) 121:132–44. doi:10.1016/j.clinph.2009.09.027
72. Uchino Y, Kushiro K. Differences between otolith- and semicircular canal-activated neural circuitry in the vestibular system. *Neurosci Res* (2011) 71:315–27. doi:10.1016/j.neures.2011.09.001
73. Colebatch JG. Sound conclusions? *Clin Neurophysiol* (2010) 121:124–6. doi:10.1016/j.clinph.2009.09.026
74. Curthoys IS. A balanced view of the evidence leads to sound conclusions. A reply to J.G. Colebatch "Sound conclusions?" *Clin Neurophysiol* (2010) 121:977–8. doi:10.1016/j.clinph.2010.01.025
75. Manzari L, Tedesco A, Burgess AM, Curthoys IS. Ocular vestibular-evoked myogenic potentials to bone-conducted vibration in superior vestibular neuritis show utricular function. *Otolaryngol Head Neck Surg* (2010) 143:274–80. doi:10.1016/j.otohns.2010.03.020
76. Curthoys IS, Iwasaki S, Chihara Y, Ushio M, McGarvie LA, Burgess AM. The ocular vestibular-evoked myogenic potential to air-conducted sound; probable superior vestibular nerve origin. *Clin Neurophysiol* (2011) 122:611–6. doi:10.1016/j.clinph.2010.07.018
77. Manzari L, Burgess AM, Curthoys IS. Ocular and cervical vestibular evoked myogenic potentials in response to bone-conducted vibration in patients with probable inferior vestibular neuritis. *J Laryngol Otol* (2012) 126:683–91. doi:10.1017/S0022215112000692
78. Papathanasiou ES. The evidence is finally here: ocular vestibular evoked myogenic potentials are mainly dependent on utricular pathway function. *Clin Neurophysiol* (2015) 126:1843–4. doi:10.1016/j.clinph.2015.01.007
79. Govender S, Colebatch JG. Location and phase effects for ocular and cervical vestibular-evoked myogenic potentials evoked by bone-conducted stimuli at midline skull sites. *J Neurophysiol* (2018) 119:1045–56. doi:10.1152/jn.00695.2017
80. Curthoys IS, Vulovic V, Burgess AM, Cornell ED, Mezey LE, MacDougall HG, et al. The basis for using bone-conducted vibration or air-conducted sound to test otolithic function. *Ann N Y Acad Sci* (2011) 1233:231–41. doi:10.1111/j.1749-6632.2011.06147.x
81. Curthoys IS. The new vestibular stimuli: sound and vibration-anatomical, physiological and clinical evidence. *Exp Brain Res* (2017) 235:957–72. doi:10.1007/s00221-017-4874-y
82. Carey JP, Hirvonen TP, Hullar TE, Minor LB. Acoustic responses of vestibular afferents in a model of superior canal dehiscence. *Otol Neurotol* (2004) 25:345–52. doi:10.1097/00129492-200405000-00024
83. Curthoys IS, Grant JW. How does high-frequency sound or vibration activate vestibular receptors? *Exp Brain Res* (2015) 233:691–9. doi:10.1007/s00221-014-4192-6